UNIVERSITY OF CALIFORNIA,
IRVINE

Study of Amyloid Oligomers and Facile Access to Aβ Peptides and Labeled Aβ

DISSERTATION

submitted in partial satisfaction of the requirements
for the degree of

DOCTOR OF PHILOSOPHY

in Chemistry

by

Stan Yoo

Dissertation Committee:
Professor James S. Nowick, Chair
Professor Andy S. Borovik
Professor Zhibin Guan

2019

DEDICATION

To my parents and grandparents.

TABLE OF CONTENTS

LIST OF FIGURES

LIST OF TABLES

ACKNOWLEDGEMENTS

I would like to thank my advisor, Professor James Nowick. When he wrote me back a very nice email back when I inquired him whether he would be taking any students before I was admitted, I already knew James would be an amazing person and mentor. James really cares about students' personal growths and career pathways. His excitement in science, humble personality, and dedication in mentorship really resonated with the group and fostered his lab's culture very well. I feel incredibly fortunate to have him as my advisor.

I would like to thank my thesis committee, Professor Zhibin Guan and Professor Andy Borovik. Zhibin served as a member of my committee for second year report and advancement to candidacy exam and kindly agreed to be a part of my thesis committee. It was nice to interact with Zhibin and I learned from his astute questions. Andy is one of the nicest people I have met at UCI. I really appreciate all the encouragement and consolation that Andy has given me over last few years.

I would like to thank my past and present labmates, especially the two that I got to work closely with – Dr. Adam Kreutzer and Sheng Zhang. Adam and I made a good team and we got to work together since the very beginning to end of my graduate career. I learned so much from him and I will always be thankful for his kindness. Sheng and I worked together for last two years, and I am proud of what we have achieved. We established protein expression and purification procedures in our lab for the first time. I really appreciate his hard work.

I would like to thank my former mentors, Dr. Ron Zuckermann, and Dr. Michael Kienzler. I was fortunate to have worked with Ron and Michael before coming to UCI. Without their mentorship, graduate school would have been much more difficult. I am really thankful for their continued support.

I would like to thank my friends. I was fortunate to have these people at UCI: Nick Foy, Tyler Heiss, Eric Kuenstner, Dr. Colin Rathbun, Alex Reath, Hyunjun Yang, and many more. Going out to eat delicious food and going to climbing with friends made my time at UCI enjoyable.

Lastly, I would like to thank my family. My parents sacrificed their life in Korea and moved to America for my education. My grandparents supported me throughout the time I studied in America. I would not have made this far without their scarification and love.

CURRICULUM VITAE
Stan Yoo

EDUCATION

Ph. D., Chemistry, **University of California – Irvine, Irvine, CA** (2014 – 2019)

B.S., Chemistry, **University of California – Berkeley, Berkeley, CA** (2009 – 2013)

RESEARCH EXPERIENCE

Professor James Nowick's lab – *Graduate Student Researcher* (2014 – current)

- Developed and optimized method for expression and purification of amyloid-beta peptides
- Constructed recombinant plasmids of aggregation-prone amyloid-beta peptides and their mutants via molecular cloning, expressed and purified the peptides, and conduct biological and biophysical studies
- Synthesized macrocyclic β-sheet peptides as the chemical models to study supramolecular assembly of amyloids, specifically Amyloid beta and transthyretin
- Screened and optimized crystals of peptides; collected and processed X-ray crystallography data
- Mentored three junior lab members and two undergraduate students

Dr. Ron Zuckermann's lab at LBNL – *Post-Baccalaureate Fellow* (2013 – 2014)

- Synthesized polypeptoids, N-substituted glycines, using automated synthesizer and manual synthesis, then purified and analyzed the resulting compounds with LC/MS, MALDI, and analytical HPLC.
- Managed LC/MS instrument and maintain laboratory supplies and the reagents for peptoid synthesis.

Professor Ehud Isacoff's lab – *Undergraduate Student Researcher* (2012 – 2013)

- Executed the multistep organic synthesis of azobenzene photoswitch for neurobiological studies.
- Carried out experiments by setting up organic reactions, purifying the resulting products through flash column chromatography, and characterizing them with NMR and mass spectrometry.

Professor Len Bjeldanes' lab – *Undergraduate Student Researcher* (2011 – 2013)

- Screened for natural compounds for anti-cancer and anti-inflammatory activities
- Treated cancer and inflammatory cells with natural compounds to analyze anti-cancer or anti-inflammatory activities with various cytotoxicity assays.

PUBLICATIONS | MyNCBI publication list: tinyurl.com/yoostan-myncbi

12. Zhang, S.[‡]; **Yoo, S.**[‡]; Kreutzer, A.; Nowick, J. Discovery of a unique oligomer-forming Aβ by disulfide stabilization, *In preparation for submission to Biochemistry* **2019** ([‡] equal contribution)

11. **Yoo, S.**; Zhang, S.; Guaglinone, G.; Nowick, J. An efficient expression system for N-terminal cysteine Aβ for bioconjugation, *In preparation for submission to Bioconjugate Chem*. **2019**

10. Moser, B.; Steinhardt, R.; Escalante-Buendia, Y.; Boltz, D.; Barker, K.; **Yoo, S.**; McGonnigal, B.; Esser-Kahn, E. Immune potentiator for increased safety and improved protection of vaccines by NF-kB modulation. preprint to *bioRxiv*

9. Salveson, P.; Haerianardakani, S.; Thuy-Boun, A.; **Yoo, S.**; Kreutzer, A.; Demeler, B.; Nowick, J.; Repurposing triphenylmethane dyes to bind to trimers derived from Aβ. *J. Am. Chem. Soc.* **2018**, *140*, 11745-11754

8. **Yoo, S**[‡].; Zhang, S.[‡]; Kreutzer, A.; Nowick, J. An efficient method for the expression and purification of Aβ(M1-42). *Biochemistry* **2018**, *57*, 3861-3966 ([‡] equal contribution)

7. Kreutzer, A.; Spencer R.; McKnelly, K.; **Yoo, S.**; Hamza, I.; Salveson, P.; Nowick, J. A Hexamer of a Peptide Derived from $A\beta_{16\text{-}36}$. *Biochemistry*. **2017**, *56*, 6061-6071

6. Kreutzer, A.; **Yoo, S.**; Spencer, R.; Nowick, J. Stabilization, Assembly, and Toxicity of Trimers Derived from Aβ. *J. Am. Chem. Soc.* **2017**, *139*, 966-975

5. **Yoo, S.**; Kreutzer, A.; Truex, N.; Nowick, J. Square Channels Formed by a Peptide Derived from Transthyretin. *Chem. Sci.* **2016**, *7*, 6946-6951

4. Robertson, E.; Proulx, C.; Su, J.; Garcia, R.; **Yoo, S.**; Nehls, E., Connolly, M.; Taravati, L.; Zuckermann, R. Molecular Engineering of the Peptoid Nanosheet Hydrophobic Core. *Langmuir*, **2016**, *32*, 11946-11957

3. Proulx, C.; Noë, F,; **Yoo, S.**; Connolly, M.; Zuckermann, R. On-Resin *N*-Terminal Peptoid Degradation: Toward Mild Sequencing Conditions. *Pept. Sci.* **2016**, *106*, 726-736.

2. Proulx, C.; **Yoo, S.**; Connolly, M.; Zuckermann, R. Accelerated Submonomer Solid-Phase Synthesis of Peptoids Incorporating Multiple Substituted N-Aryl Glycine Monomers. *J. Org. Chem.* **2015**, *80*, 10490-10497

1. Kienzler, M. [‡]; Reiner, A. [‡]; Trautman, E.; **Yoo, S.**; Trauner, D.; Isacoff, E. A Red-Shifted, Fast Relaxing Azobenzene Photoswitch for Visible Light Control of an Ionotropic Glutamate Receptor. *J. Am. Chem. Soc*. **2013**, *135*, 17683-17686 ([‡] equal contribution)

PRESENTATIONS

12. **Yoo, S.**; Zheng, S.; Kreutzer, A.; Nowick, J. Facile access to Aβ peptides and studies of stapled and labeled analogues. The 26th American Peptide Symposium, Monterery, CA, June 22-27, 2019

11. **Yoo, S.**; Zheng, S.; Kreutzer, A.; Nowick, J. An Efficient Method for the Expression and Purification of Aβ(M1–42) and N-terminal Cysteine Aβ for Cysteine-conjugation. the 13th Annual Peptide. Therapeutics Symposium, La Jolla, CA, October 25-26, 2018.

10. McKnelly, K.; **Yoo, S.**; Kreutzer, A.; Hart, C.; Laayouni, M.; Nowick, J. Effects of Familial Mutations on the Structural Assembly and Biophysical Properties of a Peptide Derived from $A\beta_{16-36}$. The American Chemical Society 25th National Meeting, New Orleans, LA, March, 2018.

9. Kreutzer, A.; **Yoo, S.**; Spencer, R.; Hamza, I.; Diab, M.; Nowick, J. Recognition of Aβ Oligomers by Antibodies Generated Against Triangular Trimers Derived from Aβ. Gordon Research Symposium & Conference, Chemistry and Biology of Peptides, February 11th, 2018.

8. **Yoo, S**‡.; Zhang, S.‡; Kreutzer, A.; Nowick, J. Expression and Purification of β-Hairpin-pinched Aβ. Orange County Section ACS Meeting, Irvine, CA, September 28th, 2017. (‡equal contribution)

7. Hart, C.; **Yoo. S.**; Salveson, P.; Truex, N.; Nowick, J. Detecting Amyloid Oligomer Assemblies using Triarylmethane Dyes. The 24th Annual UC Irvine Undergraduate Research Symposium, Irvine, CA, May, 2017.

6. **Yoo, S**.; Salveson, P.; Kreutzer, A.; Hart, C.; Nowick, J. Detecting Amyloid Oligomer Assembly in a Chemical Model System. The American Chemical Society 253rd National Meeting, San Francisco, CA, April, 2017.

5. **Yoo, S.**; Truex, N.; Kreutzer, A.; Nowick, J. A β-hairpin Derived from Transthyretin 106-121 that Forms Square Hydrophobic Channels. The American Chemical Society 251st National Meeting, San Diego, CA, March, 2016.

4. **Yoo, S.**; Truex, N.; Kreutzer, A.; Nowick, J. A β-hairpin Derived from Transthyretin 106-121 that Forms Square Hydrophobic Channels. The 45th Western Regional Meeting of ACS, San Marcos, CA. November, 2015.

3. **Yoo, S.**; Proulx, C.; Zuckermann. R. Improved Synthesis of Electron-deficient Side Chains and Their Application in Controlling Chain Confirmation in Peptoids. The 248th ACS National Meeting, San Francisco, CA. August, 2014.

2. **Yoo, S.**; Kienzler, M.; Isacoff, E. Synthesis of Novel Red-Shifted Maleimide Azobenzene Glutamate Photoswitches. College of Chemistry Saegebarth Undergraduate Research Fair, Berkeley, CA. April, 2013.

1. **Yoo, S.**; Gooding, M.; Blum, A. Toxic Prioritization of Organohalogens. The Green Science Policy Institute Symposium, Berkeley, CA. August, 2011.

TEACHING EXPERIENCE

▪ Get Fit Faculty-in-Training Program (Spring 18)
Participated in NSF-sponsored program in career development in teaching; observed and gave a lecture in an organic chemistry course at Harvey Mudd College

▪ Teaching Internship with Experienced Support (T.I.E.S.) Program (Spring 18)
Participated in teaching internship program at Orange Community College; observed and taught in a preparatory general chemistry course in Orange Coast College

▪ Senior lead teaching assistant (Fall 17 – Spring 18)
Facilitated and participated in discussions on pedagogical topics with professors and other teaching assistants. Led discussion sections, managed exam grading, mentored other teaching assistants

▪ Course instructor for CHEM 51LB – Organic Chemistry Laboratory (Summer 17)
Facilitated and taught an accelerated organic chemistry laboratory course. Led laboratory lectures, managed the course logistics, teaching assistants, and students

▪ Head teaching assistant for CHEM 51–Organic Chemistry Laboratory (Fall 16, Winter 17, Spring 17)
Assisted with logistics and course materials for the large lower division organic chemistry laboratory courses and mentored other teaching assistants for the courses

▪ Teaching assistant for CHEM 51C – Organic chemistry lecture (Spring 18)

▪ Teaching assistant for CHEM 51B – Organic chemistry lecture (Winter 18)

▪ Teaching assistant for CHEM H/M52LA – Honors/Majors Organic chemistry laboratory (Fall 17)

▪ Teaching assistant for CHEM 125 – Advanced organic chemistry lecture (Spring 16)

▪ Teaching assistant for CHEM 128L – Chemical biology laboratory (Winter 15, Winter 16)

▪ Teaching assistant for CHEM 51LC – Organic chemistry laboratory (Spring 15)

▪ Teaching assistant for CHEM 51LD – Organic chemistry laboratory (Fall 14, Summer 15, Fall 15)

EXTRA-CURRICULAR ACTIVITIES

▪ Graduate Safety Team at UC Irvine - *Chair of Public Relations committee* (2017 – 2018)
Designed and posted posters, stall wall moments, and the general publicity of graduate safety team and cultivated a positive relationship with industrial partners by communication with the company liaisons.

▪ Safety Representative of the Nowick group (2017 – current)
Managed the safety matters in the research group. Handled safety inspections and gave on-the-job safety trainings for incoming lab group members. Organized chemical inventory update and lab clean-up.

▪ Recruitment coordinator for UCI Chemistry Department (2017, 2018)
Coordinated after-events during recruitment weekends for prospective students
▪ GPS-BIOMED trainee (2014 – current)
Participated in NIH-sponsored program in professional development program, GPS-BIOMED

▪ Dept. of Chemistry graduate student and post-doctoral colloquium organizing committee (2016 – 2018)
Organized monthly colloquium where the graduate students and post-doctoral fellows in organic chemistry and chemical biology share their research.

▪ UC Irvine Chemistry Outreach - *Volunteer* (2014 – 2016)
Participated in Chemistry Outreach program and presented chemistry demonstrations in K-12 schools.

▪ Organic Chemistry storeroom - *Laboratory facilitator* (2011 – 2013)
Organized chemicals for the undergraduate organic chemistry laboratory and assisted students with their in-lab needs.

▪ *Science of Wellness* Magazine – *Copy editor/Layout designer* (2012 –2013)
Edited and designed articles for the student-run publication to inform the public on various health-related issues.

▪ Organic Chemistry laboratory development – *Volunteer* (2012 – 2013)
Recorded NMR spectra data for students in the advanced organic chemistry laboratory. Developed green organic chemistry experiments for use in undergraduate laboratory courses.

▪ Green Science Policy Institute with Dr. Arlene Blum – *Volunteer* (2011 – 2012)
Collected and analyzed foam samples using XRF analyzer for harmful halogenated flame retardants.

ABSTRACT OF THE DISSERTATION

STUDY OF AMYLOID OLIGOMERS AND

FACILE ACCESS TO Aβ PEPTIDES AND LABELED Aβ

by

Stan Yoo

Doctor of Philosophy in Chemistry

University of California, Irvine

2019

Professor James S. Nowick, Chair

Amyloidogenic peptides or proteins self-assemble to form oligomers and fibrils in many neurodegenerative diseases such as Alzheimer's disease, Parkinson's disease, and type-2 diabetes. Fibrils formed by amyloidogenic peptides or proteins are observed as plaques in patients, and the build-up of these plaques are the hallmark of amyloid diseases. The amyloid fibrils were believed to be the cause of neurodegenerative diseases because they were observed in patients' brains. Amyloid fibrils are stable, and their structures are extensively characterized over the years through solid-state NMR and cryogenic electron microscopy.

In the last few decades, the intermediate form, soluble amyloid oligomers, have emerged as the neurotoxic form of amyloids rather than amyloid fibrils. Amyloid oligomers are short-lived and inherently heterogeneous, forming various species of many different sizes and morphologies The heterogeneous nature of amyloid oligomers makes them difficult to elucidate their structures by common structural techniques such as NMR, X-ray crystallography, and cryo-EM. While not much is known about amyloid oligomers, many studies have found that amyloid oligomers are comprised of amyloid monomers adapting an antiparallel β-hairpin conformation.

Effort to gain insights into structures of elusive amyloid oligomers, the Nowick laboratory has developed a chemical model system which mimics β-hairpin of amyloid peptides or proteins. In the last few years, structural studies of these model systems have shed light on how amyloid oligomers may assemble in disease pathology. Among many amyloid peptides and proteins, amyloid beta (Aβ) is the most intensively studied amyloid peptide and is central to the pathology of Alzheimer's disease. Thus, advances in amyloid research rely on improved access to Aβ. In the first two chapters of my thesis, I describe an efficient method of expression and purification of Aβ(M1-42) and its mutants, by combining protein expression and peptide purification method, as well as of efficient expression and labeling N-terminal cysteine Aβ with fluorophores or biotin

using maleimide conjugation reagents. In the Chapters 3 and 4, I describe my effort in studying amyloid oligomers by stabilizing β-hairpin region of Aβ and by a chemical model system derived from transthyretin. Lastly, in the epilogue, I describe my collaborative efforts during my time in the Nowick laboratory.

PREFACE

For my graduate work, my efforts went into solving three challenges in the amyloid field: The first challenge was the difficulty in facile production of large quantities of high-quality amyloid beta peptides. The second challenge was the difficulty in site-specific labeling of Aβ peptides with functional moieties such as fluorophores. The last challenge was the difficulty in studying neurotoxic amyloid oligomers as they are inherently heterogeneous and short-lived. In each chapter, I describe my approaches to solve those challenges.

Chapter 1 presents an efficient method for expression and purification of N-terminal methionine extended Aβ, Aβ(M1–42). Expression of Aβ(M1–42) is simple to execute and avoids an expensive and often difficult enzymatic cleavage step associated with expression and isolation of Aβ(1–42). This chapter reports an efficient method for expression and purification of Aβ(M1–42) and ^{15}N-labeled Aβ(M1–42). The method affords the pure peptide at about 19 mg per liter of bacterial culture through simple and inexpensive steps in three days. This chapter also reports a simple method for construction of recombinant plasmids, and the expression and purification of Aβ(M1–42) peptides containing familial mutations.

Chapter 2 describes the extension of previously developed method for Aβ(M1–42) to express and purify N-terminal cysteine Aβ, Aβ(C1–42). This chapter also describes utility of Aβ(C1–42) through fluorescent labeling and biotin labeling using cysteine-maleimide conjugation. Biophysical and biological studies of labeled Aβ peptides show similar behavior as the unlabeled peptide.

Chapter 3 presents an approach to study Aβ oligomers by stabilization of β-hairpin within full-length Aβ peptides by installing a disulfide linkage formed by two cysteines. This chapter details the expression of β-hairpin stabilized Aβ peptides and their biophysical studies. One mutant

with its β-hairpin stabilized forms unprecedented oligomer formation and further studies are underway.

Chapter 4 describes the design, synthesis, and X-ray crystallographic structure of a macrocyclic peptide derived from transthyretin (TTR). This chapter explores the supramolecular assembly of a β-sheet-forming peptide derived from TTR. X-ray crystallography reveals that the peptide does not form a tetramer, but rather assembles to form square channels. The square channels are formed by extended networks of β-sheets and pack in a "tilted windows" pattern. This unexpected structure represents an emergent property of the peptide and broadens the scope of known supramolecular assemblies of β-sheets.

Finally, the epilogue describes my collaborative efforts during my time in the Nowick laboratory. Throughout my time in the Nowick laboratory, I was fortunate to work with many laboratory members with many different projects. I briefly introduce each collaborative project in this chapter.

Overall, through projects that will be described, I was able to tackle the three challenges in the amyloid fields: (1) facile access of Aβ peptides, (2) site-specific labeling of Aβ, and (3) study of amyloid oligomers. I hope that these works will benefit researchers in the field by providing efficient methods to produce Aβ and labeled Aβ for their studies and by providing new insights in understanding how amyloid oligomers assemble.

Chapter 1

An Efficient Method for the Expression and Purification of Aβ(M1–42)

Introduction

Aggregation of the amyloid-β peptide, Aβ, is central to the pathology of Alzheimer's disease.[1-3] Aβ peptides are cleaved from amyloid precursor protein and aggregate to form amyloid deposits and oligomers in Alzheimer's disease (Figure 1.1). The two major forms of Aβ *in vivo* are the 40- and 42-amino acid alloforms of Aβ, where they differ by two additional hydrophobic residues at the C-terminus. The 42-amino acid alloform, Aβ(1–42) is considered as the main amyloidogenic species and aggregates more rapidly and is more toxic than Aβ(1–40), despite of its 10-fold lower concentration *in vivo* as compared to Aβ(1–40).[4, 5]

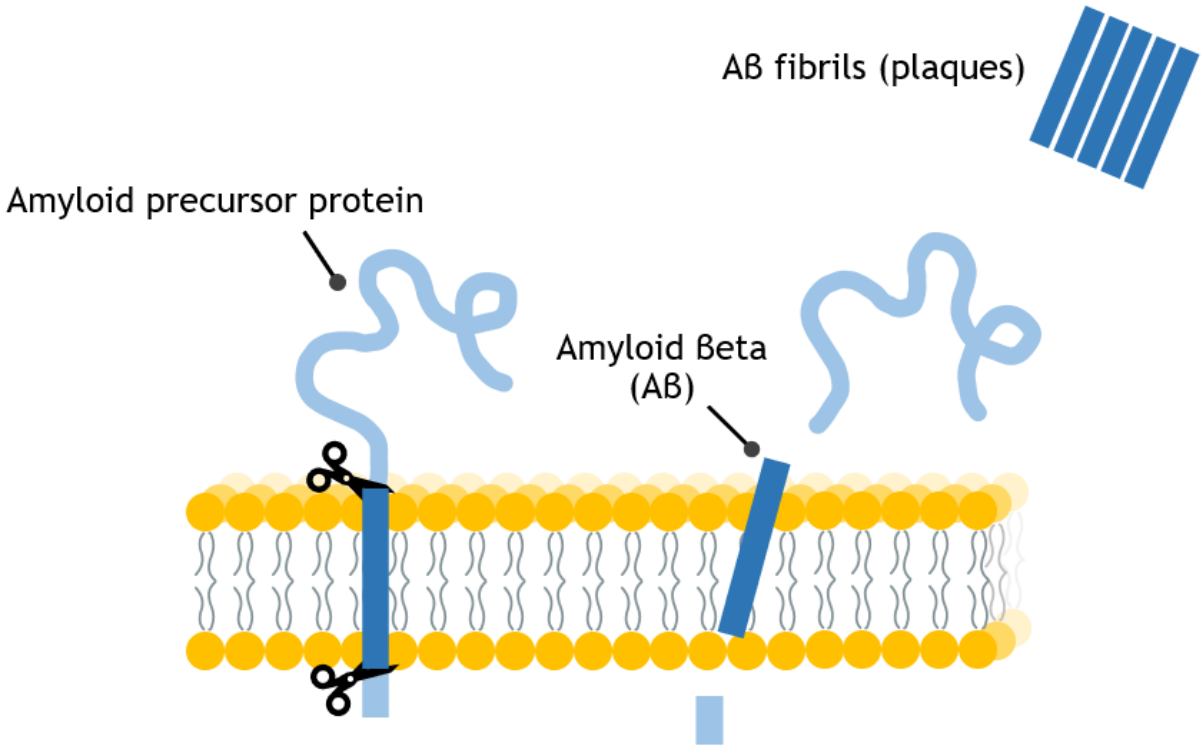

Figure 1.1. Aβ is cleaved from amyloid precursor protein (APP) and aggregates to form Aβ fibrils.

In 1907, Alois Alzheimer, a German psychiatrist and neuropathologist discovered amyloid plaques in the postmortem brains of demented patients and wondered if these deposits are related to neurodegeneration.[6] About 80 years later, Aβ peptide was first sequenced from meningeal blood vessels from Alzheimer's disease patients.[7] A year later, another research group purified and characterized Aβ peptide from the senile plaques in brain tissue of Alzheimer's disease patients.[8] These discoveries led scientists to believe in the amyloid hypothesis, which postulates that accumulation of Aβ in the brains is the primary influence driving Alzheimer's disease pathogenesis.[9, 10] Even though the amyloid hypothesis has been one of leading hypotheses of Alzheimer's disease for last three decades, it is currently lacking in detail and is still under debate. One of the bottlenecks in studies with Aβ is insufficient access to large quantities of highly pure Aβ peptides. A plentiful source of pure Aβ peptides, including isotopically labeled Aβ and various mutants associated with familial Alzheimer's disease, is essential to progress in research in Aβ aggregation and Alzheimer's disease.

Early efforts to generate Aβ focused on chemical synthesis of the peptide, and chemical synthesis of Aβ continues to be valuable tool as it allows chemical modification or incorporation of unnatural amino acid. However, chemical synthesis of Aβ can lead to impurities, such as amino acid deletion products, that are difficult to eliminate during purification.[11, 12] Aggregation-prone nature of Aβ makes solid-phase peptide synthesis (SPPS) difficult to efficiently synthesize homogeneous peptide. Even though peptide chemists have developed various synthetic methods to circumvent aggregation issue that occurs during SPPS over the last two decades, the yields and levels of purity of synthetic Aβ peptides are less than desirable.[13-15] Furthermore, SPPS of Aβ peptides can be costly to produce good quantities of the peptides and not environmentally-friendly as it produces large volume of waste of dimethylformamide.

Within the past two decades, expression has emerged as a useful alternative for preparing Aβ of superior purity. Expressed Aβ has been reported to aggregate three times faster and be significantly more toxic toward neuronal cells than synthetic Aβ.[11] Expressed Aβ is typically generated as a fusion protein that is cleaved after expression using a protease.[11, 16, 17] The first reported expression method employed a solubilizing tag protein and a histidine affinity tag to facilitate expression and purification.[18] This approach requires expression and purification of the protease and an affinity purification step, which can make the preparation of Aβ costly and time-intensive. Since the discovery of expression method of Aβ, many research groups put efforts in developing more efficient expression and purification methods. Few of these methods involved incorporation of ubiquitin extension, maltose binding protein, and a tobacco etch virus (TEV) cleavage site. [11, 19, 20] These developments provided approaches to produce homogeneous and pure Aβ peptides, but still suffer from low yields and cumbersome procedures.

In 2009, Walsh and co-workers have introduced an Aβ expression system that circumvents the need for protease cleavage and affinity chromatography. In this expression system, Aβ(1–40) and Aβ(1–42) are expressed as variants Aβ(M1–40) and Aβ(M1–42) that contain an N-terminal methionine residue that originates from the translational start codon (Figure 1.2).[21] Aβ(M1–40) and Aβ(M1–42) behave almost identically to the native peptides in aggregation and toxicity assays, and the additional N-terminal methionine has little impact on the fibril structure.[22, 23] Because of these characteristics, Aβ(M1–40) and Aβ(M1–42) have emerged as widely used alternatives to the native Aβ peptides.[24-29] Although this expression system provides ready access to Aβ(M1–40) with yields of 5-20 mg per liter of bacterial culture, the preparation of Aβ(M1–42) gives substantially lower yields.[21]

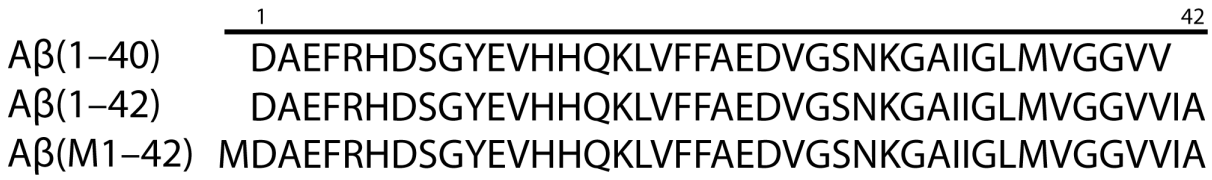

Figure 1.2. Sequences of Aβ(1–40), Aβ(1–42), and Aβ(M1–42).

In this chapter, I report an efficient method for expression and purification of Aβ(M1–42) and associated homologues, including the uniformly ^{15}N-labeled peptide and familial mutants. I also report simple and versatile method to construct recombinant plasmids containing desired mutations. Our method simplifies the construction of plasmids containing mutant Aβ sequences and bypasses cumbersome steps in previously reported purification procedures. Our approach offers several major advantages over previous procedures: (1) a short preparation time of only three days, (2) minimal expense, (3) easier laboratory techniques, and (4) production of substantial amounts of highly pure Aβ peptides at about 19 mg per liter of bacterial culture.

Results and Discussion

The following describes the procedures that I have developed for the preparation of the Aβ(M1–42) wild-type and mutant peptides (Table 1.1): For expression of the wild-type Aβ(M1–42) peptide, I use the commercially available plasmid, pET-Sac-Aβ(M1–42).[21] For expression of mutant Aβ(M1–42) peptides, I construct recombinant plasmids containing mutant Aβ(M1–42) gene sequences using standard cloning techniques. Upon expression in *E. coli*, the peptides form inclusion bodies. The inclusion bodies are subjected to multiple rounds of washing, followed by

solubilization in urea buffer. The resulting solution is filtered using a hydrophilic syringe filter and then immediately applied to a reverse-phase HPLC column. Pure HPLC fractions are then combined and lyophilized to give the peptide as a white powder. For biophysical and biological studies, the purified peptide is further treated with NaOH and then re-lyophilized. Yields are assessed both gravimetrically and by UV absorption. The composition and purity of the peptides are assessed by analytical HPLC, MALDI-MS, and SDS-PAGE with silver staining.

Table 1.1. A representative schedule for expression and purification of Aβ(M1–42).

Day	Time	Steps
Monday	Evening	Starter culture
Tuesday	Morning	Daytime culture
	Afternoon	IPTG Induced expression
	Evening	Cell pelleting
Wednesday	Morning	Sonication; urea extraction
	Afternoon	**Syringe filter** using a hydrophilic membrane Purification by **prep-HPLC at 80 °C** Collecting pure fractions, freeze, and lyophilize
Thursday	Afternoon	NaOH treatment, freeze, and lyophilize

Expression of Aβ(M1–42)

To express Aβ(M1–42), pET-Sac-Aβ(M1–42) plasmid is transformed into BL21(DE3)pLysS competent *E. coli*. Expression is induced by isopropyl β-D-1-thiogalactopyranoside (IPTG). The expressed peptide is pelleted with the inclusion bodies, which are washed several times and then solubilized with 8 M urea. The yield of Aβ(M1–42) depends on the extent of cell growth prior to IPTG induction, with an OD_{600} of ca. 0.45 proving optimal for wild-type Aβ(M1–42) production. Growth to substantially higher or lower OD_{600} values gives lower yields of peptide.

Purification of Aβ(M1–42) by preparative HPLC

At this point in the procedure, the expressed peptide is handled like a synthetic peptide, and HPLC is used to purify it. The solution of the inclusion bodies in 8 M urea is filtered to prevent damaging the HPLC column. Initially, a 0.22 µm nylon syringe filter was used, but doing so resulted in substantial loss of peptide. The hydrophobicity and propensity of Aβ to aggregate appear to make Aβ particularly prone to loss in filters. I screened several types of syringe filters to optimize peptide recovery, monitoring the relative concentrations of peptide by UV absorbance at 280 nm (Table 1.2).Syringe filters with large pore sizes (0.45 µm) result in incomplete filtration of the peptide and risk damaging HPLC columns. I found that a 0.22 µm hydrophilic filter, such as hydrophilic polyvinylidene fluoride (PVDF) or polyethersulfone (PES), provided satisfactory peptide recovery. Syringe filters with large pore sizes (0.45 µm) result in incomplete filtration of the peptide and risk damaging HPLC columns.

Table 1.2. The effect of different syringe filters on Aβ(M1–42) recovery.

Filter type	UV absorbance at 280 nm	Peptide recovery
non-filtered Aβ sample	0.7279 ± 0.0052	N/A
Millex-HV PES (0.22 μm)	0.6294 ± 0.0001	86.5%
Fisher hydrophilic PVDF (0.22 μm)	0.6279 ± 0.0009	86.3%
Millex-GV hydrophilic PVDF (0.22 μm)	0.5703 ± 0.0003	78.3%
Fisher nylon (0.22 μm)	0.2907 ± 0.0001	39.9%
Millex-GV MCE (0.22 μm)	0.2273 ± 0.0001	31.2%

A typical HPLC trace of unpurified Aβ(M1–42) shows three major peaks (Figure 1.4A). The first peak is the largest and contains mostly monomer, and the second and the third peaks appear to be oligomers. For preparative HPLC, a reverse-phase silica-based C8 column is used as the stationary phase, and a gradient of water and acetonitrile containing 0.1% trifluoroacetic acid is used as the mobile phase. To enhance resolution and reduce peak tailing, it was necessary to heat the column. Without heating, the resolution and yield of peptide are substantially lower. Aβ(M1–42) peptide monomer generally elutes at around 34% acetonitrile when the C8 column is heated to 80 °C in a water bath (Figure 1.3). HPLC fractions containing pure peptide were combined, and the purity was confirmed by analytical HPLC (Figure 1.4B). Acetonitrile was removed by rotary evaporation, and the aqueous solution of pure peptide was then frozen and lyophilized. These procedures typically yield about 19 mg of Aβ(M1–42) as the trifluoroacetate salt from one liter of bacterial culture.

This purification procedure does not require specialized equipment or costly reagents and is not time-consuming. It avoids the use of specialized and costly columns, such as cation-exchange chromatography columns and size-exclusion chromatography columns. Another advantage of this procedure is that it yields lyophilized powder as the final peptide product. Working with lyophilized peptide is convenient for subsequent studies as it can be dissolved in any appropriate buffer at a desired concentration.

The purity and composition of the Aβ(M1–42) peptide were further assessed through MALDI-MS, and SDS-PAGE with silver staining. MALDI-MS confirms that the observed mass of Aβ(M1–42) matches the expected mass (Figure 1.4C). The silver-stained SDS-PAGE gel shows that at low concentrations, the Aβ(M1–42) peptide exists as a monomer. At higher concentrations, Aβ(M1–42) begins to form oligomers with molecular weights consistent with trimers and tetramers (Figure 1.4D). The fibrillization property of expressed Aβ(M1–42) was assessed by transmission electron microscopy (TEM) after 1 day of incubation in 1X PBS at 37 °C (Figure 1.5)

Figure 1.3. The reverse-phase HPLC column was heated to 80 °C using a commonly available sous vide immersion circulator.

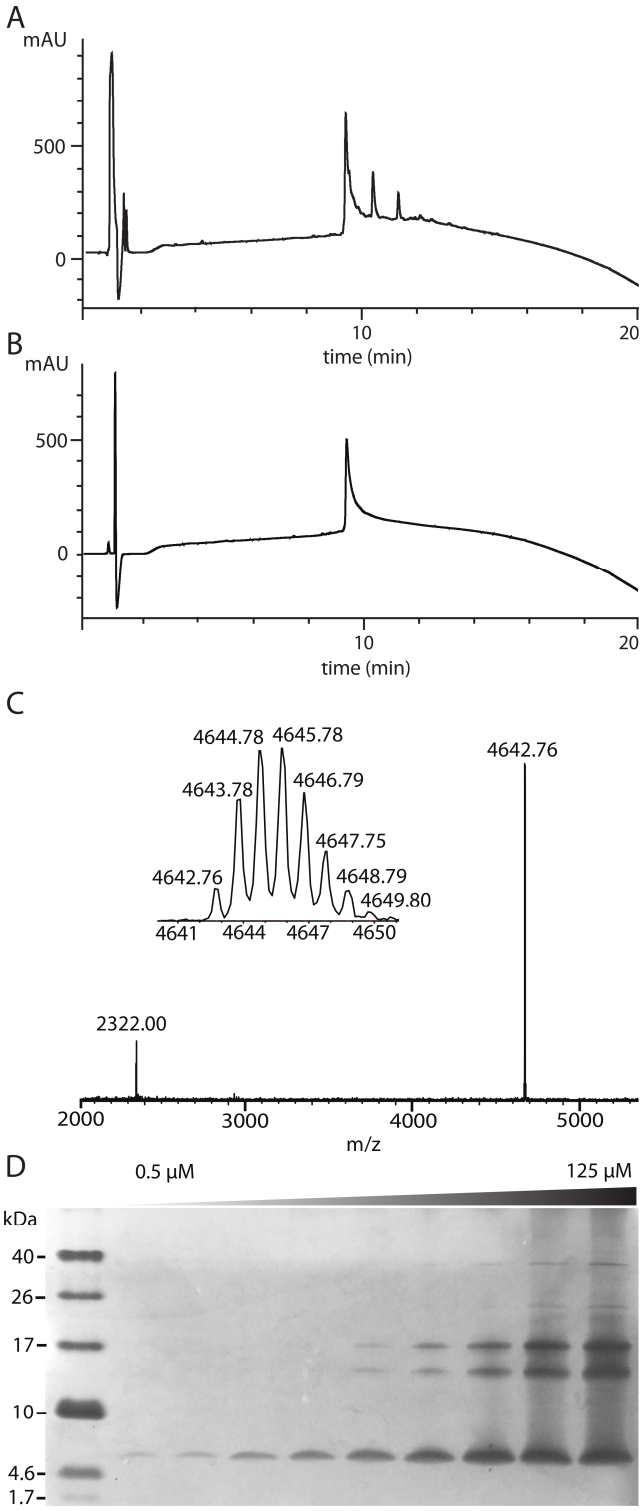

Figure 1.4. Purification and characterization of Aβ(M1–42). (A) Typical analytical HPLC trace of filtered crude Aβ(M1–42) sample. (B) Typical analytical HPLC trace of purified Aβ(M1–42). (C) MALDI mass spectrum of purified Aβ(M1–42). (D) Silver-stained SDS-PAGE gel (16% polyacrylamide) of increasing concentrations of Aβ(M1–42) from 0.5 to 125 µM. A 12-µL aliquot was loaded in each lane of the gel.

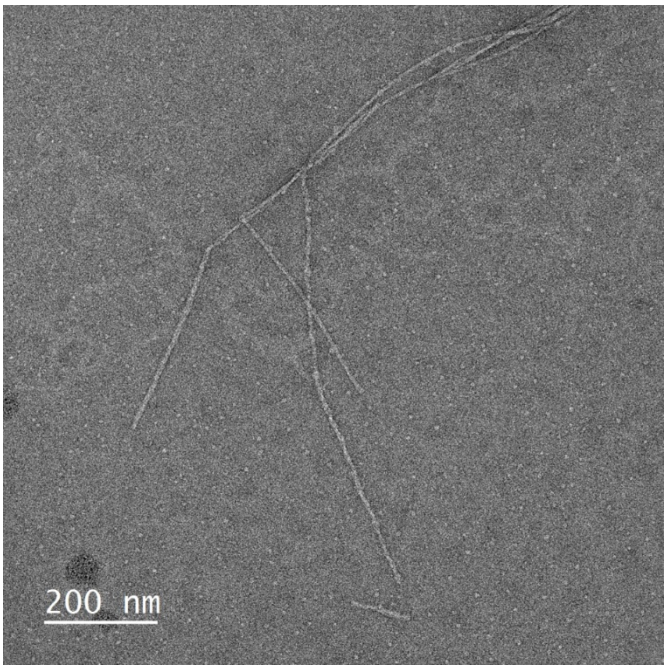

Figure 1.5. A TEM image of Aβ(M1–42) after 1 day of incubation at in 1X PBS.

Sample preparation for biophysical and biological studies

The propensity of Aβ to aggregate necessitates the preparation of monomeric Aβ for subsequent studies.[30] Without any sample preparation, studies are reported to be irreproducible.[31] Fezoui and co-workers reported that treatment of Aβ with NaOH disrupts aggregates and generates Aβ that is monomeric or nearly monomeric.[32] This NaOH-treated Aβ is used in subsequent aggregation studies.[30]

I applied this procedure to each batch of expressed Aβ to generate aliquots for further studies. Thus, the lyophilized powder was dissolved in 2 mM NaOH, and the pH was adjusted, if necessary, by addition of 0.1 M NaOH, to give a pH 10.5 solution. The solution was sonicated for one minute, the concentration was determined by UV absorbance at 280 nm, and the yield of Aβ(M1–42) was calculated. The solution was then aliquoted in 0.0055 or 0.020 micromole portions into small tubes, and these samples were frozen and lyophilized. The lyophilized aliquots are stored in a desiccator at -20 °C.

Expression of ^{15}N-labeled Aβ(M1–42)

^{15}N-labeled Aβ peptides are useful tools for structural studies by NMR and for studying binding profiles of Aβ. For expression of ^{15}N-labeled Aβ(M1–42), *E. coli* are grown to an OD_{600} of ca. 0.45 in LB media, then the LB media is exchanged to M9 minimal media containing $^{15}NH_4Cl$. Expression is induced in the ^{15}N-enriched M9 media for 16 hours with IPTG. Purification and sample preparation of ^{15}N-labeled Aβ(M1–42) is performed identically to unlabeled Aβ(M1–42). The composition of the ^{15}N-labeled Aβ(M1–42) was assessed by MALDI-MS (Figure 1.6A). A ^{1}H-^{15}N HSQC NMR spectrum of 160 μM ^{15}N-labeled Aβ(M1–42) in 50 mM potassium phosphate buffer in 10% D_2O was recorded at 5 °C with a 500 MHz NMR spectrometer equipped with a cryogenic probe (Figure 1.6B). This spectrum matches the NMR spectrum reported by Macao and co-workers.[9]

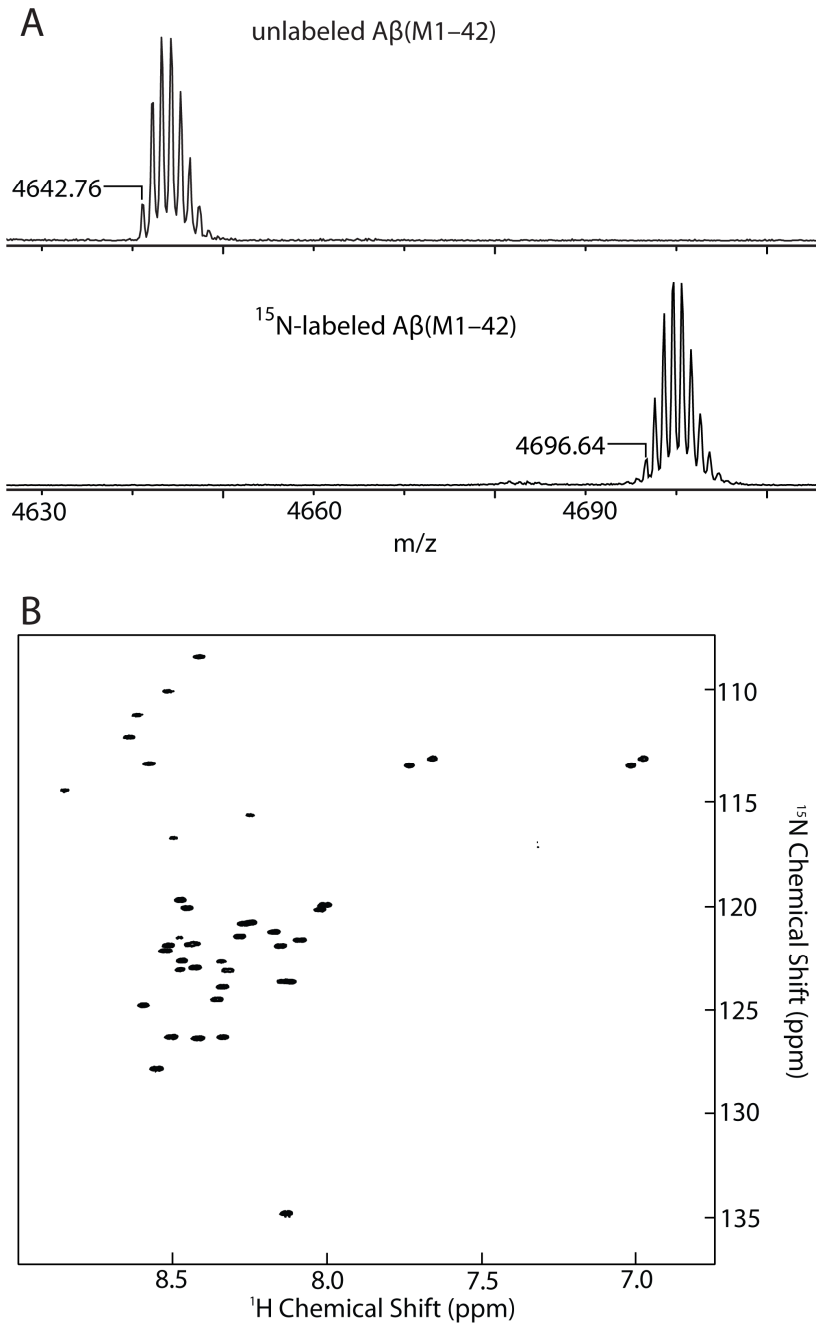

Figure 1.6. (A) MALDI spectra of unlabeled Aβ(M1–42) and ^{15}N-labeled Aβ(M1–42) peptides. (B) ^{1}H-^{15}N HSQC NMR spectrum of 160 µM ^{15}N-labeled Aβ(M1–42) peptide at 5 °C at 500 MHz equipped with a cryogenic probe.

The yield of the ^{15}N-labeled Aβ(M1–42) peptide is comparable to that of the unlabeled Aβ(M1–42) peptide, at around 19 mg per liter of bacterial culture. Access to such amounts of the ^{15}N-labeled peptide at low cost is enabling for performing experiments such as SAR by NMR spectroscopy.[33]

Construction of recombinant plasmids for expression of mutant Aβ(M1–42) peptides

To express Aβ(M1–42) peptides containing familial mutations, I construct recombinant plasmids by ligating enzymatically digested pET-Sac-Aβ(M1–42) and DNA sequences that encode Aβ(M1–42) mutants (Figure 1.7). In this procedure, pET-Sac-Aβ(M1–42) is first digested with *Nde*I and *Sac*I restriction enzymes to remove the wild-type Aβ(M1–42) sequence. Next, the digested pET-Sac vector is treated with shrimp alkaline phosphatase (rSAP) to remove the terminal phosphate groups. The digested vector is isolated by agarose gel electrophoresis purification using a commercially available kit. Synthetic DNA encoding each mutant Aβ(M1–42) is purchased and then digested with *NdeI* and *SacI* to generate the insert. The vector and insert are ligated using T4 ligase and then transformed into TOP 10 competent *E. coli*. *E. coli* transformed with ligated plasmid form colonies on agar containing carbenicillin. Plasmids are isolated from colonies, and the sequences are verified by DNA sequencing. For this chapter, I constructed five plasmids with familial mutations: A21G, E22G, E22K, E22Q, and D23N.

This cloning strategy is inexpensive and is simpler to execute than site-directed mutagenesis. The entire cloning procedure takes two days, and many mutants can be generated concurrently. Another advantage of this strategy is that Aβ(M1–42) plasmids containing multiple point mutations can be prepared as easily as plasmids containing single point mutations.

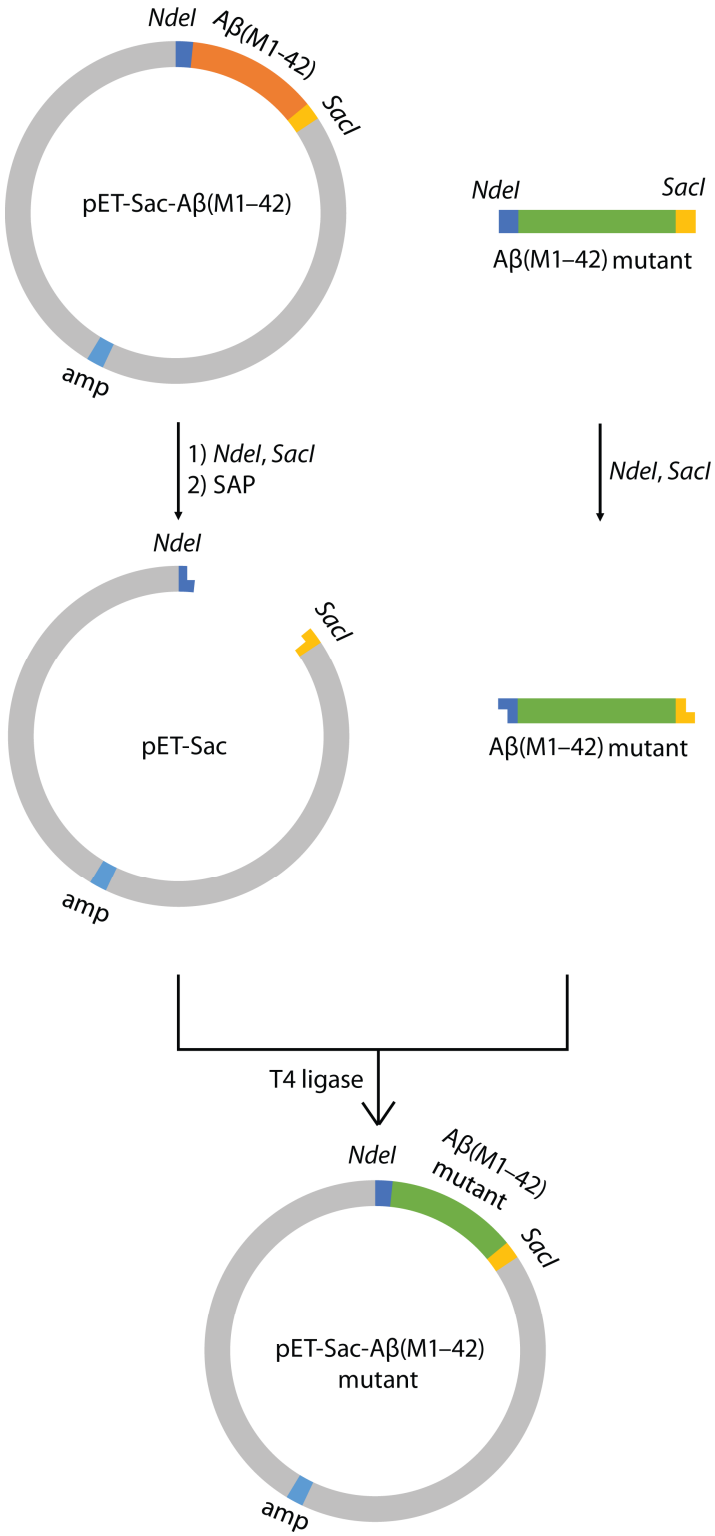

Figure 1.7. Molecular cloning strategy to construct recombinant plasmids of Aβ(M1–42) containing familial mutations.

The purification and preparation of Aβ(M1–42) containing familial mutations is performed identically to that of Aβ(M1–42). The composition of familial mutant Aβ(M1–42) peptides was assessed using MALDI-MS (Figure 1.8). The expression levels and yields of the Aβ(M1–42) familial mutants varied due to different aggregation propensities of the peptides. Analytical HPLC traces of crude samples of the A21G and E22Q mutants showed smaller first peaks and larger second and third peaks, suggesting that more oligomers are formed after dissolving the inclusion bodies. Table 1.3 shows typical yields of the peptides. Our expression and purification procedures proved unsuitable for the E22Q mutant, which showed very little monomer in the HPLC trace.

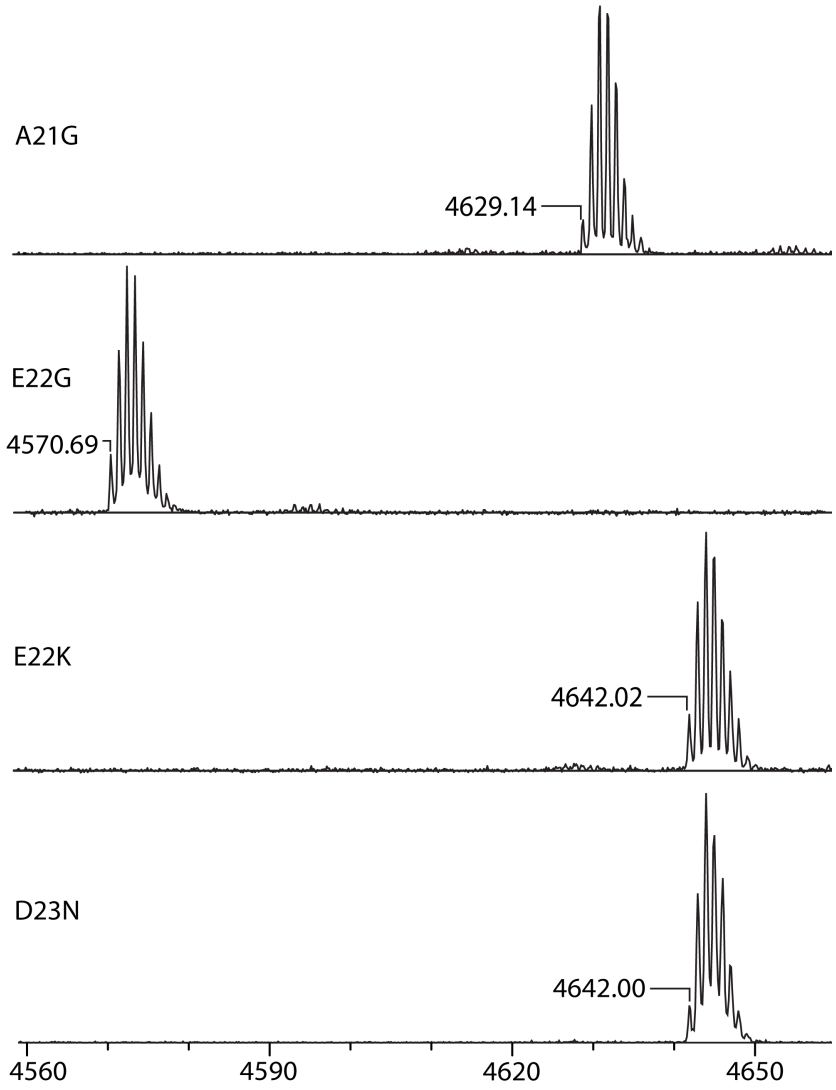

Figure 1.8. MALDI mass spectra of Aβ(M1–42) peptides with A21G, E22G, E22K, and D23N mutations.

Table 1.3. Yields of Aβ(M1–42), ^{15}N-labeled Aβ(M1–42), and familial mutants of Aβ(M1–42).

Aβ (M1–42) peptides	Yield (per liter of bacterial culture)
Aβ (M1–42)	19.4 mg
^{15}N-labeled Aβ (M1–42)	18.6 mg
Aβ (M1–42/D23N)	19.4 mg
Aβ (M1–42/E22K)	17.6 mg
Aβ (M1–42/E22G)	6.2 mg
Aβ (M1–42/A21G)	5.3 mg

Conclusion

The procedures described herein provide an efficient method for expression and purification of Aβ(M1–42), ^{15}N-labeled Aβ(M1–42), and Aβ(M1–42) containing several familial mutations. Our method employs the most convenient features of protein expression and peptide purification to provide ready access to good quantities of the pure peptides. I anticipate that our method will provide new opportunities to pilot experiments that require large amounts of Aβ. I also anticipate that this method can be adjusted for the expression and purification of other amyloidogenic proteins.

References and Notes

1. Benilova, I.; Karran, E.; De Strooper, B., The toxic Aβ oligomer and Alzheimer's disease: an emperor in need of clothes. *Nat. Neurosci.* **2012**, *15*, 349-357.

2. Haass, C.; Selkoe, D. J., Soluble protein oligomers in neurodegeneration: lessons from the Alzheimer's amyloid β-peptide. *Nat Rev Mol Cell Biol.* **2007**, *8*, 101-112.

3. Chiti, F.; Dobson, C. M., Protein misfolding, amyloid formation, and human disease: a summary of progress over the last decade. *Annu. Rev. Biochem.* **2017**, *86*, 27-68.

4. Irie, K.; Masuda, Y.; Morimoto, A.; Ohigashi, H.; Ohashi, R.; Takegoshi, K.; Nagao, M; T, S.; Shirasawa, T. Structure of beta-amyloid fibrils and its relevance to their neurotoxicity: implications for the pathogenesis of Alzheimer's disease. *J. Biosci. Bioeng.*, **2005**, *99*, 437-447.

5. Jarrett, J. T.; Berger, E. P.; Lansbury, P. T., The carboxy terminus of the β-amyloid protein is critical for the seeding of amyloid formation: Implications for the pathogenesis of Alzheimer's disease. *Biochemistry* **2002**, *32*, 4693-4697.

6. Alzheimer, A., Über eine eigenartige Erkrankung der Hirnrinde. *Psychisch. Gerichtl. Med.* **1907**, *64*, 146–148.

7. Glenner, G.G.; Wong, C.W. Alzheimer's disease: initial report of the purification and characterization of a novel cerebrovascular amyloid protein. *Biochem. Biophys. Res. Commun.* **1984**, *120*, 885-890.

8. Masters, C.L.; Simms, G.; Weinman, N.A.; Multhaup, G.; McDonald, B.L.; Beyreuther, K.; Amyloid plaque core protein in Alzheimer disease and Down syndrome. *Proc. Natl. Acad. Sci. U.S.A.* **1985**, *82*, 4245-4249.

9. Hardy, J.; Selkoe, D.J. The amyloid hypothesis of Alzheimer's disease: progress and problems on the road to therapeutics. *Science*, **2002**, *297*, 353-356.

10. Hardy, J.A.; Higgins, G.A. Alzheimer's disease: the amyloid cascade hypothesis. *Science*, **1992,** *256*, 184-185.

11. Finder, V. H.; Vodopivec, I.; Nitsch, R. M.; Glockshuber, R., The recombinant amyloid-β peptide Aβ1-42 aggregates faster and is more neurotoxic than synthetic Aβ1-42. *J. Mol. Biol.* **2010**, *396*, 9-18.

12. Zagorski, M.G.; Yang, J.; Shao, H.; Ma, K.; Zeng, H.; Hong, A. Methodological and chemical factors affecting amyloid beta peptide amyloidogenicity. *Methods Enzymol.* **1999**, *309*, 189-204.

13. Bacsa, B.; Bosze, S.; Kappe, C.O. Direct solid-phase synthesis of the beta-amyloid (1-42) peptide using controlled microwave heating. *J, Org. Chem.* **2010**, *75*, 2103-2106.

14. Collins, J.M.; Porter, K.A.; Singh, S.K.; Vanier, G.S. High-efficiency solid phase peptide synthesis (HE-SPPS) *Org. Lett.* **2014**, *16*, 940-943.

15. Karas, J.A.; Noor, A. Schieber, C.; Connell, T.U.; Separovic, F.; Donnelly, P.S. The efficient synthesis and purification of amyloid-β(1-42) using an oligoethylene glycol-containing photocleavable lysine tag. *Chem. Commun*, **2017**, *53*, 6903-6905.

16. Hortschansky, P.; Schroeckh, V.; Christopeit, T.; Zandomeneghi, G.; Fandrich, M., The aggregation kinetics of Alzheimer's β-amyloid peptide is controlled by stochastic nucleation. *Protein Sci.* **2005**, *14*, 1753-1759.

17. Liao, Y. H.; Chen, Y. R., A novel method for expression and purification of authentic amyloid-β with and without ^{15}N labels. *Protein Expr. Purif.* **2015**, *113*, 63-71.

18. Döbeli, H.; Draeger, N.; Huber, G.; Jakob, P.; Schmidt, D,; Seilheimer, B.; Stüber, D.; Wipf, B.; Zulauf, M. A biotechnological method provides access to aggregation competent monomeric Alzheimer's 1-42 residue amyloid peptide. *Nat. Biotechnol.* **1995**, *13*, 988-993.

19. Sharpe, S.; Yau, W.M.; Tycko, R. Expression and purification of a recombinant peptide from

the Alzheimer's beta-amyloid protein for solid-state NMR. *Protein Expr. Purif.* **2005,** *42*, 200-210.

20. Caine, J.; Volitakis, I.; Cherny, R.; Varghese, J.; Macreadie I. Abeta produced as a fusion to maltose binding protein can be readily purified and stably associates with copper and zinc. *Protein Pept Lett.* **2007**, *14*, 83-86.

21. Walsh, D. M.; Thulin, E.; Minogue, A. M.; Gustavsson, N.; Pang, E.; Teplow, D. B.; Linse, S., A facile method for expression and purification of the Alzheimer's disease-associated amyloid β-peptide. *FEBS J.* **2009**, *276*, 1266-1281.

22. Macao, B.; Hoyer, W.; Sandberg, A.; Brorsson, A. C.; Dobson, C. M.; Hard, T., Recombinant amyloid β-peptide production by coexpression with an affibody ligand. *BMC biotechnol.* **2008**, *8*, 82.

23. Silvers, R.; Colvin, M. T.; Frederick, K. K.; Jacavone, A. C.; Lindquist, S.; Linse, S.; Griffin, R. G., Aggregation and fibril structure of AβM01-42 and Aβ1-42. *Biochemistry* **2017**, *56*, 4850-4859.

24. Sandberg, A.; Luheshi, L. M.; Sollvander, S.; Pereira de Barros, T.; Macao, B.; Knowles, T. P.; Biverstal, H.; Lendel, C.; Ekholm-Petterson, F.; Dubnovitsky, A.; Lannfelt, L.; Dobson, C. M.; Hard, T., Stabilization of neurotoxic Alzheimer amyloid-β oligomers by protein engineering. *Proc. Natl. Acad. Sci. U.S.A.* **2010**, *107*, 15595-600.

25. Cohen, S. I.; Linse, S.; Luheshi, L. M.; Hellstrand, E.; White, D. A.; Rajah, L.; Otzen, D. E.; Vendruscolo, M.; Dobson, C. M.; Knowles, T. P., Proliferation of amyloid-β 42 aggregates occurs through a secondary nucleation mechanism. *Proc. Natl. Acad. Sci. U. S. A.* **2013**, *110*, 9758-9763.

26. Bertini, I.; Gonnelli, L.; Luchinat, C.; Mao, J.; Nesi, A., A new structural model of Aβ40 fibrils. *J. Am. Chem. Soc.* **2011**, *133*, 16013-16022.

27. Colvin, M. T.; Silvers, R.; Ni, Q. Z.; Can, T. V.; Sergeyev, I.; Rosay, M.; Donovan, K. J.;

Michael, B.; Wall, J.; Linse, S.; Griffin, R. G., Atomic resolution structure of monomorphic Aβ42 amyloid fibrils. *J. Am. Chem. Soc.* **2016**, *138*, 9663-9674.

28. Meisl, G.; Yang, X.; Hellstrand, E.; Frohm, B.; Kirkegaard, J. B.; Cohen, S. I.; Dobson, C. M.; Linse, S.; Knowles, T. P., Differences in nucleation behavior underlie the contrasting aggregation kinetics of the Aβ40 and Aβ42 peptides. *Proc. Natl. Acad. Sci. U. S. A.* **2014**, *111*, 9384-9389

29. Munke, A.; Persson, J.; Weiffert, T.; De Genst, E.; Meisl, G.; Arosio, P.; Carnerup, A.; Dobson, C. M.; Vendruscolo, M.; Knowles, T. P. J.; Linse, S., Phage display and kinetic selection of antibodies that specifically inhibit amyloid self-replication. *Proc. Natl. Acad. Sci. U. S. A.* **2017**, *114*, 6444-6449.

30. Teplow, D. B., Preparation of amyloid β-protein for structural and functional studies. *Methods Enzymol.*. **2006**, *413*, 20-33

31. Wood, S. J.; Maleeff, B.; Hart, T.; Wetzel, R., Physical, Morphological and functional differences between pH 5.8 and 7.4 aggregates of the Alzheimer's amyloid peptide Aβ. *J. Mol. Biol.* **1996**, *256*, 870-877.

32. Fezoui, Y.; Hartley, D. M.; Harper, J. D.; Khurana, R.; Walsh, D. M.; Condron, M. M.; Selkoe, D. J.; Lansbury, P. T.; Fink, A. L.; Teplow, D. B., An improved method of preparing the amyloid β-protein for fibrillogenesis and neurotoxicity experiments. *Amyloid* **2009**, *7*, 166-178.

33. Shuker, S. B.; Hajduk, P. J.; Meadows, R. P.; Fesik, S. W., Discovering high-affinity ligands for proteins: SAR by NMR. *Science* **1996**, *274*, 1531-1534.

Supporting Information

Table of Contents

Materials and Methods

General information on materials and methods

All chemicals were used as received unless otherwise noted. Deionized water (18 MΩ) was obtained from a Thermo Scientific Barnstead Genpure Pro water purification system. The pET-Sac-Aβ(M1–42) was a gift from Dominic Walsh (Addgene plasmid # 71875).[1] DNA sequences that encode Aβ(M1–42) familial mutants were purchased in 500 ng quantities from Genewiz. *NdeI* and *SacI* restriction enzymes, CutSmart buffer, and shrimp alkaline phosphatase (rSAP) were purchased from New England Biolabs (NEB). TOP10 Ca^{2+}-competent *E. coli* and BL21 DE3 PLysS Star Ca^{2+}-competent *E. coli*, T4 ligase, and ethidium bromide were purchased from Thermo Fisher Scientific. Zymo ZR plasmid miniprep kit was purchased from Zymo Research. Zymoclean Gel DNA Recovery Kit was purchased from Zymo Research. Carbenicillin and chloramphenicol were purchased from RPI Research Products. The carbenicillin was added to culture media as a 1000X stock solution (50 mg/mL) in water. The chloramphenicol was added to culture media as a 1000X stock solution (34 mg/mL) in EtOH. The $^{15}NH_4Cl$ was purchased from Cambridge Isotope Laboratories.

The concentration of the DNA sequences was measured using a Thermo Scientific NanoDrop spectrophotometer. *E. coli* were incubated in a Thermo Scientific MaxQ Shaker 6000. *E. coli* were lysed using a QSonica Q500 ultrasonic homogenizer. Analytical reverse-phase HPLC was performed on an Agilent 1200 instrument equipped with a Phenomonex Aeris PEPTIDE 2.6u XB-C18 column with a Phenomonex SecurityGuard ULTRA cartridges guard column for C18 column. Preparative reverse-phase HPLC was performed on a Rainin Dynamax instrument SD-200 equipped with an Agilent ZORBAX 300SB-C8 semi-preparative column (9.4 x 250 mm) with

a ZORBAX 300SB-C3 preparative guard column (9.4 x 15 mm). During purifications, the C8 column and the guard column were heated to 80 °C in a Sterlite plastic bin equipped with a Kitchen Gizmo Sous Vide immersion circulator. [Any water heater large enough to submerge a HPLC column is sufficient.] HPLC grade acetonitrile and deionized water (18 MΩ), each containing 0.1% trifluoroacetic acid (TFA), were used for analytical and preparative reverse-phase HPLC. MALDI-TOF mass spectrometry was performed using an AB SCIEX TOF/TOF 5800 System. ^{1}H-^{15}N HSQC NMR was performed using a Bruker DRX500 500 MHz spectrometer equipped with a cryogenic probe.

Isolation of pET-Sac-Aβ(M1–42) plasmid

I received the pET-Sac-Aβ(M1–42) plasmid from Addgene as a bacterial stab and immediately streaked the bacteria onto a LB agar-plate containing carbenicillin (50 mg/L). Colonies grew in < 24h. Single colonies were picked and used to inoculate 5 mL of LB broth containing carbenicillin (50 mg/L). The cultures were shaken at 225 rpm overnight at 37˚C. To isolate the pET-Sac-Aβ(M1–42) plasmids, minipreps were performed using a Zymo ZR plasmid miniprep kit. The concentration of the plasmids was measured using a Thermo Scientific Nanodrop instrument.

Bacterial expression of Aβ(M1–42)

Transformation and expression of Aβ(M1–42)

All liquid cultures were performed in culture media (LB broth containing 50 mg/L carbenicillin and 34 mg/L chloramphenicol). For Aβ(M1–42) wild-type and mutant peptides: Wild-type or mutant plasmids were transformed into BL21 DE3 PLysS Star Ca^{2+}-competent *E. coli* through heat shock method. The cell cultures were spread on LB agar plates containing carbenicillin (50 mg/L) and chloramphenicol (34 mg/L). Single colonies were picked to inoculate 5 mL of culture media for overnight culture. (A glycerol stock of BL21 DE3 PLysS Star Ca^{2+}-competent *E. coli* bearing the plasmids was made, and the future expressions were started by inoculating culture media with an aliquot of the glycerol stock). The next day, all 5 mL of the overnight culture were used to inoculate 1 L of culture media. After inoculation, the culture was shaken at 225 rpm at 37 ˚C until the cell density reached an OD_{600} of approximately 0.45 (after around 3 h 45 min). Protein expression was then induced by the addition of isopropyl β-D-1-thiogalactopyranoside (IPTG) to a final concentration of 0.1 mM, and the cells were shaken at 225 rpm at 37 °C for 4 h with IPTG. The cells were then harvested by centrifugation at 4000 rpm using a JA-10 rotor (2800 x g) at 4 ˚C for 25 min, and the cell pellets were then stored at -80°C.

For ^{15}N-labeled Aβ(M1–42): Wild-type plasmids were transformed into BL21 DE3 PLysS Star Ca^{2+}-competent *E. coli* through heat shock method. The cell cultures were spread on LB agar plates containing carbenicillin (50 mg/L) and chloramphenicol (34 mg/L). Single colonies were picked to inoculate 5 mL of culture media for overnight culture. [A glycerol stock of BL21 DE3 PLysS Star Ca^{2+}-competent *E. coli* bearing the plasmids was made, and the subsequent expressions were started by inoculating culture media with an aliquot of the glycerol stock.] The next day, all 5 mL of the overnight culture were used to inoculate 1 L of culture media. After inoculation, the

culture was shaken at 225 rpm at 37 ˚C until the cell density reached an OD_{600} of approximately 0.45–0.50 (after around 3 h 50 min). The cells were harvested by centrifugation in sterile 500-mL thick-walled centrifuge bottles at 4000 rpm using a JA-10 rotor (2800 x g) at 4 ˚C for 25 min. The cell pellets were then resuspended in sterile M9 minimal media supplemented with $^{15}NH_4Cl$, carbenicillin (50 mg/L), and chloramphenicol (34 mg/L) (Table 1.S1), and incubated for 1 h at 225 rpm at 37 °C. Protein expression was then induced by the addition of isopropyl β-D-1-thiogalactopyranoside (IPTG) to a final concentration of 0.1 mM, and the cells were shaken at 225 rpm at 25 °C for ~20 h with IPTG. The cells were then harvested by centrifugation 4000 rpm using a JA-10 rotor (2800 x g) at 4 ˚C for 25 min, and the cell pellets were stored at -80°C.

Table 1.S1. M9 minimal media.

Reagents	Amount
5X M9 salts solution (34.0 g of Na_2HPO_4, 15.0 g of KH_2PO_4, and 2.5 g of NaCl in 1.0 L of H_2O)	200.0 mL
1.0 M $MgSO_4 \cdot 7H_2O$ solution	2.0 mL
1.0 M $CaCl_2$ solution	0.1 mL
$^{15}NH_4Cl$	1.0 g
D-Glucose	10.0 g
Carbenicillin (50 mg/mL)	1.0 mL
Chloramphenicol (34 mg/mL in EtOH)	1.0 mL
H_2O	Fill up to 1.0 L

Cell lysis and inclusion body preparation

To lyse the cells, the cell pellet was resuspended in 20 mL of buffer A (10 mM Tris/HCl, 1 mM EDTA, pH 8.0) and sonicated for 2 min on ice (50% duty cycle) until the lysate appeared homogenous. The lysate was then centrifuged for 25 min at 16000 rpm using a JA-18 rotor (38000 x g) at 4˚C. The supernatant was removed, and the pellet was resuspended in buffer A, sonicated and centrifuged as described above. The sonication and centrifugation steps were repeated three times. After the fourth supernatant was removed, the remaining pellet was resuspended in 15 mL of freshly prepared buffer B (8 M urea, 10 mM Tris/HCl, 1 mM EDTA, pH 8.0), and was sonicated as described above, until the solution became clear.

Peptide purification

The solution (15 mL) was then diluted with 10 mL of buffer A and filtered through a Fisher Brand 0.22 µm non-sterile hydrophilic PVDF syringe filter (Catalog No. 09-719-00). Analytical reverse-phase HPLC was performed to evaluate if expression of Aβ(M1–42) was successful. A 40-µL sample of the above solution was injected onto an Agilent 1200 instrument equipped with a Phenomonex Aeris PEPTIDE 2.6u XB-C18 column with a Phenomonex SecurityGuard ULTRA cartridges guard column for C18 column. HPLC grade acetonitrile (ACN) and 18 MΩ deionized water, each containing 0.1% trifluoroacetic acid, were used as the mobile phase. The sample was eluted at 1.0 mL/min with a 5–100% acetonitrile gradient over 20 min, at 35 °C. Figure 1.S1 shows an example HPLC trace of the crude Aβ(M1–42) solution.

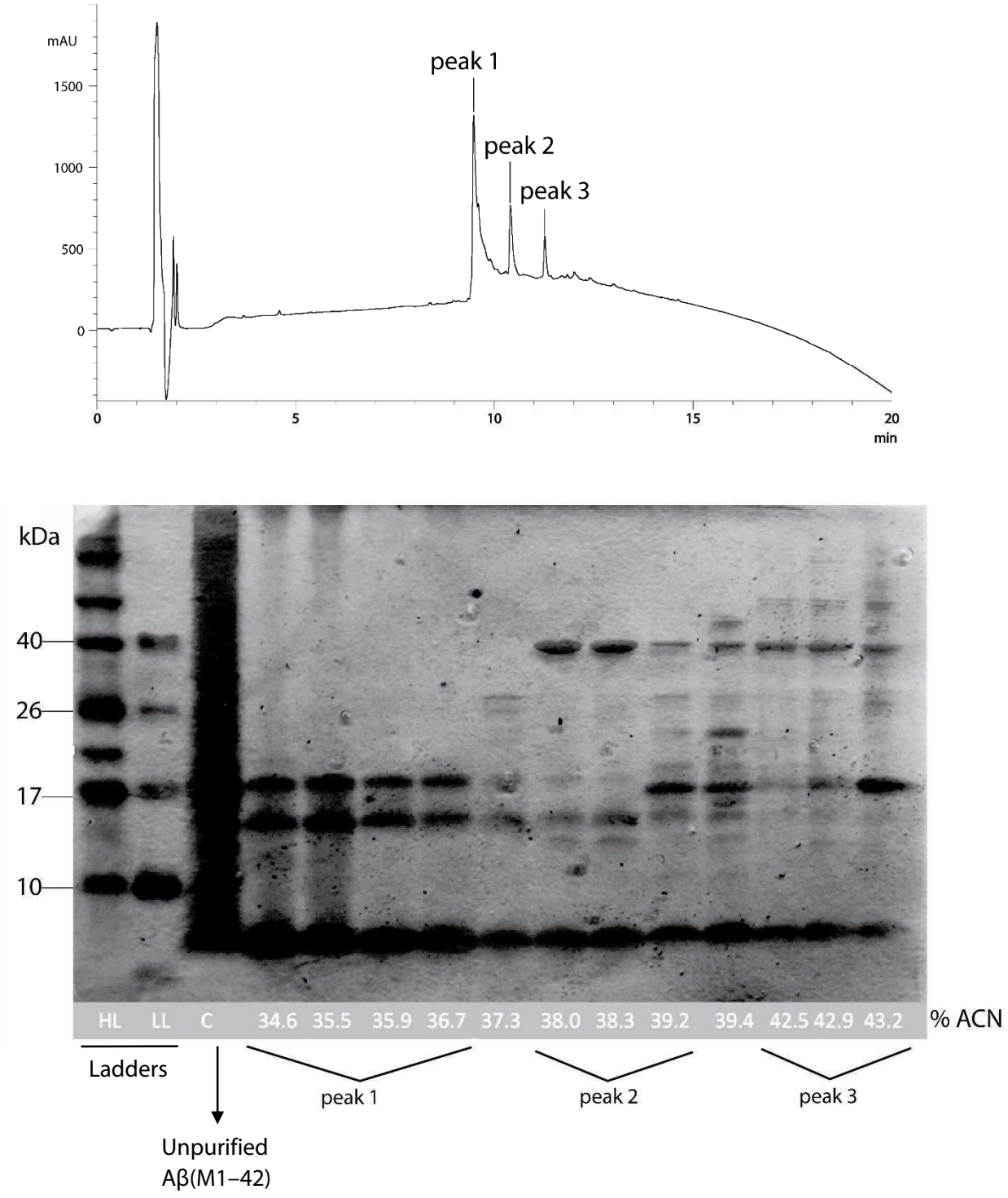

Figure 1.S1. HPLC trace of filtered urea-solubilized Aβ(M1–42) and silver-stained SDS-PAGE gel of HPLC fractions. HL: Precision Plus Protein Dual Color Standards from Bio-Rad; LL: Spectra Multicolor Low Range Protein Ladder from ThermoFisher.

Aβ(M1–42) peptides were then purified by preparative reverse-phase HPLC equipped with an Agilent ZORBAX 300SB-C8 semi-preparative column (9.4 x 250 mm) with a ZORBAX 300SB-C3 preparative guard column (9.4 x 15 mm). The C8 column and the guard column were heated to 80 °C in a water bath. HPLC grade acetonitrile (ACN) and 18 MΩ deionized water, each containing 0.1% trifluoroacetic acid, were used as the mobile phase at a flow-rate of 5 mL/min. The peptide solution was split into three ~8 mL aliquots, and purified in three separate runs. The peptide was loaded onto the column by flowing 20% ACN for 10 min and then eluted with a gradient of 20–40% ACN over 20 min. Fractions containing the monomer generally eluted from 34% to 38% ACN. After the peptide was collected, the column was washed by injecting 5 mL of filtered buffer B (8 M urea, 10 mM Tris/HCl, 1 mM EDTA, pH 8.0) while flushing at 95% ACN for 15 minutes. This cleaning procedure ensures elution of all peptide that is retained in the column and avoids problems of cross-contamination between runs.

The purity of each fraction was assessed using analytical reverse-phase HPLC. A 40-µL sample was injected onto the analytical HPLC. The sample was eluted at 1.0 mL/min with a 5–100% acetonitrile gradient over 20 min, at 35 °C. Pure fractions were combined and the purity of the combined fractions were checked using analytical HPLC. The combined fractions were concentrated by rotary evaporation to remove ACN, and then frozen with dry ice, liquid nitrogen, or a -80 °C freezer. [It is recommended to combine and freeze the purified fractions within 5 hours after purification to avoid oxidation of methionine.] The frozen sample was then lyophilized to give a fine white powder.

NaOH treatment and peptide concentration determination

The lyophilized peptide was then dissolved in 2 mM NaOH to achieve a concentration of ~0.5 mg/mL. The pH was adjusted (if necessary) by addition of 0.1 M NaOH to give a solution of pH ~10.5. The sample was sonicated in a water ultrasonic bath at room temperature for 1 min or until the solution became clear. When preparing samples, pH should not be near pH 5.5 where the peptide is prone to aggregate, and solution become opaque, giving inaccurate UV readings. pH should not be over 11, where tyrosine is mostly deprotonated, giving slightly different UV spectra (Figure 1.S2).

The concentration of Aβ(M1–42) was determined by absorbance at 280 nm using the extinction coefficient (ε) for tyrosine of 1490 $M^{-1}cm^{-1}$ (c = A/1490). The Aβ(M1–42) solution was then aliquoted into 0.0055 µmol or 0.020 µmol aliquots in 0.5 mL microcentrifuge tubes. The ^{15}N-labeled Aβ(M1–42) solution was aliquoted into appropriate volume that contains 0.5 mg in 1.6 mL Eppendorf tubes. The aliquots were lyophilized and then stored in a desiccator at -20 °C for future use.

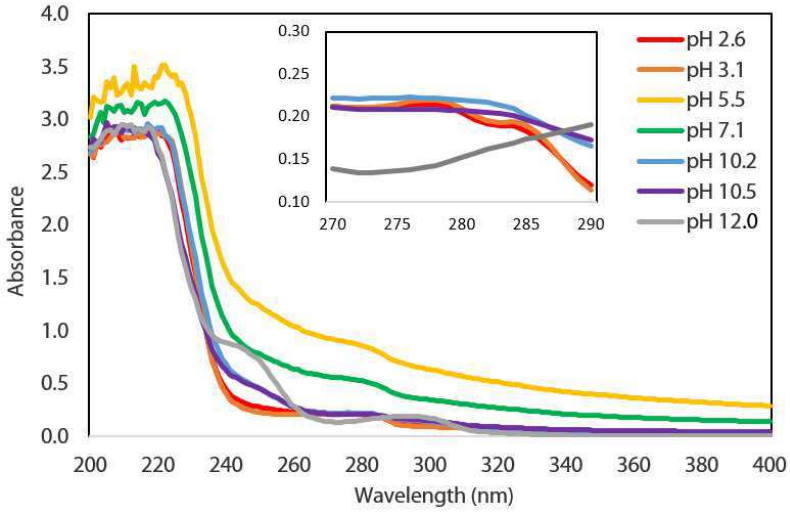

Figure 1.S2. UV absorption spectra of Aβ(M1–42) at different pH.

Table 1.S2 shows a representative schedule for expression of Aβ(M1–42). Table 1.S3 shows a representative schedule for expression of ^{15}N-labeled Aβ(M1–42).

Table 1.S2. A representative schedule for expression of Aβ(M1–42).

Day	Time	Steps
Monday	Evening	Starter culture
Tuesday	Morning	Daytime culture
	Afternoon	IPTG Induced expression
	Evening	Cell pelleting
Wednesday	Morning	Sonication; urea extraction
	Afternoon	Purification by prep-HPLC Collecting pure fractions, freeze, and lyophilize
Thursday	Afternoon	NaOH treatment, freeze, and lyophilize

Table 1.S3. A representative schedule for expression of ^{15}N-labeled Aβ(M1–42).

Day	Time	Steps
Monday	Evening	Starter culture
Tuesday	Morning	Daytime culture
	Afternoon	Media exchange to ^{15}N-containing M9 media
	Evening	IPTG induction and incubation in 25 ˚C
Wednesday	Morning	Cell pelleting
	Morning	Sonication; urea extraction
	Afternoon	Purification by prep-HPLC; collecting pure fractions, freeze, and lyophilize

Mass spectrometry

MALDI mass spectrometry was performed using an AB SCIEX TOF/TOF 5800 System. 0.5 μL of 2,5-dihydroxybenzoic acid (DHB) was dispensed onto a MALDI sample support, followed by the addition of 0.5 μL peptide sample. The mixture was allowed to air-dry. All analyses were performed in positive reflector mode, collecting data with a molecular weight range of 2000–8000 Da.

SDS-PAGE

SDS-PAGE and silver staining were adapted from and in some cases taken verbatim from our previously reported procedure.[2] For the sample preparation, a 0.0055 μmol aliquot of Aβ peptide was dissolved in 11 μL of 20 mM HEPES buffer (pH 7.4) to give a 500 μM peptide stock solution, and serial diluted with 11 uL of 20 mM HEPES buffer (pH 7.4) to create 11 μL of peptide stock solutions with concentrations of 250 μM to 1.0 μM. The peptide stock solutions were then immediately diluted with 11 μL of 2X SDS-PAGE loading buffer (100 mM Tris buffer at pH 6.8, 20% (v/v) glycerol, and 4% w/v SDS) to give 11 μL of peptide working solutions with concentrations from 125 μM to 0.5 μM. A 12.0-μL aliquot of each working solution was run on a 16% polyacrylamide gel with a 4% stacking polyacrylamide gel. The gels were run at a constant 90 volts at room temperature.

Staining with silver nitrate was used to visualize peptides in the SDS-PAGE gel. Briefly, the gel was first rocked in fixing solution (50% (v/v) methanol and 5% (v/v) acetic acid in deionized water) for 20 min. Next, the fixing solution was discarded and the gel was rocked in 50% (v/v) aqueous methanol for 10 min. Next, the 50% methanol was discarded and the gel was rocked

in deionized water for 10 min. Next, the water was discarded and the gel was rocked in 0.02% (w/v) sodium thiosulfate in deionized water for 1 min. The sodium thiosulfate was discarded and the gel was rinsed twice with deionized water for 1 min (2X). After the last rinse, the gel was submerged in chilled 0.1% (w/v) silver nitrate in deionized water and rocked at 4 °C for 20 min. Next, the silver nitrate solution was discarded and the gel was rinsed with deionized water for 1 min (2X). To develop the gel, the gel was incubated in developing solution (2% (w/v) sodium carbonate, 0.04% (w/v) formaldehyde until the desired intensity of staining was reached (~1–3 min). When the desired intensity of staining was reached, the development was stopped by discarding the developing solution and submerging the gel in 5% aqueous acetic acid.

NMR spectroscopy

Approximately 0.5 mg of NaOH-treated, lyophilized ^{15}N-labeled Aβ(M1–42) was dissolved in 0.6 mL of 50 mM potassium phosphate buffer containing the internal standard, 4,4-dimethyl-4-silapentane-1-ammonium trifluoroacetate (DSA) at a concentration of 30 μM and 10% D_2O (pH 7.4) to give a 160 μM peptide solution. The exact concentration of the peptide solution was determined by absorbance at 280 nm using the extinction coefficient for tyrosine of 1490 $M^{-1}cm^{-1}$. The NMR sample was prepared immediately prior to the NMR experiment. NMR was performed using a Bruker DRX500 500 MHz spectrometer equipped with a cryogenic probe. The temperature was maintained at 5 °C to reduce peptide aggregation. NMR data were processed using XWinNMR. ^{1}H-^{15}N heteronuclear single quantum correlation (HSQC) spectra were acquired using GARP decoupling. The number of points acquired in the direct dimension (^{1}H) was 2048, and the number of increments in the indirect dimension (^{15}N) was 256 experiments.

Molecular cloning

DNA sequences for Aβ(M1–42) familial mutant

DNA sequences for Aβ(M1–42) familial mutant peptides were ordered from Genewiz. Figure S3 shows the design of the DNA sequences for Aβ(M1–42) mutants.

3' and 5' overhangs *NdeI* restriction site/start codon stop codons

SacI restriction site familial mutation

>Aβ(M1–42)

GATATA CAT ATG GAC GCT GAA TTC CGT CAC GAC TCT GGT TAC GAA GTT CAC CAC CAG AAG CTG GTG TTC TTC GCT GAA GAC GTG GGT TCT AAC AAG GGT GCT ATC ATC GGT CTG ATG GTT GGT GGC GTT GTG ATC GCT TAA TAG GAGCTC GATCCG

>Aβ(M1–42/A21G)

GATATA CAT ATG GAC GCT GAA TTC CGT CAC GAC TCT GGT TAC GAA GTT CAC CAC CAG AAG CTG GTG TTC TTC GGT GAA GAC GTG GGT TCT AAC AAG GGT GCT ATC ATC GGT CTG ATG GTT GGT GGC GTT GTG ATC GCT TAA TAG GAGCTC GATCCG

>Aβ(M1–42/E22G)

GATATA CAT ATG GAC GCT GAA TTC CGT CAC GAC TCT GGT TAC GAA GTT CAC CAC CAG AAG CTG GTG TTC TTC GCT GGT GAC GTG GGT TCT AAC AAG GGT GCT ATC ATC GGT CTG ATG GTT GGT GGC GTT GTG ATC GCT TAA TAG GAGCTC GATCCG

>Aβ(M1–42/E22K)

GATATA CAT ATG GAC GCT GAA TTC CGT CAC GAC TCT GGT TAC GAA GTT CAC CAC CAG AAG CTG GTG TTC TTC GCT AAG GAC GTG GGT TCT AAC AAG GGT GCT ATC ATC GGT CTG ATG GTT GGT GGC GTT GTG ATC GCT TAA TAG GAGCTC GATCCG

>Aβ(M1–42/E22Q)

GATATA CAT ATG GAC GCT GAA TTC CGT CAC GAC TCT GGT TAC GAA GTT CAC CAC CAG AAG CTG GTG TTC TTC GCT CAG GAC GTG GGT TCT AAC AAG GGT GCT ATC ATC GGT CTG ATG GTT GGT GGC GTT GTG ATC GCT TAA TAG GAGCTC GATCCG

>Aβ(M1–42/D23N)

GATATA CAT ATG GAC GCT GAA TTC CGT CAC GAC TCT GGT TAC GAA GTT CAC CAC CAG AAG CTG GTG TTC TTC GCT GAA AAC GTG GGT TCT AAC AAG GGT GCT ATC ATC GGT CTG ATG GTT GGT GGC GTT GTG ATC GCT TAA TAG GAGCTC GATCCG

Figure 1.S3. Design of the DNA sequences for Aβ(M1–42) mutants.

Restriction enzyme digestion of pET-Sac-Aβ(M1–42) and Aβ(M1–42) familial mutant DNA sequences

The pET-Sac-Aβ(M1–42) plasmid was digested using *SacI* and *NdeI* restriction enzymes. Table 3.S4 details the restriction reaction conditions. Reagents were added in the order they are listed.

Table 1.S4. Double-digestion of the pET- Sac Aβ(M1–42) plasmid.

Reagents	Amount
pET-Sac Aβ(M1–42)	20 µL of 50 ng/uL plasmid solution (1.0 µg in total)
10X CutSmart buffer	5.0 µL
H_2O	23.0 µL
NdeI restriction enzyme	1.0 µL (1 U)
SacI-HF restriction enzyme	1.0 µL (1 U)
Total	50.0 µL
Time	1.0 h
Temperature	37.0 °C

Next, to prevent backbone self-ligation, the digested plasmid was treated with shrimp alkaline phosphatase (rSAP). Table 3.S5 details the rSAP reaction conditions.

Table 1.S5. SAP treatment of the vectors.

Reagents	Amount
Double-digestion mixture	50.0 µL
rSAP	1.0 µL (1U)
Total	51.0 µL
Time	0.5 h
Temperature	37.0 °C
Heat inactivation	65.0 °C for 20 min

After the rSAP reaction and heat inactivation were complete, the reaction mixture was mixed with DNA loading buffer and loaded onto a 1% agarose gel containing ethidium bromide (5 µL per 100 mL gel). The agarose gel was run at 100 V for ~30 min. A UV box was used to visualize the digested pET-Sac vector (~4500 bp), which was excised from the gel using a razor blade. The digested pET-Sac vector was purified from the agarose gel using a Zymoclean Gel DNA Recovery Kit. The concentration of the vector after purification was measured using a Thermo Scientific Nanodrop instrument. The purified digested pET-Sac linear vector was used in the subsequent ligation step.

The Aβ(M1–42) mutant DNA sequences were digested using *SacI* and *NdeI* restriction enzymes. Table 3.S6 details the restriction reaction conditions. Reagents were added in the order they are listed.

Table 1.S6. Double-digestion of the inserts.

Reagents	Amount
DNA sequence encoding mutation	20 µL of 5 ng/µL DNA solution (100.0 ng in total)
10X CutSmart buffer	2.5 µL
H_2O	1.5 µL
NdeI restriction enzyme	0.5 µL (0.5 U)
SacI-HF restriction enzyme	0.5 µL (0.5 U)
Total	25.0 µL
Time	1.0 h
Temperature	37.0 °C
Heat inactivation	65.0 °C for 20 min

T4 ligation of the Aβ(M1–42) mutant DNA sequences and the linear digested pET-Sac vector

The inserts and the vectors were ligated together using T4 ligase. Table 3.S7 details the T4 ligation reaction conditions. Reagents were added in the order they are listed.

Table 1.S7. T4 ligation of the inserts and the vectors.

Reagents	Amount	
	Insert:Vector = 0:1 (molar ratio) (negative control)	Insert:Vector = 5:1 (molar ratio)
Vector	6.2 µL of 9.7 ng/µL DNA solution (60.0 ng in total)	6.2 µL of 9.7 ng/µL DNA solution (60.0 ng in total)
Insert	---	2.5 µL of 4.0 ng/µL DNA solution (10.0 ng in total)
10X T4 DNA ligase reaction buffer	2.0 µL	2.0 µL
T4 DNA ligase	1.0 µL	1.0 µL
H_2O	10.8 µL	8.3 µL
Total	20.0 µL	20.0 µL
Ligation time	10 min	
Temp	22.0 °C (room temperature)	
Heat inactivation	65.0 °C for 10 min	

2 µL of the ligation reaction mixture was then transformed into TOP10 Ca^{2+}-competent *E. coli* using the heat shock method. The cell cultures were spread on LB agar plates containing carbenicillin (50 mg/L). Single colonies were picked to inoculate 5 mL of overnight cultures in LB media with carbenicillin (50 mg/L). The plasmids were extracted from TOP10 cells using Zymo ZR plasmid miniprep kit. The concentration of the plasmids was measured through Thermo Scientific NanoDrop spectrophotometer. The DNA sequences of the Aβ(M1–42) mutants were verified by DNA sequencing.

Characterization Data

Analytical HPLC trace of Aβ(M1–42). % Purity: >99%

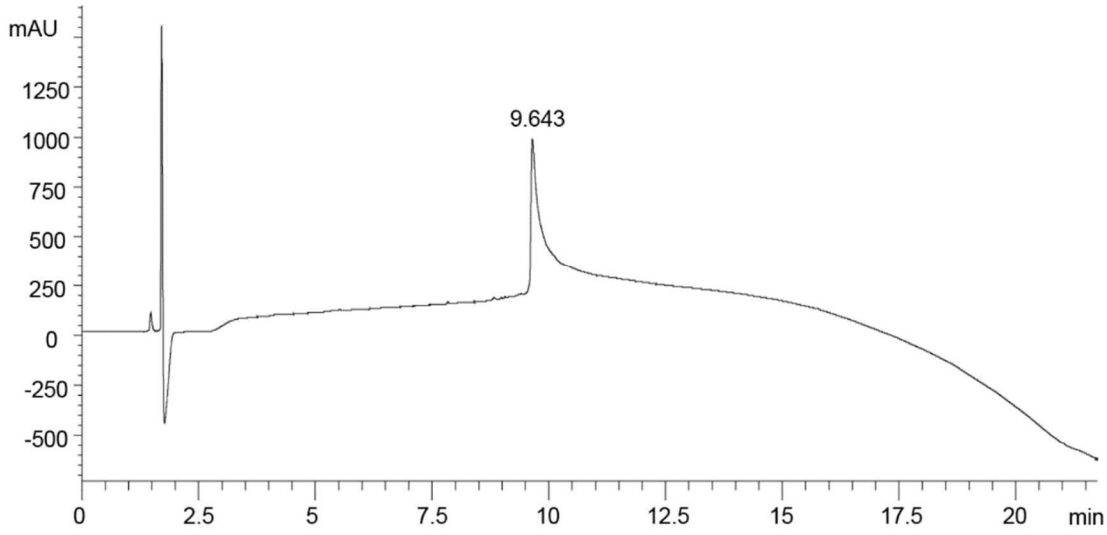

MALDI-MS trace of of Aβ(M1–42).

Positive reflector mode; Matrix: 2,5-dihydroxybenzoic acid.

Exact mass calculated for M^+: 4642.3; Exact mass calculated for $[M+H]^+$: 4643.3; Exact mass calculated for $[M+2H]^{2+}$: 2322.2. Observed $[M+H]^+$: 4642.8; Observed $[M+2H]^{2+}$: 2322.0.

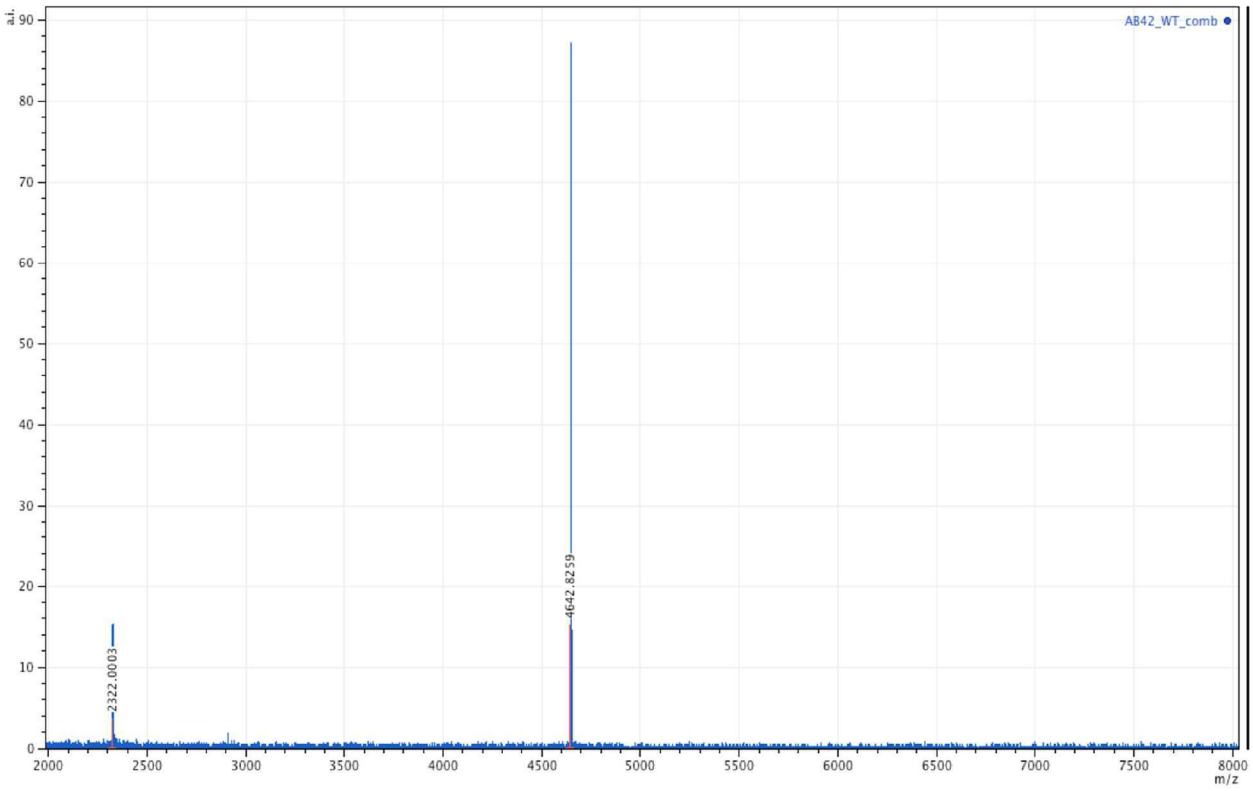

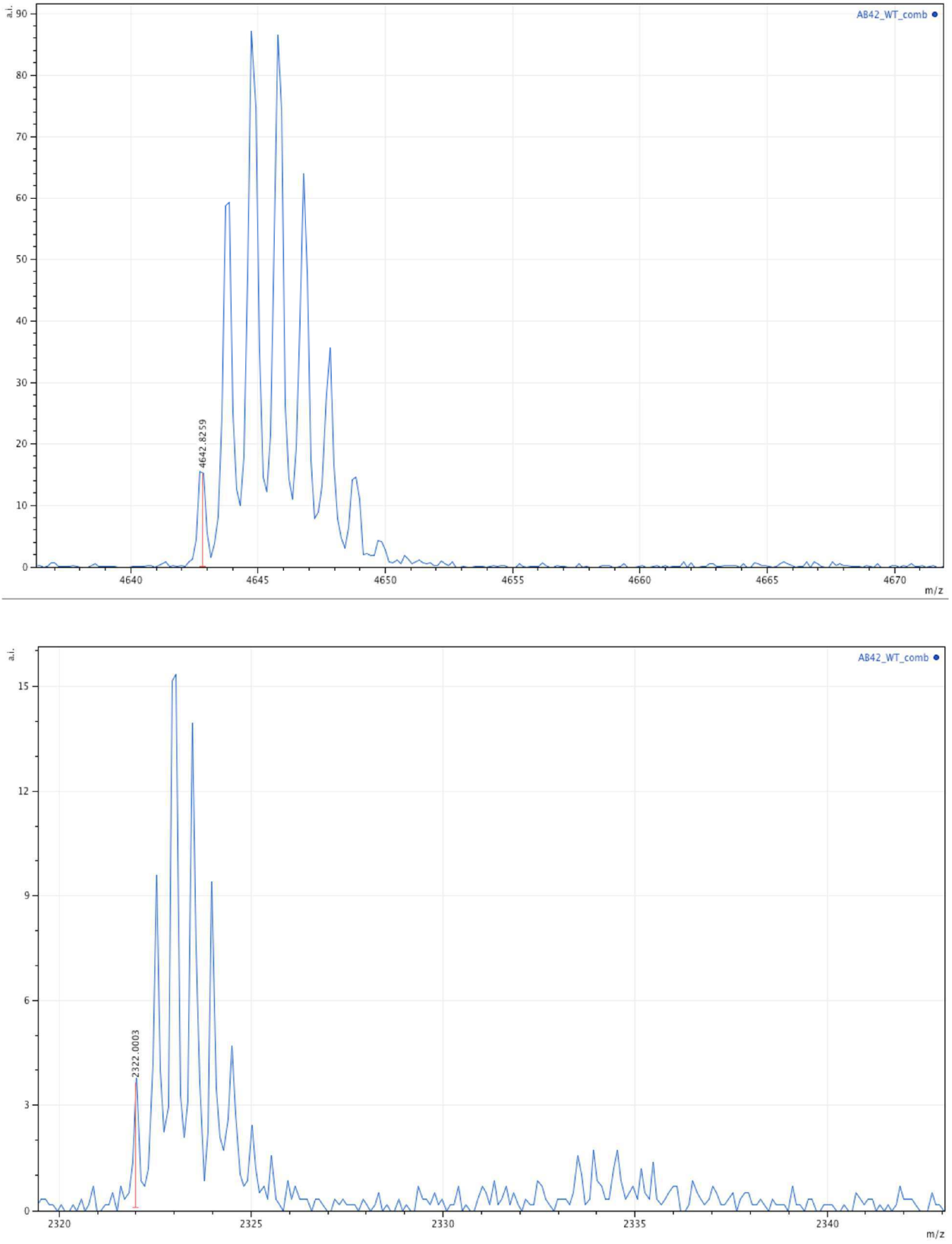

Figure 1.S4. Analytical HPLC and MALDI-MS traces of Aβ(M1–42).

Analytical HPLC trace of ^{15}N-labeled Aβ(M1–42). % Purity: >99%

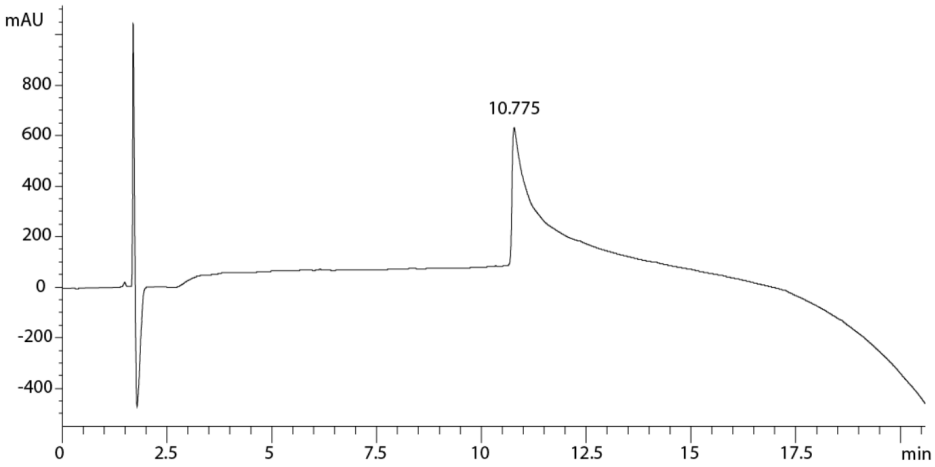

MALDI-MS trace of ^{15}N-labeled Aβ(M1–42).

Positive reflector mode. Matrix: 2,5-dihydroxybenzoic acid.

Exact mass calculated for M^+: 4698.3; Exact mass calculated for $[M+H]^+$: 4699.3; Exact mass calculated for $[M+2H]^{2+}$: 2350.2. Observed $[M+H]^+$: 4697.6; Observed $[M+2H]^{2+}$: 2349.4.

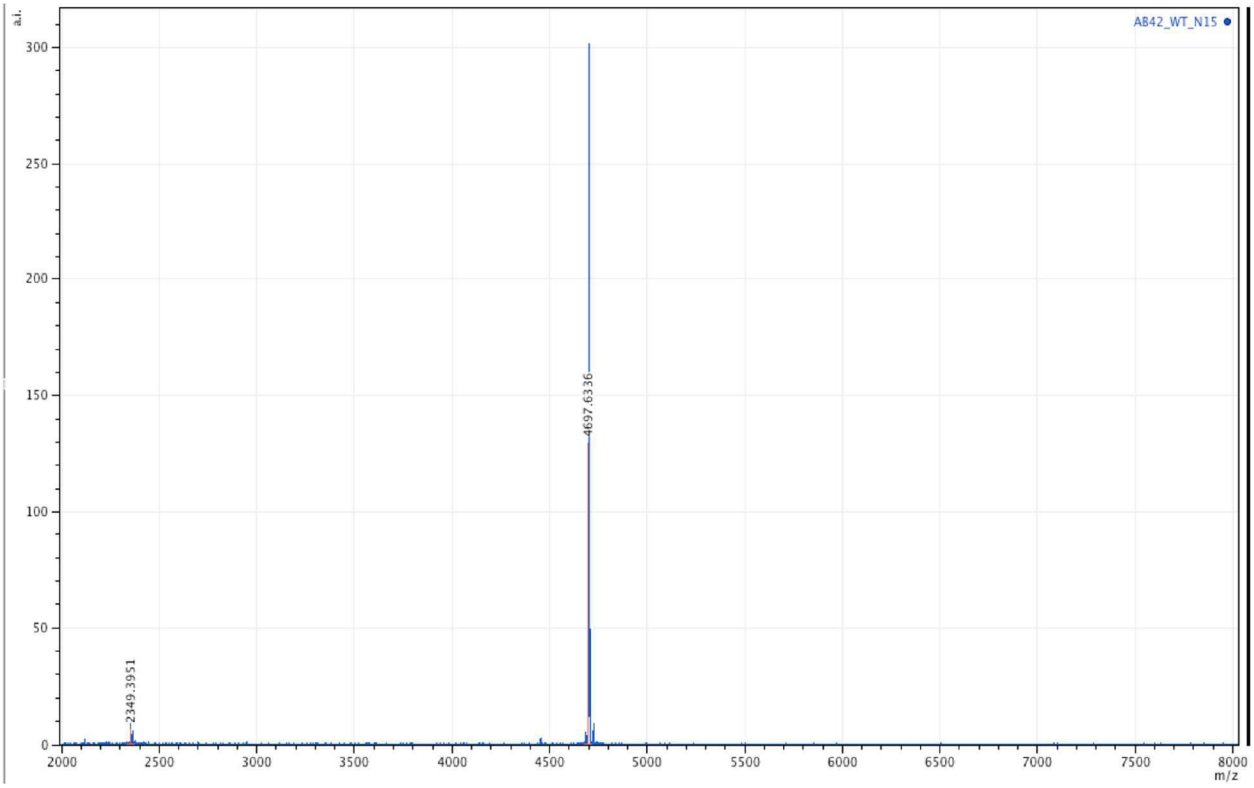

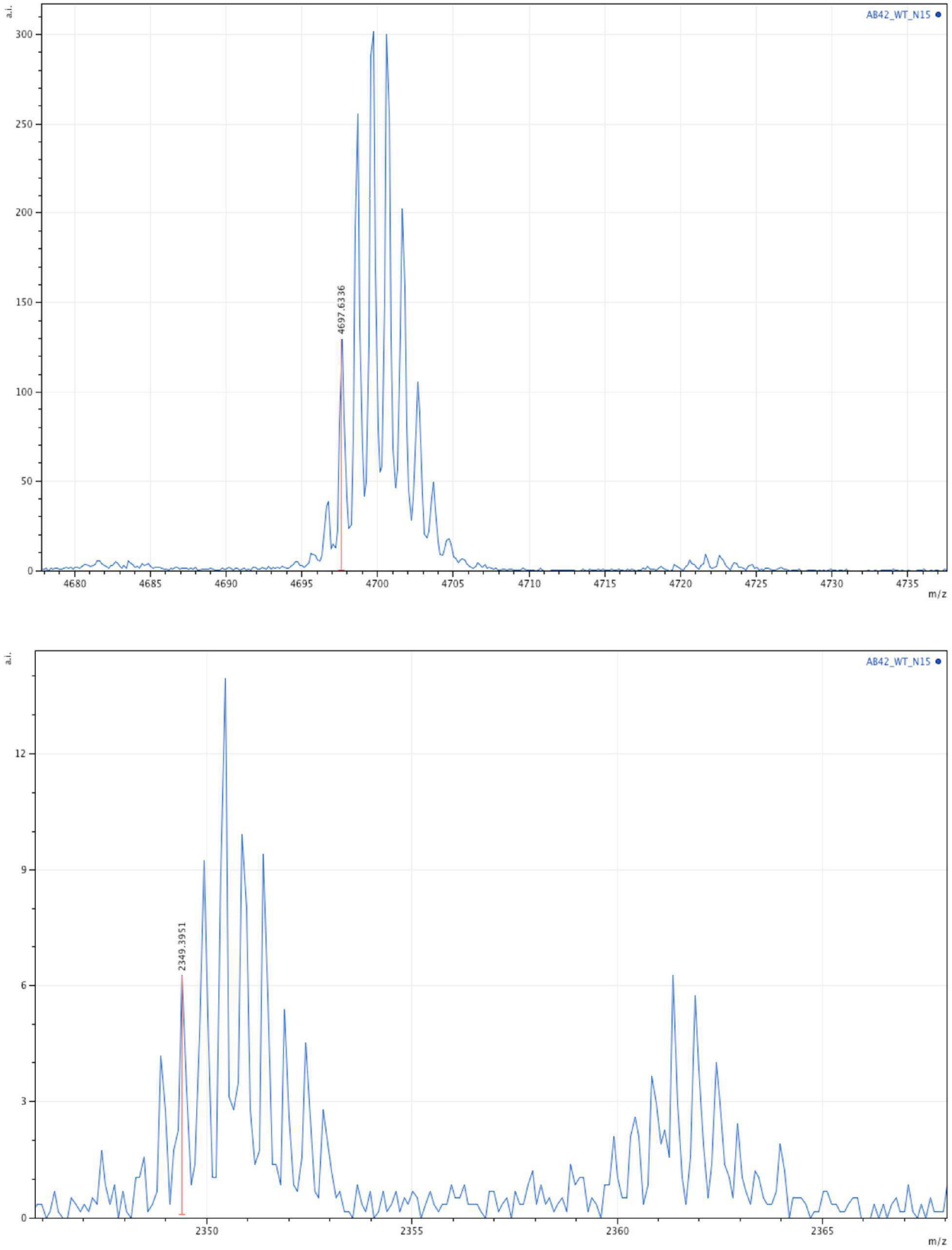

Figure 1.S5. Analytical HPLC and MALDI-MS traces of ^{15}N-labeled Aβ(M1–42).

Analytical HPLC trace of Aβ(M1–42/A21G). % purity: >99%

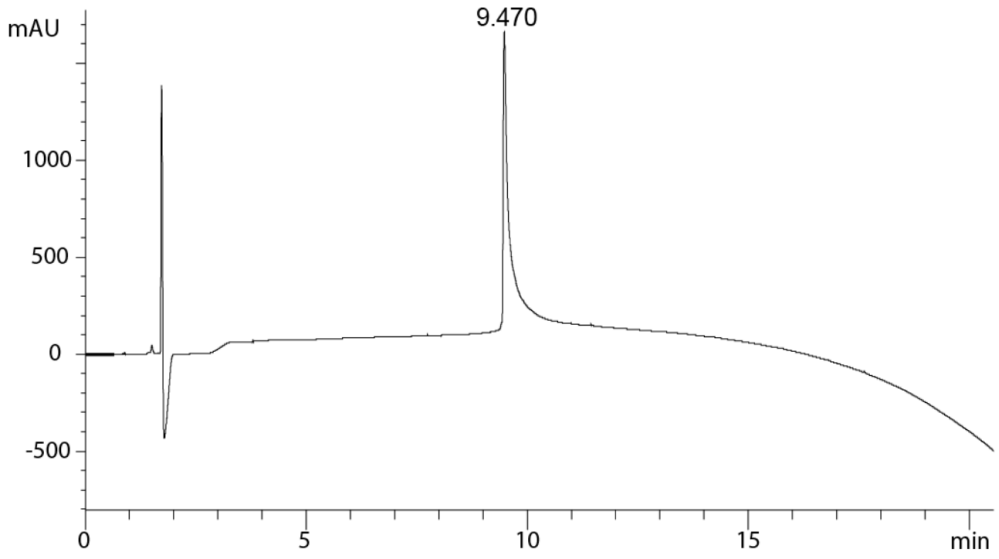

MALDI-MS trace of Aβ(M1–42/A21G).

Positive reflector mode. Matrix: 2,5-dihydroxybenzoic acid.

Exact mass calculated for M^+: 4628.3; Exact mass calculated for $[M+H]^+$: 4629.3. Observed $[M+H]^+$: 4629.1.

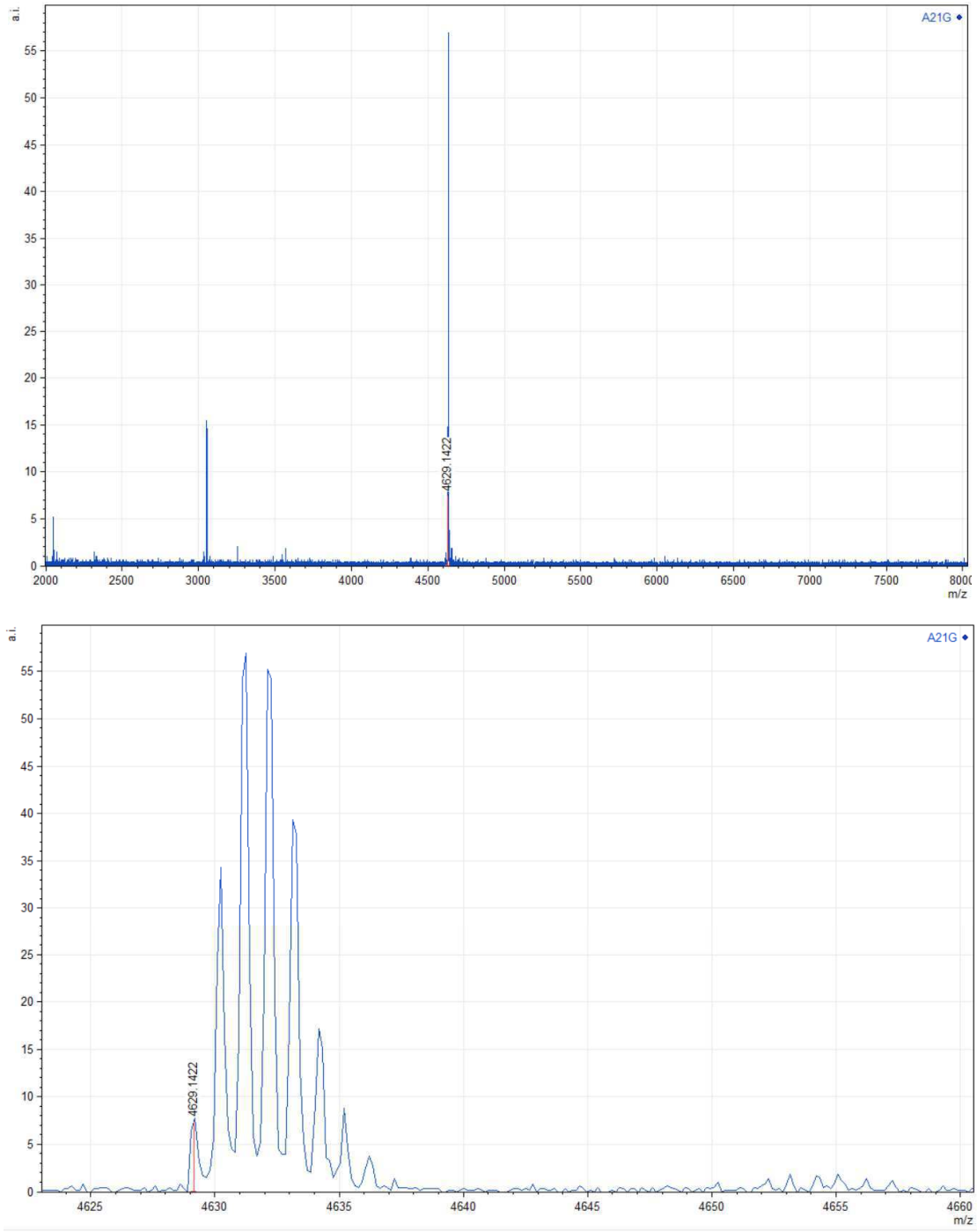

Figure 1.S6. Analytical HPLC and MALDI-MS traces of Aβ(M1–42/A21G).

Analytical HPLC trace of Aβ(M1–42/E22G). % purity: >99%

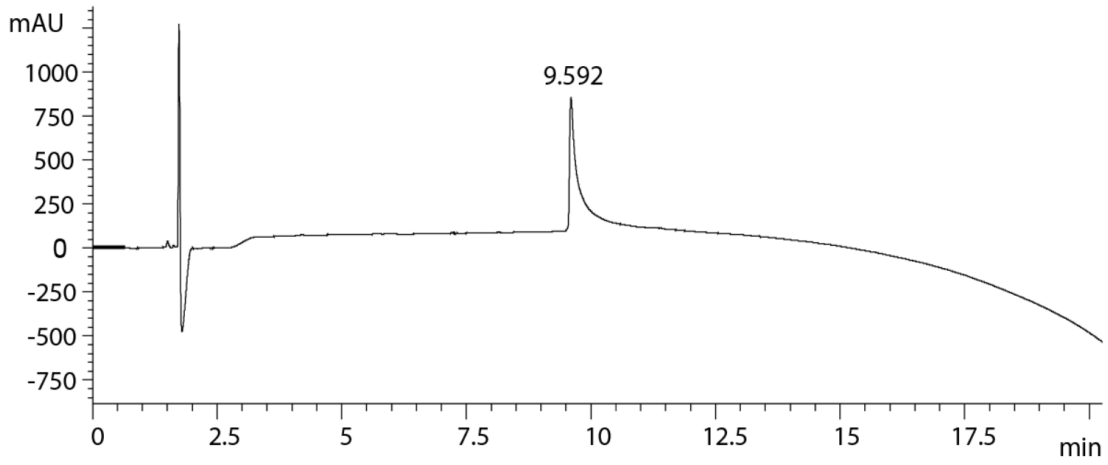

MALDI-MS trace of Aβ(M1–42/E22G).

Positive reflector mode.

Matrix: 2,5-dihydroxybenzoic acid.

Exact mass for M^+: 4570.3; Exact mass calculated for $[M+H]^+$: 4571.3; Exact mass calculated for $[M+2H]^{2+}$: 2286.2.

Observed $[M+H]^+$: 4570.6; Observed $[M+2H]^{2+}$: 2285.9.

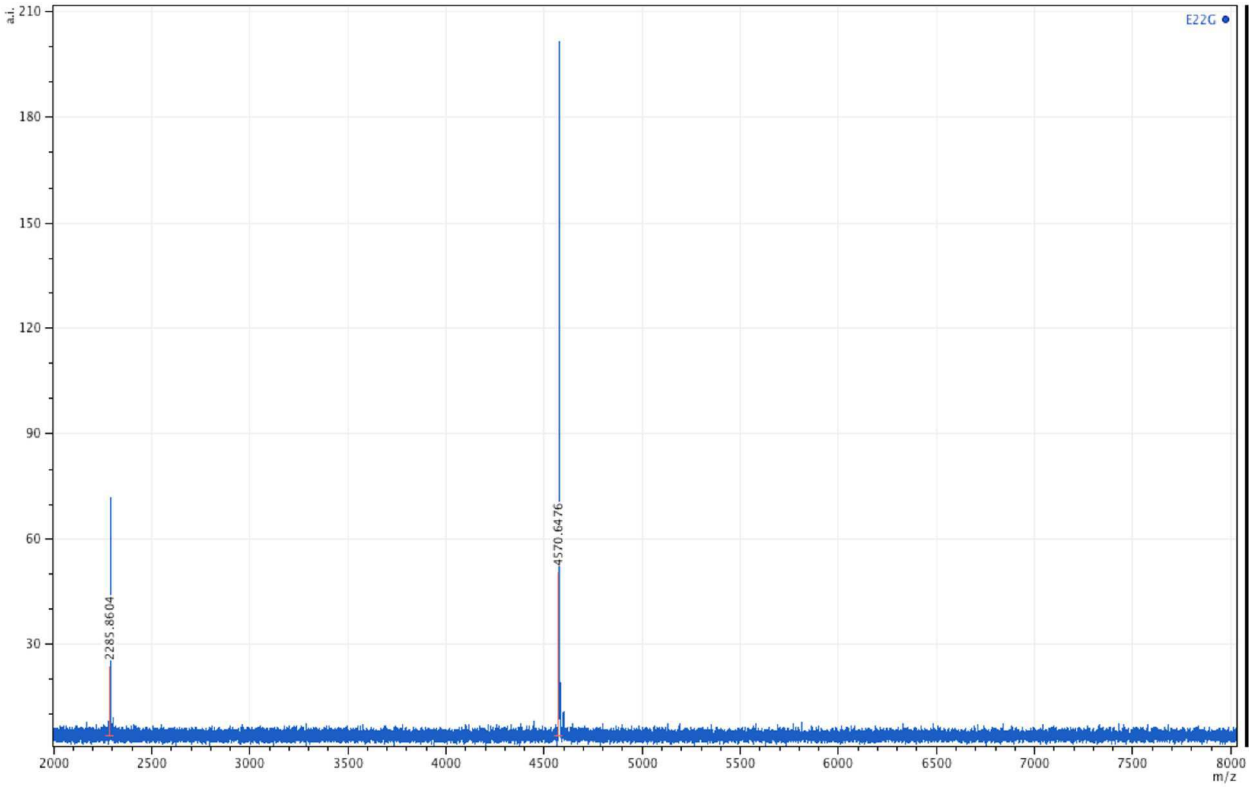

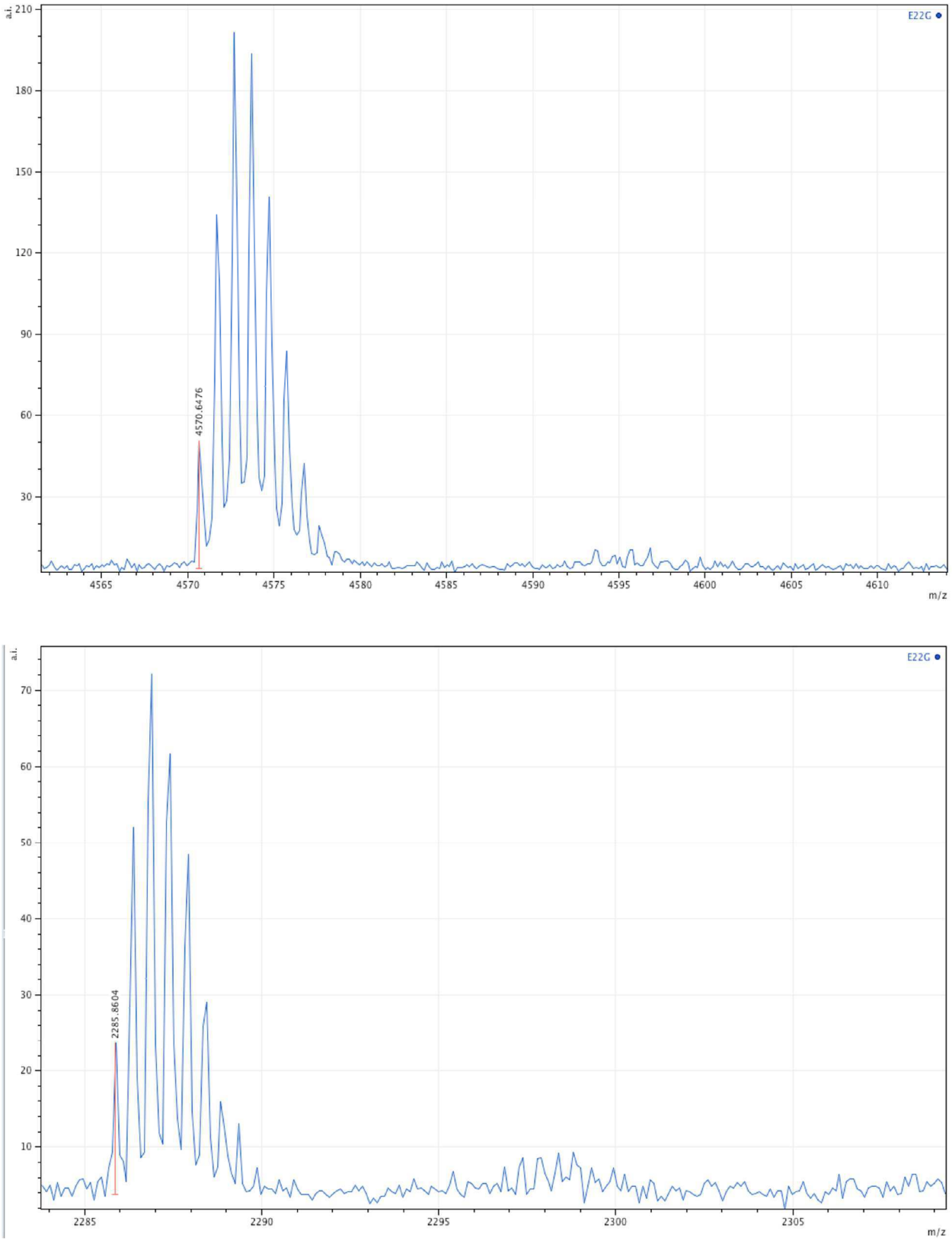

Figure 1.S7. Analytical HPLC and MALDI-MS traces of Aβ(M1–42/E22G).

Analytical HPLC trace of Aβ(M1–42/E22K). % purity: >99%

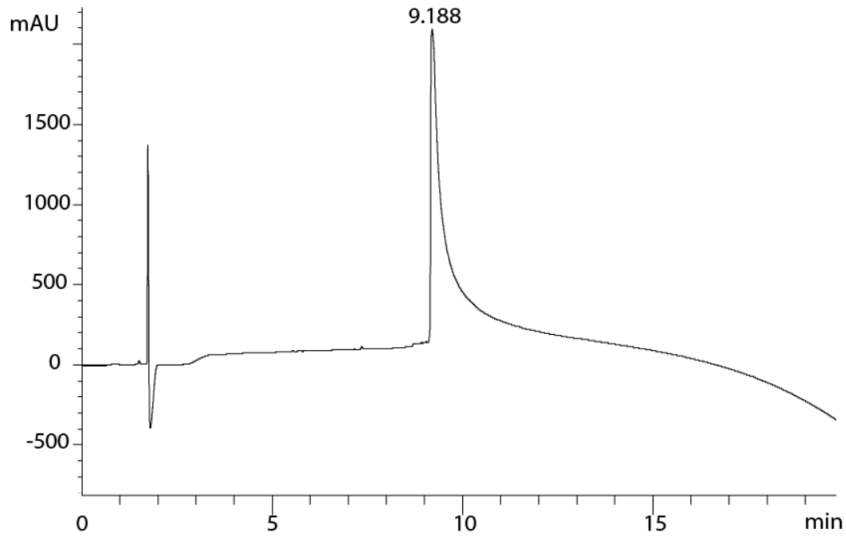

MALDI-MS trace of Aβ(M1–42/E22K).

Positive reflector mode.

Matrix: 2,5-dihydroxybenzoic acid.

Exact mass for M^+: 4641.3; Exact mass calculated for $[M+H]^+$: 4642.3; Exact mass calculated for $[M+2H]^{2+}$: 2321.7.

Observed $[M+H]^+$: 4642.0; Observed $[M+2H]^{2+}$: 2321.5.

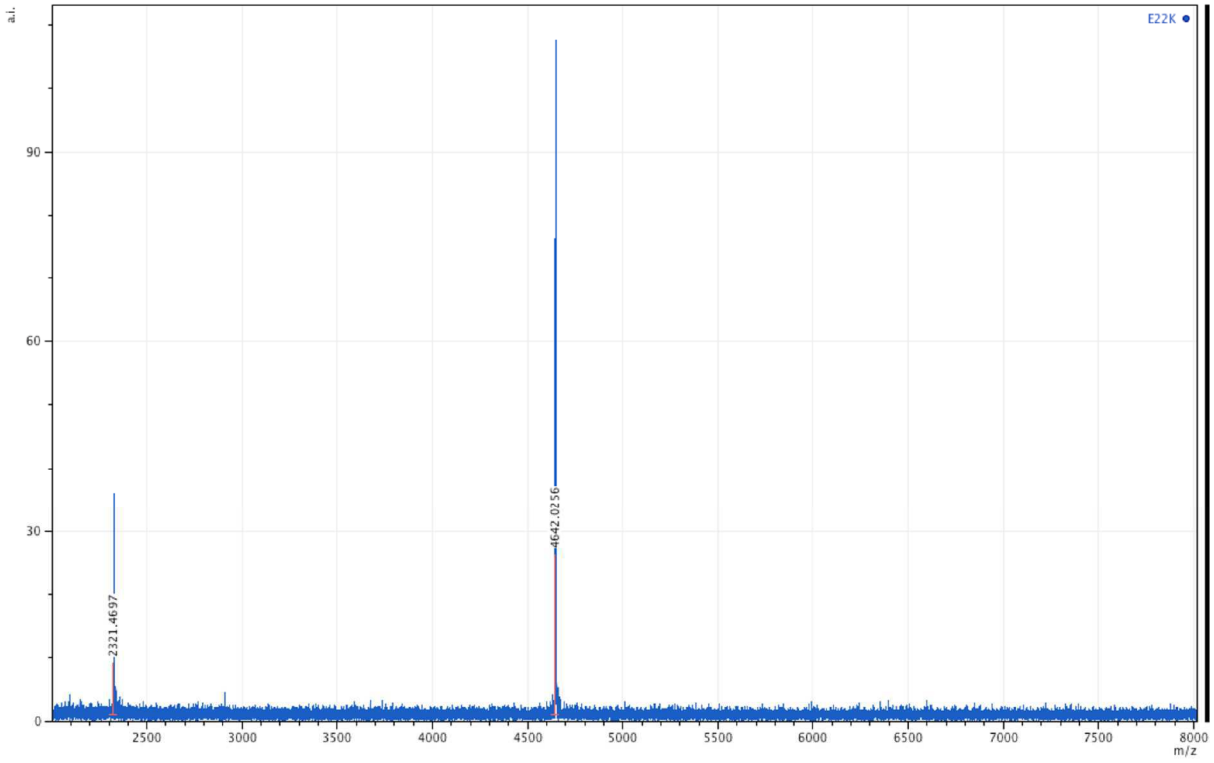

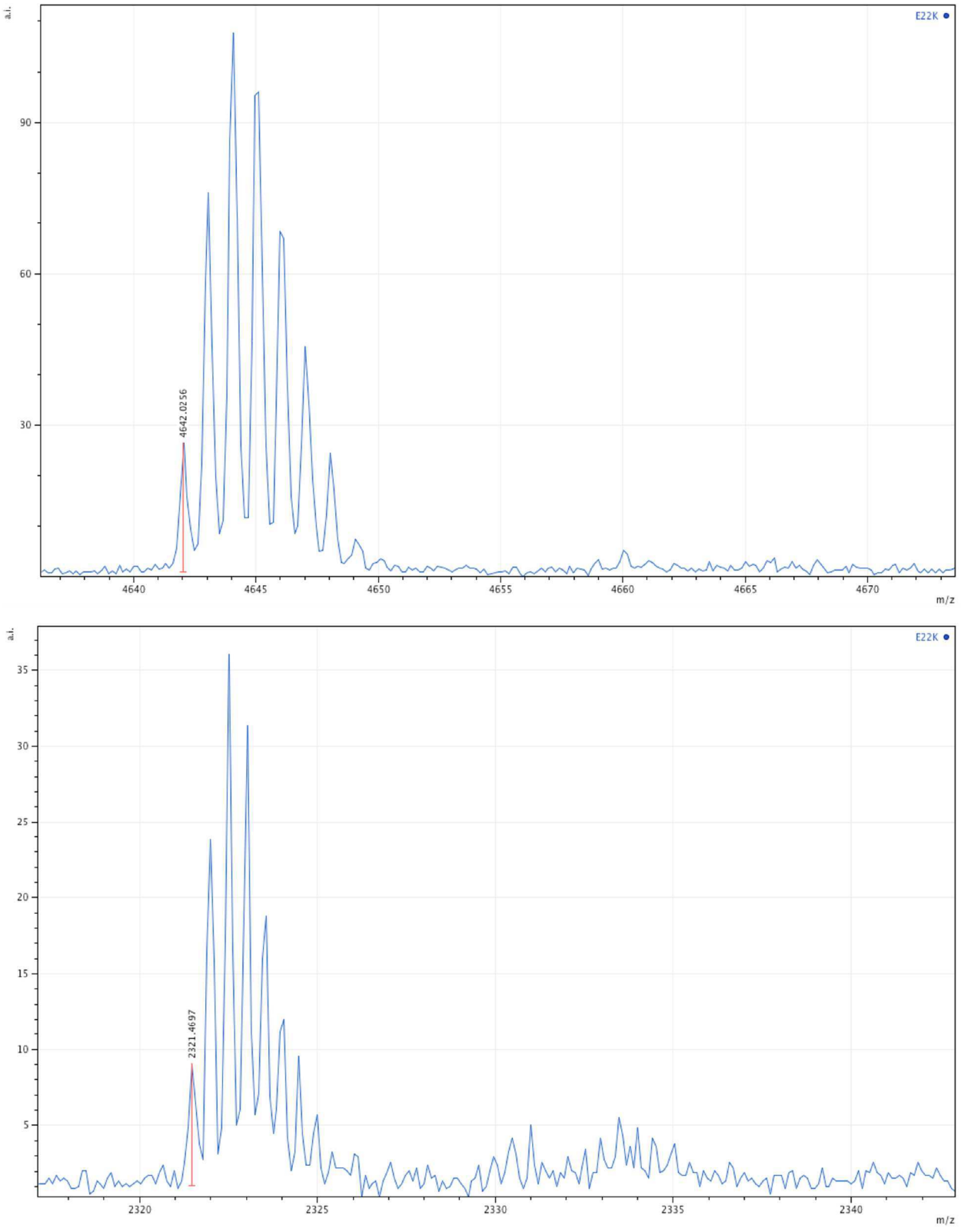

Figure 1.S8. Analytical HPLC and MALDI-MS traces of Aβ(M1–42/E22K).

Analytical HPLC trace of Aβ(M1–42/D23N). % purity: >95%

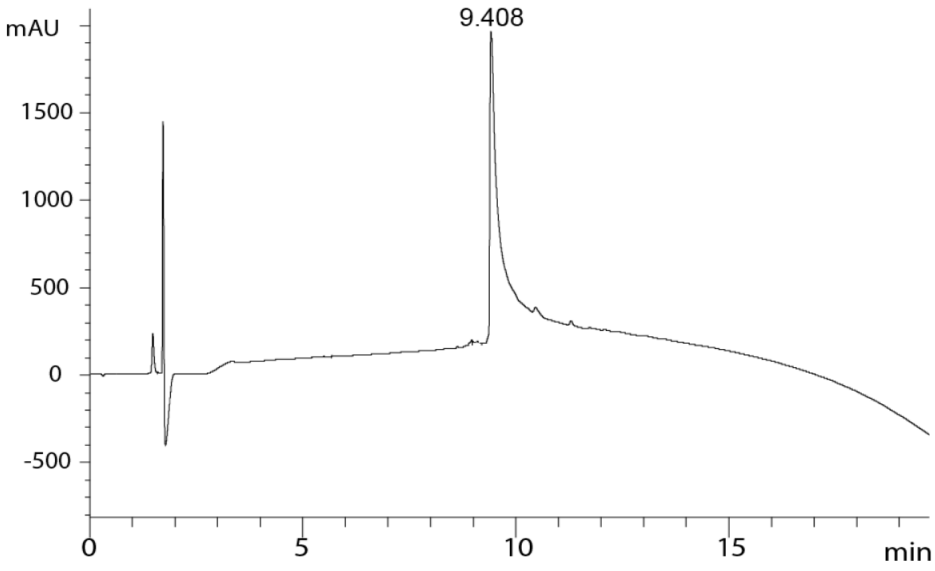

MALDI-MS trace of Aβ(M1–42/D23N).

Positive reflector mode.

Matrix: 2,5-dihydroxybenzoic acid.

Exact mass for M^+: 4641.3; Exact mass calculated for $[M+H]^+$: 4642.3; Exact mass calculated for $[M+2H]^{2+}$: 2321.7.

Observed $[M+H]^+$: 4641.9; Observed $[M+2H]^{2+}$: 2321.5.

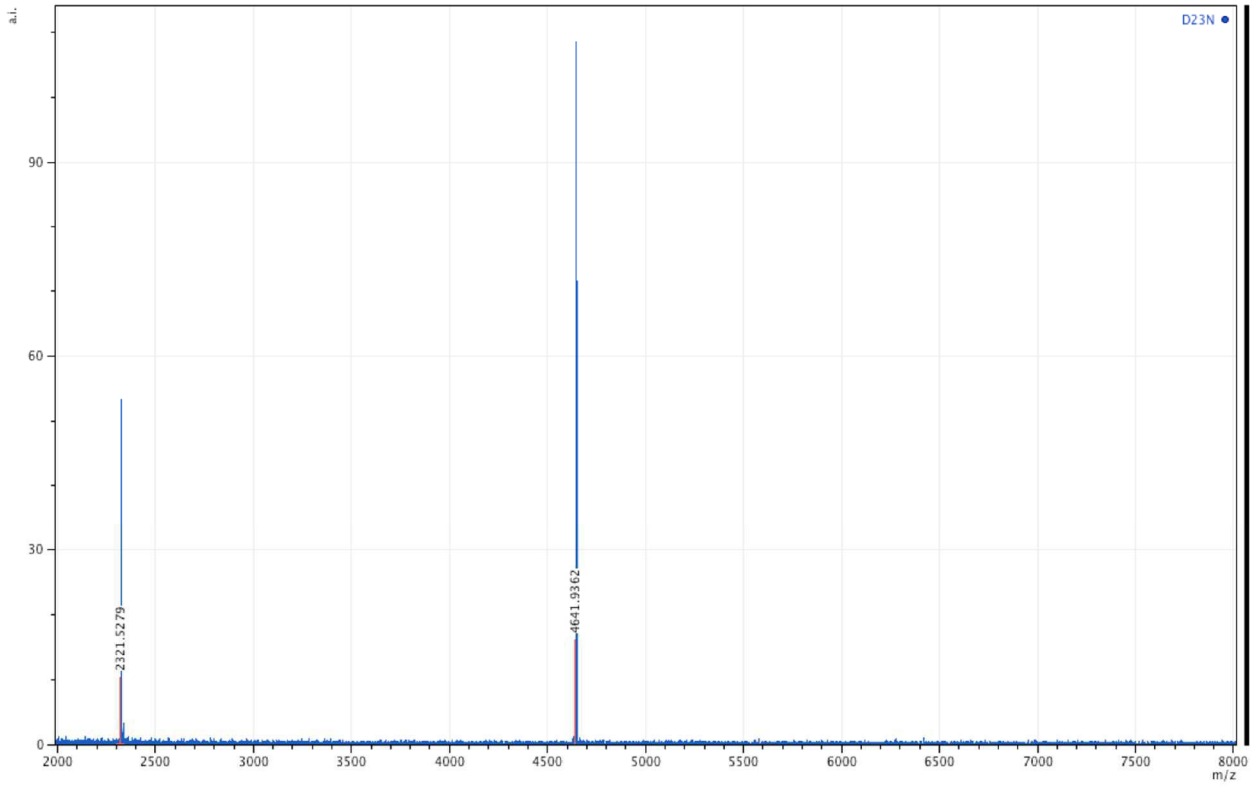

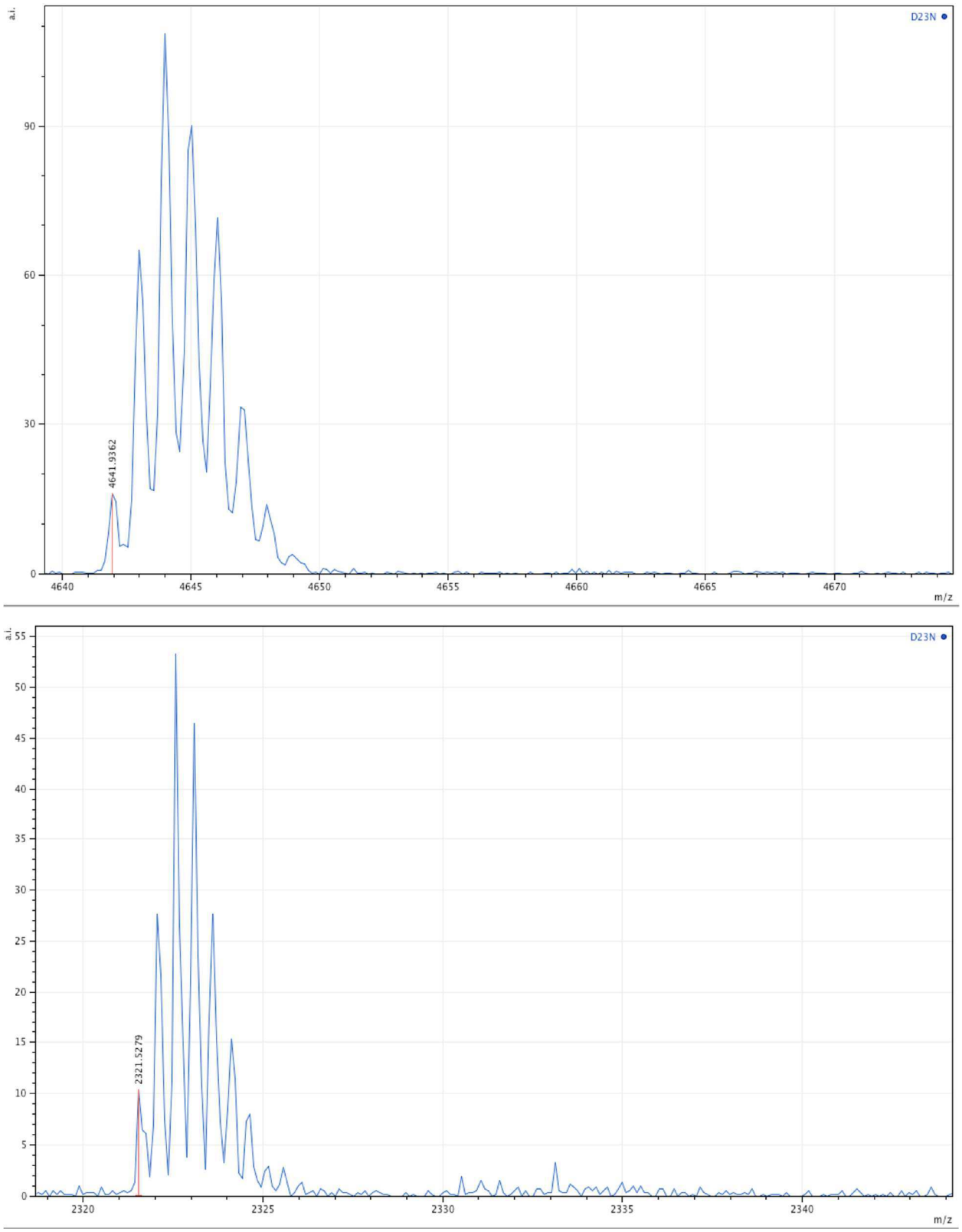

Figure 1.S9. Analytical HPLC and MALDI-MS traces of Aβ(M1–42/D23N).

References

1. Walsh, D. M., Thulin, E., Minogue, A. M., Gustavsson, N., Pang, E., Teplow, D. B., and Linse, S. A facile method for expression and purification of the Alzheimer's disease-associated amyloid β-peptide, *FEBS J.* **2009**, *276*, 1266-1281.

2. Kreutzer, A. G., Yoo, S., Spencer, R. K., and Nowick, J. S. Stabilization, Assembly, and Toxicity of Trimers Derived from Aβ, *J. Am. Chem. Soc.* **2017**, 139, 966-975.

Chapter 2

An Efficient Expression System for N-Terminal Cysteine Aβ for Bioconjugation

Introduction

Peptides and proteins bearing an N-terminal cysteine residue are valuable tools in chemical biology research, because the unique reactivity of N-terminal cysteine imparts the potential to participate in native chemical ligation, bioconjugation reactions, and other site-specific modifications.[1-4] β-Amyloid peptides (Aβ) bearing an N-terminal cysteine are versatile tools in Alzheimer's disease research, because N-terminal cysteine Aβ can be labeled with fluorophores or biotin for biological and chemical studies.[5,6] Site-specific labeling on the N-terminus of Aβ minimizes perturbation in the structure and function of the peptide, because the central and the C-terminal regions of Aβ are more important for fibril and oligomer formation (Figure 2.1).[7]

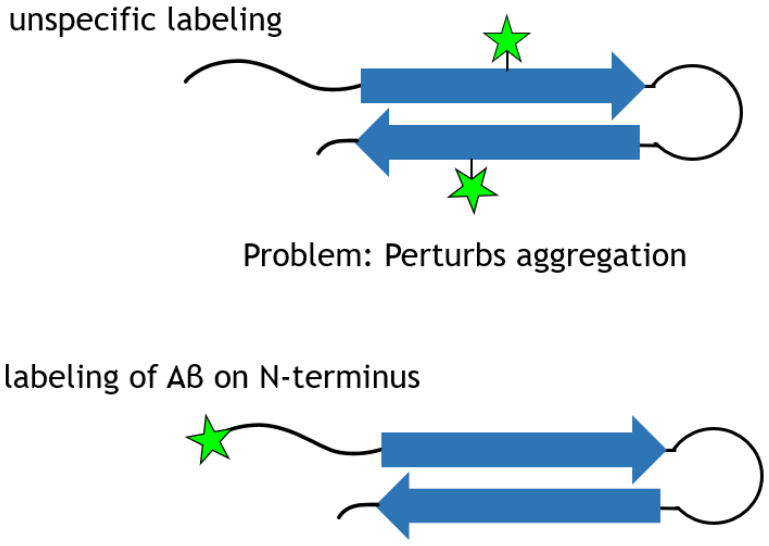

Figure 2.1. Scheme for unspecific and N-terminus labeling of Aβ.

In this chapter, I describe an efficient method for recombinant expression and purification of the Aβ peptide with an N-terminal cysteine, Aβ(C1–42), and the preparation of labeled Aβ(C1–42) conjugates (Figure 2.2). Expressed Aβ peptides are superior to chemically synthesized Aβ, because they contain fewer peptidic impurities. Expressed Aβ peptides have been found to aggregate more quickly and be more toxic than synthetic Aβ.[1] Although Aβ peptides bearing fluorescent and biotin labels can be prepared by chemical syntheses, the expressed Aβ peptide bioconjugates are preferable because they are free from amino acid deletions and chemical impurities.

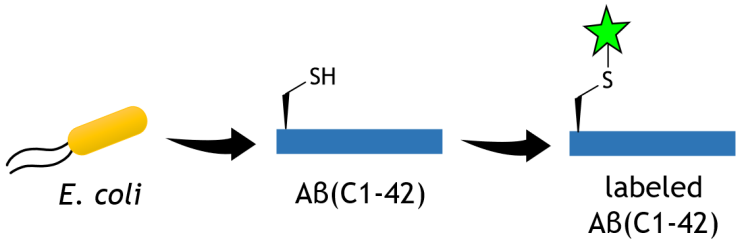

Figure 2.2. Overall scheme of this expression and labeling method.

In the preceding chapter, I described an efficient method for expression and purification of N-terminal methionine Aβ, Aβ(M1–42).[2] In the this chapter, I adapt this method by first cloning an Aβ sequence where a cysteine is placed in the penultimate position, Aβ(MC1-42) (Figure 2.3). As Aβ(MC1-42) is expressed, the N-terminal methionine is spontaneously excised by methionyl aminopeptidase (MAP) in *E. coli*, leaving cysteine on the N-terminus.[3] The expressed N-terminal cysteine Aβ is then purified using reverse-phase preparative HPLC. I also illustrate applications of Aβ(C1-42) by fluorescent and biotin labeling through cysteine-maleimide conjugation and show that a labeled peptide behaves similarly to unlabeled Aβ.

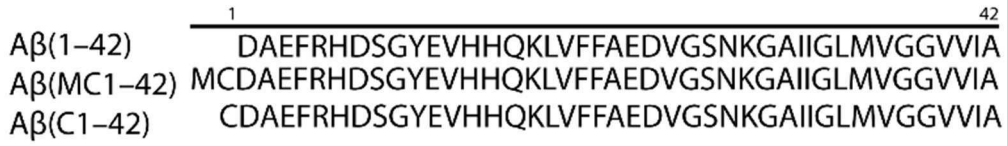

Figure 2.3. Sequences of Aβ(1–42), Aβ(MC1–42), and Aβ(C1–42).

Results and discussion

I expressed Aβ(C1–42) in *E. coli* using a plasmid for Aβ(MC1–42) that I constructed and will be available through Addgene.[11] The expressed peptide forms inclusion bodies that are isolated by multiple rounds of washing. The inclusion bodies are then solubilized in urea buffer, and the dissolved Aβ(C1–42) is purified by reverse-phase HPLC. The pure HPLC fractions are immediately used in conjugation reactions, and the conjugated peptides are purified by another round of HPLC purification.

Expression and purification of N-terminal cysteine Aβ peptides

I prepared plasmids encoding Aβ(MC1−42) and Aβ(MC1−40) sequences in the same fashion as I had previously described, and I deposited these plasmids with Addgene to make them available to others (Figure 2.4).[11] To express Aβ(C1−42), the pET-Sac-Aβ(MC1−42) plasmid is transformed into BL21(DE3)-pLysS competent *E. coli.* The transformed *E. coli* is cultured to an OD_{600} of 0.45, and expression is induced with isopropyl β-D-1-thiogalactopyranoside (IPTG). The expressed peptide is isolated as the inclusion bodies, which are washed three times with a Tris buffer and then solubilized with 8 M urea. The solution is then filtered through a 0.22 μm polyvinylidene fluoride (PVDF) filter and subjected to preparative reverse-phase HPLC on a C8 column at 80 °C. A typical HPLC trace prior to purification shows three major peaks, with the first

peak corresponding to the Aβ(C1–42) monomer (Figure 2.5A). The combined pure fractions typically show >95% purity as assessed by analytical HPLC and mass spectrometry (Figures 2.5B and 2.5C). The combined fractions of Aβ(C1–42) are then directly used for conjugation reactions. Alternatively, the combined fractions may be lyophilized, and the resulting powder may be stored for future use.

I have also applied these expression and purification procedures to Aβ(C1–40), albeit in far lower yield and lower purity (Figure 3.S8).

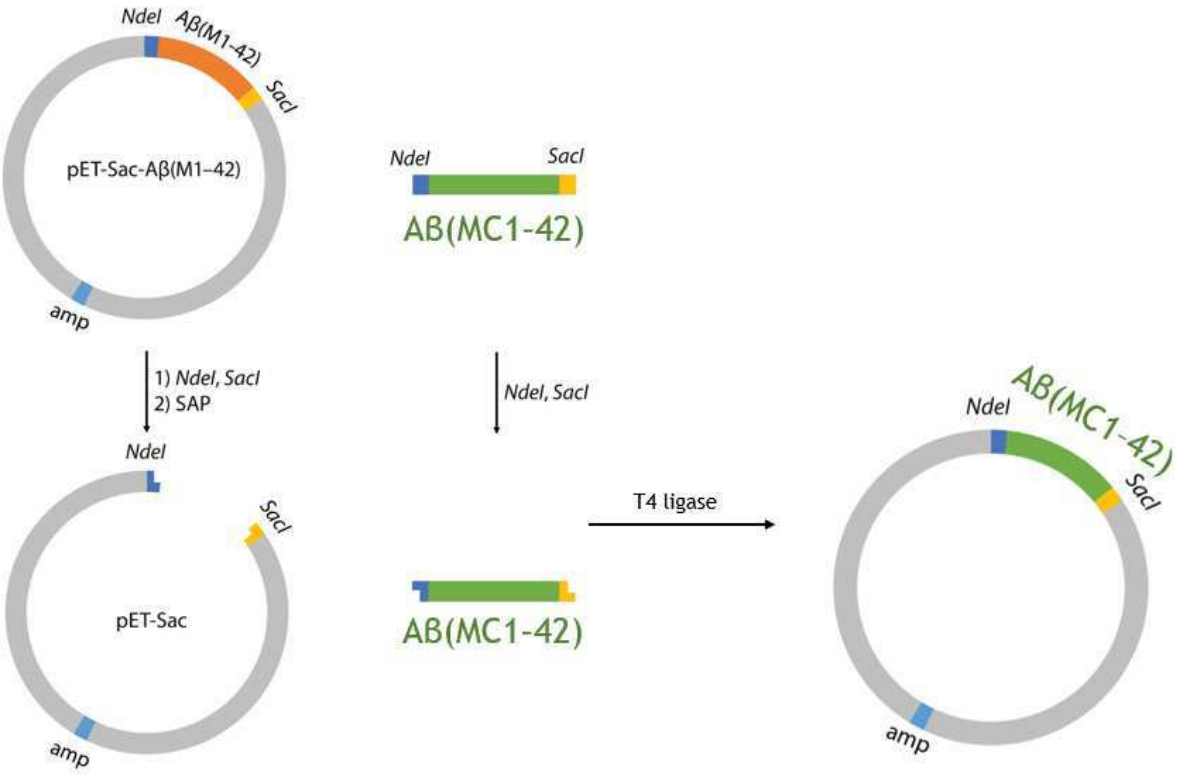

Figure 2.4. Molecular cloning strategy for recombinant plasmid for Aβ(MC1-42).

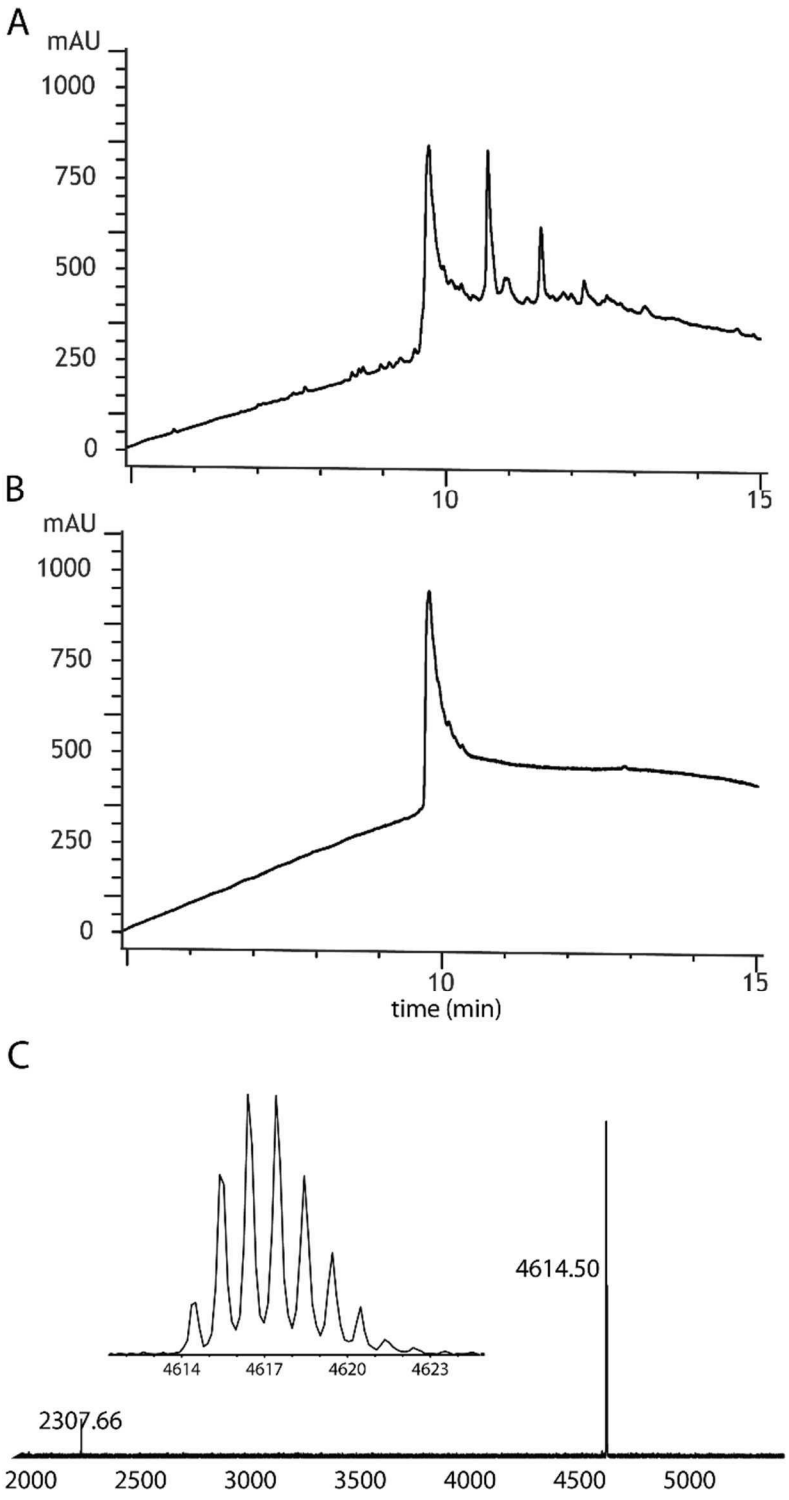

Figure 2.5. Characterization of Aβ(C1–42). (A) Analytical HPLC trace of a filtered crude Aβ(C1–42) sample dissolved in 8 M urea. (B) Analytical HPLC trace of purified Aβ(C1–42). (C) MALDI-MS spectrum of purified Aβ(C1–42).

Labeling of Aβ(C1–42)

I developed a protocol for directly labeling the combined pure fractions of Aβ(C1–42) to save time and prevent aggregation of the peptide. The optimization for conjugation reactions are still in development and optimized procedure will be reported on a publication.

Using current reaction condition, conjugation reactions are performed by mixing the combined pure fractions of Aβ(C1–42) with a 2- to 5-fold molar excess of the bioconjugation reagent. The pH of the reaction mixture is adjusted to pH 6-7 with aqueous NaOH for 5 minutes, and then is acidified to pH 2-3. (Figure 2.6). The conjugation reactions were monitored by disappearance of Aβ(C1-42) and appearance of conjugated peptide on an analytical HPLC on a C18 column. Then, the solution is subjected to purification by preparative HPLC on a C8 column at 80 °C, and the pure fractions of the conjugated Aβ(C1–42) peptide are combined and lyophilized. Again, further optimization of conjugation reaction is underway.

I labeled with three different maleimide reagents: fluorescein-5-maleimide, 6-TAMRA-maleimide, and maleimide-PEG2-biotin (Figure 2.7). Fluorescein and TAMRA are commonly used fluorescent dyes for cell imaging and biotins are common functional groups for pull-down experiments.

MALDI mass spectra of purified fractions show singly labeled Aβ(C1–42) peptide conjugates with the respective maleimide reagents (Figure 2.8). The lyophilized powders of the conjugated Aβ(C1–42) are stored in a desiccator at -20 °C.

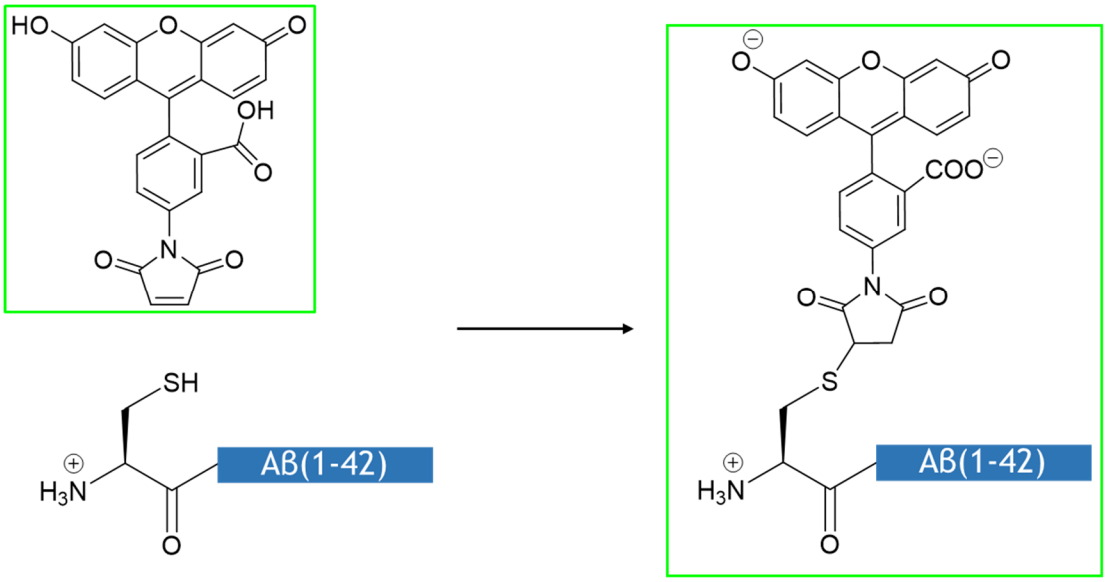

Figure 2.6. Conjugation reaction scheme with Aβ(C1–42) and fluorescein-5-maleimide to synthesize fluorescein-conjugated Aβ.

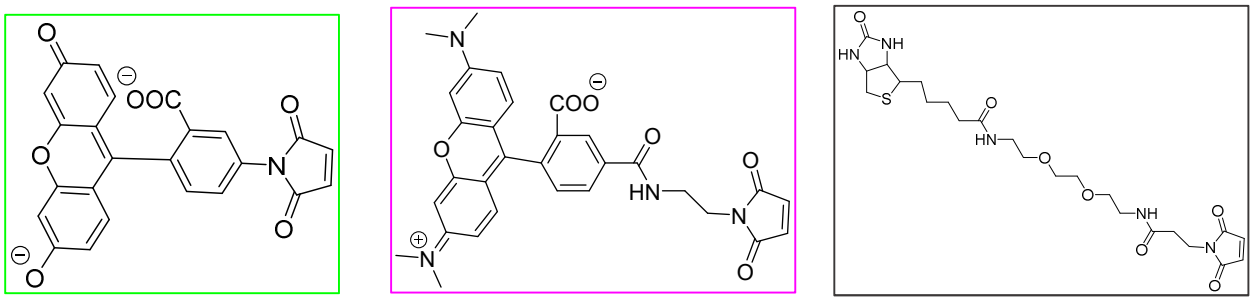

Figure 2.7. Chemical structures of the three maleimide reagents used: fluorescein-5-maleimide, 6-TAMRA-maleimide, and maleimide-PEG2-biotin.

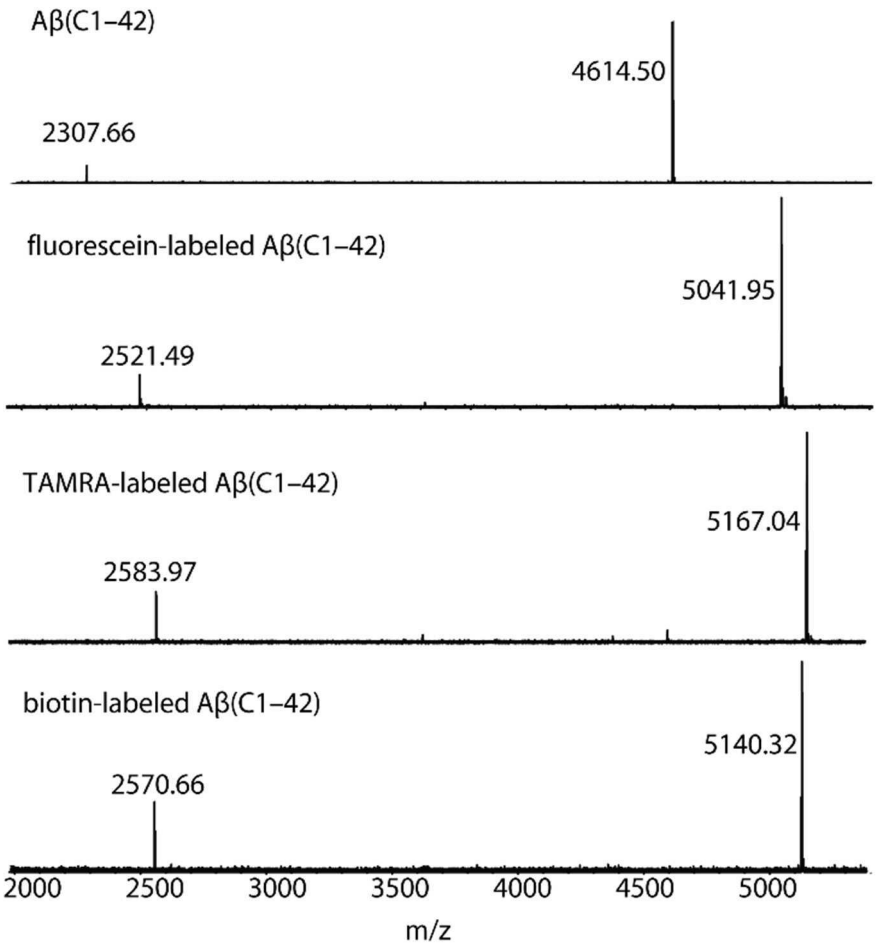

Figure 2.8. MALDI-MS spectra of Aβ(C1–42) and fluorescent or biotin labeled Aβ(C1–42).

Challenge in sample preparation

In the previous chapter, I described the sample preparation by treating lyophilized TFA salt samples with 2 mM NaOH solution. This was necessary for quantification of Aβ peptides and for prepare aliquots containing accurate amount of peptide samples for future experiments. For preparation of fluorescently labeled Aβ samples in this chapter, I initially followed the same sample preparation procedure. However, it was found that the succinimide rings within the fluorescently labeled peptides was partially hydrolyzed as the [M+!8] masses were detected on their MALDI mass spectra. Figure 2.9 shows an example of hydrolysis product detected on a MALDI mass spectrum of NaOH treated lyophilized powder of fluorescein-labeled Aβ(C1-42). For this procedure, NaOH treatment step deemed not necessary as the labeled peptides are quantified gravimetrically and as hydrolysis reaction by NaOH produces undesired side product.

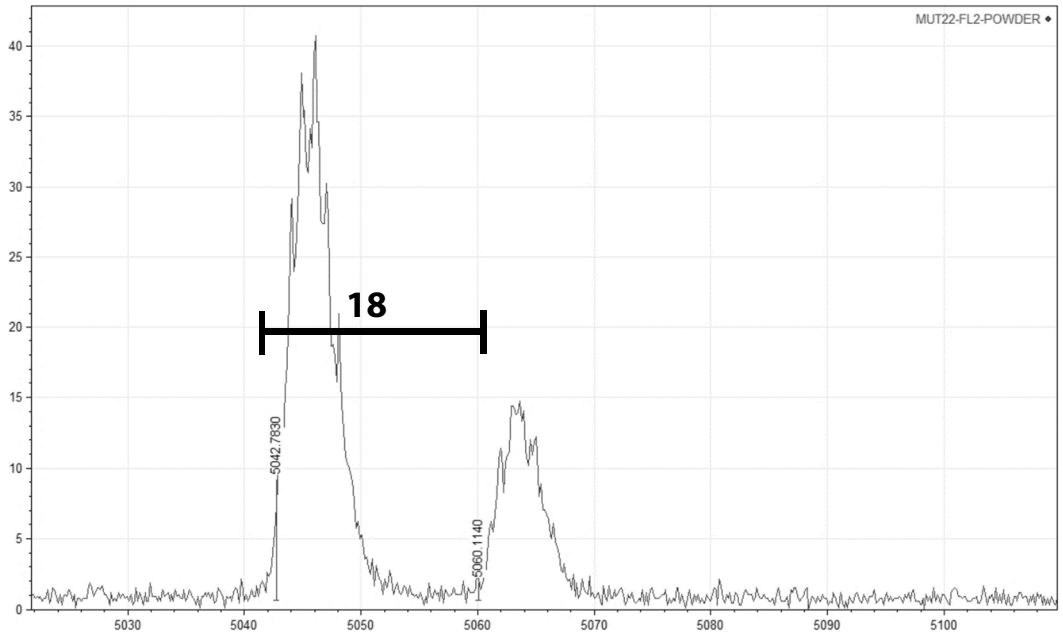

Figure 2.9. MALDI mass spectrum of NaOH treated lyophilized power of fluorescein-labeled Aβ(C1-42). The peak at 5042.8 is the [M+1] mass of fluorescein-labeled Aβ(C1-42) and the peak at 5060.1 is the [M+1] mass of the succinimide ring-opened form of fluorescein-labeled Aβ(C1-42).

Biophysical and biological studies of fluorescein-labeled Aβ(C1-42)

To confirm the utility of conjugated Aβ(C1-42) peptides, I studied fluorescein-labeled Aβ(C1-42) by SDS-PAGE, transmission electron microscopy (TEM), and fluorescence microscopy with human neuroblastoma cell line SH-SY5Y. Aliquots of fluorescein-labeled Aβ(C1-42) ranging from 50 μg to 0.8 μg were run on an SDS-PAGE gel, and the gel was visualized by fluorescence with excitation at 494 nm (Figure 2.10). The fluorescein-labeled Aβ(C1-42) migrates in SDS-PAGE in a similar pattern as unlabeled Aβ(M1–42).[9] At low loading, the peptide shows a monomer band above the 4.6 kDa marker, while at high loading, the peptide shows two additional oligomer bands between the 10 and 15 kDa markers. Fibril formation of fluorescein-labeled Aβ(C1-42) was observed by TEM imaging after 1 day of incubation in PBS at 37 °C (Figure 2.11). Incubation of SH-SY5Y cells with fluorescein-labeled Aβ(C1-42) followed by visualization by fluorescence microscopy revealed that the peptide localizes on or within some of the cells (Figure 2.12).

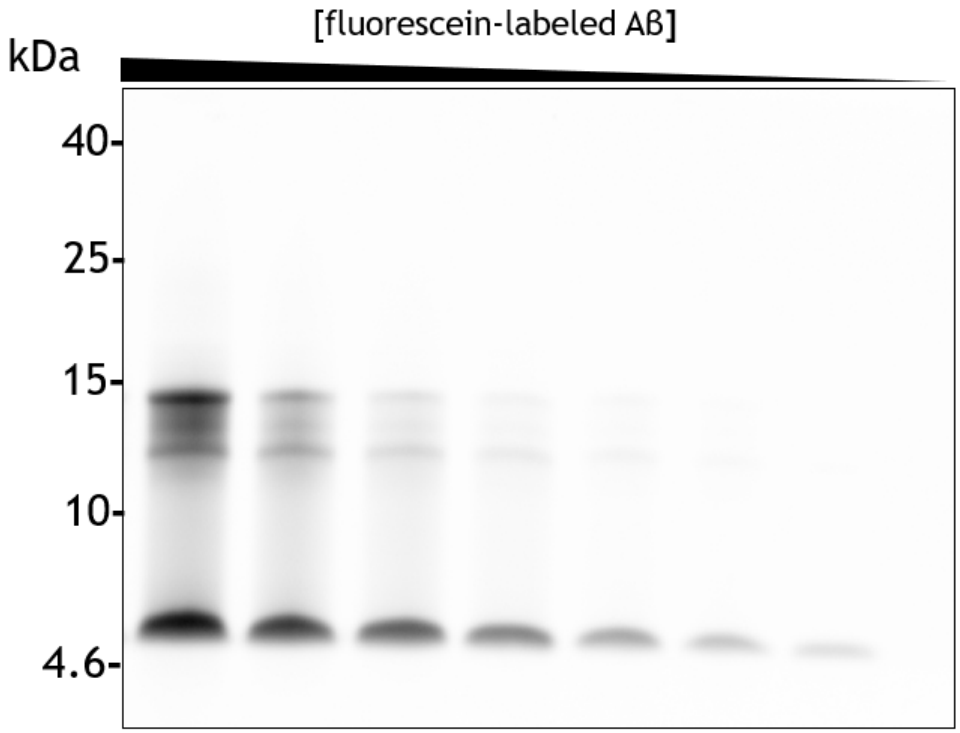

Figure 2.10. SDS-PAGE gel of fluorescein-labeled Aβ concentration gradient, visualized by fluorescence with excitation at 494 nm.

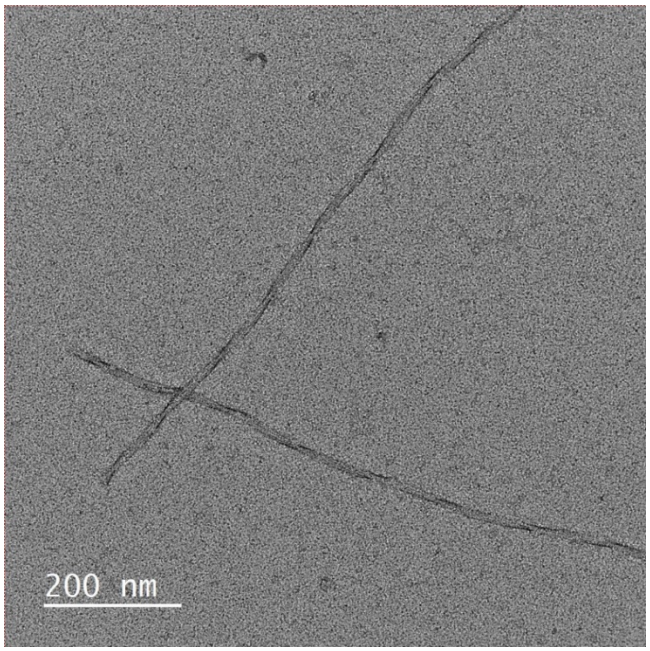

Figure 2.11. TEM image of fibrils formed by fluorescein-labeled Aβ after 1 day of incubation in PBS.

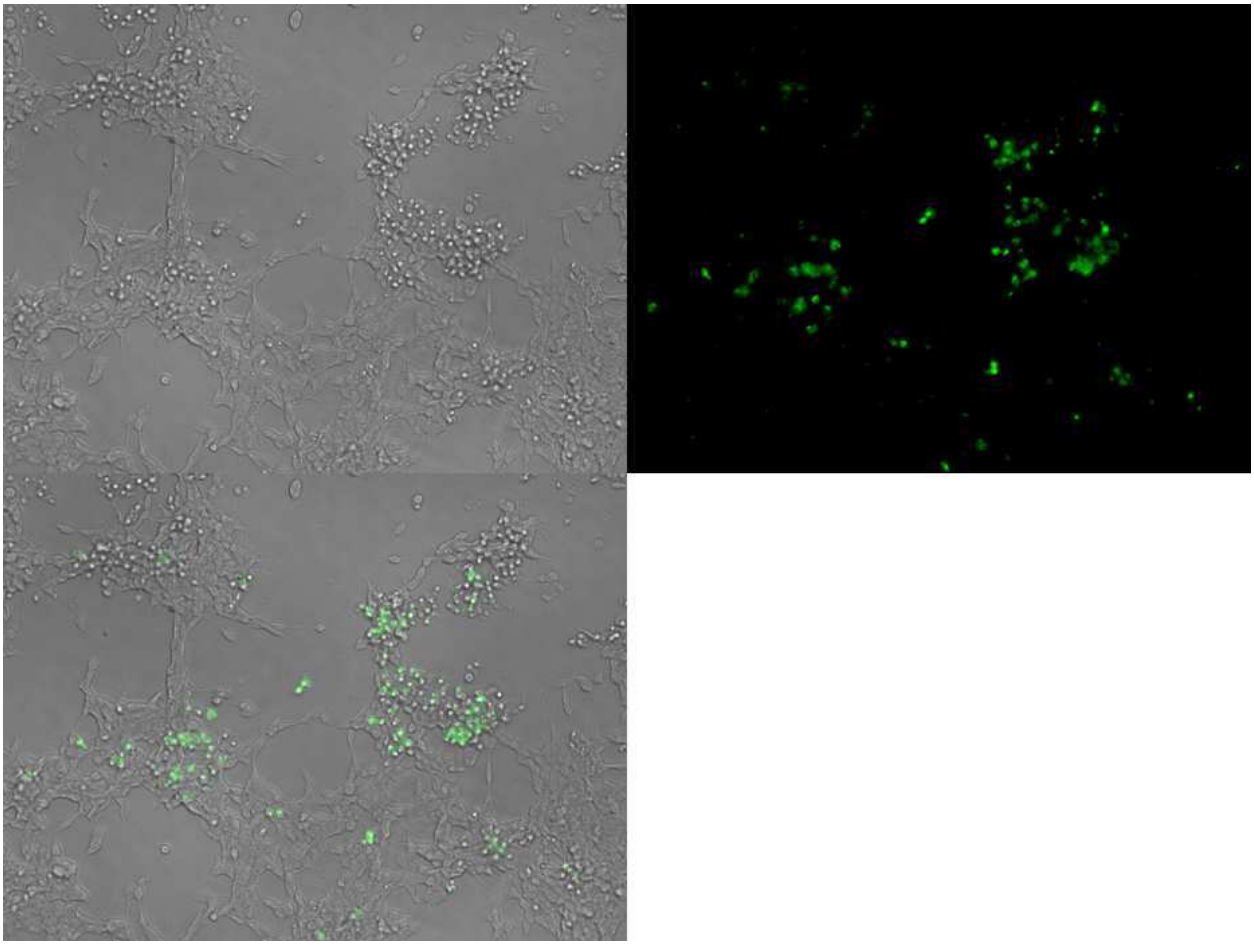

Figure 2.12. Fluorescence micrograph of fluorescein-labeled Aβ on SH-SY5Y cells after 1 day of incubation. Bright-field image of cells (top, left), fluorescent image of cells with 395nm excitation (top, right), and overlay image (bottom, left).

Conclusion

Expression of Aβ(MC1-42) in *E. coli* affords Aβ(C1-42) in practical yield. The expressed peptide is readily purified by reverse-phase HPLC and can be elaborated to useful conjugates upon treatment with maleimide bearing fluorophores or biotin. The procedure is efficient and economical. HPLC and MALDI analyses show that the N-terminal cysteine Aβ and labeled Aβ are pure and homogeneous. SDS-PAGE and TEM imaging of fibrils show that N-terminal labeled Aβ behaves similarly to unlabeled Aβ. I anticipate that this method can be adapted for the expression and purification of other amyloidogenic peptides or proteins bearing N-terminal cysteine.

References and notes

1. Rosen, C. B.; Francis, M. B. Targeting the N terminus for site-selective protein modification. *Nat. Chem. Biol.* **2017**, *13*, 697-705.

2. Bandyopadhyay, A.; Cambray, S.; Gao, J. Fast and selective labeling of N-terminal cysteines at neutral pH via thiazolidino boronate formation. *Chem. Sci.* **2016**, *7*, 4589-4593.

3. Wang, P.; Zhang, C. J.; Chen, G.; Na, Z.; Yao, S. Q.; Sun, H. Site-specific immobilization of biomolecules by a biocompatible reaction between terminal cysteine and 2-cyanobenzothiazole. *Chem. Commun.* **2013**, *49*, 8644-8646.

4. Ren, H.; Xiao, F.; Zhan, K.; Kim, Y. P.; Xie, H.; Xia, Z.; Rao, J. A biocompatible condensation reaction for the labeling of terminal cysteine residues on proteins. *Angew. Chem., Int. Ed.* **2009**, *48*, 9658-9662.

5. Dunning, C. J.; McGauran, G.; Willen, K.; Gouras, G. K.; O'Connell, D. J.; Linse, S. Direct High affinity interaction between Aβ42 and GSK3alpha stimulates hyperphosphorylation of Tau. A new molecular link in Alzheimer's disease? *ACS Chem. Neurosci.* **2016**, *7*, 161-170.

6. LeVine, H. III, Biotin-avidin interaction-based screening assay for Alzheimer's β-peptide oligomer inhibitors. *Anal. Biochem.* **2006**, *356*, 265-272.

7. Jungbauer, L. M.; Yu, C.; Laxton, K. J.; LaDu, M. J. Preparation of fluorescently-labeled amyloid-β peptide assemblies: the effect of fluorophore conjugation on structure and function. *J. Mol. Recognit.* **2009**, *22*, 403-413.

8. Finder, V. H.; Vodopivec, I.; Nitsch, R. M.; Glockshuber, R. The recombinant amyloid-β peptide Aβ1-42 aggregates faster and is more neurotoxic than synthetic Aβ1-42. *J. Mol. Biol.* **2010**, *396*, 9-18.

9. Yoo, S.; Zhang, S.; Kreutzer, A. G.; Nowick, J. S. An efficient method for the expression and purification of Aβ(M1-42). *Biochemistry* **2018**, *57*, 3861-3866.

10. In *E. coli*. N-terminal methionine excision occurs most readily for glycine, alanine, proline, serine, threonine, valine, and cysteine. Hirel, P. H., Schmitter, M. J., Dessen, P., Fayat, G., Blanquet, S. Extent of N-terminal methionine excision from *Escherichia coli* proteins is governed by the side-chain length of the penultimate amino acid, *Proc. Natl. Acad. Sci. U. S. A.* **1989**, *86*, 8247-8251.

11. Aβ(MC1−42): plasmid # 127151; http://n2t.net/addgene:127151; RRID:Addgene_127151; Aβ(MC1−40): plasmid # 127152; http://n2t.net/addgene:127152; RRID:Addgene_127152

12. Walsh, D. M.; Thulin, E.; Minogue, A. M.; Gustavsson, N.; Pang, E.; Teplow, D. B.; Linse, S. A facile method for expression and purification of the Alzheimer's disease-associated amyloid β-peptide. *FEBS J.* **2009**, *276*, 1266-1281.

Supporting Information

Table of Contents

Characterization Data

Materials and Methods[1]

General information on materials and methods

All chemicals were used as received unless otherwise noted. Deionized water (18 MΩ) was obtained from a Thermo Scientific Barnstead Genpure Pro water purification system. The pET-Sac-Aβ(M1–42) was a gift from Dominic Walsh via Addgene (plasmid # 71875).[2] DNA sequences that encode Aβ(MC1–42) and Aβ(MC1–40) were purchased in 500 ng quantities from Genewiz. *NdeI* and *SacI* restriction enzymes, CutSmart buffer, and shrimp alkaline phosphatase (rSAP) were purchased from New England Biolabs (NEB). TOP10 Ca^{2+}-competent *E. coli* and BL21 DE3 PLysS Star Ca^{2+}-competent *E. coli*, T4 ligase, and ethidium bromide were purchased from Thermo Fisher Scientific. Zymo ZR plasmid miniprep kit and Zymoclean Gel DNA recovery kit was purchased from Zymo Research. Carbenicillin and chloramphenicol were purchased from RPI Research Products. The carbenicillin was added to culture media as a 1000X stock solution (50 mg/mL) in water. The chloramphenicol was added to culture media as a 1000X stock solution (34 mg/mL) in EtOH.

The concentration of the DNA sequences was measured using a Thermo Scientific NanoDrop spectrophotometer. *E. coli* were incubated in a Thermo Scientific MaxQ Shaker 6000. *E. coli* were lysed using a QSonica Q500 ultrasonic homogenizer. Analytical reverse-phase HPLC was performed on an Agilent 1200 instrument equipped with a Phenomonex Aeris PEPTIDE 2.6u XB-C18 column with a Phenomonex SecurityGuard ULTRA cartridges guard column for C18 column. Preparative reverse-phase HPLC was performed on a Rainin Dynamax instrument SD-200 equipped an Agilent ZORBAX 300SB-C8 semi-preparative column (9.4 x 250 mm) with a ZORBAX 300SB-C3 preparative guard column (9.4 x 15 mm). During purifications, the C8

column and the guard column were heated to 80 °C in a Sterlite plastic bin equipped with a Kitchen Gizmo Sous Vide immersion circulator. HPLC grade acetonitrile and deionized water (18 MΩ), each containing 0.1% trifluoroacetic acid (TFA), were used for analytical and preparative reverse-phase HPLC. MALDI-TOF mass spectrometry was performed using an AB SCIEX TOF/TOF 5800 System.

Isolation of pET-Sac-Aβ(M1–42) plasmid

I received the pET-Sac-Aβ(M1–42) plasmid from Addgene as a bacterial stab and immediately streaked the bacteria onto a LB agar-plate containing carbenicillin (50 mg/L). Colonies grew in < 24h. Single colonies were picked and used to inoculate 5 mL of LB broth containing carbenicillin (50 mg/L). The cultures were shaken at 225 rpm overnight at 37˚C. To isolate the pET-Sac-Aβ(M1–42) plasmids, minipreps were performed using a Zymo ZR plasmid miniprep kit. The concentration of the plasmids was measured using a Thermo Scientific Nanodrop instrument.

Molecular cloning

DNA sequences for Aβ(MC1–42) and Aβ(MC1–40)

DNA sequences for Aβ(MC1–42) and Aβ(MC1–40) were ordered from Genewiz. Figure S1 shows the design of the DNA sequences for Aβ(MC1–42) and Aβ(MC1–40).

3' and 5' overhangs *Nde1* restriction site/start codon stop codons

Sac1 restriction site codon for cysteine

>Aβ(MC1–42)

GATATA CAT ATG TGC GAC GCT GAA TTC CGT CAC GAC TCT GGT TAC GAA GTT CAC CAC CAG AAG CTG GTG TTC TTC GCT GAA GAC GTG GGT TCT AAC AAG GGT GCT ATC ATC GGT CTG ATG GTT GGT GGC GTT GTG ATC GCT TAA TAG GAGCTC GATCCG

>Aβ(MC1–40)

GATATA CAT ATG TGC GAC GCT GAA TTC CGT CAC GAC TCT GGT TAC GAA GTT CAC CAC CAG AAG CTG GTG TTC TTC GCT GAA GAC GTG GGT TCT AAC AAG GGT GCT ATC ATC GGT CTG ATG GTT GGT GGC GTT GTG TAA TAG GAGCTC GATCCG

Figure 2.S1. Design of the DNA sequences for Aβ(MC1–42) and Aβ(MC1–40).

Restriction enzyme digestion of pET-Sac-Aβ(M1–42)

The pET-Sac-Aβ(M1–42) plasmid was digested using *SacI* and *NdeI* restriction enzymes. Table 2.S1 details the restriction reaction conditions. Reagents were added in the order they are listed.

Table 2.S1. Double-digestion of the pET- Sac Aβ(M1–42) plasmid.

Reagents	Amount
pET-Sac Aβ(M1–42)	20 µL of 50 ng/uL plasmid solution (1.0 µg in total)
10X CutSmart buffer	5.0 µL
H_2O	23.0 µL
NdeI restriction enzyme	1.0 µL (1 U)
SacI-HF restriction enzyme	1.0 µL (1 U)
Total	50.0 µL
Time	1.0 h
Temperature	37.0 °C

Next, to prevent backbone self-ligation, the digested plasmid was treated with shrimp alkaline phosphatase (rSAP). Table 2.S2 details the rSAP reaction conditions.

Table 2.S2. SAP treatment of the vectors.

Reagents	Amount
Double-digestion mixture	50.0 µL
rSAP	1.0 µL (1U)
Total	51.0 µL
Time	0.5 h
Temperature	37.0 °C
Heat inactivation	65.0 °C for 20 min

After the rSAP reaction and heat inactivation were complete, the reaction mixture was mixed with DNA loading buffer and loaded onto a 1% agarose gel containing ethidium bromide (5 µL per 100 mL gel). The agarose gel was run at 100 V for ~30 min. A UV box was used to visualize the digested pET-Sac vector (~4500 bp), which was excised from the gel using a razor blade. The digested pET-Sac vector was purified from the agarose gel using a Zymoclean gel DNA recovery kit. The concentration of the vector after purification was measured using a Thermo Scientific Nanodrop instrument. The purified digested pET-Sac linear vector was used in the subsequent ligation step.

The Aβ(MC1–42) and Aβ(MC1–40) DNA sequences were digested using *SacI* and *NdeI* restriction enzymes. Table 2.S3 details the restriction reaction conditions. Reagents were added in the order they are listed.

Table 2.S3. Double-digestion of the inserts.

Reagents	Amount
DNA sequence encoding mutation	20 µL of 5 ng/µL DNA solution (100.0 ng in total)
10X CutSmart buffer	2.5 µL
H_2O	1.5 µL
NdeI restriction enzyme	0.5 µL (0.5 U)
SacI-HF restriction enzyme	0.5 µL (0.5 U)
Total	25.0 µL
Time	1.0 h
Temperature	37.0 °C
Heat inactivation	65.0 °C for 20 min

T4 ligation of the Aβ(MC1–42) and Aβ(MC1–40) DNA sequences and the linear digested pET-Sac vector

The inserts and the vectors were ligated together using T4 ligase. Table 2.S4 details the T4 ligation reaction conditions. Reagents were added in the order they are listed.

Table 2.S4. T4 ligation of the inserts and the vectors.

Reagents	Amount	
	Insert:Vector = 0:1 (molar ratio) (negative control)	Insert:Vector = 5:1 (molar ratio)
Vector	9.1 µL of 6.6 ng/µL DNA solution (60.0 ng in total)	9.1 µL of 6.6 ng/µL DNA solution (60.0 ng in total)
Insert	---	2.5 µL of 4.0 ng/µL DNA solution (10.0 ng in total)
10X T4 DNA ligase reaction buffer	2.0 µL	2.0 µL
T4 DNA ligase	1.0 µL	1.0 µL
H_2O	7.9 µL	5.4 µL
Total	20.0 µL	20.0 µL
Ligation time	10 min	
Temp	22.0 °C (room temperature)	
Heat inactivation	65.0 °C for 10 min	

2 µL of the ligation reaction mixture was then transformed into TOP10 Ca^{2+}-competent *E. coli* using the heat shock method. The cell cultures were spread on LB agar plates containing carbenicillin (50 mg/L). Single colonies were picked to inoculate 5 mL of overnight cultures in LB media with carbenicillin (50 mg/L). The plasmids were extracted from TOP10 cells using

Zymo ZR plasmid miniprep kit. The concentration of the plasmids was measured through Thermo Scientific NanoDrop spectrophotometer. The DNA sequences of the Aβ(MC1–42) and Aβ(MC1–40) were verified by DNA sequencing.

Bacterial expression of Aβ(C1–42) and Aβ(C1–40)

Transformation of Aβ(MC1–42) and Aβ(MC1–40) and expression of Aβ(C1–42) and Aβ(C1–40)

All liquid cultures were performed in culture media (LB broth containing 50 mg/L carbenicillin and 34 mg/L chloramphenicol). Aβ(MC1–42) and Aβ(MC1–40) plasmids were transformed into BL21 DE3 PLysS Star Ca^{2+}-competent *E. coli* through heat shock method. The cell cultures were spread on LB agar plates containing carbenicillin (50 mg/L) and chloramphenicol (34 mg/L). Single colonies were picked to inoculate 5 mL of culture media for overnight culture. [A glycerol stock of BL21 DE3 PLysS Star Ca^{2+}-competent *E. coli* bearing the plasmids was made, and the future expressions were started by inoculating culture media with an aliquot of the glycerol stock.] The next day, all 5 mL of the overnight culture were used to inoculate 1 L of culture media. After inoculation, the culture was shaken at 225 rpm at 37 ˚C until the cell density reached an OD_{600} of approximately 0.45. Protein expression was then induced by the addition of isopropyl β-D-1-thiogalactopyranoside (IPTG) to a final concentration of 0.1 mM, and the cells were shaken at 225 rpm at 37 °C for 4 h with IPTG. The cells were then harvested by centrifugation at 4000 rpm using a JA-10 rotor (2800 x g) at 4 ˚C for 25 min, and the cell pellets were then stored at -80°C.

Cell lysis and inclusion body preparation

To lyse the cells, the cell pellet was resuspended in 20 mL of buffer A (10 mM Tris/HCl, 1 mM EDTA, pH 8.0) and sonicated for 2 min on ice (50% duty cycle) until the lysate appeared homogenous. The lysate was then centrifuged for 25 min at 16000 rpm using a JA-18 rotor (38000 x g) at 4˚C. The supernatant was removed, and the pellet was resuspended in buffer A, sonicated and centrifuged as described above. The sonication and centrifugation steps were repeated three times for Aβ(C1–42) or two times for Aβ(C1–40). After the last round of sonication and centrifugation, the supernatant was removed, the remaining pellet was resuspended in 15 mL of freshly prepared buffer B (8 M urea, 10 mM Tris/HCl, 1 mM EDTA, pH 8.0), and was sonicated as described above, until the solution became clear.

Peptide purification

The solution (15 mL) was then diluted with 10 mL of buffer A and filtered through a Fisher Brand 0.22 µm non-sterile hydrophilic PVDF syringe filter (Catalog No. 09-719-00). Analytical reverse-phase HPLC was performed to evaluate if expression of Aβ(C1–42) or Aβ(C1–40) was successful. A 20-µL sample of the above solution was injected onto an Agilent 1200 instrument equipped with a Phenomonex Aeris PEPTIDE 2.6u XB-C18 column with a Phenomonex SecurityGuard ULTRA cartridges guard column for C18 column. HPLC grade acetonitrile (ACN) and 18 MΩ deionized water, each containing 0.1% trifluoroacetic acid, were used as the mobile phase. The sample was eluted at 1.0 mL/min with a 5–100% acetonitrile gradient over 20 min, at 60 °C.

Aβ(C1–42) and Aβ(C1–40) were then purified by preparative reverse-phase HPLC equipped with an Agilent ZORBAX 300SB-C8 semi-preparative column (9.4 x 250 mm) with a ZORBAX 300SB-C3 preparative guard column (9.4 x 15 mm). The C8 column and the guard column were heated to 80 °C in a water bath. HPLC grade acetonitrile (ACN) and 18 MΩ deionized water, each containing 0.1% trifluoroacetic acid, were used as the mobile phase at a flow-rate of 5 mL/min. The peptide solution was split into three ~8 mL aliquots, and purified in three separate runs. The peptide was loaded onto the column by flowing 20% ACN for 10 min and then eluted with a gradient of 20–40% ACN over 20 min. Fractions containing the monomer generally eluted from 34% to 38% ACN. After the peptide was collected, the column was washed by flushing with 100% isopropanol for 15 minutes. This cleaning procedure ensures elution of all peptide that is retained in the column and avoids problems of cross-contamination between runs.

The purity of each fraction was assessed using analytical reverse-phase HPLC. A 20-µL sample was injected onto the analytical HPLC. The sample was eluted at 1.0 mL/min with a 5–100% acetonitrile gradient over 20 min, at 35 °C. Pure fractions were combined and the purity of the combined fractions were checked using analytical HPLC. The combined fractions were directly used in desired conjugation reactions. Alternatively, the combined fractions were concentrated by rotary evaporation to remove ACN, and then frozen with dry ice, liquid nitrogen, or a -80 °C freezer. [It is recommended to combine and freeze the purified fractions within 5 hours after purification to avoid oxidation of methionine.] The frozen sample was then lyophilized to give a fine white powder.

Labeling of Aβ(C1–42) and Aβ(C1–40)

Conjugation reactions were performed by mixing combined pure fractions of Aβ(C1–42) or Aβ(C1–40) and concentrated bioconjugate reagents in molar excess. Maleimide reagents were dissolved in 100% DMSO in 10 mg/mL and 2-5 excess molar equivalent was added to the combined fractions with a micropipette. The pH of the reaction mixture is adjusted to pH 6-7 with aqeous NaOH for 5 minutes, and then is acidified to pH 2-3. The reaction progress was monitored using an analytical HPLC. Then, the solution is centrifuged to pellet unreacted dyes, and the supernatant is subjected to purification by preparative HPLC and pure fractions of conjugated Aβ(C1–42) or Aβ(C1–40) peptide are combined and lyophilized, and the sample was then lyophilized and the powders were kept in -20 °C in a desiccator.

Mass spectrometry

MALDI mass spectrometry was performed using an AB SCIEX TOF/TOF 5800 System. 0.5 µL of sinapinic acid was dispensed onto a MALDI sample support, followed by the addition of 0.5 µL peptide sample. The mixture was allowed to air-dry. All analyses were performed in positive reflector mode, collecting data with a molecular weight range of 2000–8000 Da.

For the fragmentation experiment (Figure 2.S3 and 2.S4), MALDI mass spectrometry was performed in MS/MS mode targeting m/z = 4617 mass. The expected fragmentation masses of Aβ(C1-42) were generated via fragment ion calculator[3].

SDS-PAGE

For the sample preparation, a 0.3 mg aliquot of Aβ(C1–42) peptide was dissolved in 50 μL of deionized water to give a 6 mg/mL peptide stock solution. A 20 μL aliquot of the 6 mg/mL stock solution was set aside. Another 20 μL aliquot of the 6 mg/mL stock solution was then serial diluted with 20 μL of deionized water to create 20 μL of peptide stock solutions with concentrations of 3 mg/mL to 0.09 mg/mL. 4 μL of 6X SDS-PAGE loading buffer (100 mM Tris buffer at pH 6.8, 20% (v/v) glycerol, and 4% w/v SDS) was then added each peptide stock solutions to give 24 μL of peptide working solutions with concentrations from 5 mg/mL to 0.08 mg/mL. A 10 μL aliquot of each working solution was run on a 16% polyacrylamide gel with a 4% stacking polyacrylamide gel. The gels were run at a constant 90 volts at room temperature.

The SDS-PAGE gel of fluorescein-labeled Aβ(C1-42) was visualized with a Bio-Rad ChemiDoc Imager with fluorescence with excitation at 494 nm.

TEM imaging

TEM images of fluorescein-labeled Aβ(C1-42) were taken with a JEM-2100F transmission electron microscope (JEOL, Peabody, MA, USA) at 200 kV with an electron dose of approximately 15 e^-/A^2. The microscope was equipped with Gatan K2 Summit direct electron detector (Gatan, Pleasanton, CA, USA) at 15,000x or 25,000x magnification. The sample was cooled at liquid nitrogen temperature through the cryostage. Contrast and brightness of the images were adjusted as appropriate.

Fluorescent microscopy with SH-SY5Y cells

SH-SY5Y cells were plated in a 96-well plate at 50,000 cells per well. Cells were incubated in 100 µL of a 1:1 mixture of DMEM:F12 media supplemented with 10% fetal bovine serum, 100 U/mL penicillin, and 100 µg/mL streptomycin at 37 °C in a 5% CO2 atmosphere and allowed to adhere to the bottom of the plate for 24 hours. Working solutions of fluorescein-Aβ were prepared by dissolving a 0.1 µmol aliquot of fluorescein-Aβ in 10 µL of 20 mM NaOH and 90 µL of media. After 24 hours, cells were treated with 10 µL of fluorescein-Aβ working solution. Treated wells were incubated for an additional 24 hours and then imaged in the 96-well plate using a Keyence BZ-X810 with 20x magnification.

Characterization Data

Analytical HPLC trace of Aβ(C1–42)

% Purity: >97%

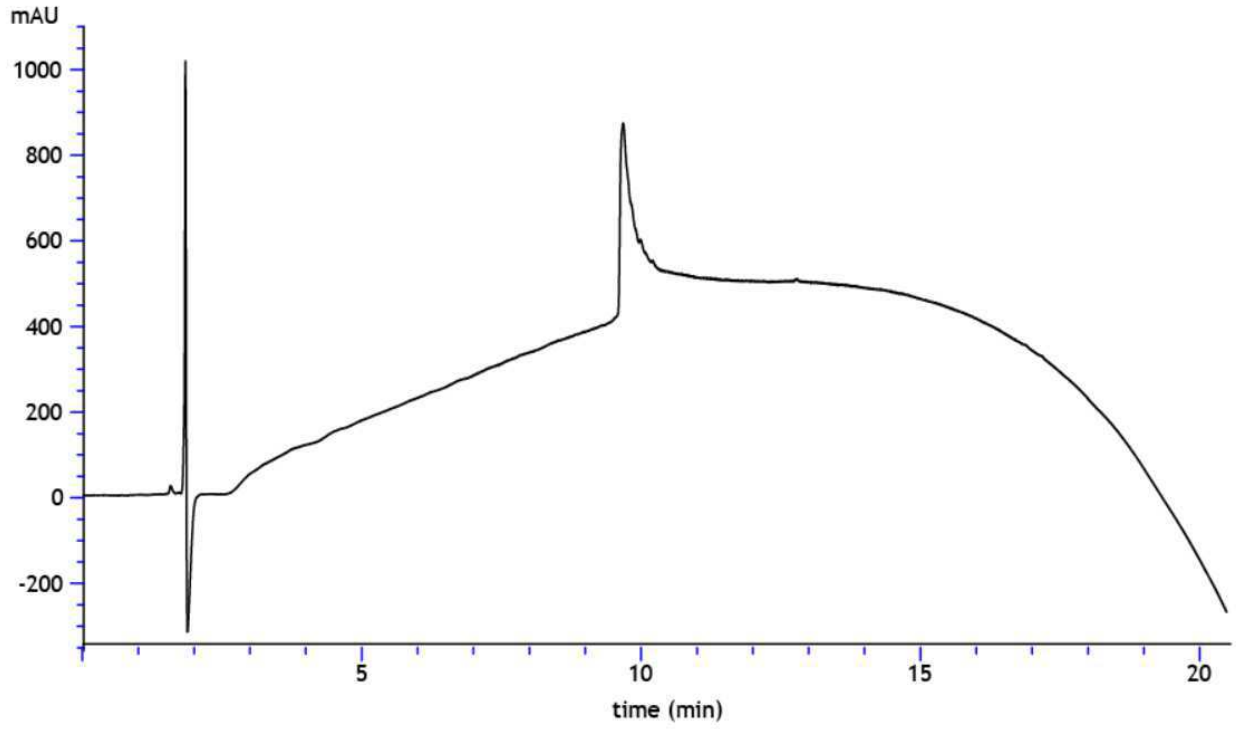

MALDI-MS trace of Aβ(C1–42)

Positive reflector mode; Matrix: Sinapinic acid

Exact mass calculated for M^+: 4613.3; Exact mass calculated for $[M+H]^+$: 4614.3; Exact mass calculated for $[M+2H]^{2+}$: 2307.7. Observed $[M+H]^+$: 4614.5; Observed $[M+2H]^{2+}$: 2307.7.

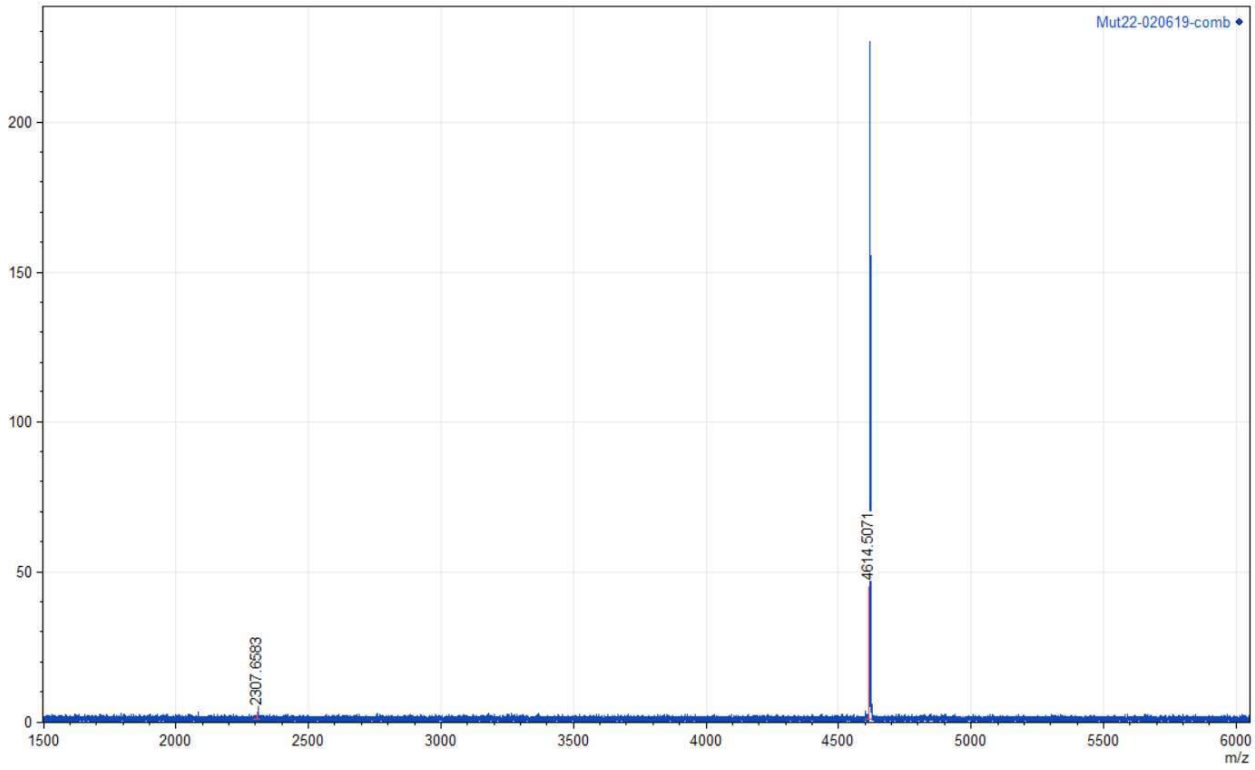

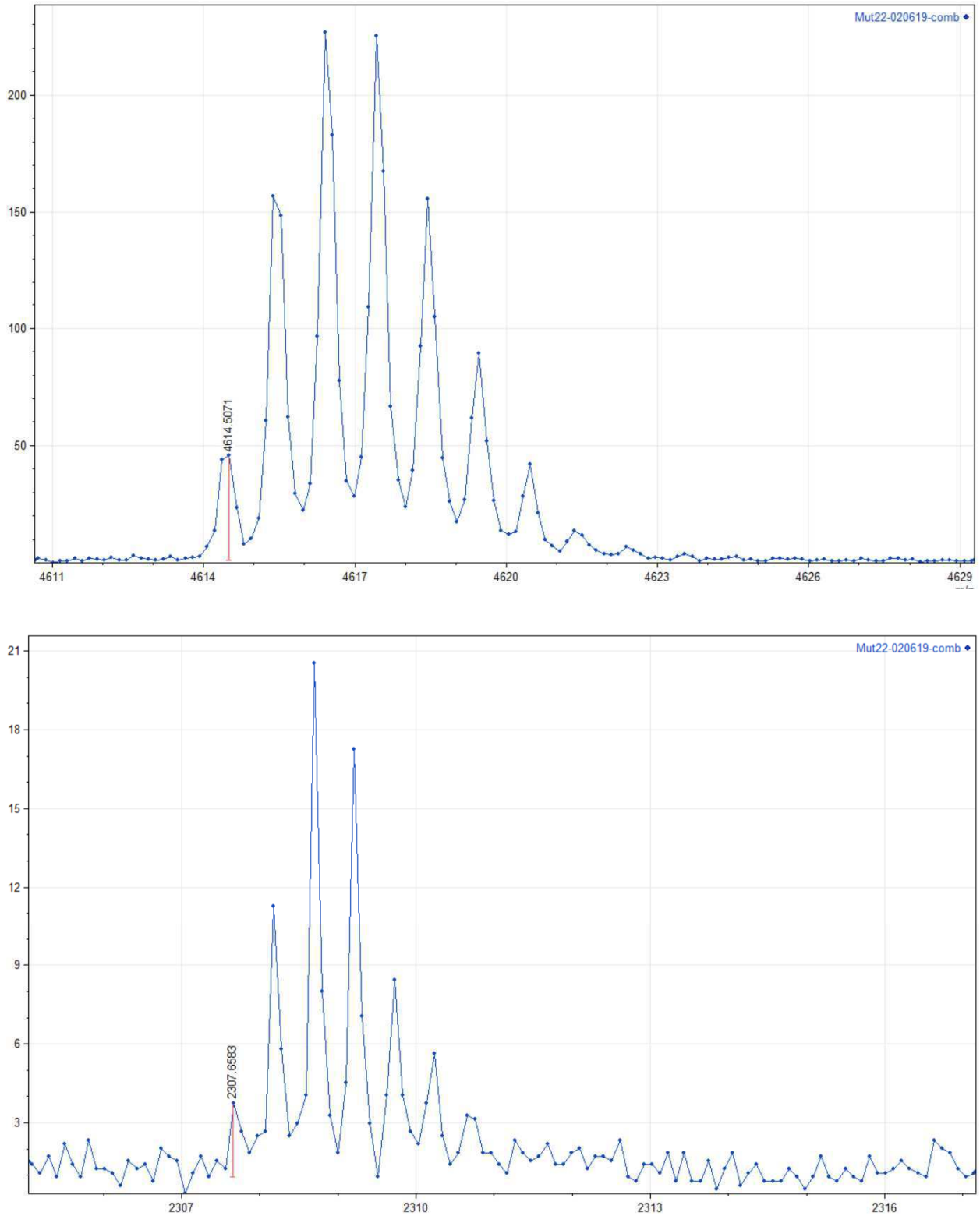

Figure 2.S2. Analytical HPLC and MALDI-MS traces of Aβ(C1–42).

MS/MS fragmentation at m/z = 4617

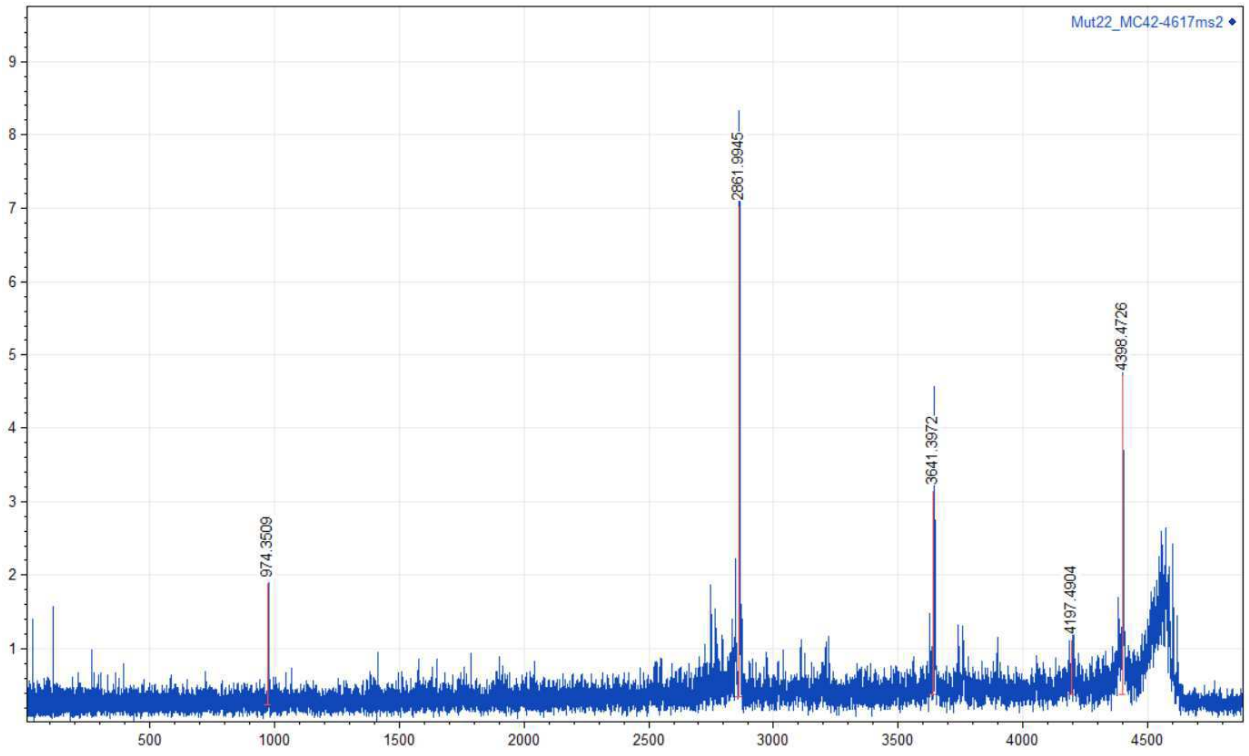

Figure 2.S3. MS/MS fragmentation spectrum of m/z = 4617.

Sequence: **CDAEFRHDSGYEVHHQKLVFFAEDVGSNKGAIIGLMVGGVVIA**, pI: **5.31109**

Fragment Ion Table, monoisotopic masses

Seq	#	B	Y	# (+1)
C	1	104.01651	4615.28610	43
D	2	219.04345	4512.27691	42
A	3	290.08056	4397.24997	41
E	4	419.12316	4326.21286	40
F	5	566.19157	4197.17027	39
R	6	722.29268	4050.10185	38
H	7	859.35159	3894.00074	37
D	8	974.37853	3756.94183	36
S	9	1061.41056	3641.91489	35
G	10	1118.43203	3554.88286	34
Y	11	1281.49535	3497.86139	33
E	12	1410.53795	3334.79807	32
V	13	1509.60636	3205.75547	31
H	14	1646.66527	3106.68706	30
H	15	1783.72418	2969.62815	29
Q	16	1911.78276	2832.56924	28
K	17	2039.87772	2704.51066	27
L	18	2152.96179	2576.41570	26
V	19	2252.03020	2463.33163	25
F	20	2399.09861	2364.26322	24
F	21	2546.16703	2217.19481	23
A	22	2617.20414	2070.12639	22
E	23	2746.24673	1999.08928	21
D	24	2861.27368	1870.04669	20
V	25	2960.34209	1755.01974	19
G	26	3017.36355	1655.95133	18
S	27	3104.39558	1598.92987	17
N	28	3218.43851	1511.89784	16
K	29	3346.53347	1397.85491	15
G	30	3403.55494	1269.75995	14
A	31	3474.59205	1212.73848	13
I	32	3587.67611	1141.70137	12
I	33	3700.76018	1028.61731	11
G	34	3757.78164	915.53324	10
L	35	3870.86570	858.51178	9
M	36	4001.90619	745.42772	8
V	37	4100.97460	614.38723	7
G	38	4157.99607	515.31882	6
G	39	4215.01753	458.29735	5
V	40	4314.08594	401.27589	4
V	41	4413.15436	302.20748	3
I	42	4526.23842	203.13906	2
A	43	4597.27554	90.05500	1

Figure 2.S4. Fragmentation ion table for Aβ(C1-42). B

Analytical HPLC trace of Fluorescein-labeled Aβ(C1–42)

% Purity: >95%

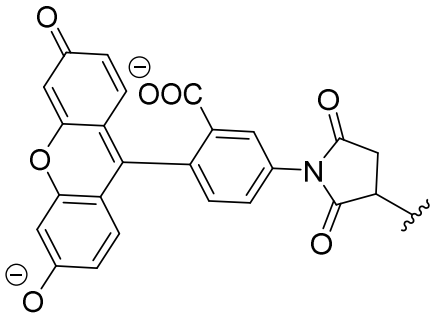

(Fluorescein-5-Maleimide)

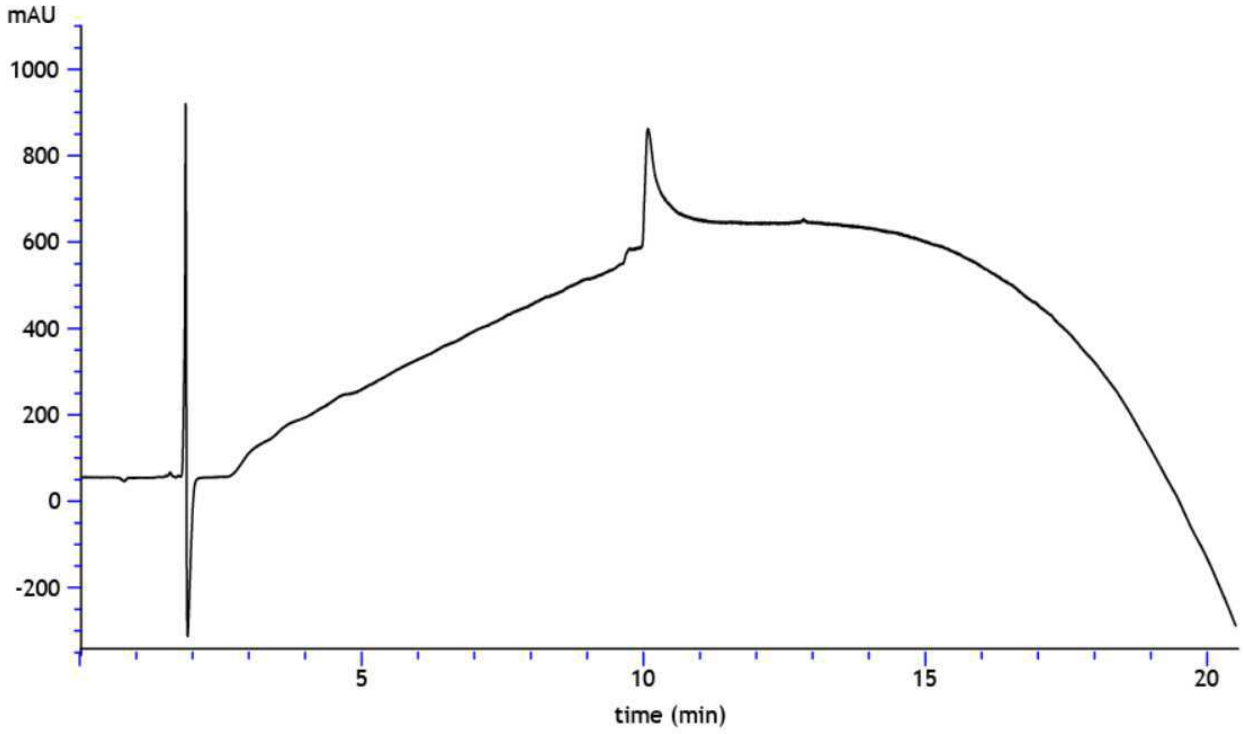

MALDI-MS trace of fluorescein-labeled Aβ(M1–42)

Positive reflector mode. Matrix: Sinapinic acid.

Exact mass calculated for M^+: 5040.6; Exact mass calculated for $[M+H]^+$: 5041.6; Exact mass calculated for $[M+2H]^{2+}$: 2521.3. Observed $[M+H]^+$: 5041.9; Observed $[M+2H]^{2+}$: 2521.4.

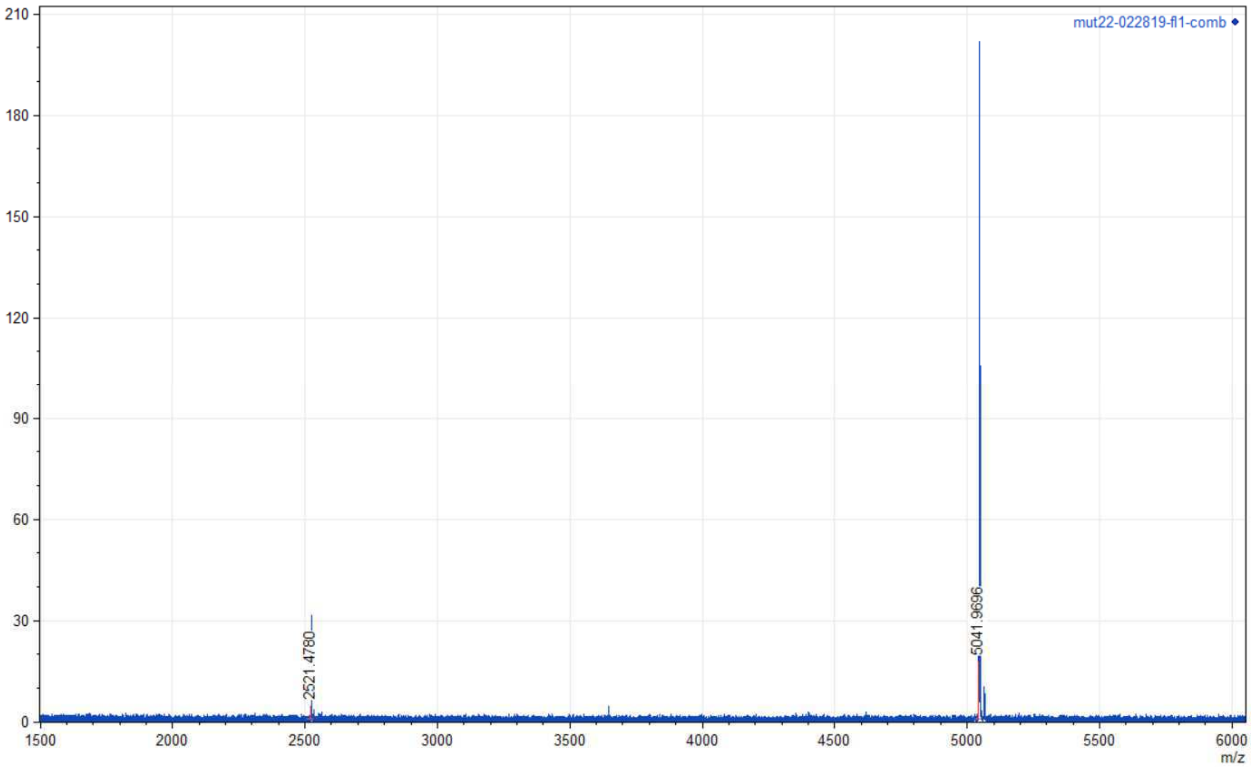

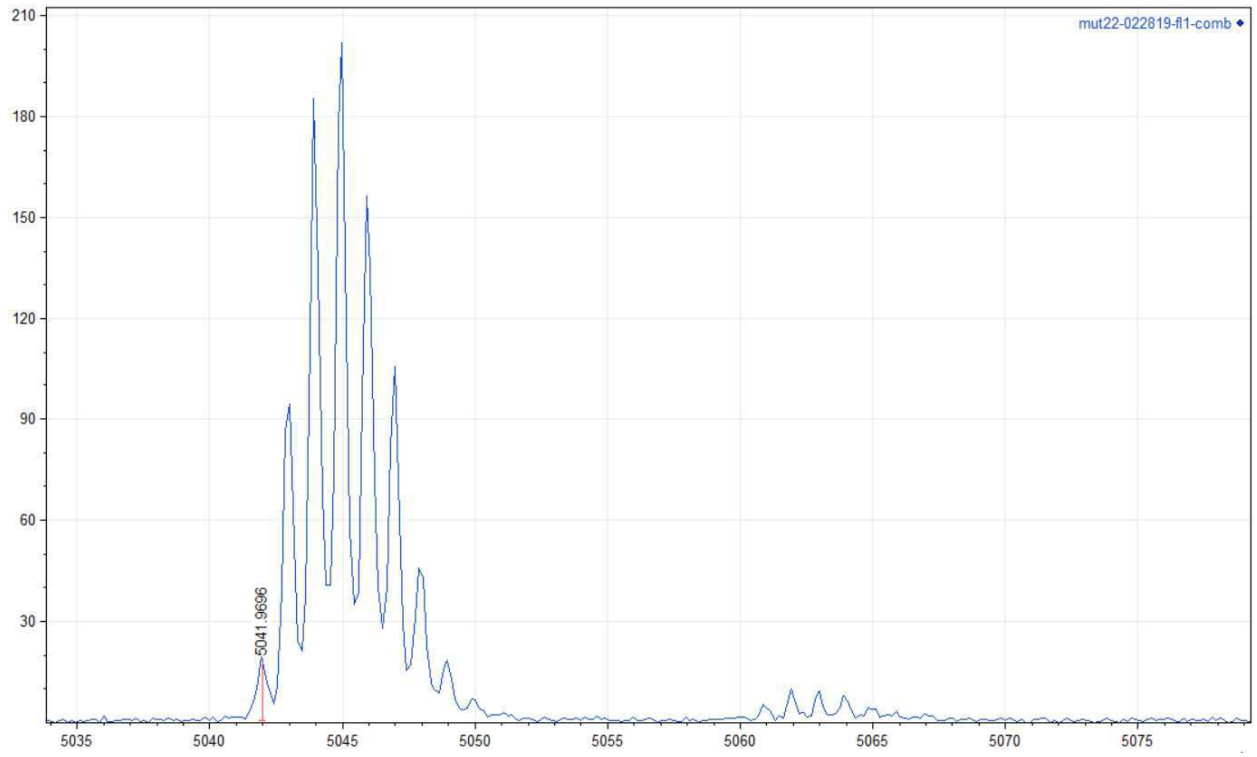

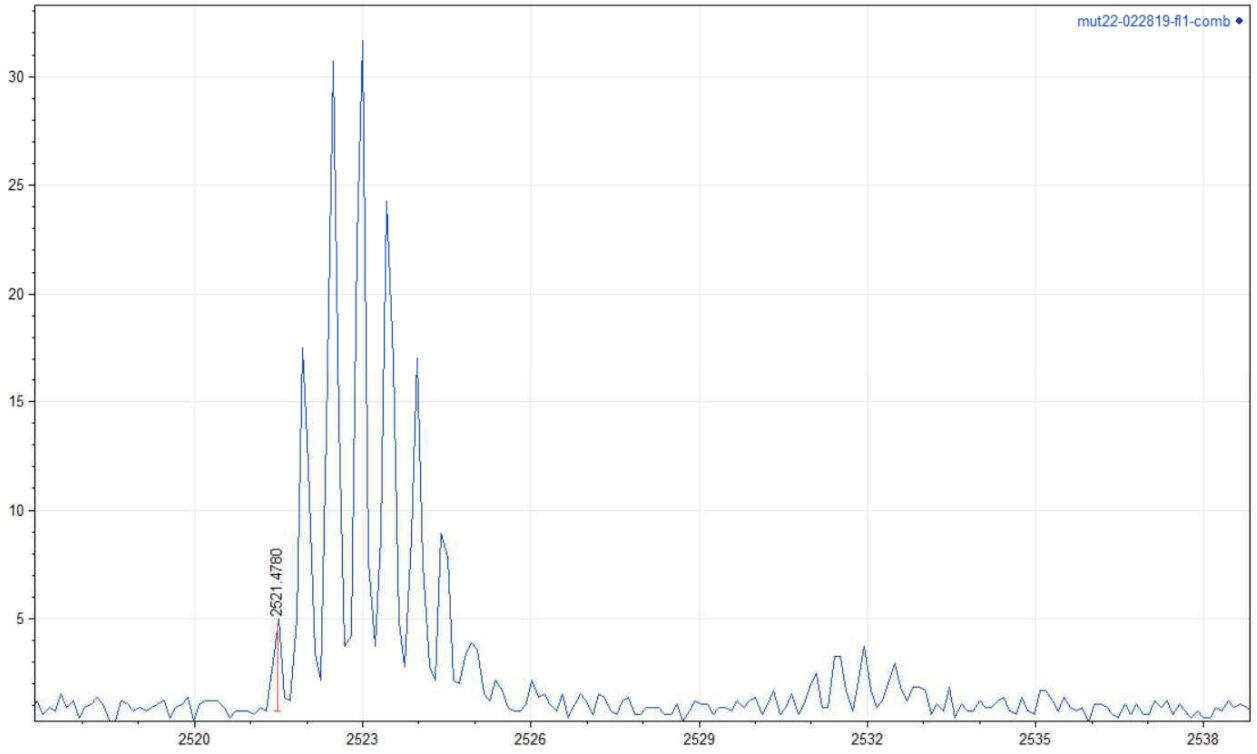

Figure 4.S5. Analytical HPLC and MALDI-MS traces of Fluorescein-labeled Aβ(C1–42).

Analytical HPLC trace of TAMRA-labeled Aβ(C1–42)

% Purity: >95%

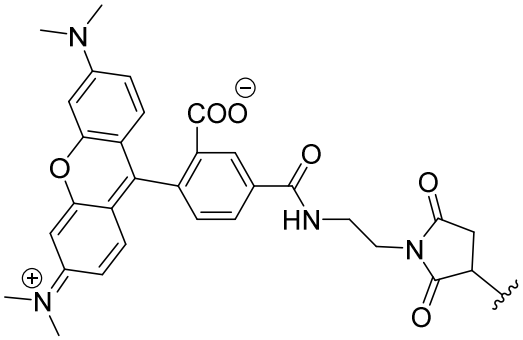

(TAMRA maleimide, 6-isomer)

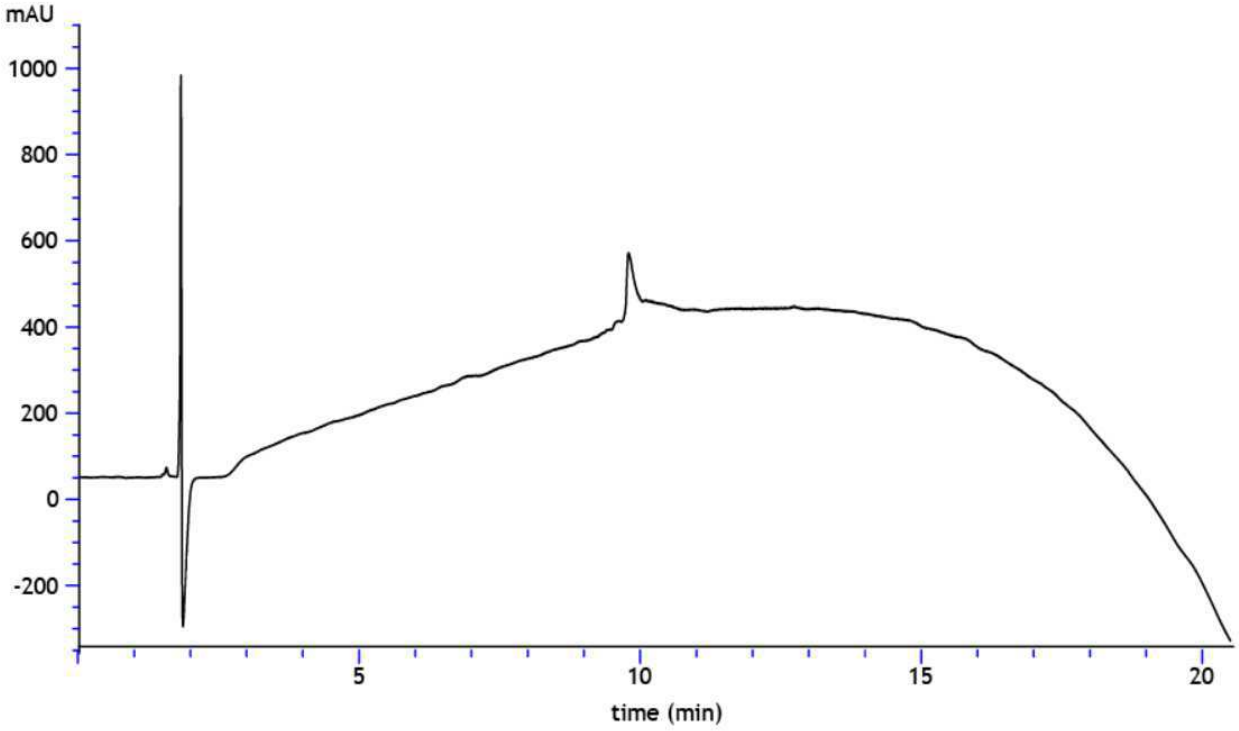

MALDI-MS trace of TAMRA-labeled Aβ(C1-42)

Positive reflector mode. Matrix: Sinapinic acid.

Exact mass calculated for M^+: 5165.9; Exact mass calculated for $[M+H]^+$: 5166.9, Exact mass calculated for $[M+2H]^{2+}$: 2583.9. Observed $[M+H]^+$: 5167.0; Observed $[M+2H]^{2+}$: 2583.9.

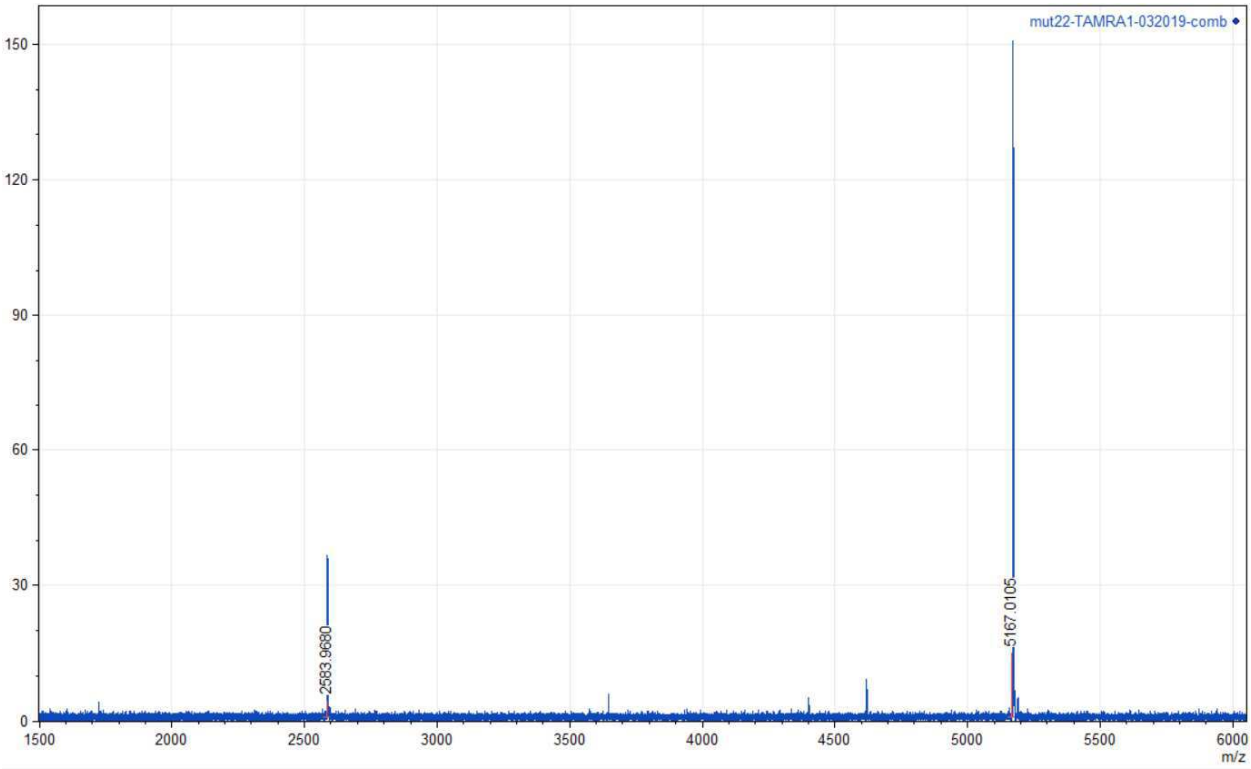

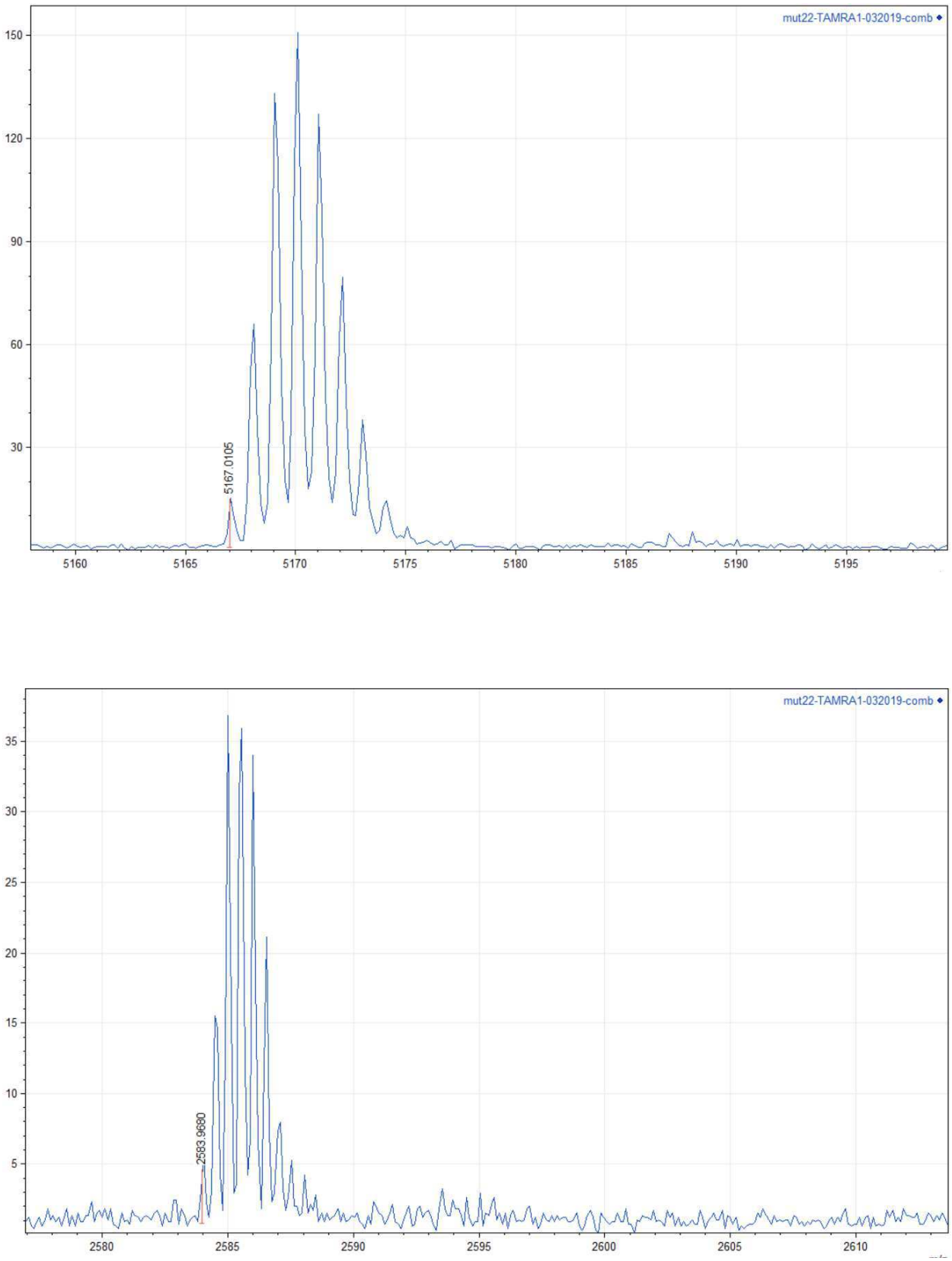

Figure 4.S6. Analytical HPLC and MALDI-MS traces of TAMRA-labeled Aβ(C1-42).

Analytical HPLC trace of Biotin-labeled Aβ(C1–42)

% Purity: >95%

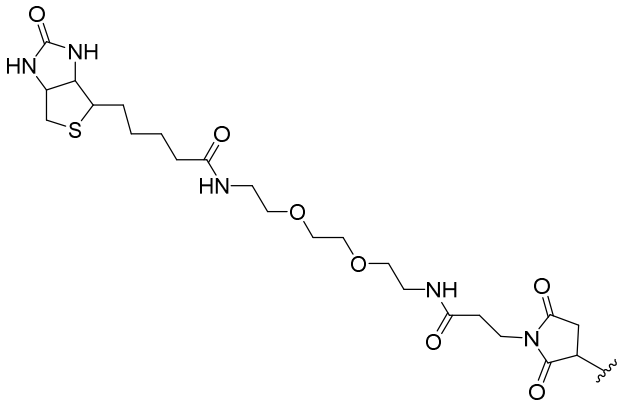

(Maleimide-PEG$_2$-Biotin)

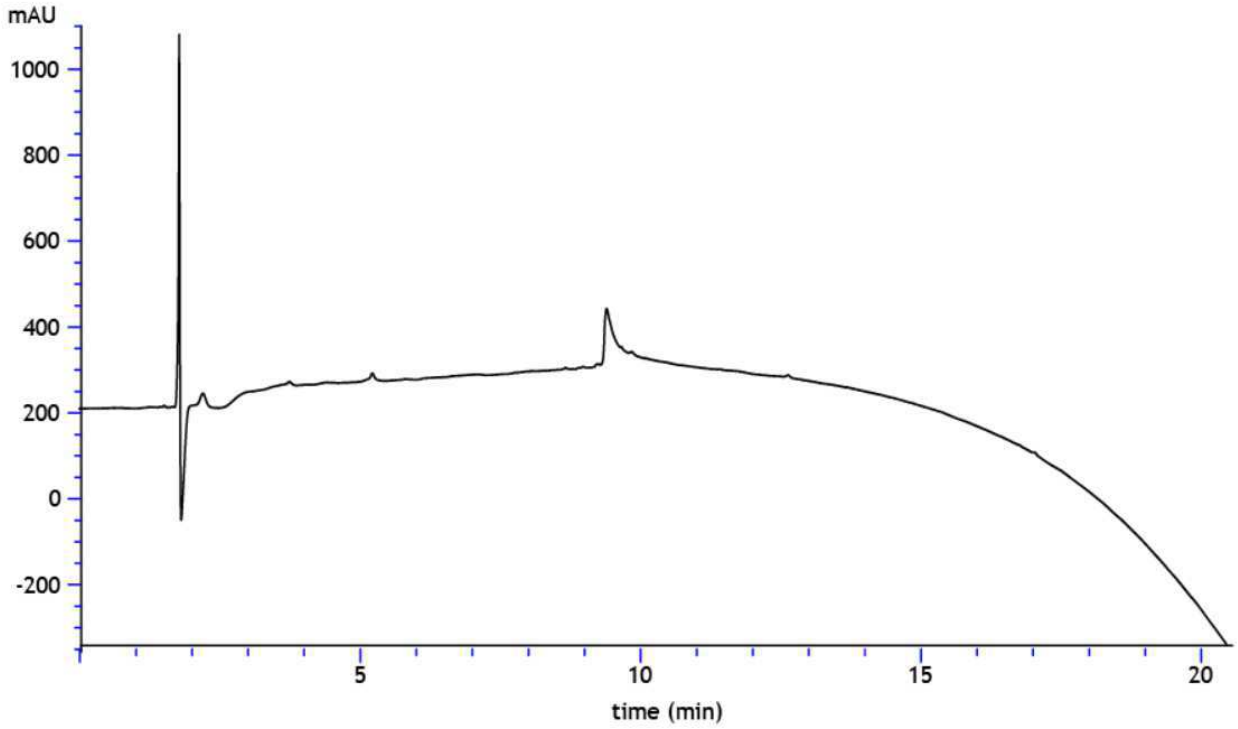

MALDI-MS trace of biotin-labeled Aβ(C1-42).

Positive reflector mode.

Matrix: Sinapinic acid.

Exact mass for M^+: 5138.9; Exact mass calculated for $[M+H]^+$: 5139.9; Exact mass calculated for $[M+2H]^{2+}$: 2570.5. Observed $[M+H]^+$: 5140.3; Observed $[M+2H]^{2+}$: 2570.6.

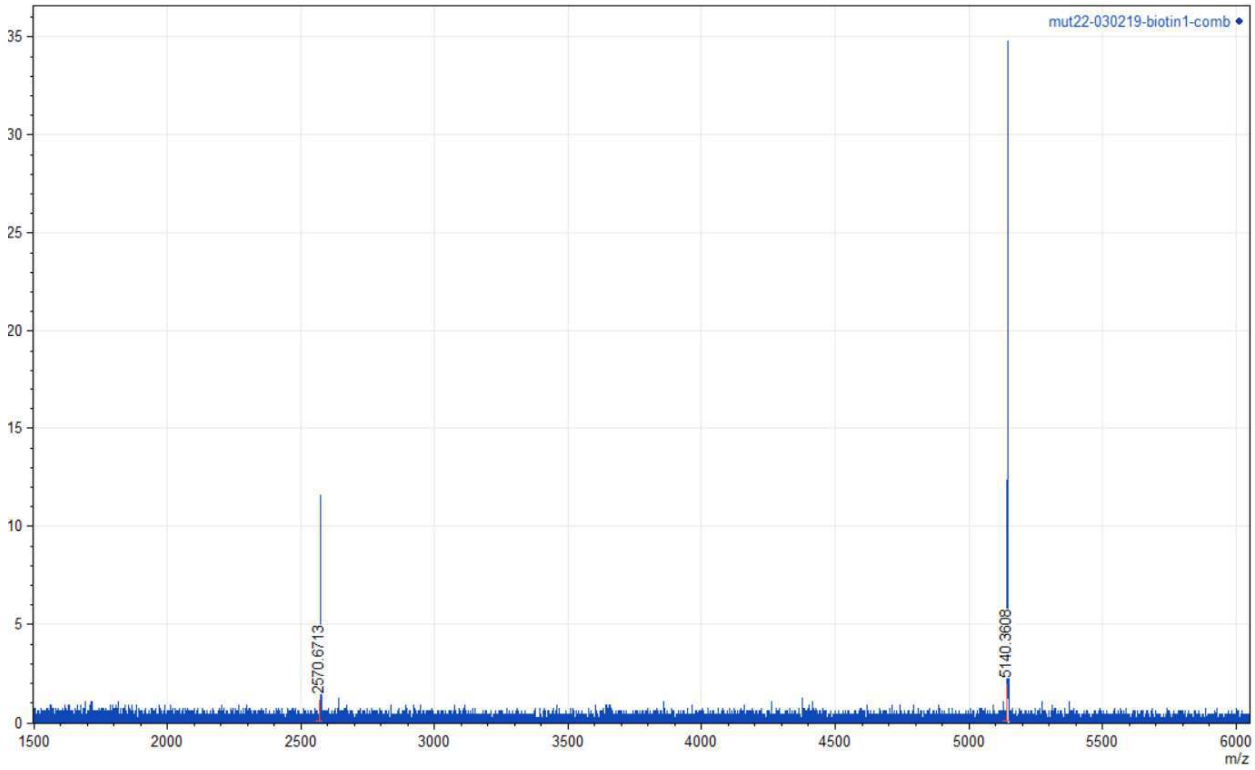

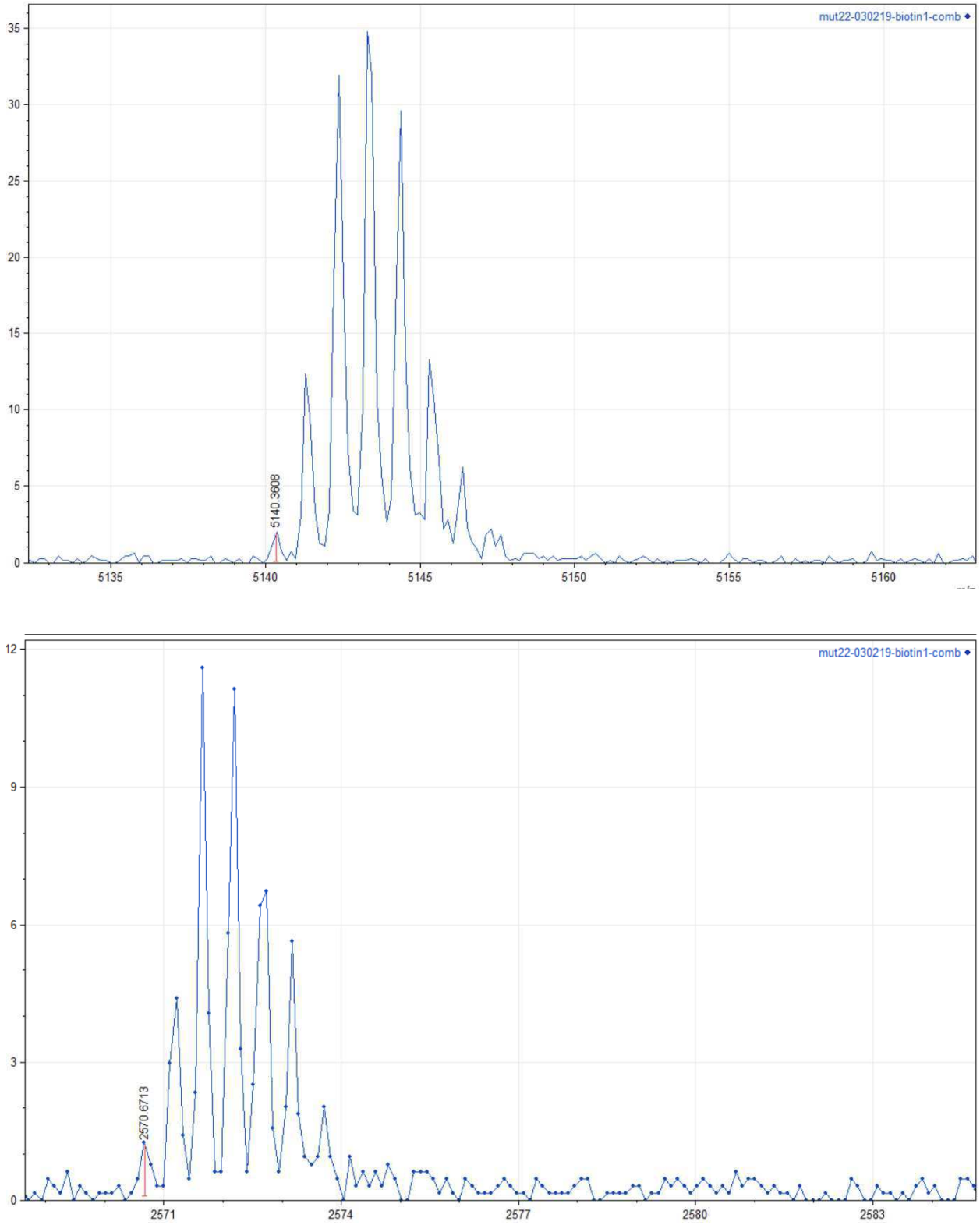

Figure 4.S7. Analytical HPLC and MALDI-MS traces of biotin-labeled Aβ(C1–42).

Analytical HPLC trace of Aβ(C1–40)

% Purity: >90%

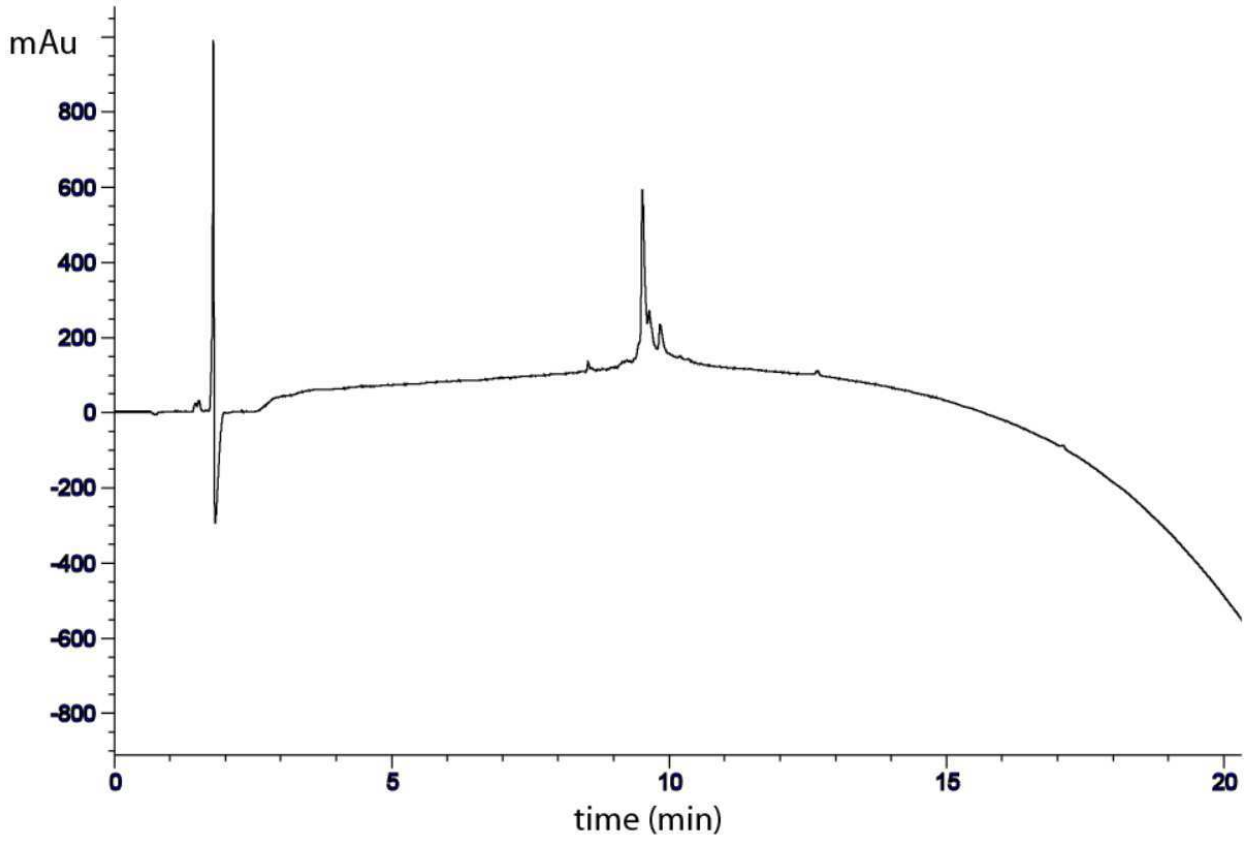

MALDI-MS trace of Aβ(C1-40).

Positive reflector mode. Matrix: Sinapinic acid.

Exact mass for M^+: 4430.1; Exact mass calculated for $[M+H]^+$: 4431.1 Observed $[M+H]^+$: 4430.6.

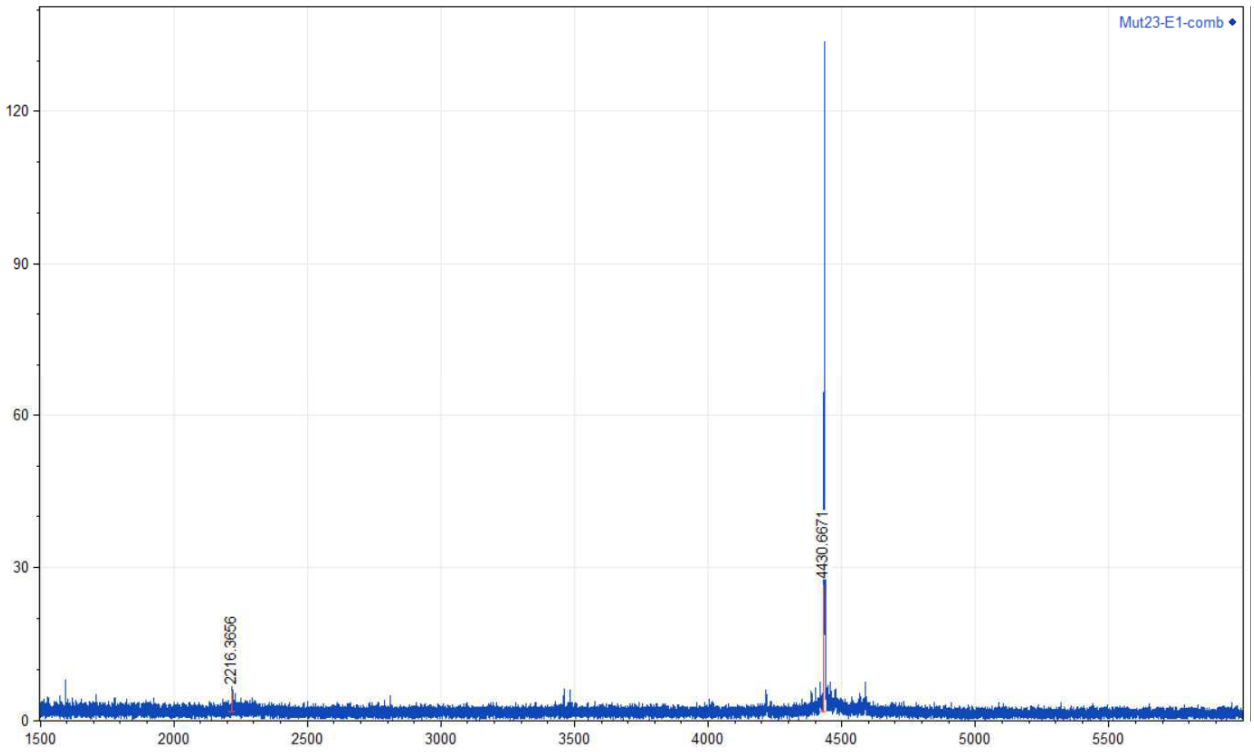

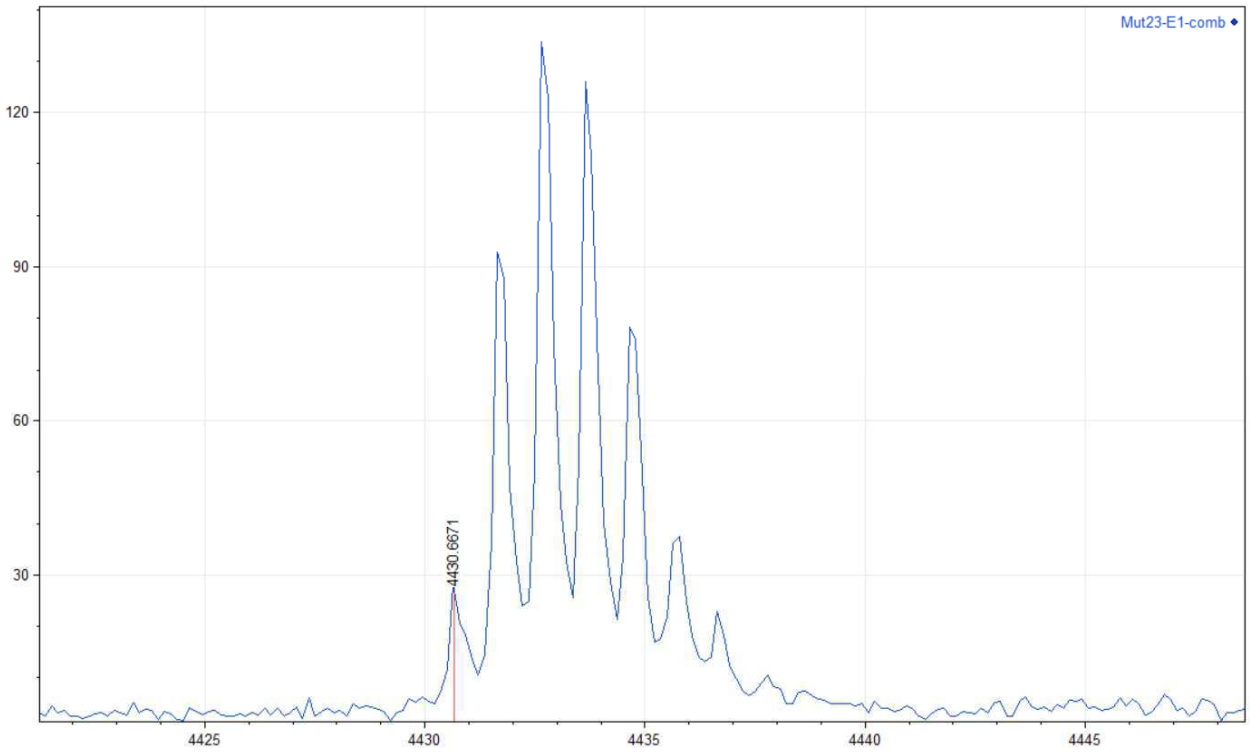

Figure 4.S8. Analytical HPLC and MALDI-MS traces of Aβ(C1–40).

References and notes

1. These procedures follow closely those that our laboratory has previously published. The procedures in this section are adapted from and in some cases taken verbatim from Yoo, S.; Zheng, S.; Kreutzer, A.; Nowick, J. Biochemistry, 2018, 57, 3861–3866.

2. Walsh, D. M.; Thulin, E.; Minogue, A. M.; Gustavsson, N.; Pang, E.; Teplow, D. B.; Linse, S., A facile method for expression and purification of the Alzheimer's disease-associated amyloid β-peptide. *FEBS J.* **2009**, *276*, 1266-1281.

3. Institute for Systems Biology: db.systemsbiology.net:8080/proteomicsToolkit/FragIonServlet.html

Chapter 3

Favoring Aβ Oligomer Formation by β-Hairpin Stabilization

Introduction

Amyloidogenic peptides or proteins self-assemble to form oligomers and fibrils in many neurodegenerative diseases such as Alzheimer's disease, Parkinson's disease, and type-2 diabetes.[1] Fibrils formed by amyloidogenic peptides or proteins are observed as plaques in patients, and the build-up of these plaques are the hallmark of amyloid diseases. The amyloid fibrils were believed to be the cause of amyloid diseases because they were observed in patients' organs. Amyloid fibrils are stable, and their structures are extensively characterized over the years through solid-state NMR spectroscopy (ss-NMR) and cryogenic electron microscopy (cryoEM). The ss-NMR and cryoEM structural studies had revealed that the fibrils are composed of an extended network of in-register parallel β-sheets and provided detailed molecular models of amyloid fibrils.[2-4]

High-resolution structures of amyloid oligomers and better understanding how amyloid oligomers formed are necessary in developing prevention or treatments of neurodegenerative diseases, such as Alzheimer's disease. Over the last few decades, soluble oligomers of β-amyloid peptides (Aβ) have emerged as crucial species in the pathogenesis of Alzheimer's Disease.[5-8] These neurotoxic oligomers are short-lived and heterogeneous in nature, making difficult to study their structures by high-resolution techniques such as NMR, X-ray crystallography, and cryo-EM.

Aβ oligomers are thought to be composed of antiparallel β-sheets comprising β-hairpins.[7, 8] Currently, there is no high-resolution structures of amyloid oligomers of full amyloid peptide or proteins. To study elusive amyloid oligomers, our laboratory has developed macrocyclic β-hairpin mimics, which gave insights into structures formed by amyloid oligomer, by X-ray crystallography and solution-phase studies. In the last five years, macrocyclic peptide mimicking β-hairpin of Aβ have been developed and studied (Figure 3.1). In 2014, Dr. Ryan Spencer synthesized and studied

macrocyclic β-hairpin templating L17 to D23 and A30 to V36. The X-ray crystallographic structure of this peptide revealed trimeric trimer assembly.[9] Furthermore, in 2016, Dr. Adam Kreutzer incorporated the β-turn within the β-hairpin in the macrocycle with a disulfide stabilization with in β-hairpin.[10] This larger macrocycle also crystallized to form the similar trimeric trimer assembly as the previous structure. These macrocyclic β-hairpin mimics and their assemblies gave insights into how the oligomers formed by the full-length Aβ may look like or behave. These models suggested a model for trimeric trimers assembly in amyloid oligomer formation.

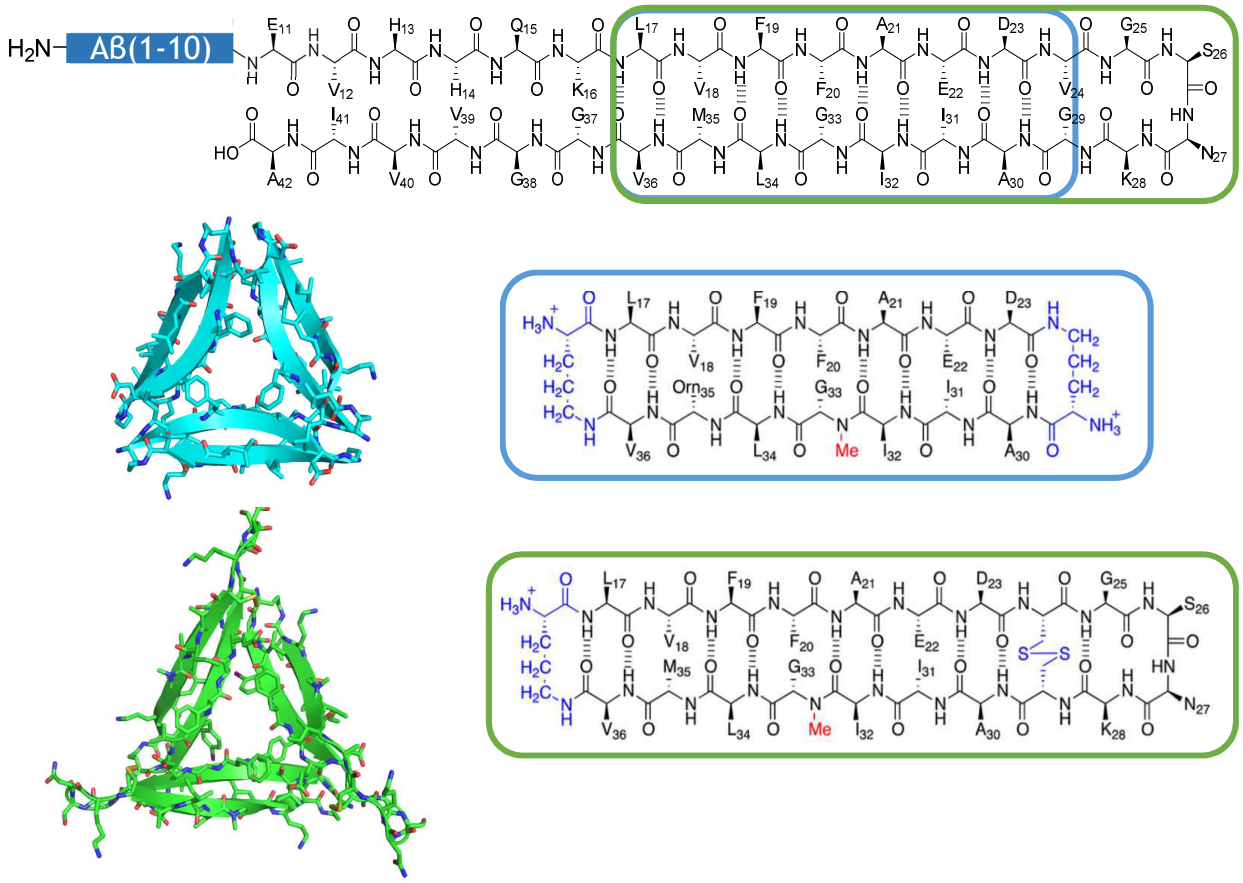

Figure 3.1. Macrocyclic peptides mimicking Aβ β-hairpin and trimeric assemblies of those peptides by X-ray crystallography.

Although macrocyclic peptides derived from Aβ β-hairpin provided unique insights into the oligomerization of Aβ, these peptides are heavily modified and engineered with functional groups and unnatural amino acids, such as N-methyl group and ornithine turns. In this chapter, I describe my effort in stabilizing β-hairpin region of Aβ and thereby favoring oligomerization and disfavoring fibrillization using the full-length peptide. Figure 3.2 illustrates the hypothesized equilibrium between Aβ monomers, oligomers, and fibrils. When Aβ monomers are stabilized within their β-hairpin regions, the pathways from monomers to fibrils and from oligomers and fibrils may be disfavored. I describe the design and expression and purification of five Aβ mutants each with two cysteine mutations, which form a disulfide linkage, within the β-hairpin region. I studied the mutants using biophysical and biological techniques.

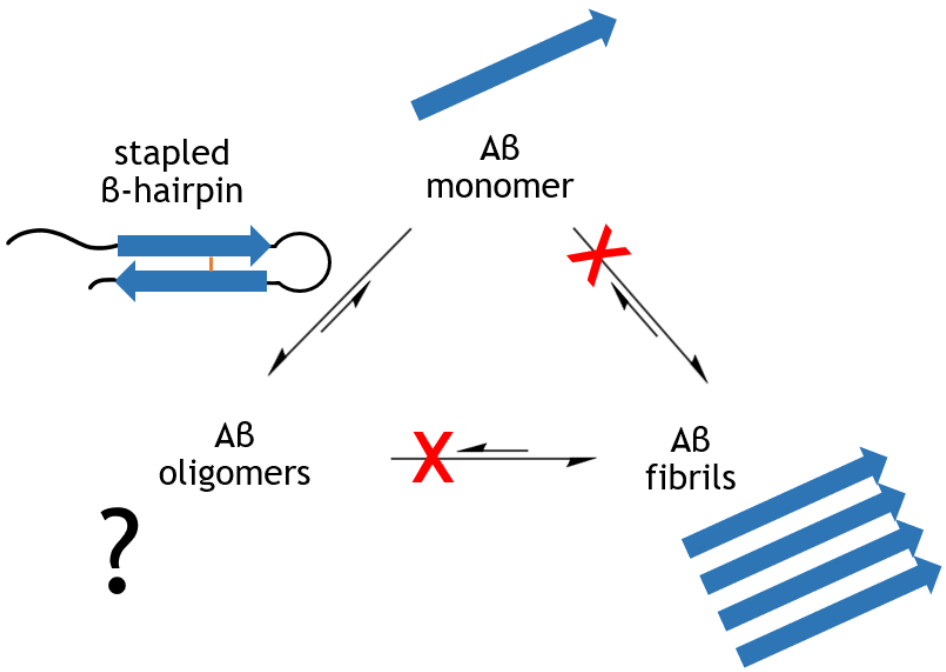

Figure 3.2. Hypothesized equilibrium between Aβ monomers, oligomers, and fibrils when the β-hairpin of Aβ monomers are stabilized. Red X's indicate hypothesized effect of disfavoring pathways from monomers to fibrils and oligomers to fibrils upon stabilization of β-hairpin.

Results and Discussion

Design of β-hairpin stabilized analogues

I chose to stabilize the β-hairpin of Aβ using a disulfide linkage formed by thiols of two cysteines. Two amino acid residues were chosen to be mutated to two cysteines for these two criteria: (1) The two amino acids need to be in close proximity and in non-hydrogen-bonded pair, which can accommodate disulfide linkages in antiparallel β-sheet conformations.[11] (2) The two mutated residues were chosen to retain the overall charge and hydrophobicity when mutated with two cysteines. This design of β-hairpin stabilization was precedented by Hoyer and coworkers who reported studies of β-hairpin stabilized monomeric Aβ.[12] In their study, they observed formation of oligomers by size exclusion chromatography and SDS-PAGE with β-hairpin stabilized Aβ.

In this study, I generated five mutants each containing two cysteines by cloning method described previously [mutant 1: A21C, A30C; mutant 2: A21C, I32C; mutant 3: V24C, G29C; mutant 4: A21C, I31C; mutant 5: V18C, G33C].[13] Expressed and purified Aβ mutants containing two cysteine residues were found to be partially oxidized, and the oxidation was monitored by MALDI-MS (Figure 3.3). Predicted isotopic patterns of fully disulfide oxidized mutants was compared with observed isotopic patterns with MALDI-MS and I was able to observe gradual shift of isotopic pattern toward the predicted isotopic pattern: increasing intensity up to the third peak and then decrease after the third peak. To fully oxidize to form homogeneous stapled mutants, DMSO was added to urea solubilized inclusion bodies and the oxidation was agitated for two days before purification (Figure 3.4).

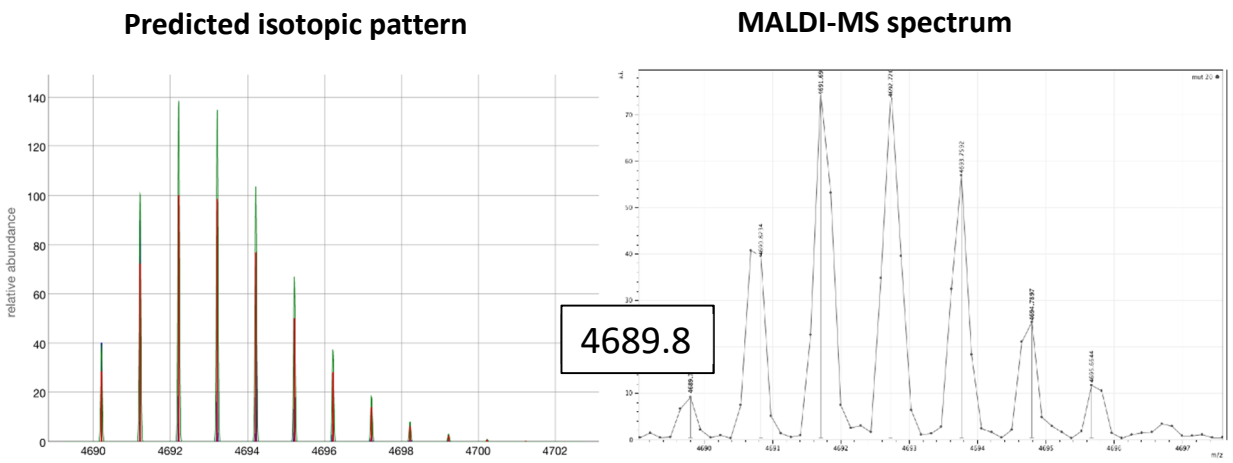

Figure 3.3. Predicted isotopic pattern of mutant 5 when it is fully oxidized (Monoisotopic mass = 4690.2) and MALDI-MS spectrum of mutant 5.

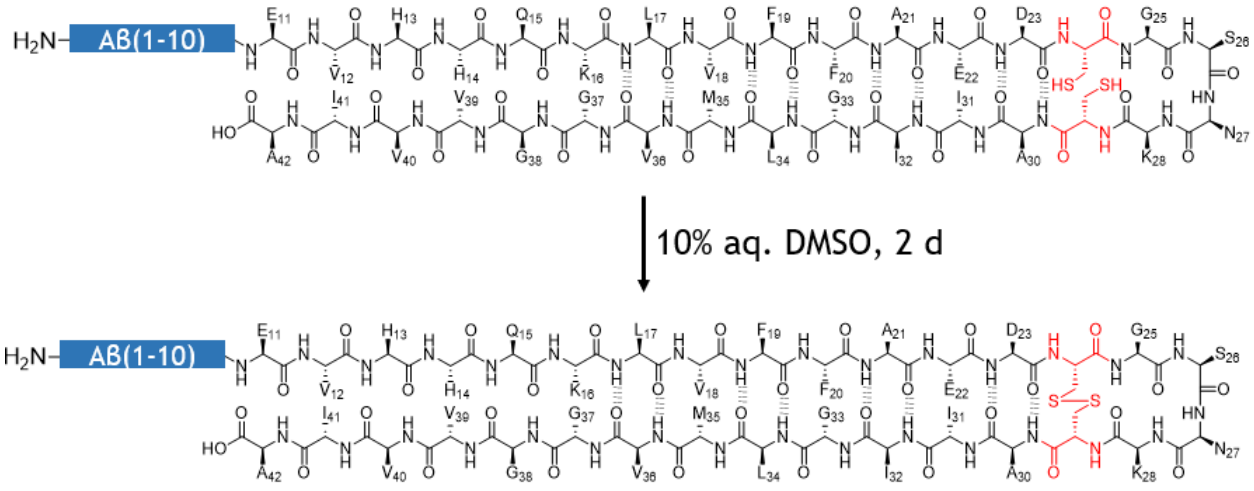

Figure 3.4. Reaction scheme for oxidation reaction to fully oxidize two thiols to form disulfide linkages.

Oligomerization observed by SDS-PAGE

Oligomerization of every Aβ mutants each with disulfide linkage in different locations along with wild-type Aβ were assessed by SDS-PAGE (Figure 3.5). The oligomerization of four mutants showed similar pattern as the wild-type Aβ. Mutant 1, containing A21C and A30C mutations, and mutant 3, containing V24C, and G29C mutations, showed higher propensity to form oligomers toward trimers and tetramers and also showed rapid equilibrium between the monomer and the trimer bands. Conversely, mutant 2 and 4 showed propensity to remain as the monomer. The most striking mutant was mutant 5, containing V18C and G33C mutations, which formed a unique oligomer species that was not observed with other mutants at slightly above 10 kDa marker. I decided to further study mutant 5 in the reminder of the project.

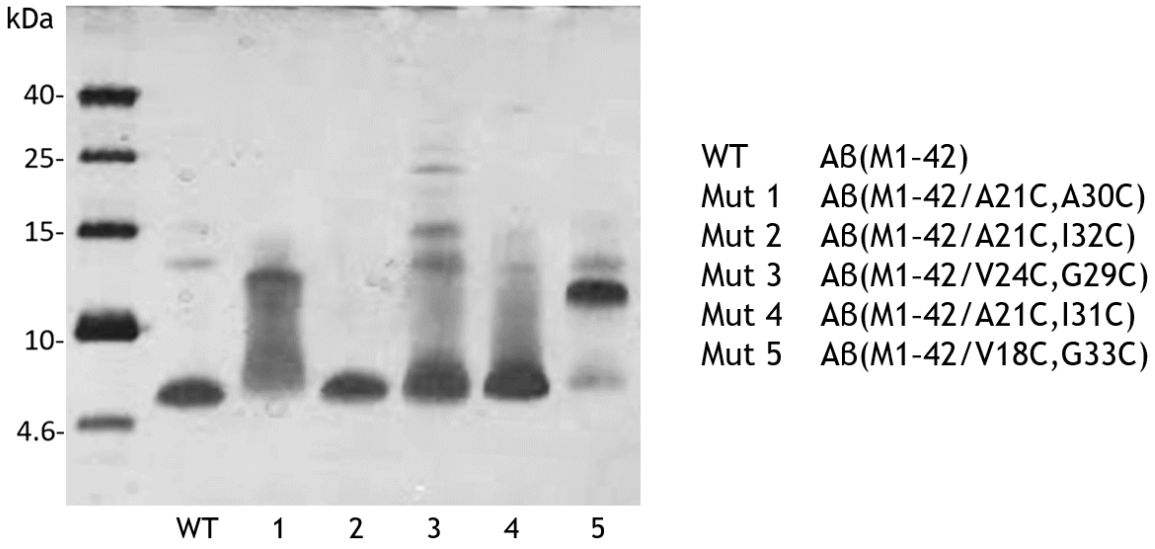

Figure 3.5. SDS-PAGE of Aβ(M1-42) and mutants containing two cysteines forming disulfide bonds within β-hairpin region.

Mutant 5, a dimeric Aβ analogue

To further investigate the oligomerization of mutant 5, Aβ(M1-42) and mutant 5 were run on SDS-PAGE with high to low loadings (Figure 3.6). The sample was prepared by dissolving NaOH treated aliquots of Aβ(M1-42) and mutant 5 in deionized water then SDS-loading buffer and diluted 2-fold multiple times. At a high loading, Aβ(M1-42) formed the trimeric and tetrameric assemblies, and at a low loading, Aβ(M1-42) mostly remained as monomer. At a high loading, mutant 5 formed a large streak between 4.6 and 15 kDa markers with large band around 12 kDa. At low loading, mutant 5 formed homogeneous band at 12 kDa. At the lowest loading of both peptides, I was able to observe striking difference in oligomerization behaviors, where Aβ(M1-42) is at its monomeric state and mutant 5 is at the dimeric state.

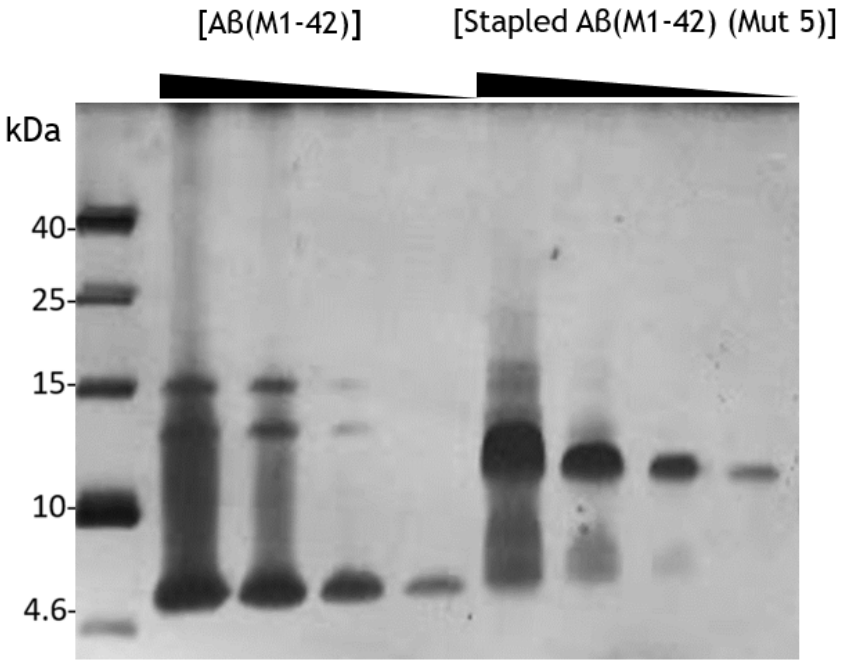

Figure 3.6. SDS-PAGE of Aβ(M1-42) and mutant 5 (Aβ(M1-42)/V18C,G33C) with different loading.

To confirm that the dimeric species of mutant 5 on SDS-PAGE is a result of intramolecular disulfide linkage rather than intermolecular, I reduced the disulfide bond with TCEP, a reducing agent, and ran reduced mutant on SDS-PAGE (figure 3.6). I had hypothesized that the reduced mutant 5 would revert back to monomer which would show monomer, trimer, and tetramer bands and would form fibril. Decreasing amounts of mutant 5 with and without disulfide reduction were loaded on an SDS-PAGE gel. The reduction reaction was performed at room temperature for 16 hours in sodium phosphate buffer containing TCEP. The gel lanes which disulfide-reduced mutant was loaded showed five major species at around 5, 11, 14, 18 kDa and a band that stayed up at the stacking gel. I believe these species are monomer, dimer, trimer, tetramer, and fibril respectively. The monomer, trimer, tetramer, and fibril bands arose from disulfide-reduced monomer, and the dimer bands must have arose from spontaneous oxidation resulting reformation of the dimer.

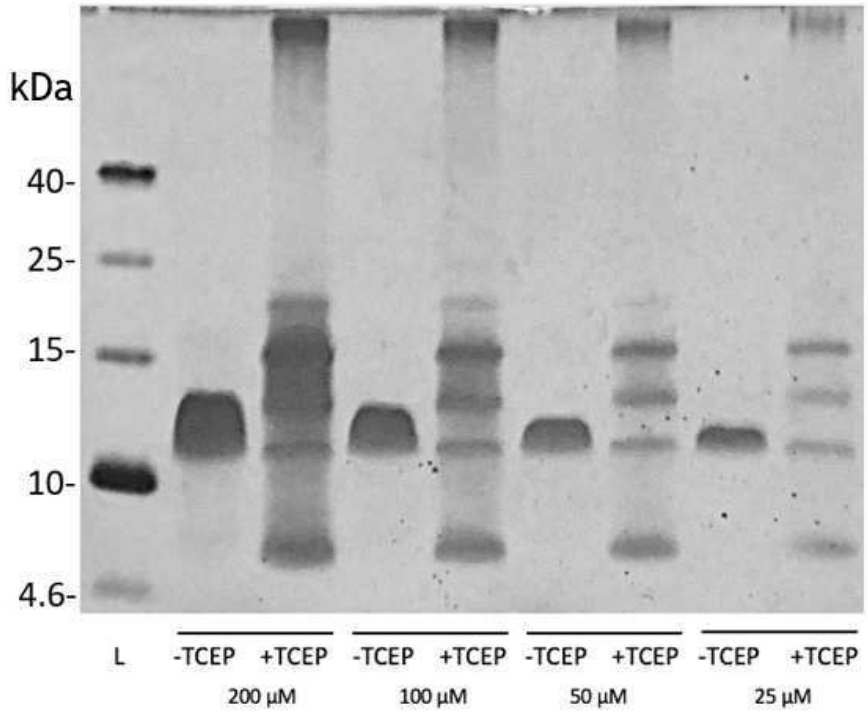

Figure 3.7. SDS-PAGE of mutant 5 with and without treatment with a reducing agent, TCEP.

Aggregation properties of a stapled Aβ, mutant 5

The aggregation properties of mutant 5 was assessed using Thioflavin (ThT) fibrillization assay, circular dichroism (CD), dynamic light scattering (DLS), and transmission electron microscopy (TEM). As hypothesized, all the assays corroborated to the fact that mutant 5 is not capable of forming large fibrils unlike Aβ(M1-42).

ThT fibrillization assay demonstrateed that Aβ(M1-42) forms fibrils within 10 minutes at 37 °C while mutant 5 does not form fibrils (Figure 3.8). The ThT samples were prepared by dissolving NaOH treated lyophilized aliquots in a buffer containing ThT, and were immediately plated on a 96-well plate for fluorescence readings. The readings were taken every 5 minutes over 24 hours. As a negative control for mutant 5, I generated the alanine variant of mutant 5, where Val 18 and Gly 33 were mutated to alanines rather than cysteines. This double alanine mutants did form fibrils after four hours of incubation. The results provided direct evidence that mutant 5 does not form fibrils as indicated by no fluorescence activity by ThT.

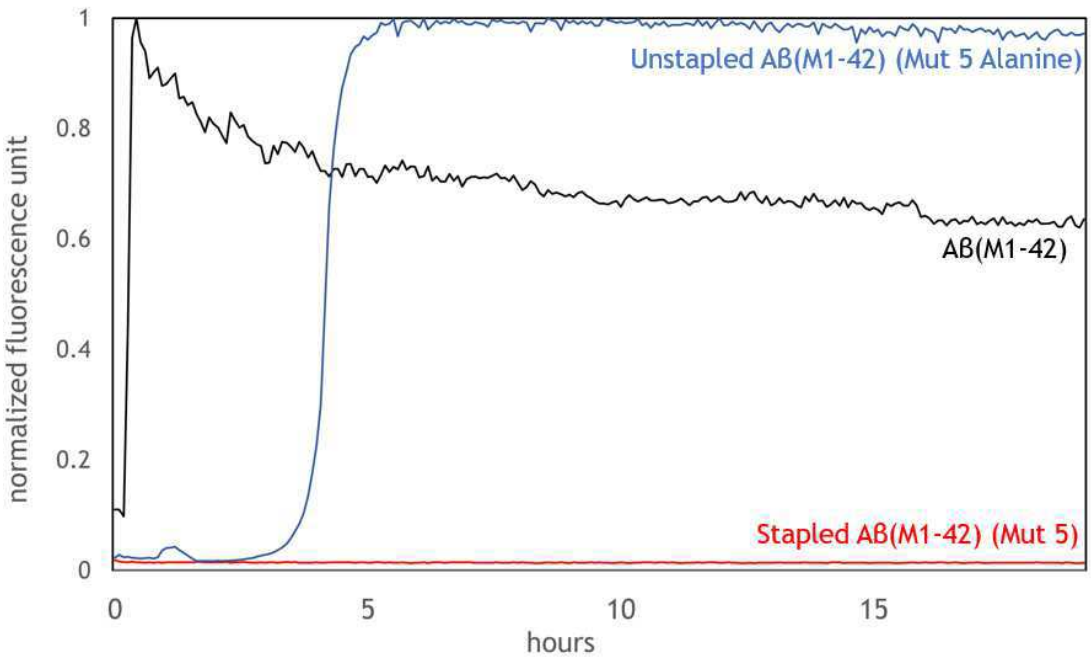

Figure 3.8. ThT fibrillization assay of Aβ(M1-42), mutant 5, and alanine variant of mutant 5.

DLS further proved that mutant 5 does not form fibrils. Aβ(M1-42) and mutant 5 were each dissolved in a phosphate buffer and were incubated at 37 °C for 16 hours. DLS measurements were performed immediately after solvation of the samples and after 16 hours of incubation (Figure 3.9). At the time of solvation, Aβ(M1-42) formed a species with hydrodynamic radius around 80 nm, and mutant 5 formed species with hydrodynamic radius around 40 nm. This result indicates that Aβ(M1-42) was already forming aggregates by the time of measurement, while mutant 5 stayed mostly as the monomer state. After 16 hours of incubation, Aβ(M1-42) formed large species with hydrodynamic radius around 1000 nm, while mutant 5 formed species with hydrodynamic radius of 50 nm. I believe that the large species formed by Aβ(M1-42) is consistent with large fibrils as observed by ThT, and the small species formed by mutant 5 is consistent with the oligomer observed SDS-PAGE.

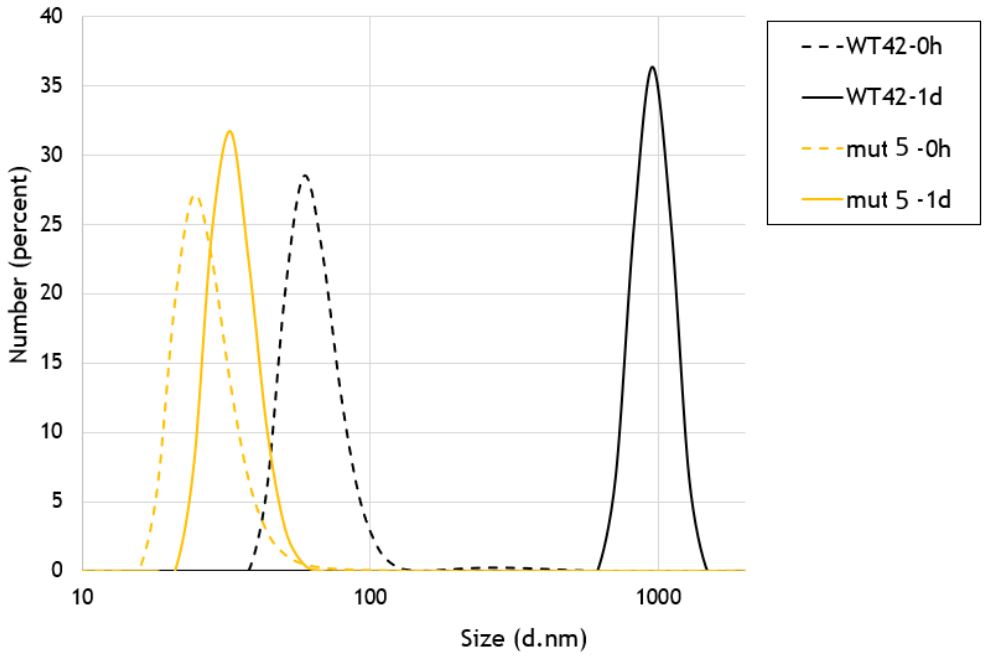

Figure 3.9. Time-course DLS of Aβ(M1-42) and mutant 5.

CD also corroborate the previous findings which indicated no fibril formation by mutant 5 (Figure 3.10). The samples for CD were prepared by dissolving NaOH aliquot powders in 10 mM sodium phosphate buffer were incubated at 37 °C for 16 hours. CD measurements were performed at the time of solvation and at 16 hour time-point. The CD spectra were deconvoluted with BeStSel (Beta structure selection) for secondary structure determination.[14] Antiparallel and parallel β-sheet characteristics were monitored for oligomer and fibril formation respectively.[7]

At the time of solvation, Aβ(M1-42) and mutant 5 showed comparable antiparallel β-sheet characteristics at 37% and 43% respectively and did not show significant parallel β-sheet characteristic. After one day of incubation, Aβ(M1-42) showed 17% parallel β-sheet characteristic, which signifies amyloid fibril formation. On the other hand, mutant 5 retained its anti-parallel characteristic at 41% and did not show any parallel β-sheet, which signifies no fibril formation.

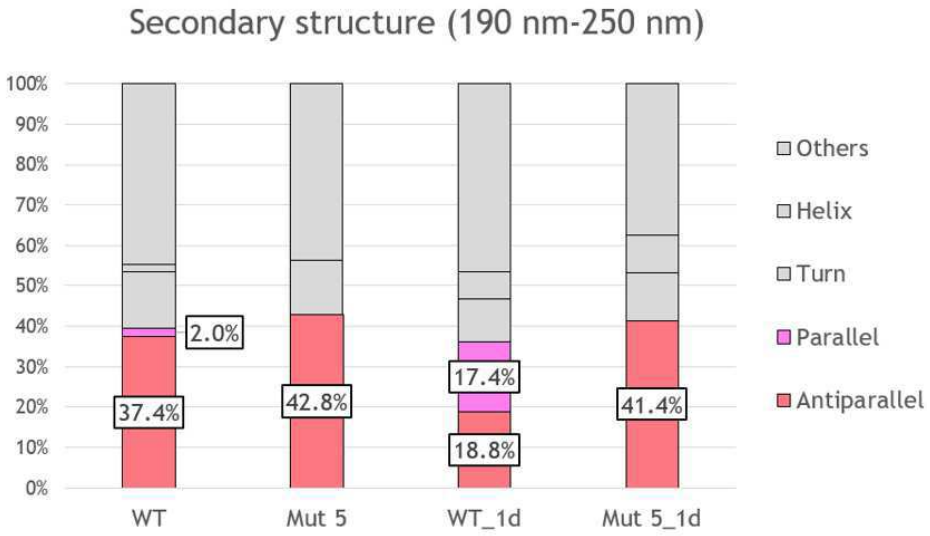

Figure 3.10. CD secondary structure deconvolution of Aβ(M1-42) and mutant 5 without incubation and one day incubation.

Lastly, TEM corroborated other experiments which further confirmed the original hypothesis about fibrillization. The TEM samples were prepared by dissolving NaOH aliquot powders in 1X PBS and were incubated without shaking at 37 °C. The glow discharged copper grids were subjected to the incubated samples then to 2% uranyl acetate for negative staining.

After one day of incubation, Aβ(M1-42) showed large fibrils, while mutant 5 showed no fibril formation (Figure 3.11). The oligomers formed by mutant 5 was not observed under TEM because the oligomers may not be uranyl acetate stain active. When disulfide bond in mutant 5 is reduced by TCEP, the fibrils were observed. These images further proved that mutant 5 do not form fibrils unlike Aβ(M1-42).

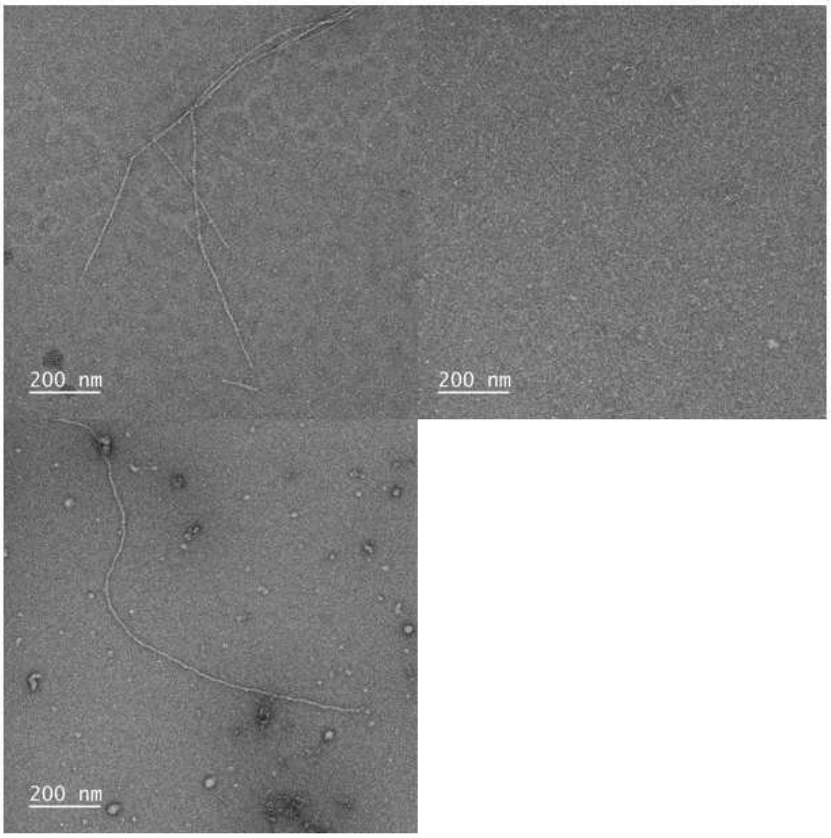

Figure 3.11. TEM images of one day incubated Aβ(M1-42) (top, left), mutant 5 (top, right), and mutant 5 with reduced disulfide bond with TCEP (bottom, left).

Mutant 6, the Aβ(M1-40) alloform of mutant 5

In order to investigate if the oligomerization behavior that is observed with mutant 5 is unique to Aβ(M1-42), mutant 6, Aβ(M1-40) alloform containing V18C and G33C mutations was prepared. DNA fragment encoding Aβ(M1-40) with V18C and G33C mutations was used to construct the recombinant plasmid. Mutant 6 was expressed, oxidized to fully oxidize thiols, and purified using the same procedure as other mutants.

The oligomerization property of mutant 6 was assessed by SDS-PAGE, similar to the gel described earlier in figure 3.6. An SDS-PGE gel was performed with decreasing loading of Aβ(M1-40) and mutant 6 (Figure 3.12). At high loading, Aβ(M1-40) formed dimeric and trimeric oligomer assemblies, and at low loading, Aβ(M1-40) mostly showed monomer. At high loading, mutant 6 formed a large streak between around 5 and 12 kDa, indicating fast equilibrium between monomer and oligomeric assemblies. As mutant 6 loading was decreased, the streaking band became shorter, at the lowest loading, mutant 6 showed similar monomeric band as Aβ(M1-40).

Although mutant 6 showed higher oligomerization propensity as Aβ(M1-40), mutant 6 did not show similar oligomerization behavior as mutant 5, which formed dimeric assembly. This result could indicate that the dimeric assembly observed with mutant 5 is unique to Aβ(M1-42) alloform.

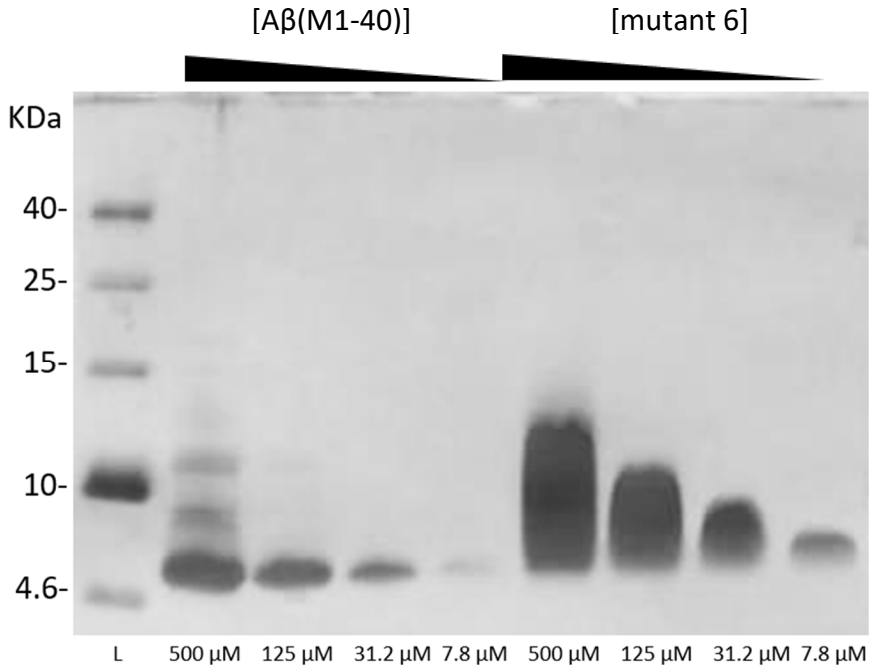

Figure 3.12. SDS-PAGE of Aβ(M1-42) and mutant 6 (Aβ(M1-40)/V18C,G33C) with different loading.

Cytotoxicity of mutant 5 and 6 with SH-SY5Y cells

Cytotoxicity profiles of Aβ(M1-42), mutant 5, Aβ(M1-40), and mutant 6, were assessed by MTT assay with SH-SY5Y human neuroblastoma cell line (Figure 5.11). Peptide samples were prepared in 10X stock in water and were added on SH-SY5Y cells on a cell culture plate. After three days of incubation, cell viability was visualized through MTT conversion to formazan assay.

The MTT assay showed that Aβ(M1-42) elicited 60% cell death without showing dose-response activity. Mutant 5 showed comparable cytotoxicity as Aβ(M1-42). This result was not expected as mutant 5, if it forms stable toxic oligomers, should be more cytotoxic. Currently, my colleague is optimizing sample preparation method for cytotoxicity to further investigate. Aβ(M1-40) showed more dose-dependency and less cytotoxicity than Aβ(M1-42). Mutant 6 was more cytotoxic than Aβ(M1-40) and as toxic as Aβ(M1-42).

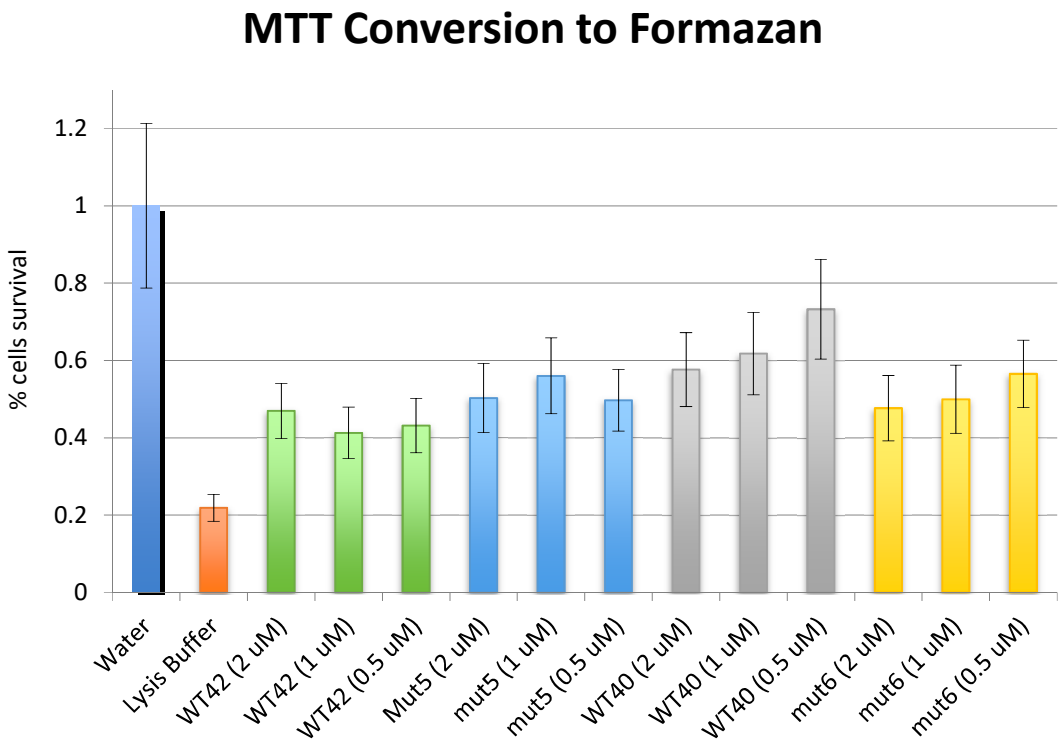

Figure 3.13. MTT conversion to formazan cytotoxicity assay for Aβ(M1-42), mutant 5, Aβ(M1-40), and mutant 6.

Conclusion

In this study, I set out to generate number of full-length Aβ with β-hairpin stabilization and study their oligomerization properties. Oligomerization properties of those peptides were assessed by SDS-PAGE and mutant 5 containing V18C and G33C mutations showed unprecedented dimeric assembly. Mutant 5's oligomerization properties were further investigated by SDS-PAGE with different loading of the peptide and with disulfide-reduced peptide. With the β-hairpin stabilization, mutant 5 was not capable of forming fibrils as evidenced by ThT fibrillization assay, DLS, CD, and TEM experiments.

Dimers of Aβ have been found and isolated from the brains of Alzheimer's patients.[15-17] Aβ dimers were found to inhibit long-term potentiation in mice and promote hyperphosphorylation of the microtubule-associated protein tau, leading to neuronal damage.[18, 19] This dimer-forming Aβ peptide may serve as a model for stable oligomer.

References and Notes

1. Chiti, F.; Dobson, C. M., Protein misfolding, amyloid formation, and human disease: A summary of the progress over the last decade. *Annu. Rev. Biochem.*, **2017**, *86*, 27-68.

2. Benzinger, T. L.; Gregory, D. M.; Burkoth, T. S.; Miller-Auer, H.; Lynn, D. G.; Botto, R. E.; Meredith, S. C., Propagating structure of Alzheimer's beta-amyloid(10-35) is parallel beta-sheet with residues in exact register. *Proc. Natl. Acad. Sci. U.S.A.* **1998**, *95*, 13407-13412.

3. Gremer, L.; Schölzel, D.; Schenk, C.; Reinartz, E.; Labahn, J.; Ravelli, R. B. G.; Tusche, M.; Lopez-Iglesias, C.; Hoyer, W.; Heise, H.; Willbold, D.; Schröder, G. F., Fibril structure of amyloid-β(1-42) by cryo-electron microscopy. *Science* **2017**, *358*, 116-119.

4. Antzutkin, O. N.; Leapman, R. D.; Balbach, J. J.; Tycko, R., Supramolecular structural constraints on Alzheimer's beta-amyloid fibrils from electron microscopy and solid-state nuclear magnetic resonance. *Biochemistry* **2002**, *41*, 15436-15450.

5. Haass, C.; Selkoe, D. J., Soluble protein oligomers in neurodegeneration: lessons from the Alzheimer's amyloid beta-peptide. *Nat. Rev. Mol. Cell. Biol.* **2007**, *8*, 101-112.

6. Yu, L.; Edalji, R.; Harlan, J. E.; Holzman, T. F.; Lopez, A. P.; Labkovsky, B.; Hillen, H.; Barghorn, S.; Ebert, U.; Richardson, P. L.; Miesbauer, L.; Solomon, L.; Bartley, D.; Walter, K.; Johnson, R. W.; Hajduk, P. J.; Olejniczak, E. T., Structural characterization of a soluble amyloid beta-peptide oligomer. *Biochemistry* **2009**, *48*, 1870-1877.

7. Scheidt, H. A.; Morgado, I.; Huster, D., Solid-state NMR reveals a close structural relationship between amyloid-beta protofibrils and oligomers. *J. Biol. Chem.* **2012**, *287*, 22822-22826.

8. Tay, W. M.; Huang, D.; Rosenberry, T. L.; Paravastu, A. K., The Alzheimer's amyloid-beta(1-42) peptide forms off-pathway oligomers and fibrils that are distinguished structurally by intermolecular organization. *J. Mol. Biol.* **2013**, *425*, 2494-2508.

9. Spencer, R. K.; Li, H.; Nowick, J. S., X-ray crystallographic structures of trimers and higher-order oligomeric assemblies of a peptide derived from Abeta(17-36). *J. Am. Chem. Soc.* **2014**, *136*, 5595-5598.

10. Kreutzer, A. G.; Hamza, I. L.; Spencer, R. K.; Nowick, J. S., X-ray Crystallographic Structures of a Trimer, Dodecamer, and Annular Pore Formed by an Abeta17-36 beta-Hairpin. *J. Am. Chem. Soc.* **2016**, *138*, 4634-4642.

11. Santiveri, C.M., León, E, Rico, M, Jiménez, M.A. Context-dependence of the contribution of disulfide bonds to beta-hairpin stability. *Chem. Eur. J.* **2008**, *14*, 488-499.

12. Hoyer, W.; Grönwall, C.; Jonsson, A.; Ståhl, S.; Härd, T., Stabilization of a beta-hairpin in monomeric Alzheimer's amyloid-beta peptide inhibits amyloid formation. *Proc. Natl. Acad. Sci. U.S.A.* **2008**, *105*, 5099-5104.

13. Yoo, S.; Zhang, S.; Kreutzer, A. G.; Nowick, J. S., An Efficient Method for the Expression and Purification of Abeta(M1-42). *Biochemistry* **2018**, *57*, 3861-3866.

14. Micsonai, A.; Wien, F.; Kernya, L.; Lee, Y. H.; Goto, Y.; Réfrégiers, M.; Kardos, J., Accurate secondary structure prediction and fold recognition for circular dichroism spectroscopy. *Proc. Natl. Acad. Sci. U.S.A.* **2015**, *112,* 3095-3103.

15. Roher, A. E.; Chaney, M. O.; Kuo, Y. M.; Webster, S. D.; Stine, W. B.; Haverkamp, L. J.; Woods, A. S.; Cotter, R. J.; Tuohy, J. M.; Krafft, G. A.; Bonnell, B. S.; Emmerling, M. R., Morphology and toxicity of Abeta-(1-42) dimer derived from neuritic and vascular amyloid deposits of Alzheimer's disease. *J. Bol. Chem.* **1996**, *271*, 20631-20635.

16. McDonald, J. M.; Savva, G. M.; Brayne, C.; Welzel, A. T.; Forster, G.; Shankar, G. M.; Selkoe, D. J.; Ince, P. G.; Walsh, D. M., The presence of sodium dodecyl sulphate-stable Abeta dimers is strongly associated with Alzheimer-type dementia. *Brain* **2010**, *133*, 1328-1341.

17. Brinkmalm, G.; Hong, W.; Wang, Z.; Liu, W.; O'Malley, T. T.; Sun, X.; Frosch, M. P.; Selkoe, D. J.; Portelius, E.; Zetterberg, H.; Blennow, K.; Walsh, D. M., Identification of neurotoxic cross-linked amyloid-beta dimers in the Alzheimer's brain. *Brain* **2019**, *142*, 1441-1457.

18. Shankar, G. M.; Li, S.; Mehta, T. H.; Garcia-Munoz, A.; Shepardson, N. E.; Smith, I.; Brett, F. M.; Farrell, M. A.; Rowan, M. J.; Lemere, C. A.; Regan, C. M.; Walsh, D. M.; Sabatini, B. L.; Selkoe, D. J., Amyloid-beta protein dimers isolated directly from Alzheimer's brains impair synaptic plasticity and memory. *Nat. Med.* **2008**, *14*, 837-842.

19. Jin, M.; Shepardson, N.; Yang, T.; Chen, G.; Walsh, D.; Selkoe, D. J., Soluble amyloid beta-protein dimers isolated from Alzheimer cortex directly induce Tau hyperphosphorylation and neuritic degeneration. *Proc. Natl. Acad. Sci. U.S.A.* **2011**, *108*, 5819-24.

Supporting Information

Table of Contents

Materials and Methods[1]

General information on materials and methods

All chemicals were used as received unless otherwise noted. Deionized water (18 MΩ) was obtained from a Thermo Scientific Barnstead Genpure Pro water purification system. The pET-Sac-Aβ(M1–42) and pET-Sac-Aβ(M1–40) were gifts from Dominic Walsh (Addgene plasmid # 71875).[2] DNA sequences that encode Aβ(M1–42/A21C–A30C), Aβ(M1–42/A21C–I32C), Aβ(M1–42/V24C–G29C), Aβ(M1–42/A21C–I31C), Aβ(M1–42/V18C–G33C), and Aβ(M1–40/V18C–G33C) were purchased in 500 ng quantities from Genewiz. *NdeI* and *SacI* restriction enzymes, CutSmart buffer, and shrimp alkaline phosphatase (rSAP) were purchased from New England Biolabs (NEB). TOP10 Ca^{2+}-competent *E. coli* and BL21 DE3 PLysS Star Ca^{2+}-competent *E. coli*, T4 ligase, and ethidium bromide were purchased from Thermo Fisher Scientific. Zymo ZR plasmid miniprep kit and Zymoclean Gel DNA recovery kit was purchased from Zymo Research. Carbenicillin and chloramphenicol were purchased from RPI Research Products. The carbenicillin was added to culture media as a 1000X stock solution (50 mg/mL) in water. The chloramphenicol was added to culture media as a 1000X stock solution (34 mg/mL) in EtOH. Dimethyl sulfoxide (DMSO) was purchased from Thermo Fisher Scientific and stored in a desiccator. 3-(4,5-Dimethylthiazol-2-yl)-2,5-Diphenyltetrazolium Bromide (MTT) reagent were purchased from Thermo Fisher Scientific.

The concentration of the DNA sequences was measured using a Thermo Scientific NanoDrop spectrophotometer. *E. coli* were incubated in a Thermo Scientific MaxQ Shaker 6000. *E. coli* were lysed using a QSonica Q500 ultrasonic homogenizer. Analytical reverse-phase HPLC was performed on an Agilent 1200 instrument equipped with a Phenomonex Aeris PEPTIDE 2.6u XB-C18 column with a Phenomonex SecurityGuard ULTRA cartridges guard column for C18

column. Preparative reverse-phase HPLC was performed on a Rainin Dynamax instrument SD-200 equipped an Agilent ZORBAX 300SB-C8 semi-preparative column (9.4 x 250 mm) with a ZORBAX 300SB-C3 preparative guard column (9.4 x 15 mm). During purifications, the C8 column and the guard column were heated to 80 °C in a Sterlite plastic bin equipped with a Kitchen Gizmo Sous Vide immersion circulator. HPLC grade acetonitrile and deionized water (18 MΩ), each containing 0.1% trifluoroacetic acid (TFA), were used for analytical and preparative reverse-phase HPLC. MALDI-TOF mass spectrometry was performed using an AB SCIEX TOF/TOF 5800 System.

Isolation of pET-Sac-Aβ(M1–42) and pET-Sac-Aβ(M1–40) plasmids

We received the pET-Sac-Aβ(M1–42) and pET-Sac-Aβ(M1–40) plasmids from Addgene as bacterial stabs and immediately streaked the bacteria onto LB agar-plates containing carbenicillin (50 mg/L). Colonies grew in < 24h. Single colonies were picked and used to inoculate 5 mL of LB broth containing carbenicillin (50 mg/L). The cultures were shaken at 225 rpm overnight at 37˚C. To isolate the pET-Sac-Aβ(M1–42) and pET-Sac-Aβ(M1–40) plasmids, minipreps were performed using a Zymo ZR plasmid miniprep kit. The concentration of the plasmids was measured using a Thermo Scientific Nanodrop instrument.

Molecular cloning

DNA sequences encoding mutant peptides

DNA sequences encoding mutant peptides were ordered from Genewiz. Figure S1 shows the design of these DNA sequences.

3' and 5' overhangs *Nde1* restriction site/start codon stop codons
Sac1 restriction site codon for cysteine

Aβ(MC1–42): 5'-GAT ATA CAT ATG GAC GCT GAA TTC CGT CAC
GAC TCT GGT TAC GAA GTT CAC CAC CAG AAG CTG GTG TTC TTC GCT GAA GAC
GTG GGT TCT AAC AAG GGT GCT ATC ATC GGT CTG ATG GTT GGT GGC GTT GTG
ATC GCT TAA TAG GAG CTC GAT CCG-3'

Aβ (M1–42/A21C–A30C): 5'-GAT ATA CAT ATG GAC GCT GAA TTC CGT CAC
GAC TCT GGT TAC GAA GTT CAC CAC CAG AAG CTG GTG TTC TTC TGC GAA GAC
GTG GGT TCT AAC AAG GGT TGC ATC ATC GGT CTG ATG GTT GGT GGC GTT GTG
ATC GCT TAA TAG GAG CTC GAT CCG-3'

Aβ (M1–42/A21C–I32C): 5'-GAT ATA CAT ATG GAC GCT GAA TTC CGT CAC
GAC TCT GGT TAC GAA GTT CAC CAC CAG AAG CTG GTG TTC TTC TGC GAA GAC
GTG GGT TCT AAC AAG GGT GCT ATC TGC GGT CTG ATG GTT GGT GGC GTT GTG
ATC GCT TAA TAG GAG CTC GAT CCG-3'

Aβ (M1–42/V24C–G29C): 5'-GAT ATA CAT ATG GAC GCT GAA TTC CGT CAC
GAC TCT GGT TAC GAA GTT CAC CAC CAG AAG CTG GTG TTC TTC GCT GAA GAC
TGC GGT TCT AAC AAG TGC GCT ATC ATC GGT CTG ATG GTT GGT GGC GTT GTG
ATC GCT TAA TAG GAG CTC GAT CCG-3'

Aβ (M1–42/A21C–I31C): 5'-GAT ATA CAT ATG GAC GCT GAA TTC CGT CAC
GAC TCT GGT TAC GAA GTT CAC CAC CAG AAG CTG GTG TTC TTC TGC GAA GAC
GTG GGT TCT AAC AAG GGT GCT TGC ATC GGT CTG ATG GTT GGT GGC GTT GTG
ATC GCT TAA TAG GAG CTC GAT CCG-3'

Aβ (M1–42/V18C–G33C): 5'- GAT ATA CAT ATG GAC GCT GAA TTC CGT CAC
GAC TCT GGT TAC GAA GTT CAC CAC CAG AAG CTG TGC TTC TTC GCT GAA GAC
GTG GGT TCT AAC AAG GGT GCT ATC ATC TGC CTG ATG GTT GGT GGC GTT GTG
ATC GCT TAA TAG GAG CTC GAT CCG -3'

Aβ(MC1–40): 5'-GAT ATA CAT ATG GAC GCT GAA TTC CGT CAC

GAC TCT GGT TAC GAA GTT CAC CAC CAG AAG CTG GTG TTC TTC GCT GAA GAC GTG GGT TCT AAC AAG GGT GCT ATC ATC GGT CTG ATG GTT GGT GGC GTT GTG TAA TAG GAG CTC GAT CCG-3’

Aβ (M1–40/V18C–G33C): 5’- GAT ATA CAT ATG GAC GCT GAA TTC CGT CAC GAC TCT GGT TAC GAA GTT CAC CAC CAG AAG CTG TGC TTC TTC GCT GAA GAC GTG GGT TCT AAC AAG GGT GCT ATC ATC TGC CTG ATG GTT GGT GGC GTT GTG TAA TAG GAG CTC GAT CCG -3’

Figure 3.S1. Design of the DNA sequences for Aβ(MC1–42) and Aβ(MC1–40) mutants.

Restriction enzyme digestion of pET-Sac-Aβ(M1–42) and pET-Sac-Aβ(M1–40)

The pET-Sac-Aβ(M1–42) plasmid and pET-Sac-Aβ(M1–40) plasmid were digested using *SacI* and *NdeI* restriction enzymes. Table 3.S1 details the restriction reaction conditions. Reagents were added in the order they are listed.

Table 3.S1. Double-digestion of the pET- Sac Aβ(M1–42) plasmid or pET- Sac Aβ(M1–40) plasmid.

Reagents	Amount
pET-Sac Aβ(M1–42) or pET-Sac Aβ(M1–40)	20 µL of 50 ng/uL plasmid solution (1.0 µg in total)
10X CutSmart buffer	5.0 µL
H_2O	23.0 µL
NdeI restriction enzyme	1.0 µL (1 U)
SacI-HF restriction enzyme	1.0 µL (1 U)
Total	50.0 µL
Time	1.0 h
Temperature	37.0 °C

Next, to prevent backbone self-ligation, the digested plasmid was treated with shrimp alkaline phosphatase (rSAP). Table 5.S2 details the rSAP reaction conditions.

Table 3.S2. SAP treatment of the vectors.

Reagents	Amount
Double-digestion mixture	50.0 µL
rSAP	1.0 µL (1U)
Total	51.0 µL
Time	0.5 h
Temperature	37.0 °C
Heat inactivation	65.0 °C for 20 min

After the rSAP reaction and heat inactivation were complete, the reaction mixture was mixed with DNA loading buffer and loaded onto a 1% agarose gel containing ethidium bromide (5 µL per 100 mL gel). The agarose gel was run at 100 V for ~30 min. A UV box was used to visualize the digested pET-Sac vector (~4500 bp), which was excised from the gel using a razor blade. The digested pET-Sac vector was purified from the agarose gel using a Zymoclean gel DNA recovery kit. The concentration of the vector after purification was measured using a Thermo Scientific Nanodrop instrument. The purified digested pET-Sac linear vector was used in the subsequent ligation step.

The Aβ(MC1–42) and Aβ(MC1–40) mutant DNA sequences were digested using *SacI* and *NdeI* restriction enzymes. Table 5.S3 details the restriction reaction conditions. Reagents were added in the order they are listed.

Table 3.S3. Double-digestion of the inserts.

Reagents	Amount
DNA sequence encoding mutation	20 µL of 5 ng/µL DNA solution (100.0 ng in total)
10X CutSmart buffer	2.5 µL
H_2O	1.5 µL
NdeI restriction enzyme	0.5 µL (0.5 U)
SacI-HF restriction enzyme	0.5 µL (0.5 U)
Total	25.0 µL
Time	1.0 h
Temperature	37.0 °C
Heat inactivation	65.0 °C for 20 min

T4 ligation of the Aβ(MC1–42) and Aβ(MC1–40) mutant DNA sequences and the linear digested pET-Sac vector

The inserts and the vectors were ligated together using T4 ligase. Table 5.S4 details the T4 ligation reaction conditions. Reagents were added in the order they are listed.

Table 3.S4. T4 ligation of the inserts and the vectors.

Reagents	Amount	
	Insert:Vector = 0:1 (molar ratio) (negative control)	Insert:Vector = 5:1 (molar ratio)
Vector	9.1 µL of 6.6 ng/µL DNA solution (60.0 ng in total)	9.1 µL of 6.6 ng/µL DNA solution (60.0 ng in total)
Insert	---	2.5 µL of 4.0 ng/µL DNA solution (10.0 ng in total)
10X T4 DNA ligase reaction buffer	2.0 µL	2.0 µL
T4 DNA ligase	1.0 µL	1.0 µL
H_2O	7.9 µL	5.4 µL
Total	20.0 µL	20.0 µL
Ligation time	10 min	
Temp	22.0 °C (room temperature)	
Heat inactivation	65.0 °C for 10 min	

2 µL of the ligation reaction mixture was then transformed into TOP10 Ca^{2+}-competent *E. coli* using the heat shock method. The cell cultures were spread on LB agar plates containing carbenicillin (50 mg/L). Single colonies were picked to inoculate 5 mL of overnight cultures in LB media with carbenicillin (50 mg/L). The plasmids were extracted from TOP10 cells using Zymo ZR plasmid miniprep kit. The concentration of the plasmids was measured through Thermo Scientific NanoDrop spectrophotometer. The DNA sequences of the recombinant Aβ(MC1–42) and Aβ(MC1–40) mutant plasmids were verified by DNA sequencing.

Bacterial expression of Aβ(M1–42) mutants and Aβ(M1–40) mutants

Transformation and expression of Aβ(M1–42) mutants and Aβ(M1–42) mutants

All liquid cultures were performed in culture media (LB broth containing 50 mg/L carbenicillin and 34 mg/L chloramphenicol). Aβ(MC1–42) and Aβ(MC1–40) mutant plasmids were transformed into BL21 DE3 PLysS Star Ca^{2+}-competent *E. coli* through heat shock method. The cell cultures were spread on LB agar plates containing carbenicillin (50 mg/L) and chloramphenicol (34 mg/L). Single colonies were picked to inoculate 5 mL of culture media for overnight culture. [A glycerol stock of BL21 DE3 PLysS Star Ca^{2+}-competent *E. coli* bearing the plasmids was made, and the future expressions were started by inoculating culture media with an aliquot of the glycerol stock.] The next day, all 5 mL of the overnight culture were used to inoculate 1 L of culture media. After inoculation, the culture was shaken at 225 rpm at 37 ˚C until the cell density reached an OD_{600} of approximately 0.45. Protein expression was then induced by the addition of isopropyl β-D-1-thiogalactopyranoside (IPTG) to a final concentration of 0.1 mM, and the cells were shaken at 225 rpm at 37 °C for 4 h with IPTG. The cells were then harvested by centrifugation at 4000 rpm using a JA-10 rotor (2800 x g) at 4 ˚C for 25 min, and the cell pellets were then stored at -80°C.

Cell lysis, inclusion body preparation, and disulfide bond formation by DMSO

To lyse the cells, the cell pellet was resuspended in 20 mL of buffer A (10 mM Tris/HCl, 1 mM EDTA, pH 8.0) and sonicated for 2 min on ice (50% duty cycle) until the lysate appeared homogenous. The lysate was then centrifuged for 25 min at 16000 rpm using a JA-18 rotor (38000 x g) at 4˚C. The supernatant was removed, and the pellet was resuspended in buffer A, sonicated and centrifuged as described above. The sonication and centrifugation steps were repeated three

times for Aβ(C1–42) mutants or two times for Aβ(C1–40) mutants. After the last round of sonication and centrifugation, the supernatant was removed, the remaining pellet was resuspended in 15 mL of freshly prepared buffer B (8 M urea, 10 mM Tris/HCl, 1 mM EDTA, pH 8.0), and was sonicated as described above, until the solution became clear. The solution was diluted with 10 mL of buffer A, and 5 mL of DMSO was added to the solution. The resulting mixture (30 mL) was incubated on a shaker at room temperature for 2-6 days.

Peptide purification

The reaction mixture was titrated with 1M NaOH to a pH of ~10.5, and was filtered through a Fisher Brand 0.22 µm non-sterile hydrophilic PVDF syringe filter (Catalog No. 09-719-00). After filtering, the solution was titrated with 1M HCl to a pH of 8.0. Analytical reverse-phase HPLC was performed to evaluate if expression of Aβ(C1–42) mutants or Aβ(C1–40) mutants were successful. A 20-µL sample of the above solution was injected onto an Agilent 1200 instrument equipped with a Phenomonex Aeris PEPTIDE 2.6u XB-C18 column with a Phenomonex SecurityGuard ULTRA cartridges guard column for C18 column. HPLC grade acetonitrile (ACN) and 18 MΩ deionized water, each containing 0.1% trifluoroacetic acid, were used as the mobile phase. The sample was eluted at 1.0 mL/min with a 5–100% acetonitrile gradient over 20 min, at 35 °C.

Aβ(C1–42) mutants and Aβ(C1–40) mutants were then purified by preparative reverse-phase HPLC equipped with an Agilent ZORBAX 300SB-C8 semi-preparative column (9.4 x 250 mm) with a ZORBAX 300SB-C3 preparative guard column (9.4 x 15 mm). The C8 column and the guard column were heated to 80 °C in a water bath. HPLC grade acetonitrile (ACN) and 18 MΩ deionized water, each containing 0.1% trifluoroacetic acid, were used as the mobile phase at

a flow-rate of 5 mL/min. The peptide solution was split into two ~15 mL aliquots, and purified in two separate runs. The peptide was loaded onto the column by flowing 20% ACN for 15 min and then eluted with a gradient of 20–40% ACN over 20 min. Fractions containing the monomer generally eluted from 34% to 38% ACN. After the peptide was collected, the column was washed by flushing with 100% isopropanol for 15 minutes. This cleaning procedure ensures elution of all peptide that is retained in the column and avoids problems of cross-contamination between runs.

The purity of each fraction was assessed using analytical reverse-phase HPLC. A 20-µL sample was injected onto the analytical HPLC. The sample was eluted at 1.0 mL/min with a 5–100% acetonitrile gradient over 20 min, at 35 °C. Pure fractions were combined and the purity of the combined fractions were checked using analytical HPLC. The combined fractions were concentrated by rotary evaporation to remove ACN, and then frozen with dry ice, liquid nitrogen, or a -80 °C freezer. [It is recommended to combine and freeze the purified fractions within 5 hours after purification to avoid oxidation of methionine.] The frozen sample was then lyophilized to give a fine white powder.

NaOH treatment and peptide concentration determination

The lyophilized peptide was then dissolved in 2 mM NaOH to achieve a concentration of ~0.5 mg/mL. The pH was adjusted by addition of 0.1 M NaOH to give a solution of pH ~10.5. The sample was sonicated in a water ultrasonic bath at room temperature for 1 min or until the solution became clear. The concentration of the peptide was determined by absorbance at 280 nm using the extinction coefficient (ε) for tyrosine of 1490 $M^{-1}cm^{-1}$ (c = A/1490). The peptide solution was then aliquoted into 0.020 µmol aliquots in 0.5 mL microcentrifuge tubes. The aliquots were lyophilized and then stored in a desiccator at -20 °C for future use.

SDS-PAGE

The concentrations of the peptide working solutions vary for different SDS-PAGE assays. Here we provide a general procedure for the SDS-PAGE assays we conducted in this project. For the sample preparation, a 0.02 μmol aliquot of peptide was dissolved in 208.4 μL of deionized water to give a 96 μM peptide stock solution. A 20 μL aliquot of the 96 μM peptide stock solution and 4 μL of 6X SDS-PAGE loading buffer (100 mM Tris buffer at pH 6.8, 20% (v/v) glycerol, and 4% w/v SDS) was then combined to give a 24 μL of peptide working solution with a concentration of 80 μM. A 10 μL aliquot of the working solution was run on a 16% polyacrylamide gel with a 4% stacking polyacrylamide gel. The gels were run at a constant 90 volts at room temperature.

Staining with silver nitrate was used to visualize peptides in the SDS-PAGE gel. Briefly, the gel was first rocked in fixing solution (50% (v/v) methanol and 5% (v/v) acetic acid in deionized water) for 20 min. Next, the fixing solution was discarded and the gel was rocked in 50% (v/v) aqueous methanol for 10 min. Next, the 50% methanol was discarded and the gel was rocked in deionized water for 10 min. Next, the water was discarded and the gel was rocked in 0.02% (w/v) sodium thiosulfate in deionized water for 1 min. The sodium thiosulfate was discarded and the gel was rinsed twice with deionized water for 1 min (2X). After the last rinse, the gel was submerged in chilled 0.1% (w/v) silver nitrate in deionized water and rocked at 4 °C for 20 min. Next, the silver nitrate solution was discarded and the gel was rinsed with deionized water for 1 min (2X). To develop the gel, the gel was incubated in developing solution (2% (w/v) sodium carbonate, 0.04% (w/v) formaldehyde until the desired intensity of staining was reached (~1–3 min). When the desired intensity of staining was reached, the development was stopped by discarding the developing solution and submerging the gel in 5% aqueous acetic acid.

Thioflavin T (ThT) fibrillization assay

1X PBS buffer containing 10 μM ThT were used to dissolve Aβ peptides, to reach a final Aβ concentration of 10 μM. The resulting solutions were filtered through 0.2 μm filters. TECP solution or the same volume of filtered water were then added to the mixture (final TCEP concentration: 5 mM). All samples were prepared on ice, and 100 μl of each sample was transferred into a 96-well plate and sealed. The ThT assays were conducted with a microplate reader using excitation and emission wavelengths of 446 and 490 nm, respectively. The assays were performed in 3 replicates in 1X PBS buffer, pH 7.4, at 37 °C with shaking.

Dynamic Light Scattering (DLS)

The dynamic light scattering (DLS) experiments were performed in disposable cuvettes using the Malvern Zetasizer μV instrument at 25 °C. A 30 μM solution of each peptide was prepared in 10 mM sodium phosphate buffer at pH 7.4. Scattering data were collected as an average of 10 scans for each measurement.

Circular Dichroism (CD)

CD spectra were acquired on a Jasco J-810 circular dichroism spectropolarimeter at room temperature. A 30 μM solution of each peptide was prepared in 10 mM sodium phosphate buffer at pH 7.4. The instrumental parameters to record the CD spectra were: 260 nm to 190 nm measurement range, 1 nm data pitch, 2 nm band width, standard sensitivity, 50 nm/min of scanning speed. The data were averaged over 3 accumulations with smoothing. The CD spectra were analyzed by the online software BeStSel.[3]

Mass spectrometry

MALDI mass spectrometry was performed using an AB SCIEX TOF/TOF 5800 System. 0.5 μL of sinapinic acid was dispensed onto a MALDI sample support, followed by the addition of 0.5 μL peptide sample. The mixture was allowed to air-dry. All analyses were performed in positive reflector mode, collecting data with a molecular weight range of 2000–8000 Da.

TEM imaging

TEM images of fluorescein-labeled Aβ(C1-42) were taken with a JEM-2100F transmission electron microscope (JEOL, Peabody, MA, USA) at 200 kV with an electron dose of approximately 15 e^-/A^2. The microscope was equipped with Gatan K2 Summit direct electron detector (Gatan, Pleasanton, CA, USA) at 15,000x or 25,000x magnification. The sample was cooled at liquid nitrogen temperature through the cryostage. Contrast and brightness of the images were adjusted as appropriate.

MTT cytotoxicity assay

a. Preparation of SH-SY5Y cells for MTT assays

Cells were cultured in the inner 60 wells (rows B–G, columns 2–11) of the 96-well plate. DMEM:F12 media (180 μL) was added to the outer wells (rows A and H and columns 1 and 12), in order to ensure the greatest reproducibility of data generated from the inner wells. SH-SY5Y cells were plated in a 96-well plate at 50,000 cells per well. Cells were incubated in 100 μL of a 1:1 mixture of DMEM:F12 media supplemented with 10% fetal bovine serum, 100 U/mL penicillin, and 100 μg/mL streptomycin at 37 °C in a 5% CO2 atmosphere and allowed to adhere

to the bottom of the plate for 24 hours. After 24 hours of incubation, the culture media was removed and replaced with 90 µL of serum-free DMEM:F12 media.

	1	2	3	4	5	6	7	8	9	10	11	12
A	Plate 1											
B		H2O	H2O	H2O	H2O	H2O	Lysis Buffer	Lysis Buffer	Lysis Buffer	Lysis Buffer	Lysis Buffer	
C		Mut20 4 uM	Mut20 4 uM	Mut20 4 uM	Mut20 4 uM	Mut20 4 uM	WT42 4 uM	WT42 4 uM	WT42 4 uM	WT42 4 uM	WT42 4 uM	
D		Mut20 2 uM	Mut20 2 uM	Mut20 2 uM	Mut20 2 uM	Mut20 2 uM	WT42 2 uM	WT42 2 uM	WT42 2 uM	WT42 2 uM	WT42 2 uM	
E		Mut20 1 uM	Mut20 1 uM	Mut20 1 uM	Mut20 1 uM	Mut20 1 uM	WT42 1 uM	WT42 1 uM	WT42 1 uM	WT42 1 uM	WT42 1 uM	
F		Mut20 0.5 uM	Mut20 0.5 uM	Mut20 0.5 uM	Mut20 0.5 uM	Mut20 0.5 uM	WT42 0.5 uM	WT42 0.5 uM	WT42 0.5 uM	WT42 0.5 uM	WT42 0.5 uM	
G		Mut20 0.25 uM	Mut20 0.25 uM	Mut20 0.25 uM	Mut20 0.25 uM	Mut20 0.25 uM	WT42 0.25 uM	WT42 0.25 uM	WT42 0.25 uM	WT42 0.25 uM	WT42 0.25 uM	
H												

Figure 3.S2. A representative cell plate layout for MTT assay.

b. Preparation of stock solutions of peptides for treatment of the SH-SY5Y cells

20 µM stock solutions of peptides were prepared by dissolving 0.2 µmol aliquot of each peptide in 1000 µL of sterile deionized water that was filtered through a 0.2 µm Millex-GS MCE syringe filter. 200 µL of the 20 µM stock solution of peptides was used directly as 20 µM working solutions of peptides. Another 200 µL of the 20 µM stock solution of peptides was serially diluted with sterile deionized water to create 200 µL of 10 µM and 5 µM working solutions of peptides.

c. Treatment of SH-SY5Y cells with peptides

A 10-μL aliquot of the working solution of peptide was added to each well, for well concentrations of 0.5-2.0 μM. Experiments were run in replicates of four. Four wells were left untreated as negative controls. Another four wells were left untreated, to be subsequently used as positive controls with lysis buffer for the LDH release assay. Cells were incubated at 37 °C in a 5% CO2 atmosphere for 72 hours.

d. MTT assay

After 72 hours, 10 μL of 10x lysis buffer (included with the LDH release assay kit) was added to the four untreated wells, and the cells were incubated for an additional 45 minutes. After incubation, the old media in each well was removed and replaced with 100 μL of serum free, phenol-red free DMEM/F12 medium supplemented with 0.2 mg/mL MTT. The cells were incubated for 24 hours in a humidified 5% CO2 atmosphere at 37 °C in the presence of the MTT containing media. Formazan crystals from the MTT reaction were dissolved in 10% SDS in 10 mM HCl for 4 h in a humidified 5% CO2 atmosphere at 37 °C. MTT plates were read spectrophotometrically at 570 nm. MTT data were graphed as a percentage versus the negative control.

Characterization Data

Analytical HPLC trace of Aβ(M1–42)[4]

% Purity: >97%

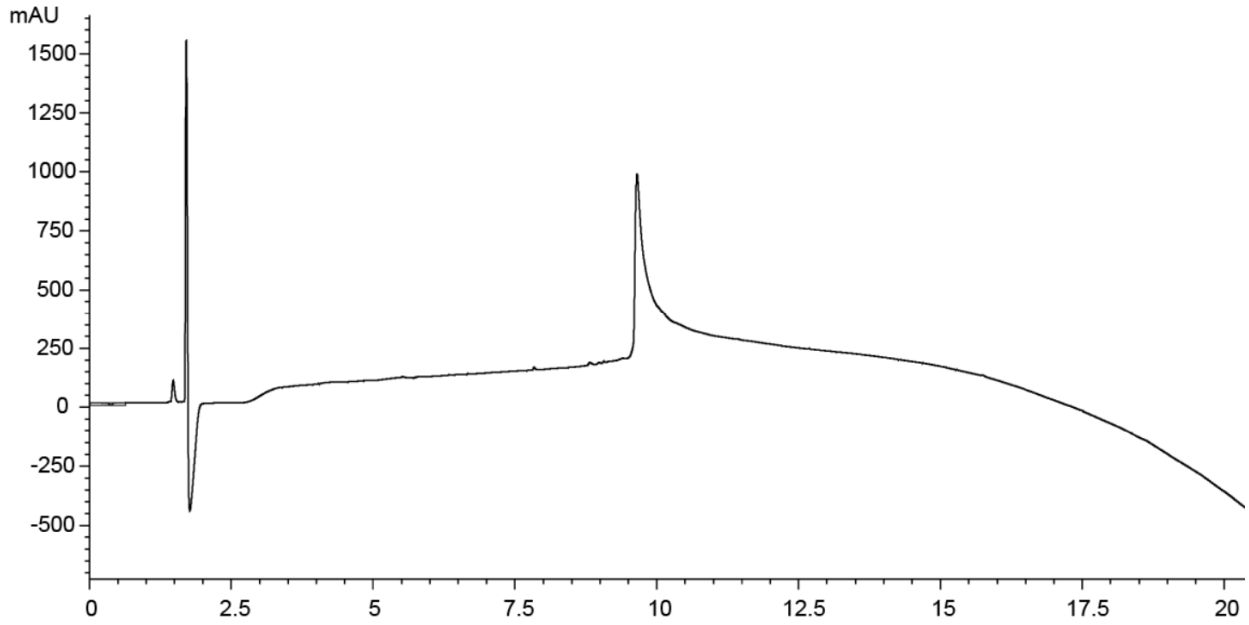

MALDI-MS trace of Aβ(M1–42)

Positive reflector mode; Matrix: Sinapinic acid

Exact mass calculated for M^+: 4642.3; Exact mass calculated for $[M+H]^+$: 4613.3; Exact mass calculated for $[M+2H]^{2+}$: 2322.2. Observed $[M+H]^+$: 4642.0; Observed $[M+2H]^{2+}$: 2321.4.

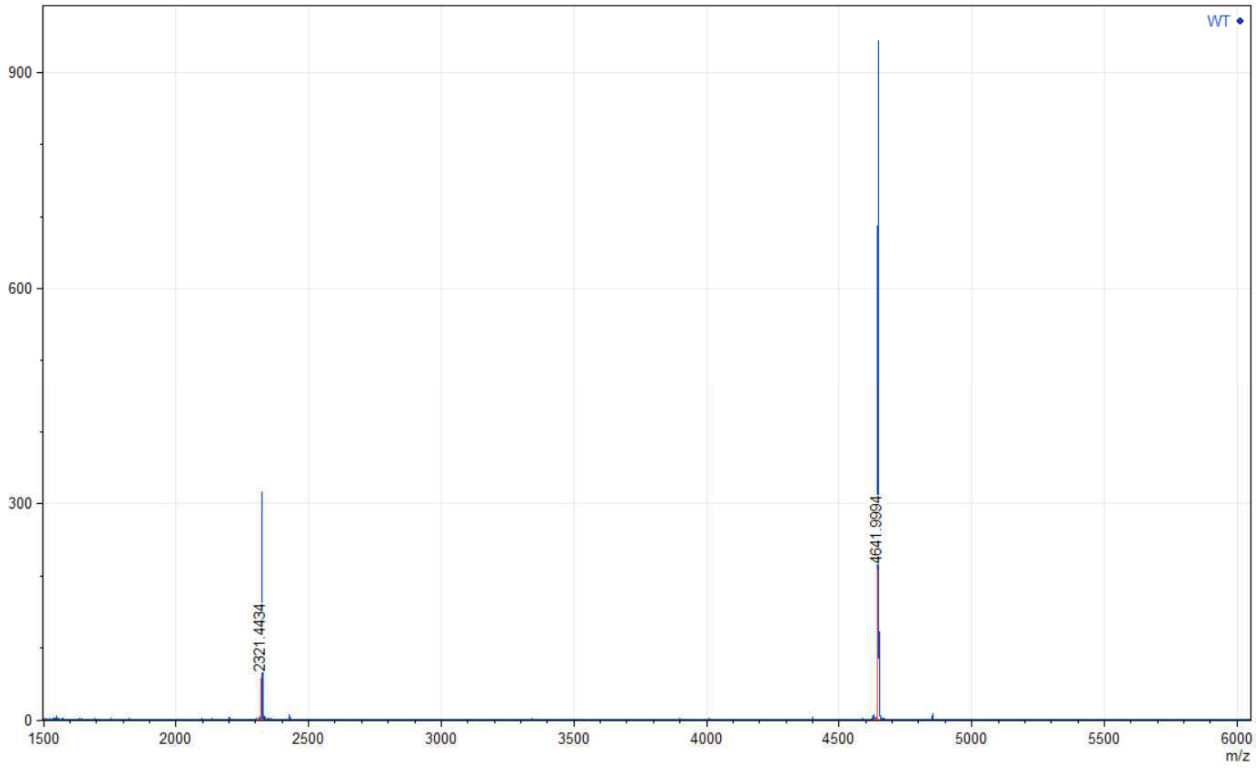

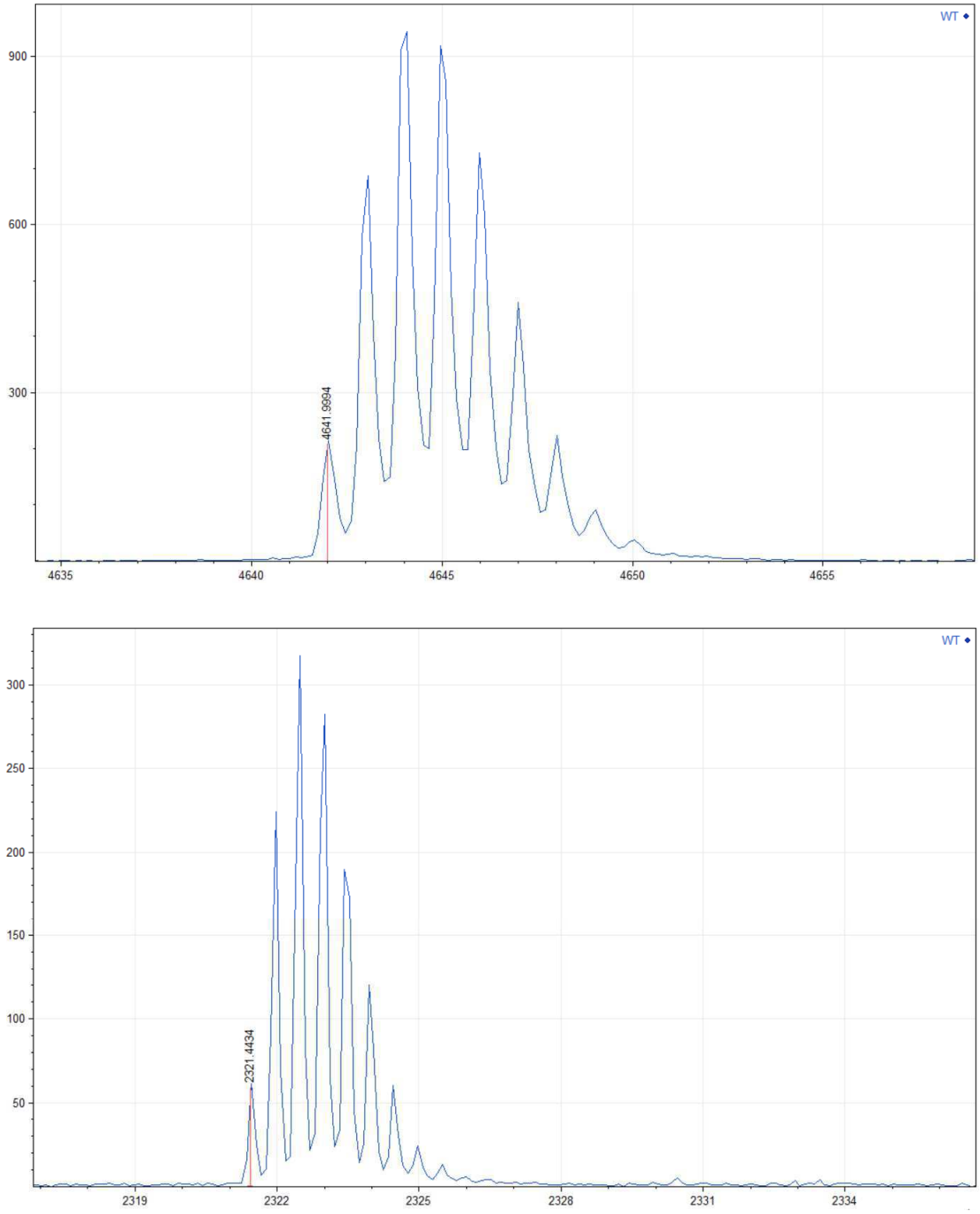

Figure 3.S3. Analytical HPLC and MALDI-MS traces of Aβ(M1–42).

Analytical HPLC trace of mutant 1 (Aβ(M1-42) | A21C, A30C)

% Purity: >97%

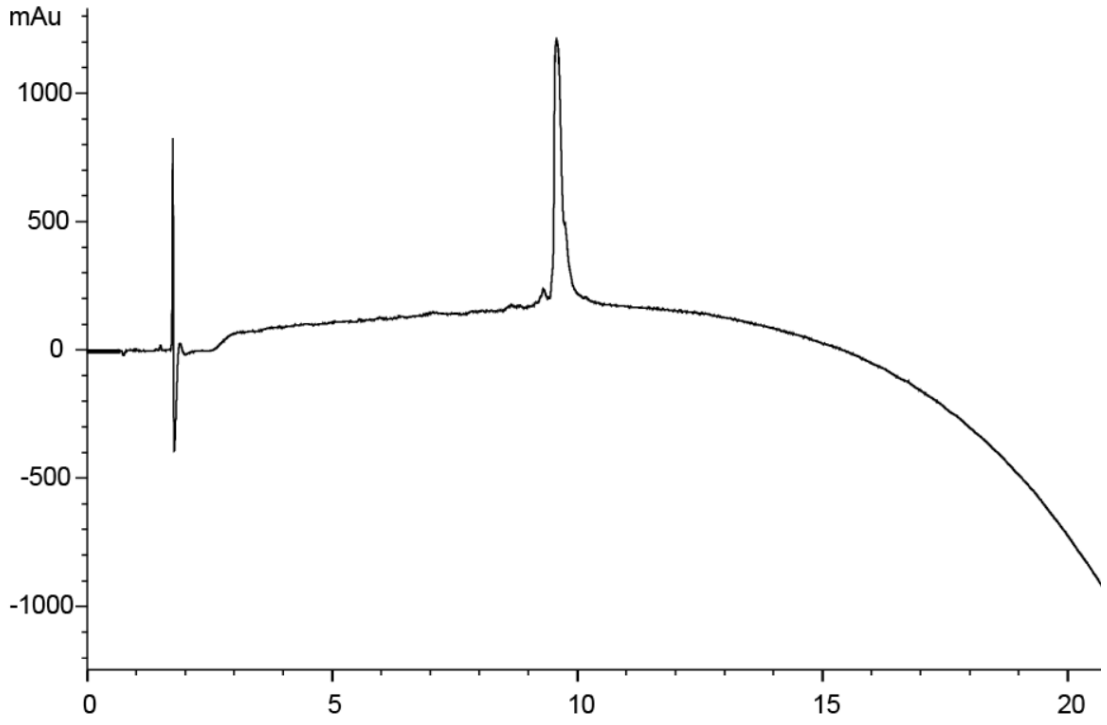

MALDI-MS trace of mutant 1 (Aβ(M1-42) | A21C, A30C)

Positive reflector mode. Matrix: Sinapinic acid.

Exact mass calculated for M^+: 4704.2; Exact mass calculated for $[M+H]^+$: 4705.2; Exact mass calculated for $[M+2H]^{2+}$: 2353.1. Observed $[M+H]^+$: 4704.0; Observed $[M+2H]^{2+}$: 2352.5.

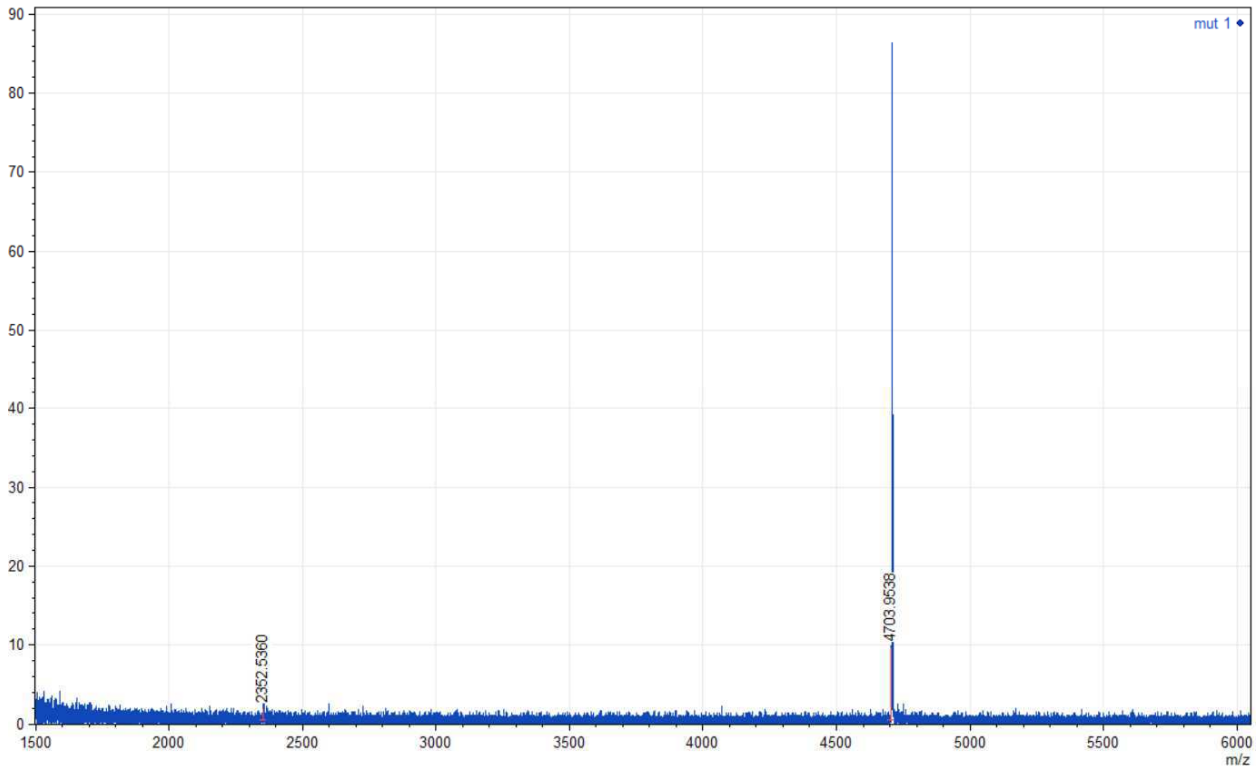

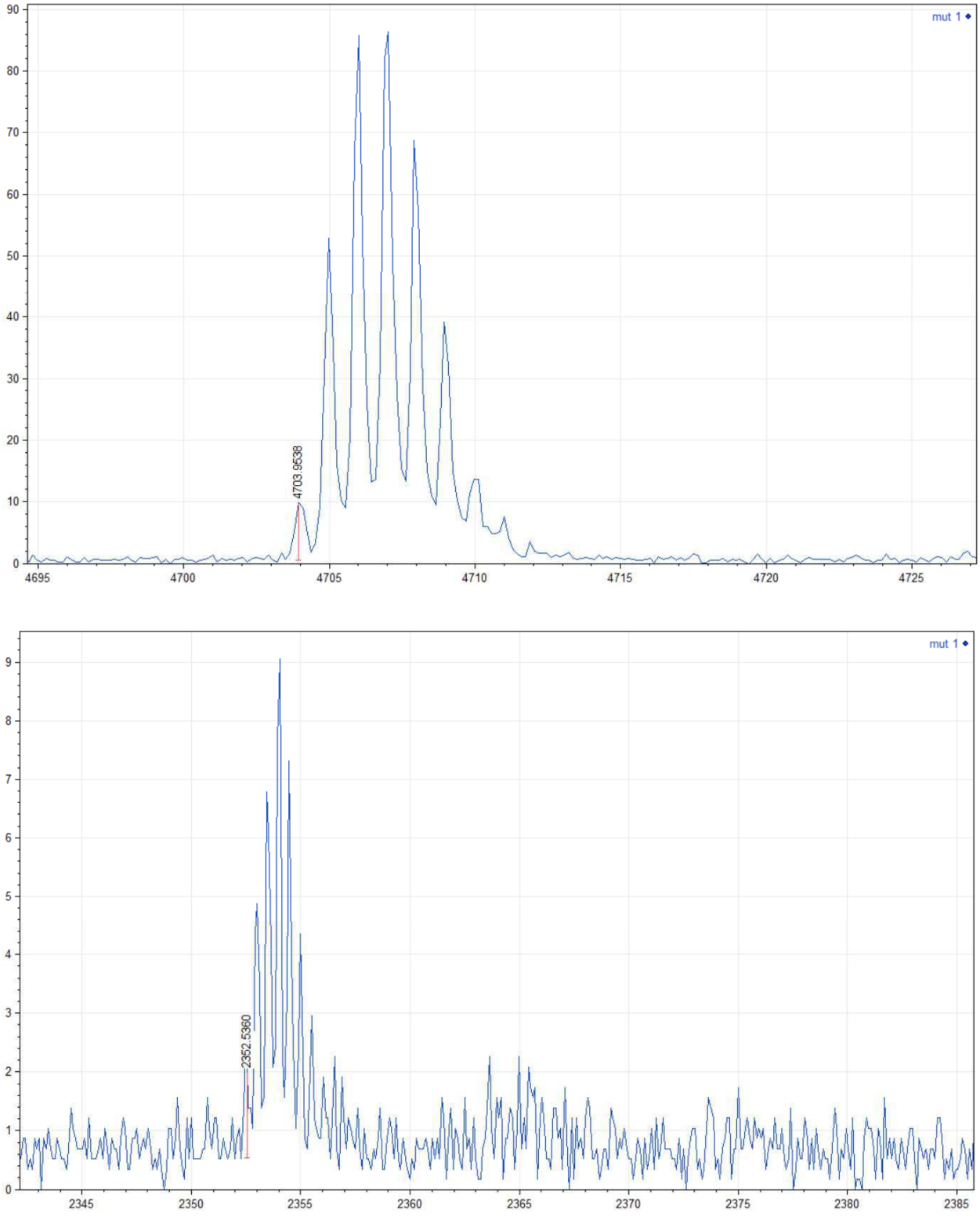

Figure 3.S4. Analytical HPLC and MALDI-MS traces of mutant 1 (Aβ(M1-42) | A21C, A30C).

Analytical HPLC trace of mutant 2 (Aβ(M1-42) | A21C, I32C)

% Purity: >95%

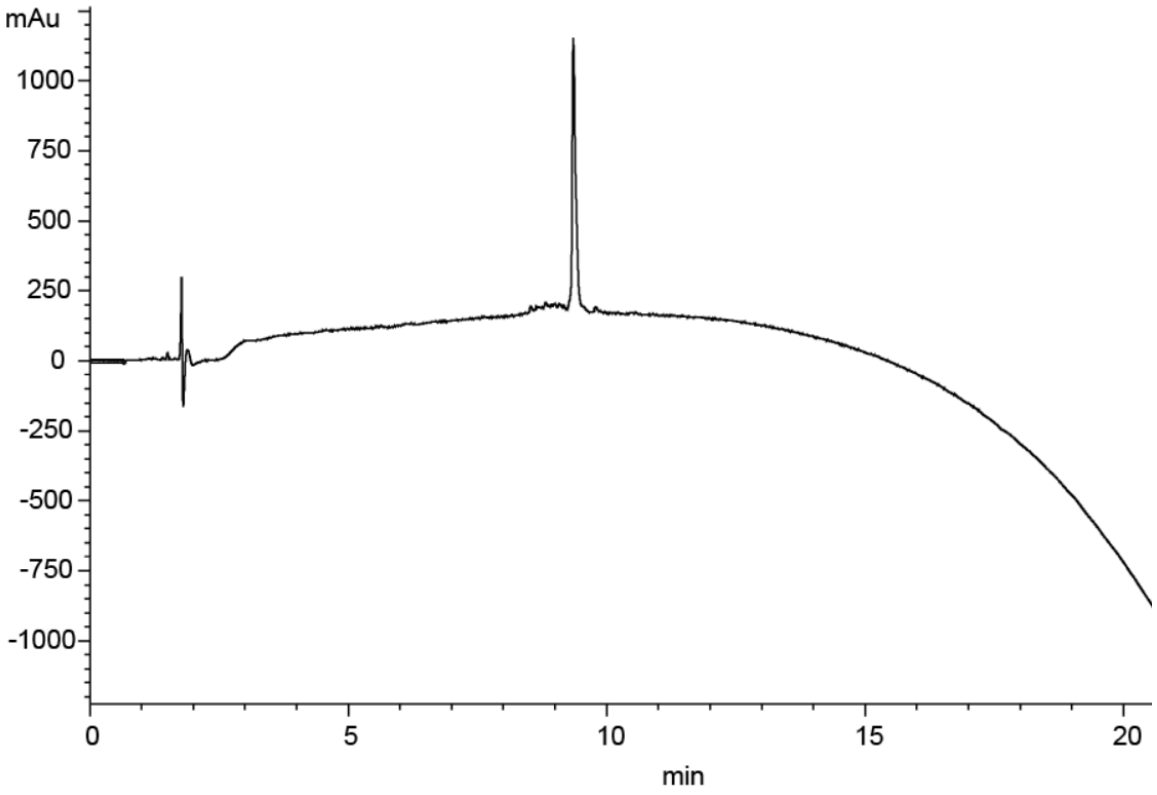

MALDI-MS trace of mutant 2 (Aβ(M1-42) | A21C, I32C)

Positive reflector mode. Matrix: Sinapinic acid.

Exact mass calculated for M^+: 4662.2; Exact mass calculated for $[M+H]^+$: 4663.2; Exact mass calculated for $[M+2H]^{2+}$: 2332.1. Observed $[M+H]^+$: 4661.8; Observed $[M+2H]^{2+}$: 2331.3.

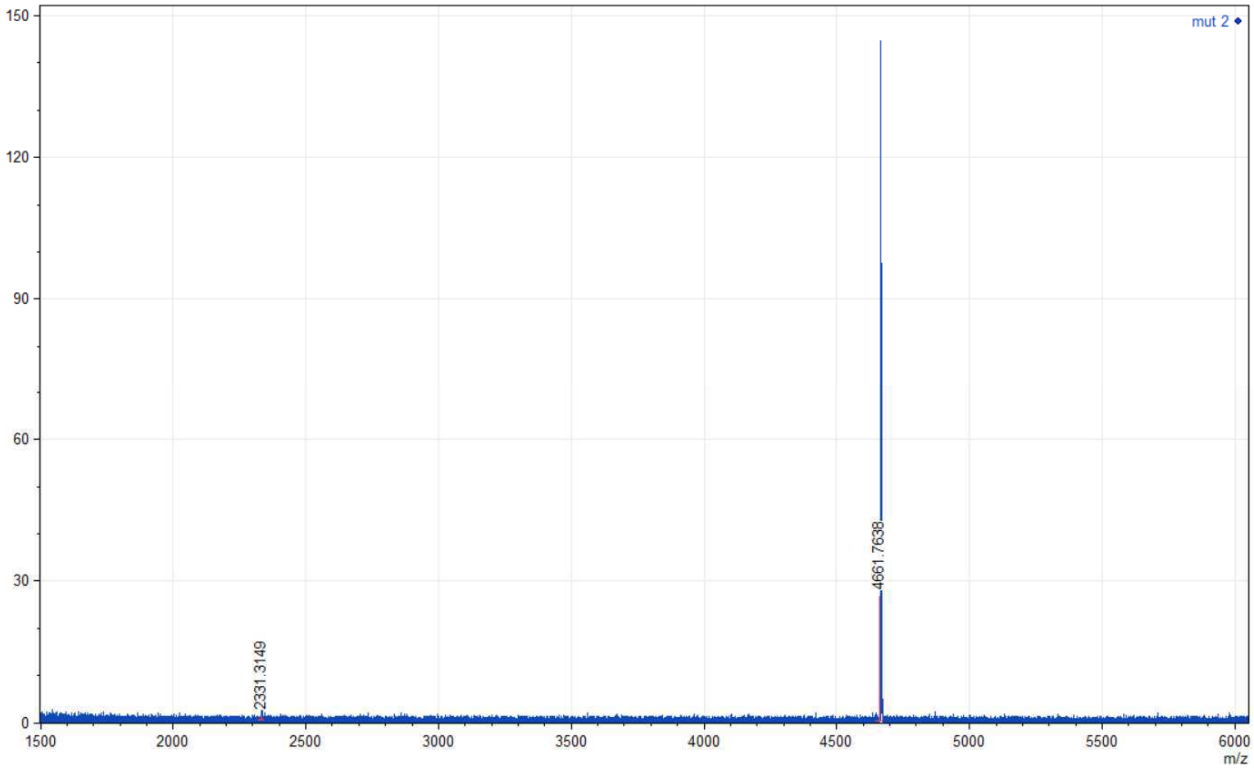

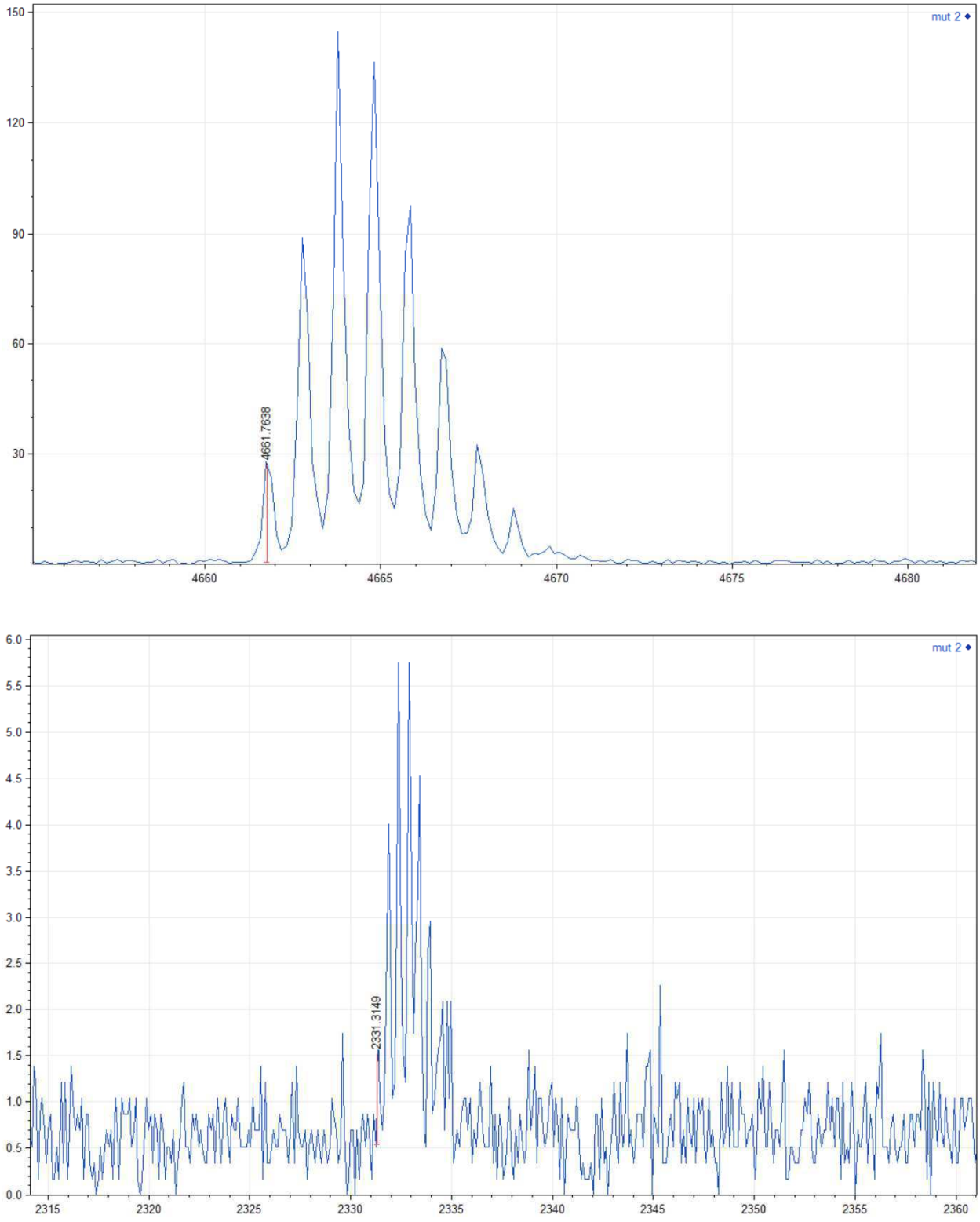

Figure 3.S5. Analytical HPLC and MALDI-MS traces of mutant 2 (Aβ(M1-42) | A21C, I32C).

Analytical HPLC trace of mutant 3 (Aβ(M1-42) | V24C, G29C)

% Purity: >95%

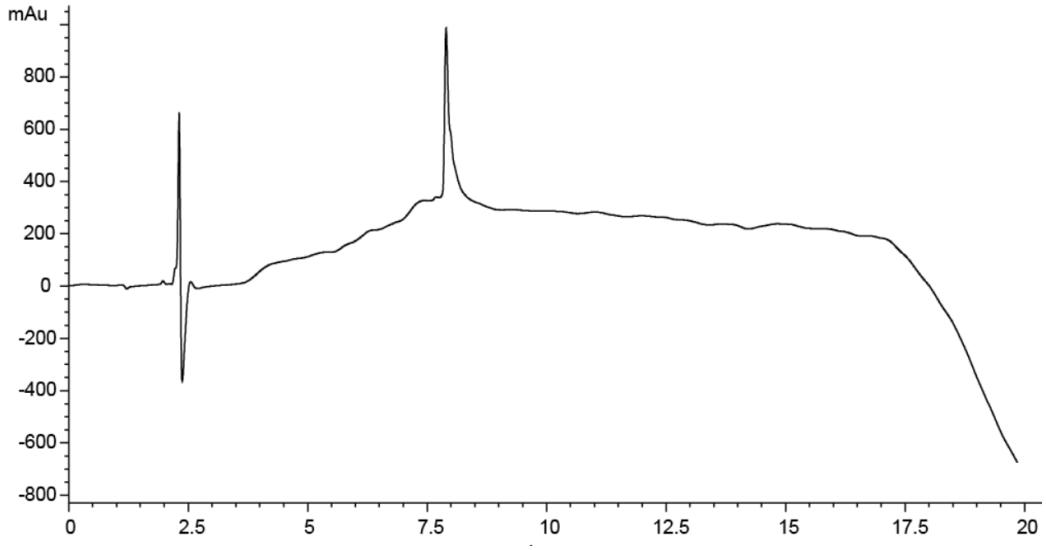

MALDI-MS trace of mutant 3 (Aβ(M1-42) | V24C, G29C)

Positive reflector mode.

Matrix: Sinapinic acid.

Exact mass for M^+: 4690.2; Exact mass calculated for $[M+H]^+$: 4691.2; Exact mass calculated for $[M+2H]^{2+}$: 2346.1. Observed $[M+H]^+$: 4691.2; Observed $[M+2H]^{2+}$: 2346.1.

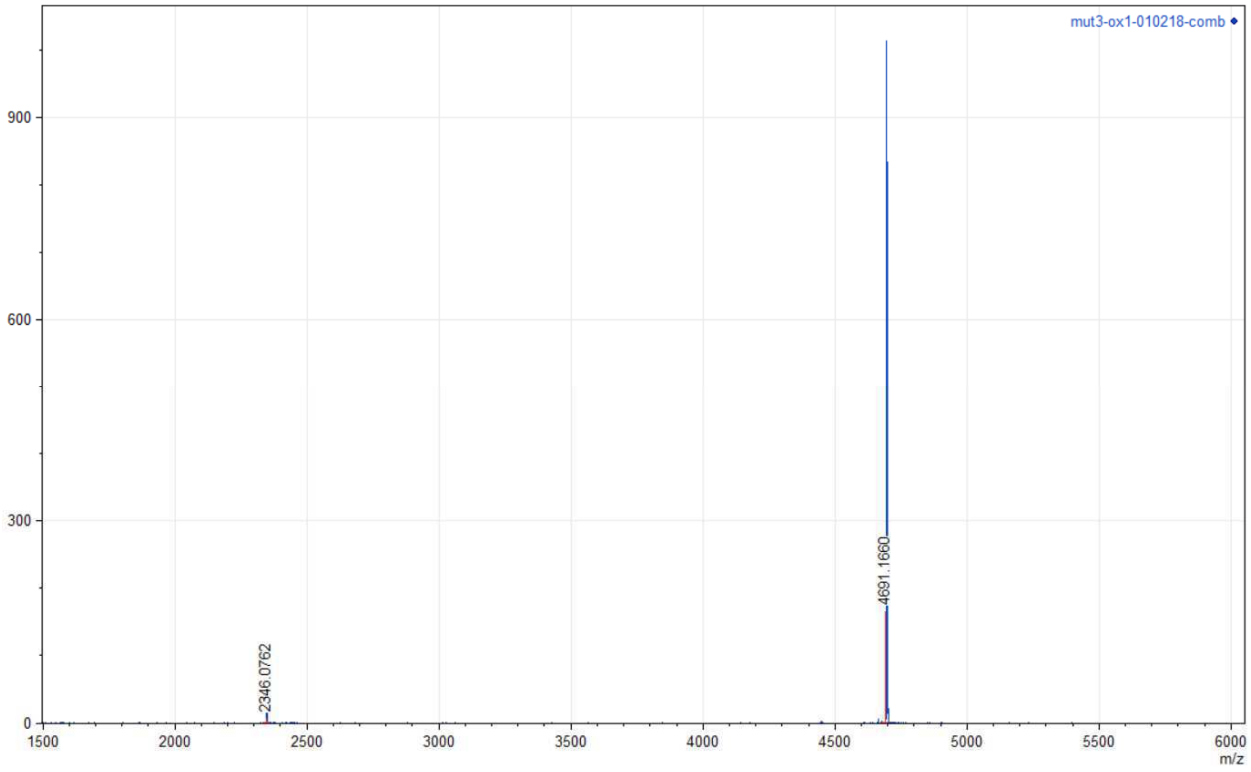

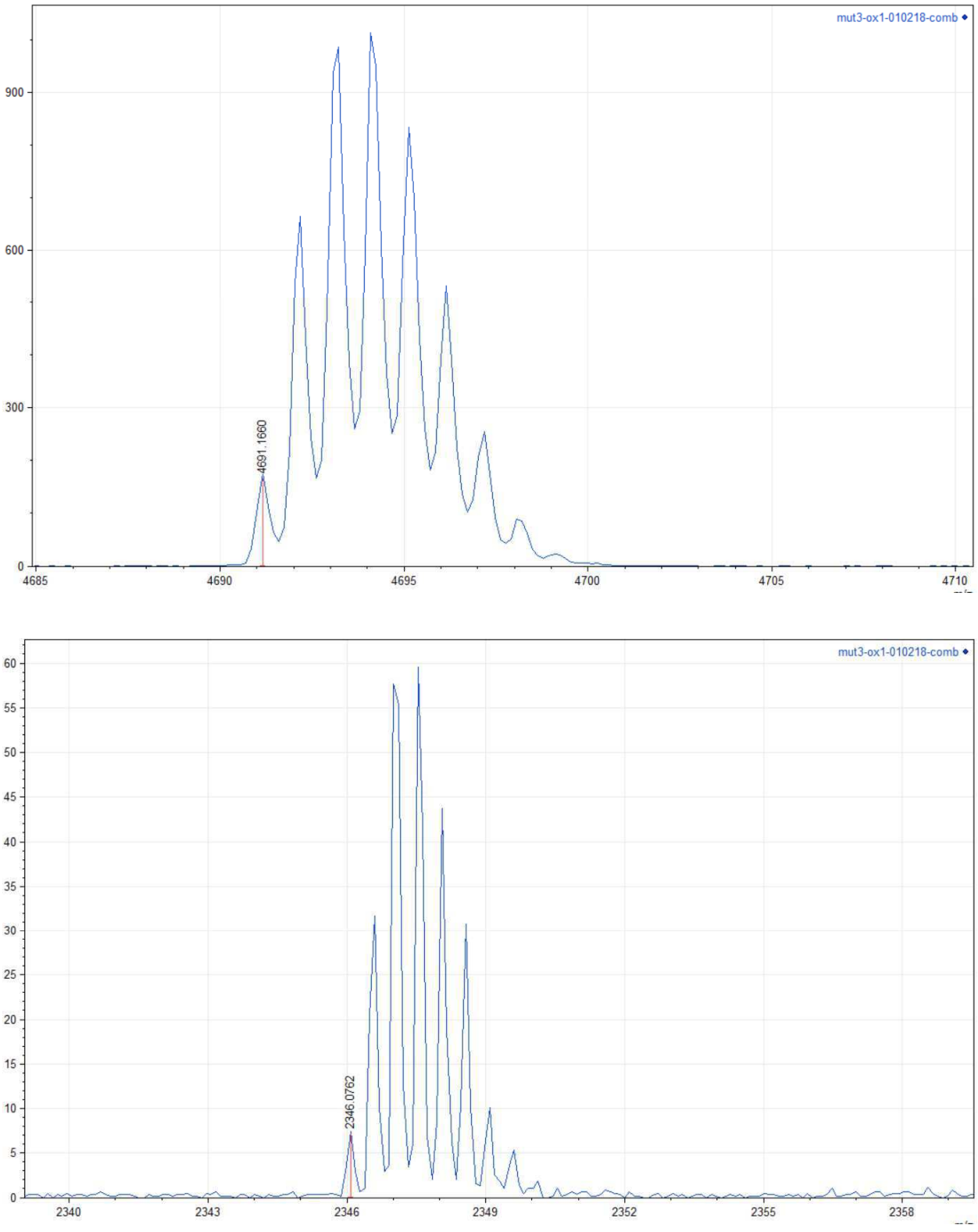

Figure 3.S6. Analytical HPLC and MALDI-MS traces of mutant 3 (Aβ(M1-42) | V24C, G29C).

Analytical HPLC trace of mutant 4 (Aβ(M1-42) | A21, I31C)

% Purity: >95%

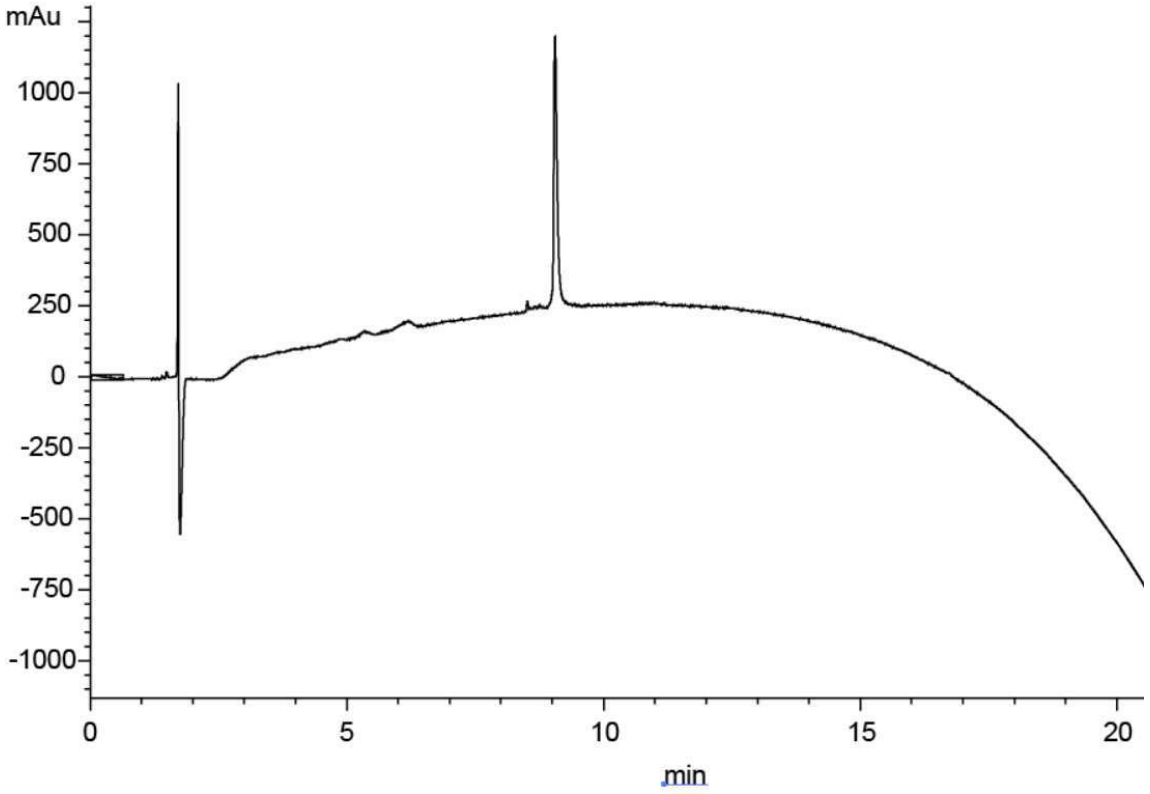

MALDI-MS trace of mutant 4 (Aβ(M1-42) | A21, I31C)

Positive reflector mode. Matrix: Sinapinic acid.

Exact mass for M^+: 4662.2; Exact mass calculated for $[M+H]^+$: 4663.2; Exact mass calculated for $[M+2H]^{2+}$: 2332.1. Observed $[M+H]^+$: 4663.0; Observed $[M+2H]^{2+}$: 2331.9.

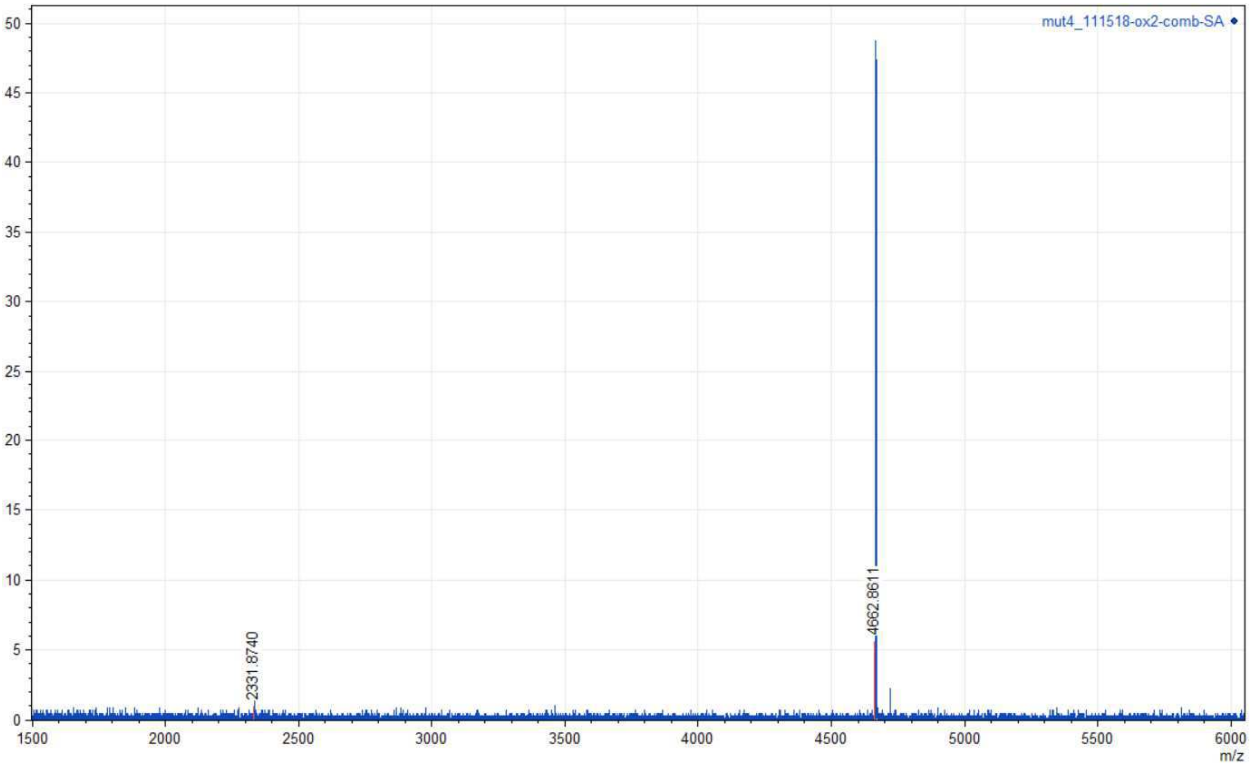

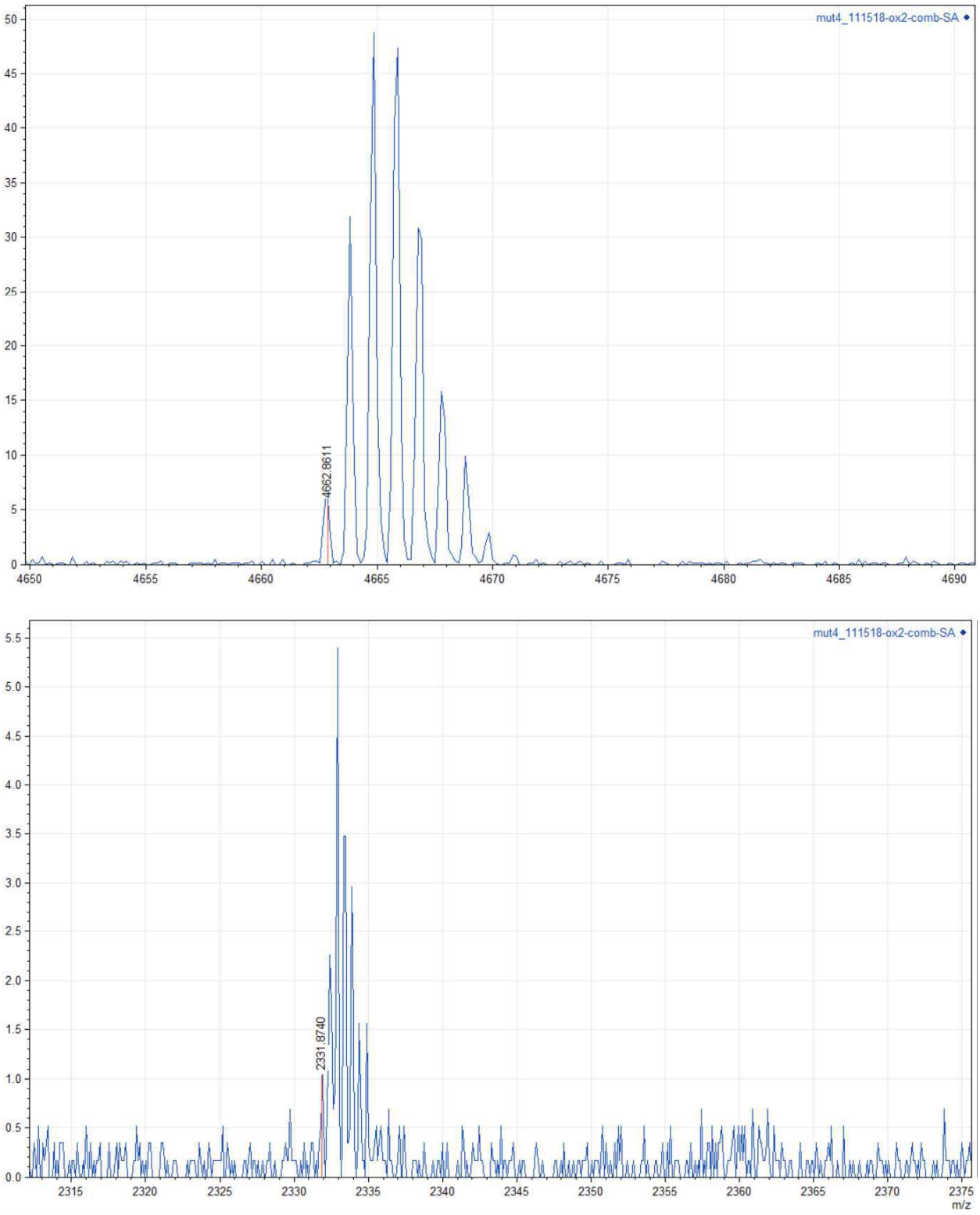

Figure 3.S7. Analytical HPLC and MALDI-MS traces of mutant 4 (Aβ(M1-42) | A21, I31C).

Analytical HPLC trace of mutant 5 (Aβ(M1-42) | V18C, G33C)

% Purity: >95%

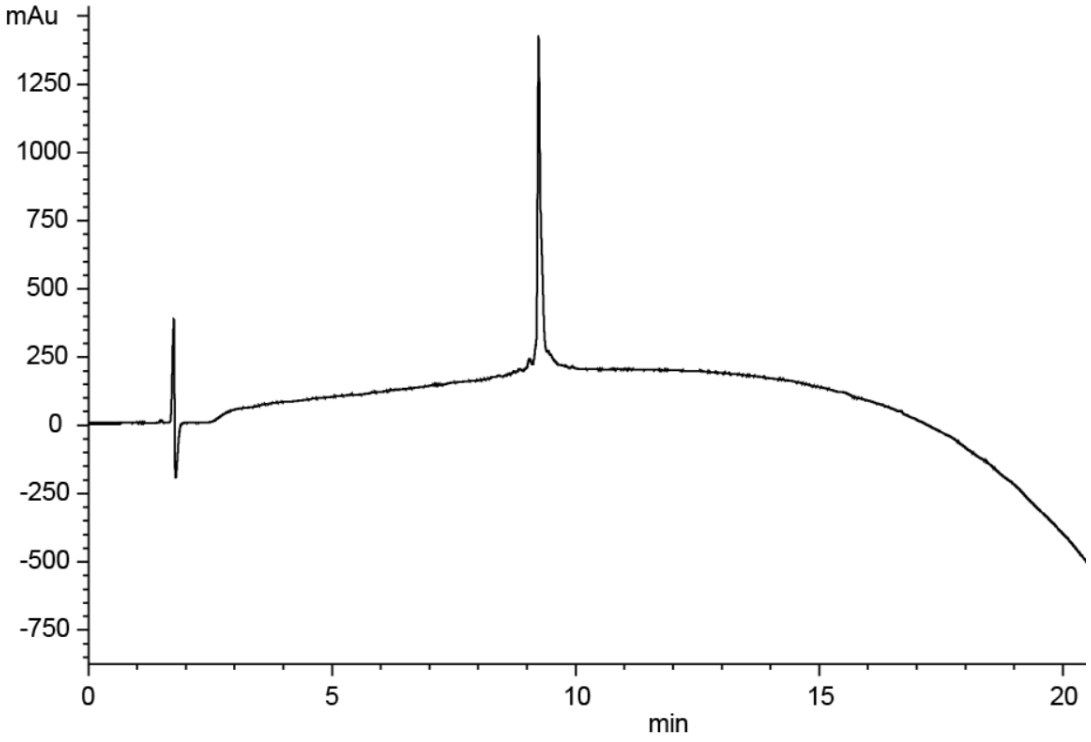

MALDI-MS trace of mutant 5 (Aβ(M1-42) | V18C, G33C)

Positive reflector mode.

Matrix: Sinapinic acid.

Exact mass for M^+: 4690.2; Exact mass calculated for $[M+H]^+$: 4691.2; Exact mass calculated for $[M+2H]^{2+}$: 2346.1. Observed $[M+H]^+$: 4690.1; Observed $[M+2H]^{2+}$: 2345.7.

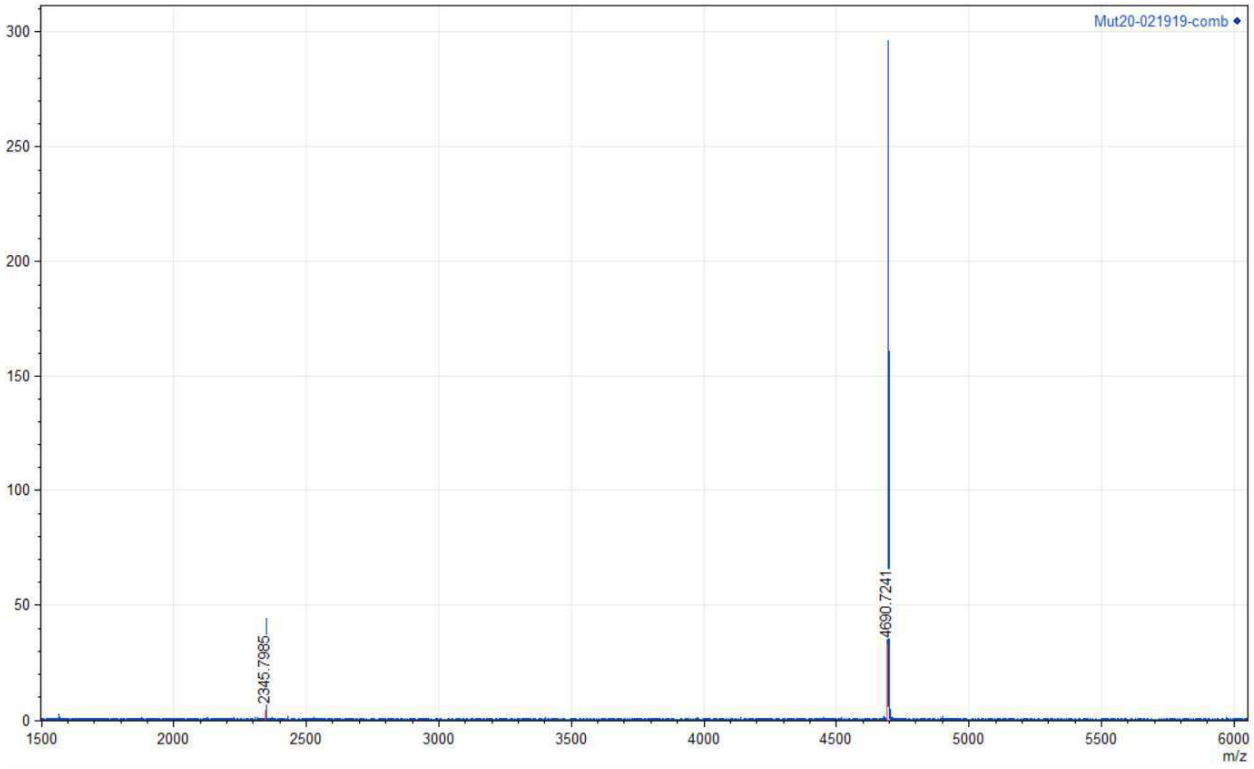

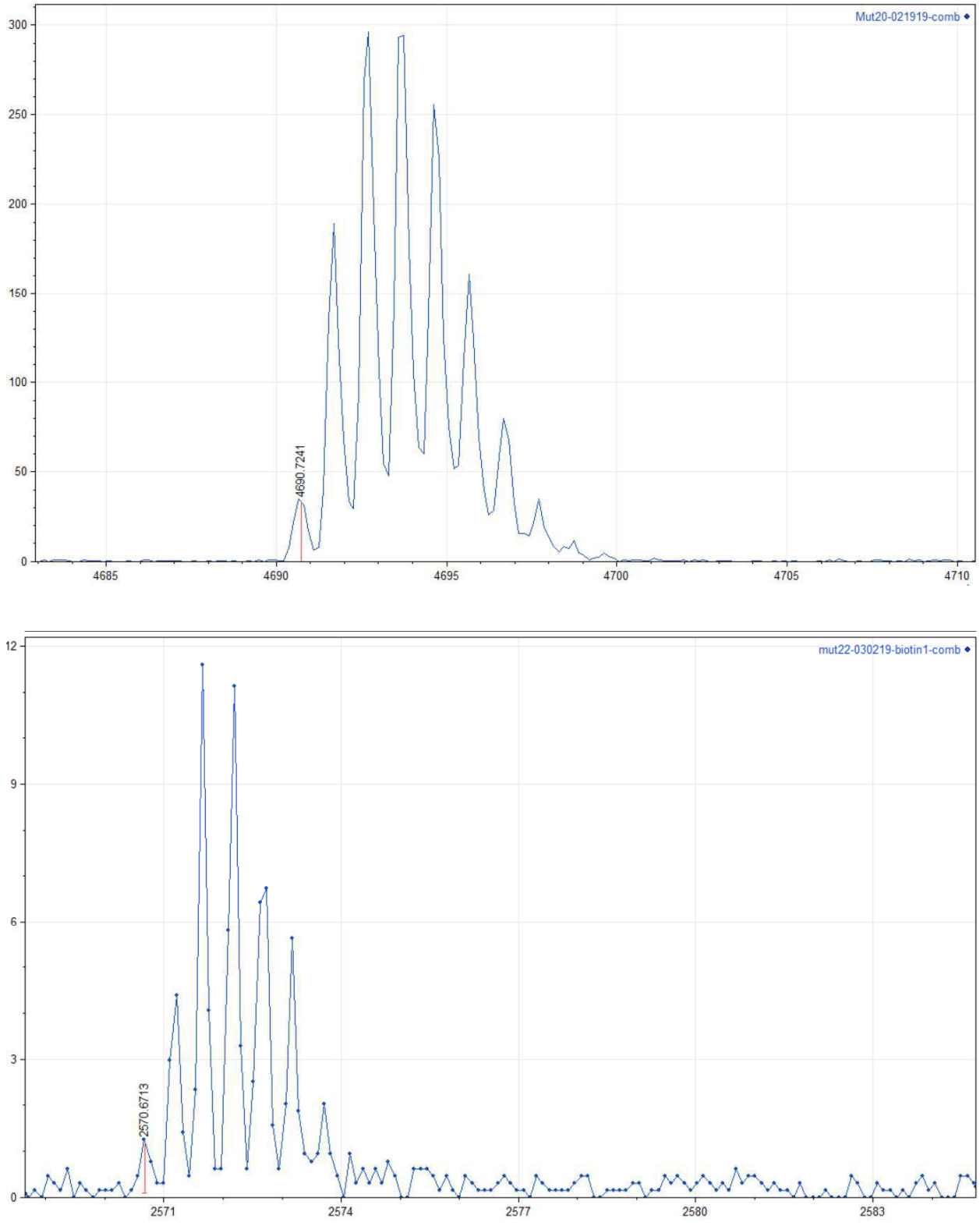

Figure 3.S8. Analytical HPLC and MALDI-MS traces of mutant 5 (Aβ(M1-42) | V18C, G33C).

Analytical HPLC trace of Aβ(M1-40)

% Purity: >95%

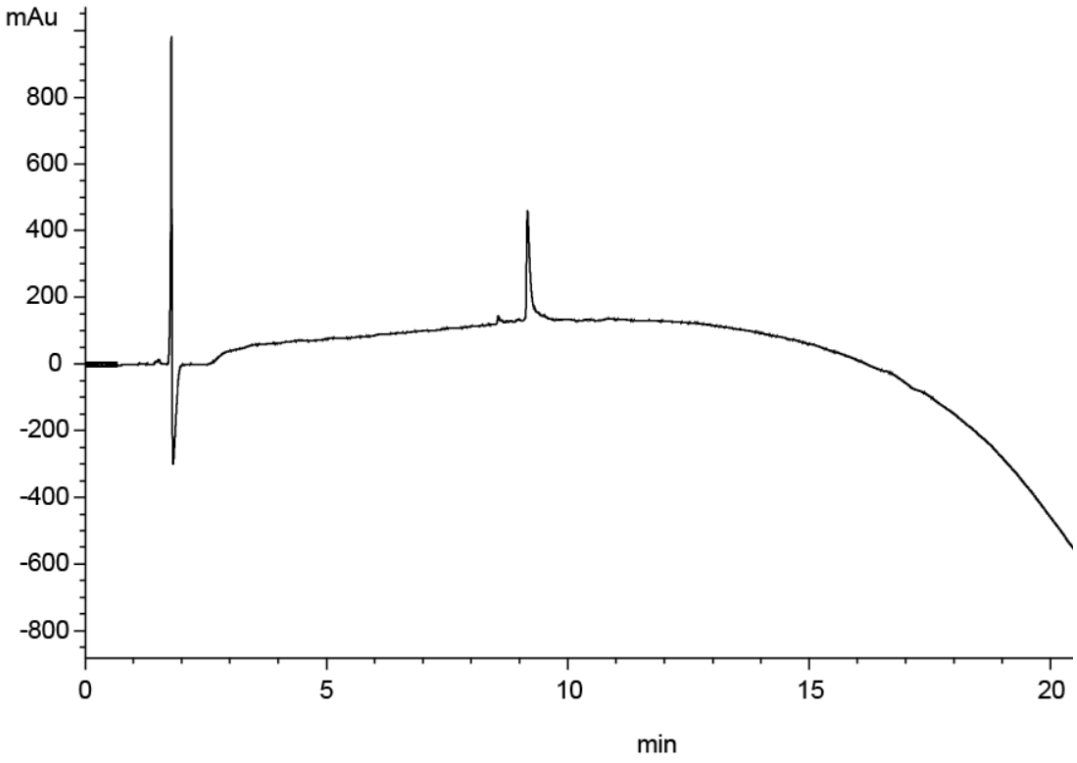

MALDI-MS trace of Aβ(M1-40)

Positive reflector mode.

Matrix: Sinapinic acid.

Exact mass for M^+: 4458.2; Exact mass calculated for $[M+H]^+$: 4459.2; Exact mass calculated for $[M+2H]^{2+}$: 2230.1. Observed $[M+H]^+$: 4458.6; Observed $[M+2H]^{2+}$: 2230.0.

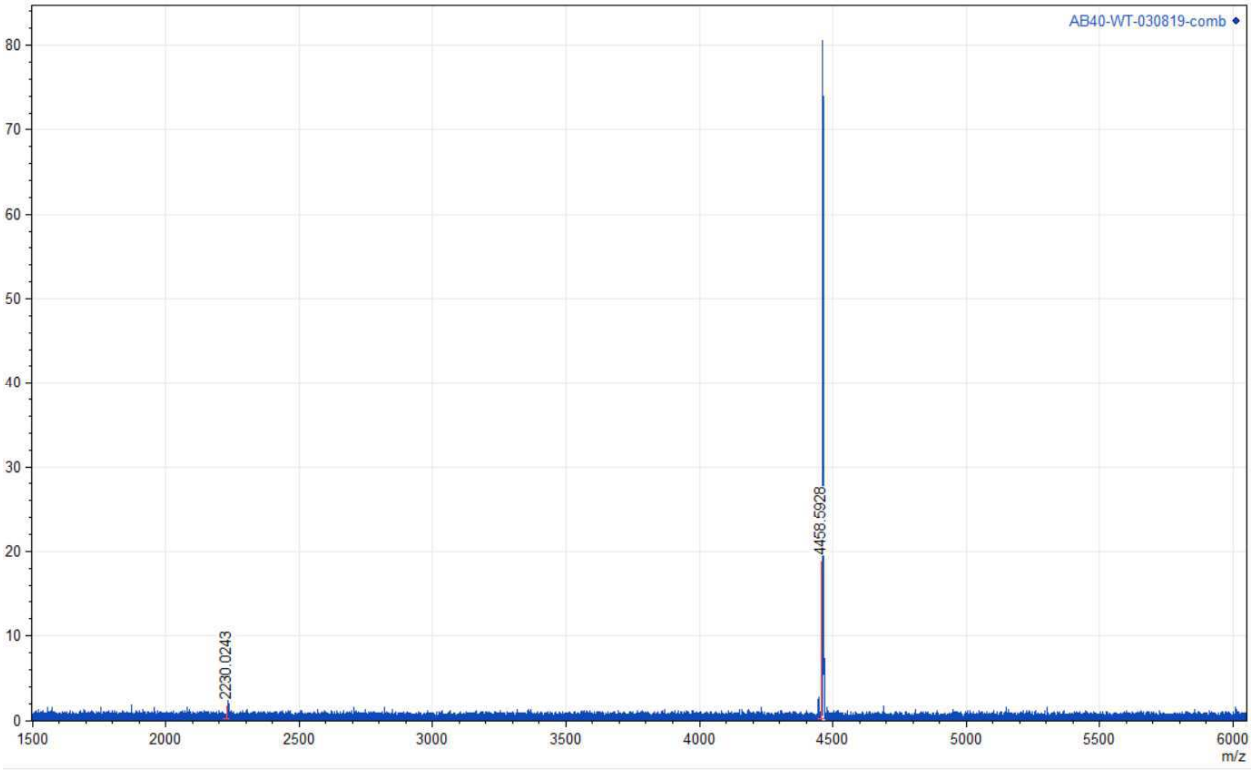

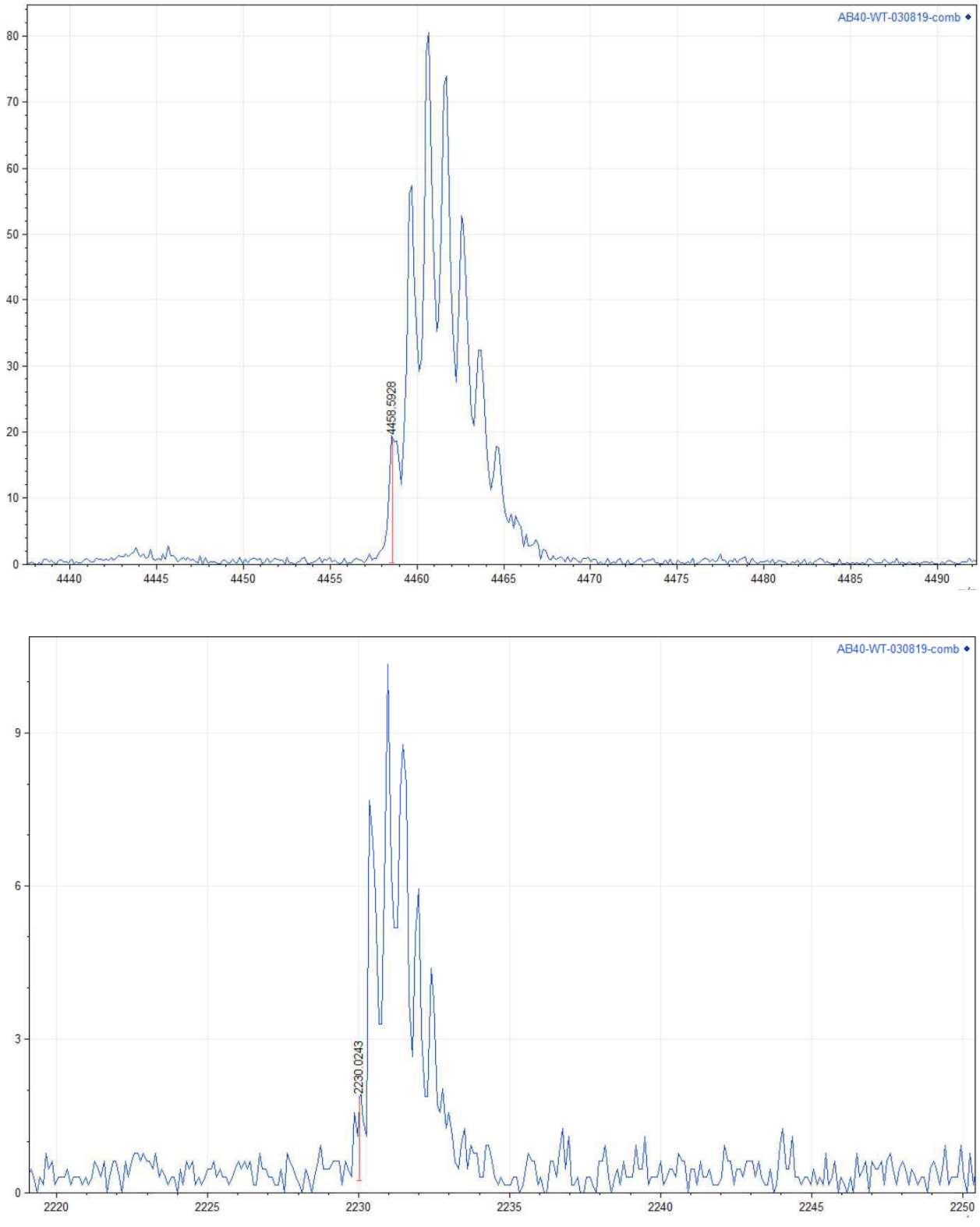

Figure 3.S9. Analytical HPLC and MALDI-MS traces of Aβ(M1-40).

Analytical HPLC trace of mutant 6 (Aβ(M1-40) | V18C, G33C)

% Purity: >97%

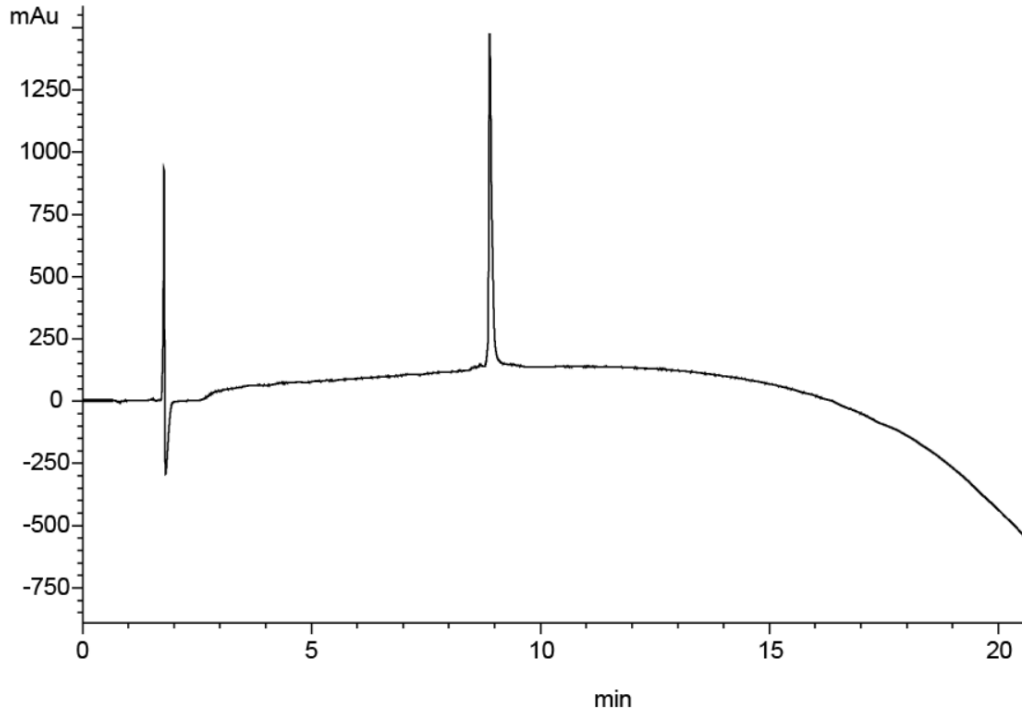

MALDI-MS trace of mutant 6 (Aβ(M1-40) | V18C, G33C)

Positive reflector mode.

Matrix: Sinapinic acid.

Exact mass for M^+: 4506.2; Exact mass calculated for $[M+H]^+$: 4507.2; Exact mass calculated for $[M+2H]^{2+}$: 2254.1. Observed $[M+H]^+$: 4507.1; Observed $[M+2H]^{2+}$: 2254.1.

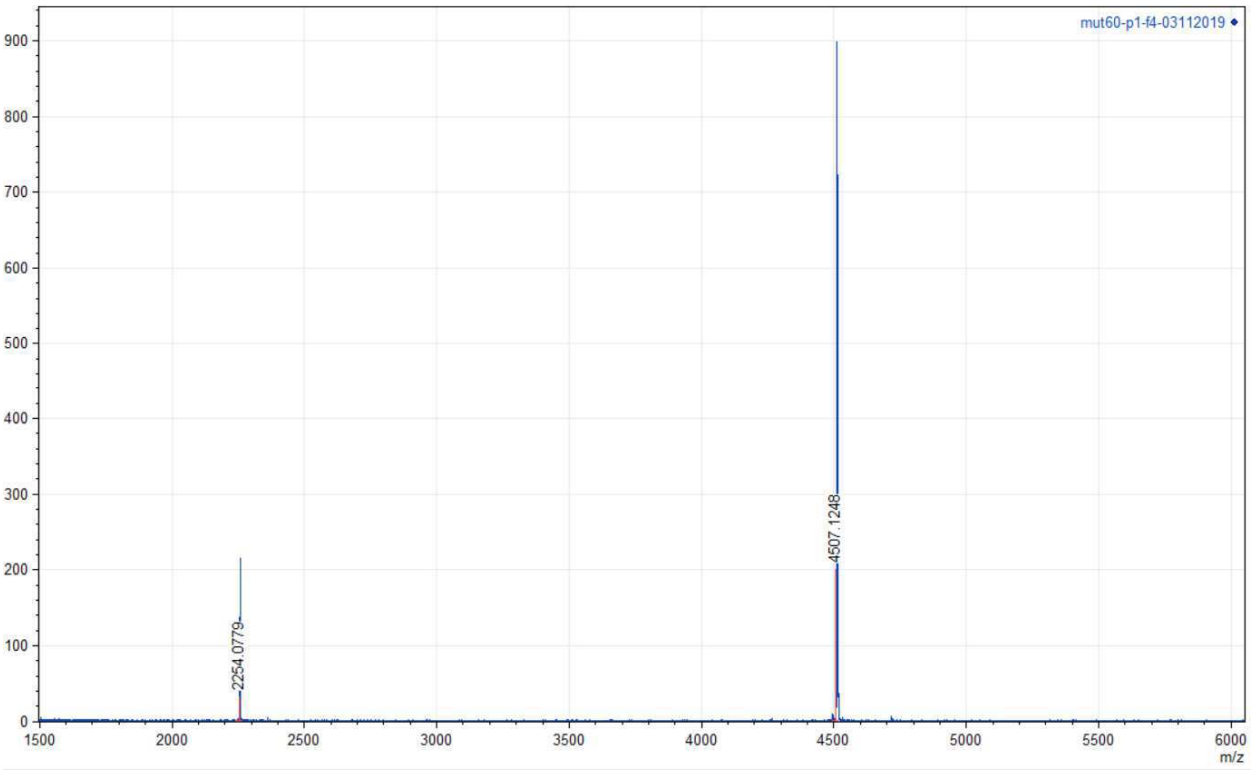

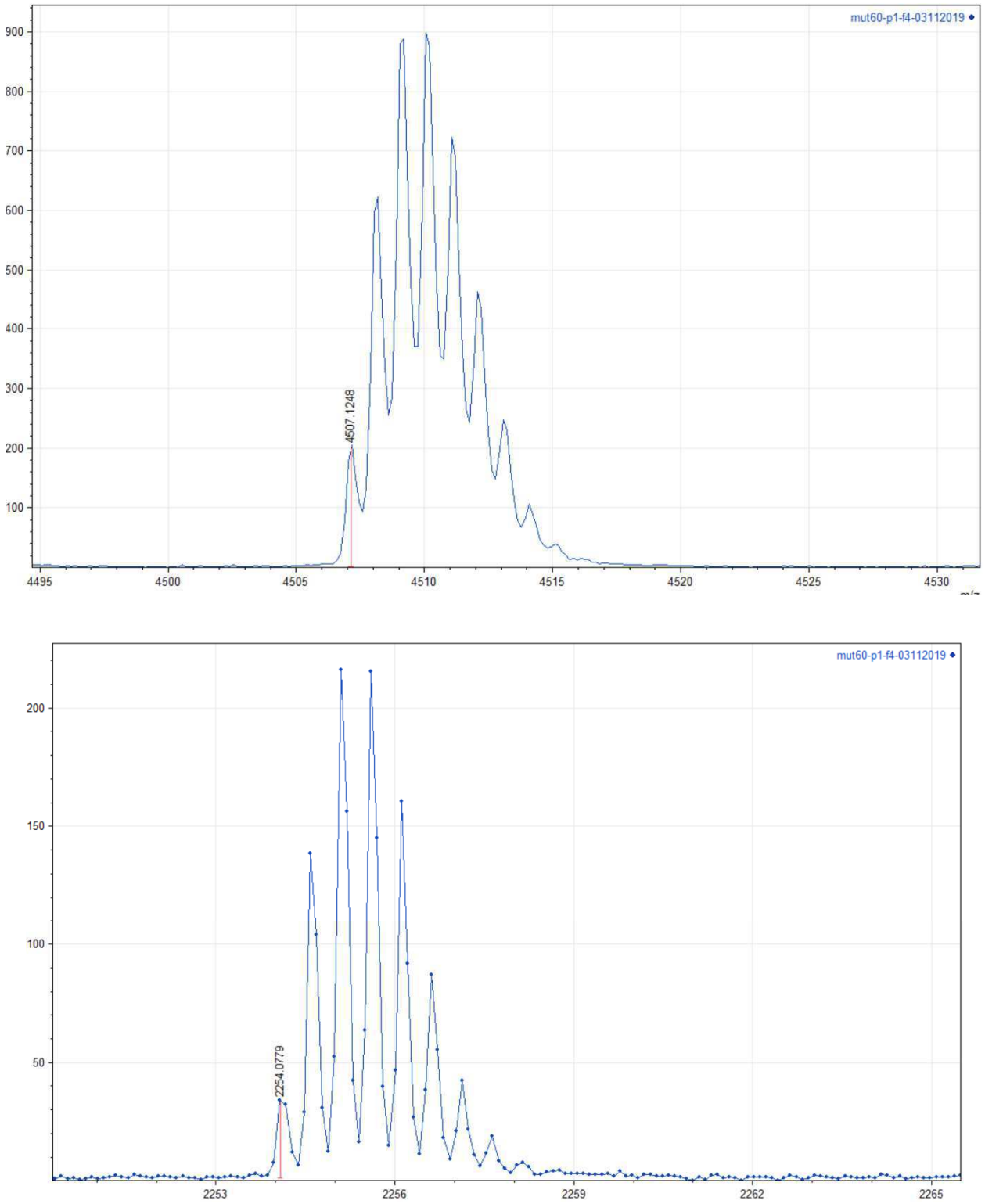

Figure 3.S10. Analytical HPLC and MALDI-MS traces of mutant 6 (Aβ(M1-40) | V18C, G33C).

References and notes

1. These procedures follow closely those that our laboratory has previously published. The procedures in this section are adapted from and in some cases taken verbatim from Yoo, S.; Zheng, S.; Kreutzer, A.; Nowick, J. Biochemistry, 2018, 57, 3861–3866.

2. Walsh, D. M.; Thulin, E.; Minogue, A. M.; Gustavsson, N.; Pang, E.; Teplow, D. B.; Linse, S., A facile method for expression and purification of the Alzheimer's disease-associated amyloid β-peptide. *FEBS J.* **2009**, *276*, 1266-1281.

3. Micsonai A.; Wien F.; Kernya L.; Lee YH.; Goto Y.; Réfrégiers M.; Kardos J. Accurate secondary structure prediction and fold recognition for circular dichroism spectroscopy. *Proc Natl. Acad. Sci. U. S. A.* **2015**, *112*,: 95-103.

4. These particular spectra were reproduced from data presented in Chapter 1, as well as Yoo, S.; Zhang, S.; Kreutzer, A. G.; Nowick, J. S., An Efficient Method for the Expression and Purification of Abeta(M1-42). *Biochemistry* **2018**, *57*, 3861-3866. However, these spectra represent purity and composition of Aβ(M1-42) used in experiments presented in this chapter.

Chapter 4

Square Channels Formed by a Peptide Derived from Transthyretin

Introduction

Elucidating the structures of amyloid fibrils and oligomers represents a vast frontier, of yet unknown scope. The fibrils and aggregates formed by amyloidogenic peptides and proteins are rich in β-sheets, and their structures are tremendously important in amyloid diseases. Many structures of amyloid fibrils have been determined by solid-state NMR spectroscopy of amyloidogenic peptides and proteins and by X-ray crystallography of smaller fragments.[1-4] Studying amyloid oligomer structures at high resolution is challenging, because amyloid oligomers are heterogeneous and dynamic, forming various species of different sizes and morphologies. Although a few structures of amyloid oligomers have been discovered in the last decade, there are not enough to provide full understanding of amyloid assemblies.[5-7]

The Nowick laboratory has pioneered the use of macrocyclic β-sheets as a tool for exploring the structures of amyloid oligomers. Macrocyclic peptides typically comprise of two β-strands that are connected by two β-turn linkers and a N-methyl group, which blocks uncontrolled aggregation to form fibrils. The β-strands of the macrocyclic peptides template β-hairpin sequences of amyloidogenic peptides or proteins of interest (Figure 4.1).[3] β-Hairpin mimicking peptide macrocycles are studied by structural elucidation techniques like NMR and X-ray crystallization, as well as by biological and biophysical techniques to observe their oligomerization in solution. In the last few years, members of the Nowick laboratory have elucidated the X-ray crystallographic structures of macrocyclic peptides derived from Aβ peptide, β_2-microglobulin, and α-synuclein.[4-6]

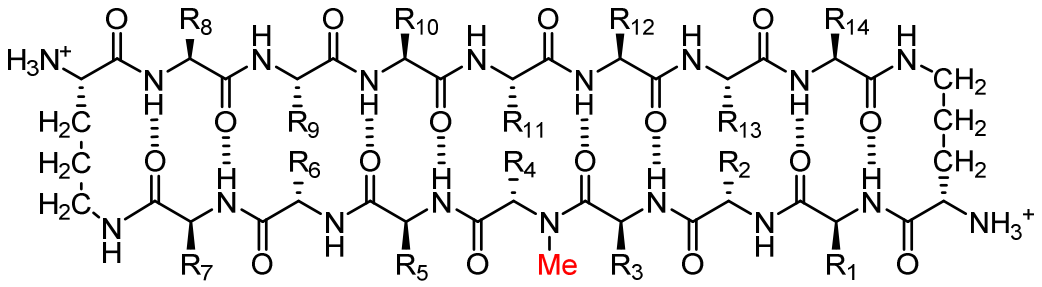

Figure 4.1. Nowick laboratory's macrocyclic scaffold mimic of β-hairpin.

Transthyretin (TTR) is a tetrameric protein that is associated with amyloid diseases, such as senile systemic amyloidosis and familial amyloid polyneuropathy.[15] Two monomers of TTR come together in an edge-to-edge fashion to form dimers. The dimers further pack in a face-to-face fashion to form tetramers. (Figure 4.2).[16] The TTR tetramers transport thyroid hormone and retinol-binding protein. Dissociation of the tetramers into monomers results in formation of the insoluble fibrils and toxic oligomers, which are associated with TTR-related amyloid diseases.[17] Kelly and coworkers have invented an innovative approach to treating familial amyloid polyneuropathy by stabilizing the tetramers with a small molecule drug called Tafamidis.[18] Tafamidis acts by binding to the dimerization interface of two dimers and preventing dissociation into monomers.

Inspired by the structure of the TTR tetramer and the propensity of TTR to form fibrils, I set out to elucidate the assembly of a β-hairpin that comprises the dimerization interface of the TTR tetramer. I incorporated the two β-strands of the TTR β-hairpin into a macrocyclic β-sheet and studied its assembly by X-ray crystallography. To my surprise, I discovered that the peptide exhibits a new mode of supramolecular assembly, forming square channels consisting of an extended network of β-sheets.

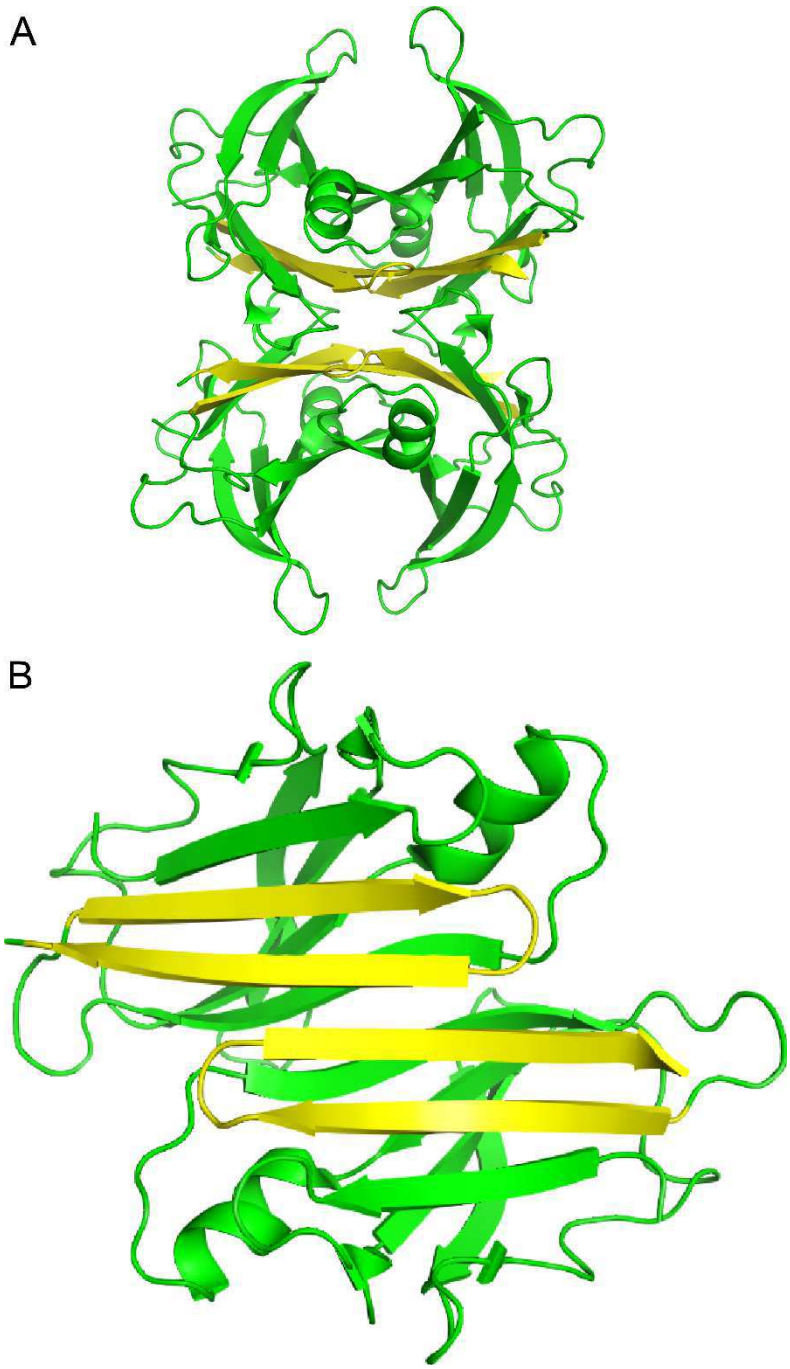

Figure 4.2. X-ray crystallographic structure of TTR protein. (A) X-ray crystallographic structure of the TTR tetramer. The β-hairpin of the tetramer interface is highlighted in yellow (PDB: 1DVQ). (B) TTR dimer subunit.

Results

Design, Synthesis, and Structural Determination of Peptide 1

I incorporated residues 106-112 from strand G and residues 115-121 from strand H into a macrocyclic β-sheet (Figure 4.3). I used two δ-linked ornithine ($^{\delta}$Orn) turn units to connect these two β-strands and form a macrocycle. I replaced the proline-tyrosine turn (residues 113 and 114) with one $^{\delta}$Orn turn to promote β-hairpin formation. I connected residues 106 and 121 with another $^{\delta}$Orn turn to reinforce the β-hairpin structure. I also incorporated an *N*-methyl group on alanine 109 (*N*-Me-A_{109}) to prevent uncontrolled aggregation.[19] I replaced tyrosine 116 with *para*-iodo-phenylalanine (F^{I}_{116}) to determine the X-ray crystallographic phases by single-wavelength anomalous diffraction (SAD) phasing.[20]

Peptide **1** was synthesized using standard Fmoc-based solid-phase synthesis, solution-phase cyclization, and RP-HPLC purification. Peptide **1** was screened with 288 crystallization conditions using Hampton Research crystallization kits (Crystal Screen, Index, and PEG/Ion). Peptide **1** grew rod-shaped crystals suitable for X-ray diffraction in 0.1 M NaOAc buffer at pH 5.3, 0.2 M $CaCl_2$, and 31% isopropanol after two weeks. X-ray diffraction data were collected to 2.08 Å using an X-ray diffractometer with a Cu rotating anode. The crystal structure of peptide **1** was solved and refined in the $P4_32_12$ space group, with one macrocycle in the asymmetric unit.

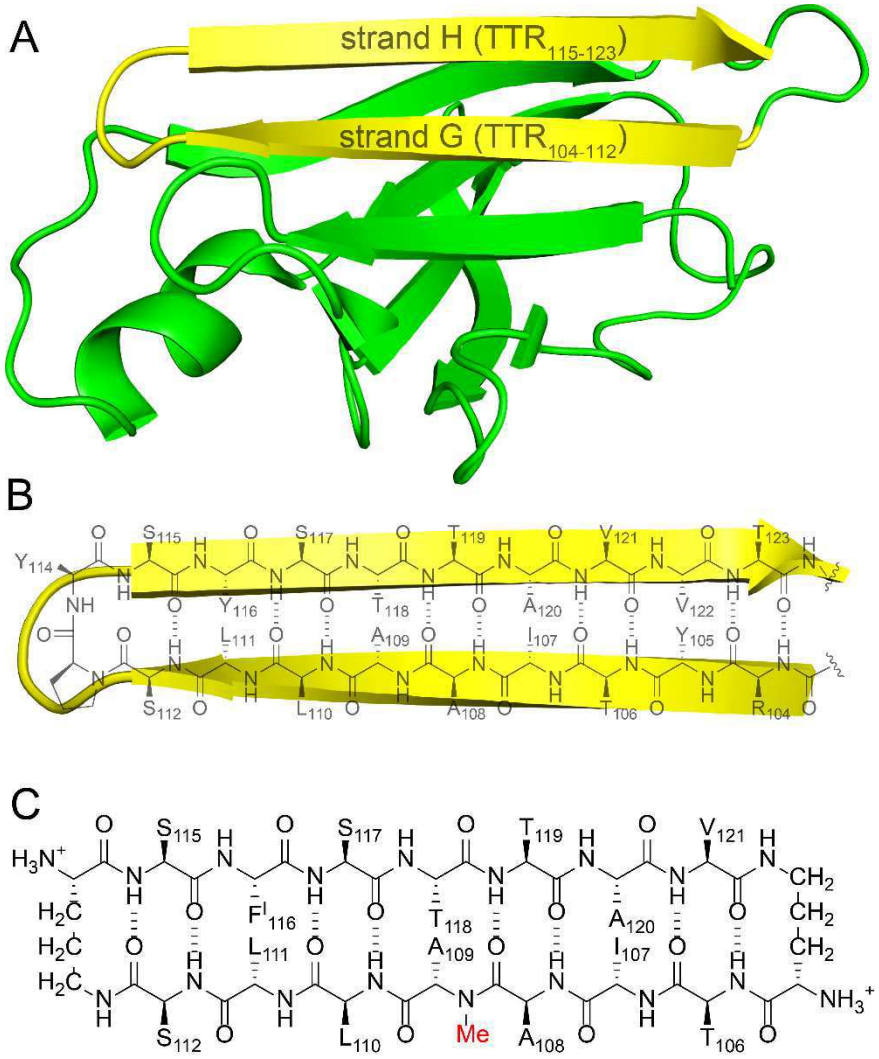

Figure 4.3. (A) TTR monomer. The β-hairpin comprising β-strands G and H is highlighted in yellow. (B) Cartoon and chemical structure of the β-hairpin comprising β-strands G and H. (C) Chemical structure of peptide **1**.

X-ray Crystallography of Peptide 1

The X-ray crystallographic structure of peptide **1** reveals a hierarchical supramolecular assembly. The peptide folds to form a β-hairpin monomer. The β-hairpin assembles to form extended β-sheets. Four extended β-sheets comprise square channels. The square channels pack in into a pattern that resembles tilted windows.

β-*Hairpin Monomer*

Peptide **1** forms a hydrogen-bonded antiparallel β-sheet (Figure 4.4). The β-sheet is relatively flat, with two distinct surfaces. One surface displays side chains from residues T_{106}, A_{108}, L_{110}, S_{112}, S_{115}, S_{117}, T_{119}, and V_{121}; the other surface displays side chains from I_{107}, *N*-Me-A_{109}, L_{111}, F^{I}_{116}, T_{118}, and A_{120}. I term these two surfaces the major and minor faces. The major face contains mostly polar side chains and the minor face contains mostly hydrophobic side chains.

Extended β-*Sheets.* Peptide **1** forms an extended network of β-sheets (Figure 4.5). The β-sheets are not fully aligned, but rather are shifted by four residues toward the C-terminus. The upper strand of one β-hairpin monomer forms four hydrogen bonds with the lower strand of the adjacent β-hairpin monomer. The δ-NH of the ornithine that connects S_{112} and S_{115} hydrogen bonds with the amide oxygen of T_{118}; the amide oxygen of A_{112} hydrogen bonds with the α-NH of T_{119}; the α-NH of L_{111} hydrogen bonds with the amide oxygen of A_{120}; the amide oxygen of *N*-Me-A_{110} hydrogen bonds with the δ-NH of the ornithine that connects T_{106} and V_{121}.

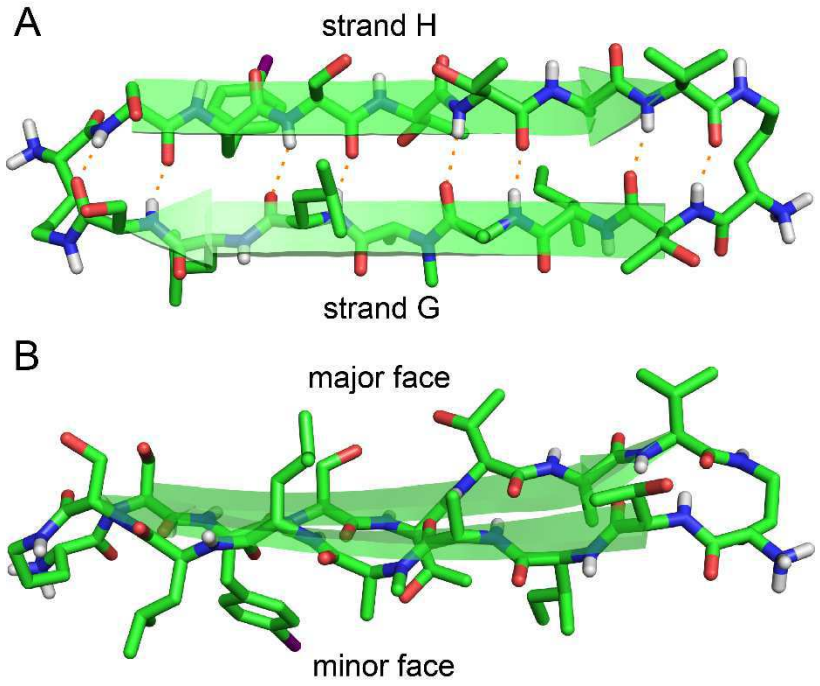

Figure 4.4. X-ray crystallographic structure of peptide **1** (PDB: 5HPP). (A) Hydrogen-bonded β-hairpin monomer. (B) Side view of the β-sheet monomer.

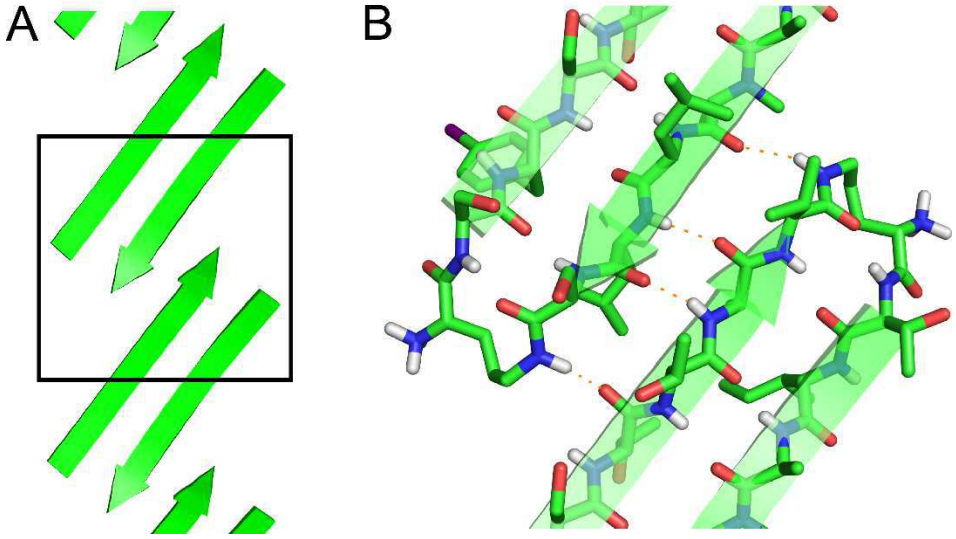

Figure 4.5. (A) Extended β-sheet formed by peptide **1**. (B) Hydrogen-bonding interactions between β-sheets.

Square Channels

Four extended β-sheets make the sides of a square channel (Figure 4.6). Each side of the square channel is approximately 22 Å long, and the inside of the channel is hollow. The side chains of I_{107}, *N*-Me-A_{109}, L_{111}, F^{I}_{116}, and A_{120} point into the square channel, creating a hydrophobic interior. The side chains of T_{106}, S_{112}, S_{115}, S_{117}, and T_{119} point outward, making the outer surface of the square channel mostly polar. Figure 5B shows a top view of the square channel and illustrates the hydrophobic interior and the polar outer surface. Each square channel is stabilized by extended networks of hydrogen bonds between the four sides. The upper strand of each β-hairpin monomer in one side forms four hydrogen bonds with the lower strand of each β-hairpin monomer in the adjacent side. (Figure 4.6C and 4.6D). The amide oxygen of A_{108} hydrogen bonds with the α-NH of the ornithine that connects S_{112} and S_{115}; the α-NH of I_{107} hydrogen bonds with the amide oxygen of S_{115}; the amide oxygen of T_{106} hydrogen bonds with the α-NH of F^{I}_{116}; the α-NH of the ornithine that connects T_{106} and V_{121} hydrogen bonds with the amide oxygen of S_{117}.

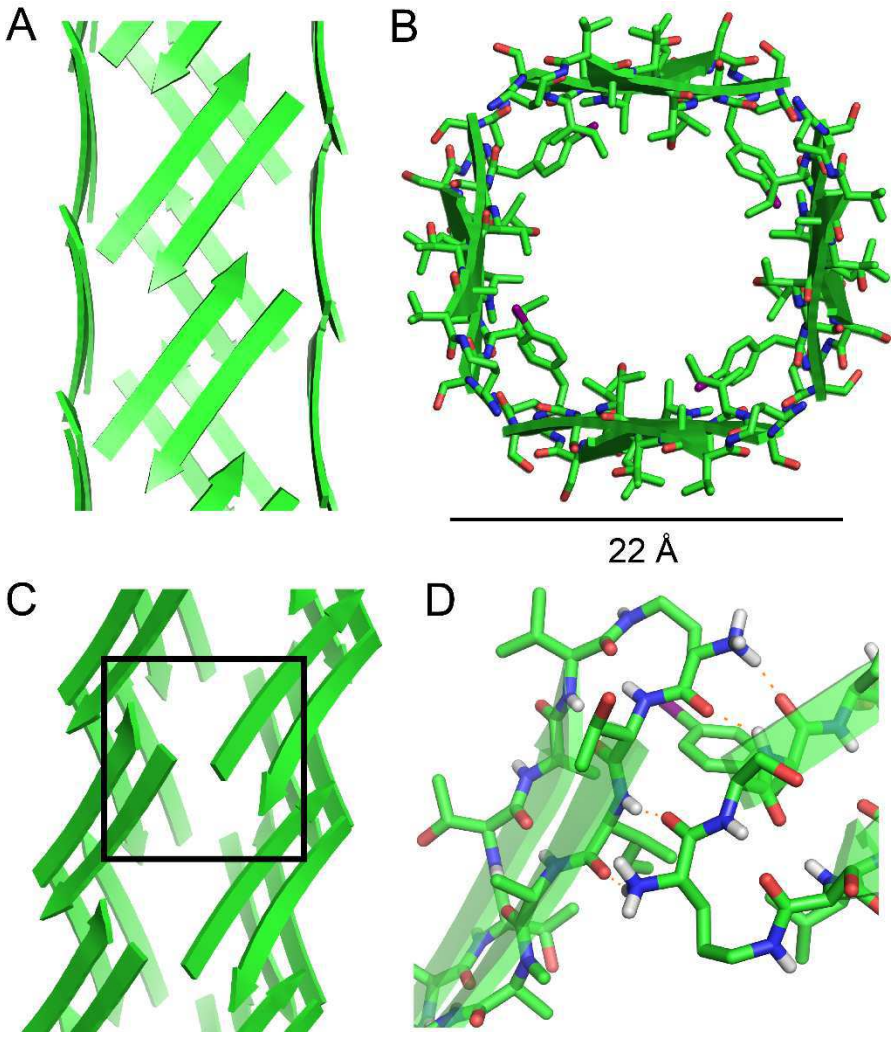

Figure 4.6. Square channel formed by peptide **1**. (A) Side view. (B) Top view. (C) Corner view of a square channel. (D) Hydrogen bonding interactions between perpendicular β-sheets in a square channel.

Each square channel is stabilized by extended networks of hydrogen bonds between the four sides. The upper strand of each β-hairpin monomer in one side forms four hydrogen bonds with the lower strand of each β-hairpin monomer in the adjacent side (Figure 4.6D).

These two networks of hydrogen bonds — those within the extended β-sheets (Figure 4.7) and those between the extended β-sheets (Figure 4.7C and 4.7D) — stabilize the square channels. All of the amide NH and carbonyl groups participate in hydrogen bonding, except the α-NH of T_{118}. To visualize how these two hydrogen-bonding networks act together to stabilize the square channels, one can imagine breaking all of the hydrogen bonds between two extended β-sheets at the corner of the square channel and unrolling and flattening the square channel (Figure 2.6).

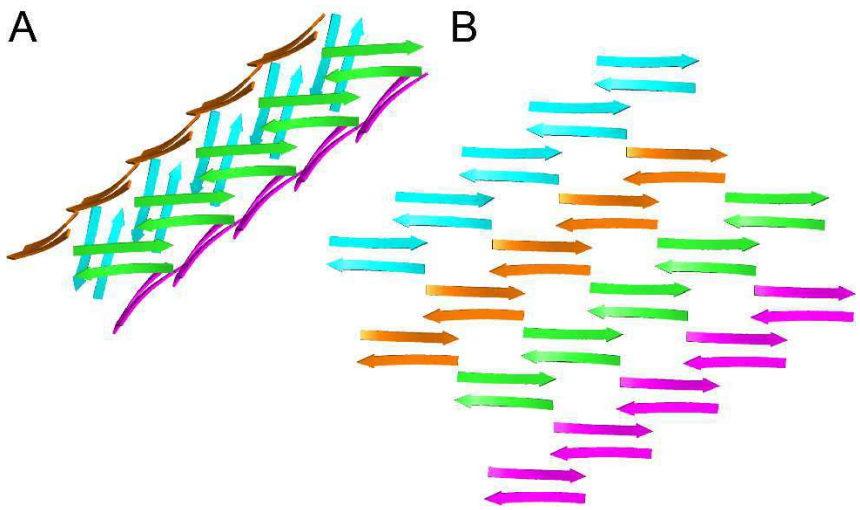

Figure 4.7. (A) Square channel. (B) "unrolled" square channel.

"Tilted Windows."

The square channels further assemble in a "tilted windows" pattern (Figure 4.8). The square channels do not align perfectly in the crystal lattice, but rather are tilted. Each channel makes limited hydrophobic contact with the neighboring channel. Although the outer surface of each channel is composed mostly of polar side chains, the hydrophobic V_{121} is located on one corner and packs against V_{121} of the adjacent square channel.

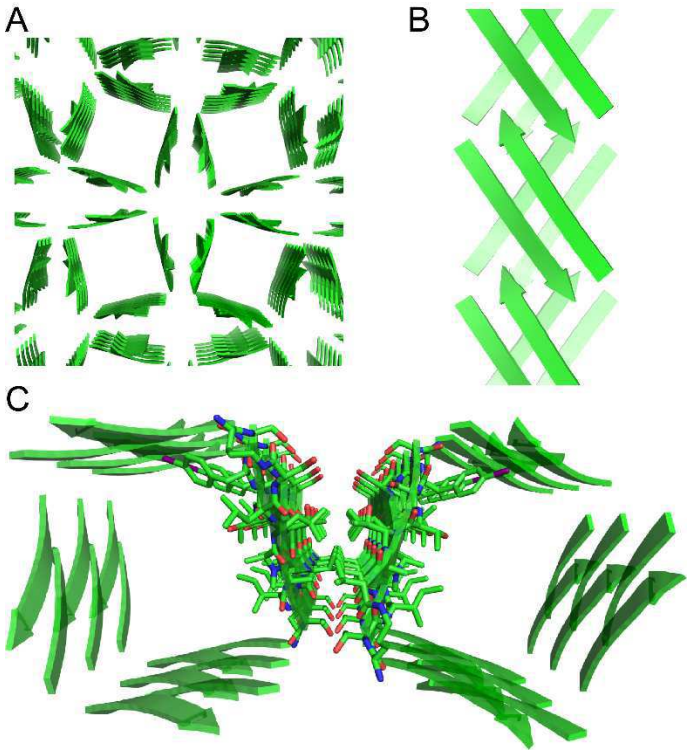

Figure 4.8. (A) Tilted windows assembly of square channels. (B) Side view of the interface between two square channels. (C) Hydrophobic contact between two square channels.

Fibril formation of peptide 1 and alternatively *N*-methylated macrocycles

After solving the crystal structure of peptide **1**, I studied behavior of peptide **1** in solution or outside of crystal lattice. The square channels assembly has characteristics of laminated layers or fibril assemblies, so I hypothesized that I could use the Thioflavin T (ThT) assay to monitor solution phase behavior of peptide **1**. I observed that peptide **1** forms ThT reactive species over time, indicating fibril formation (Figure 4.9).

To provide evidence that the ThT reactive species formed by peptide **1** in solution are the crystallographically observed square channels, I synthesized three isomeric compounds (peptides **2-4**), in which I moved the *N*-methyl group to a position predicted to block square channel assembly. In the square channel assembly of peptide **1**, the *N*-methyl group in A_{109} is essential in forming extended β-sheets and square channels. I synthesized peptide **2**, which has an *N*-methyl group on T_{118} on the opposite strand. In peptide **1**, the amide NH of T_{118} is the only place in the backbone that does not participate in hydrogen-bonding. I also synthesized peptides **3** and **4**, which have *N*-methyl groups on L_{111} and I_{107} on the same strand as peptide **1**. Both place of the *N*-methyl group in peptides **3** and **4** block hydrogen-bonding networks within the extended β-sheet and between the extended β-sheet (Figure 4.10). Peptides **2-4** did not grow crystals in the same conditions as peptide **1**. Peptides **3** and **4** grew crystals in other crystallization conditions, but the crystals were amorphous and not suitable for X-ray diffraction. These results further reinforce the importance of placement of *N*-methyl group on A_{108} in the square channel assembly.

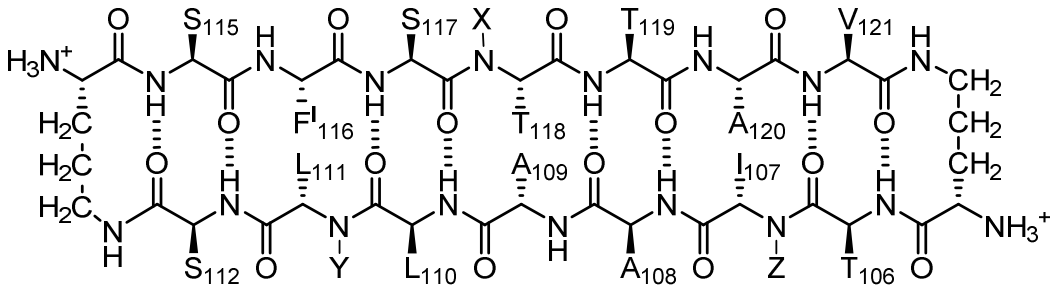

peptide **2**: X=Me, Y=H, Z=H,
peptide **3**: X=H, Y=Me, Z=H
peptide **4**: X=H, Y=H, Z=Me

Figure 4.9. Chemical structure of alternatively *N*-methylated macrocycles, peptides **2, 3,** and **4**.

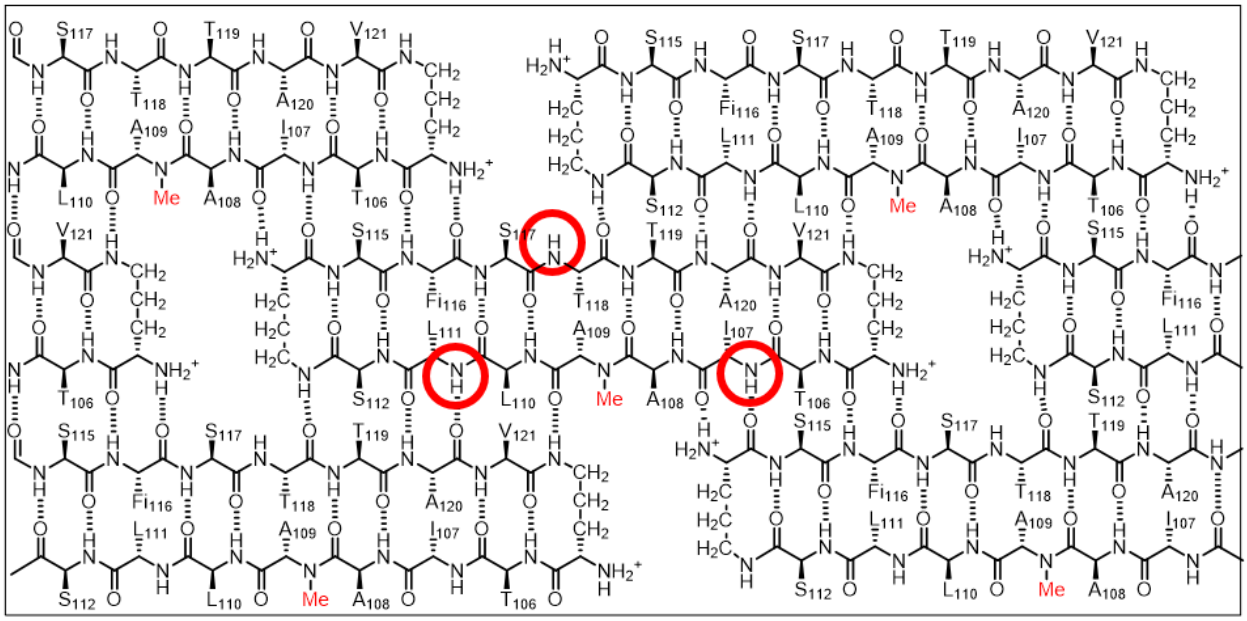

Figure 4.10. Chemical structure of peptide **1** illustrating hydrogen bonding interactions with neighboring peptides. Red circles indicate placements of N-methyl group in peptides **2-4**.

I assessed the fibril forming properties of peptides **1-4** by ThT assay (Figure 4.11). After five hours of incubation, peptide **1** showed fibril formation by ThT, while peptides **2**, **3**, and **4** did not form any fibril by ThT. This result provides evidence that the square channel assembly and fibril formation of peptide **1** may be the same species.

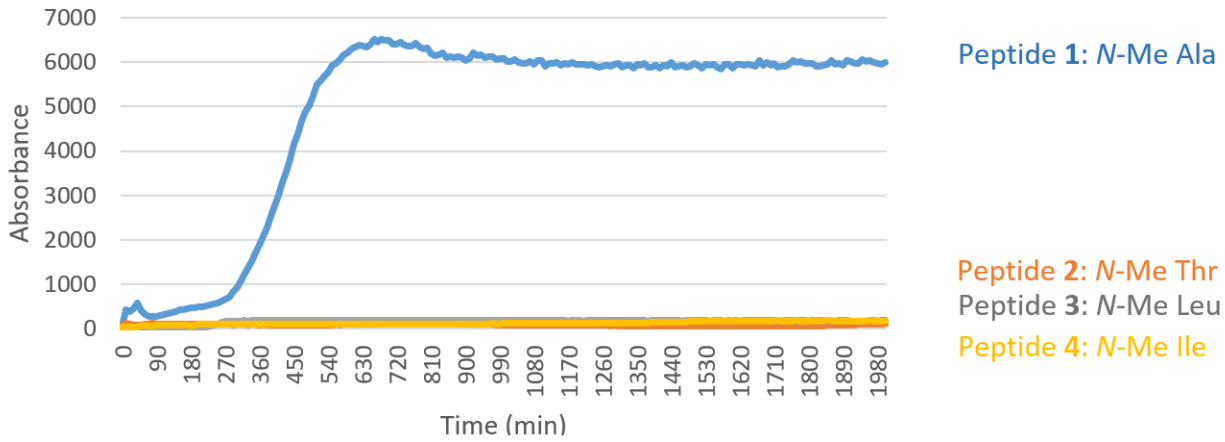

Figure 4.11. ThT fibrillization assay of peptides **1-4**. The peptides were incubated at 37 °C in 30 μM peptides / 50 μM ThT / 1X TBS.

Discussion

In designing peptide **1** to mimic the TTR tetramerization interface, I anticipated that a tetramer would form. Instead of recapitulating the natural mode of assembly of TTR, peptide **1** forms a new mode of supramolecular assembly that has not been observed previously by X-ray crystallography – square channels. In the dimer subunit of the native TTR tetramer, strand H of one monomer pairs with strand H of another monomer.

The square channels formed by peptide **1** resemble β-barrels, because both are composed of continuous networks of hydrogen-bonded β-strands. Eisenberg and coworkers found that an amyloidogenic peptide from αB crystallin forms a six-stranded β-barrel, which they termed a cylindrin (Figure 4.12).[6] The square channels formed by peptide **1** resemble the cylindrin in that the interior is hydrophobic. The structures differ in that the square channels are hollow and run the length of the crystal, while the cylindrin forms a discrete hexamer with a tightly packed interior.

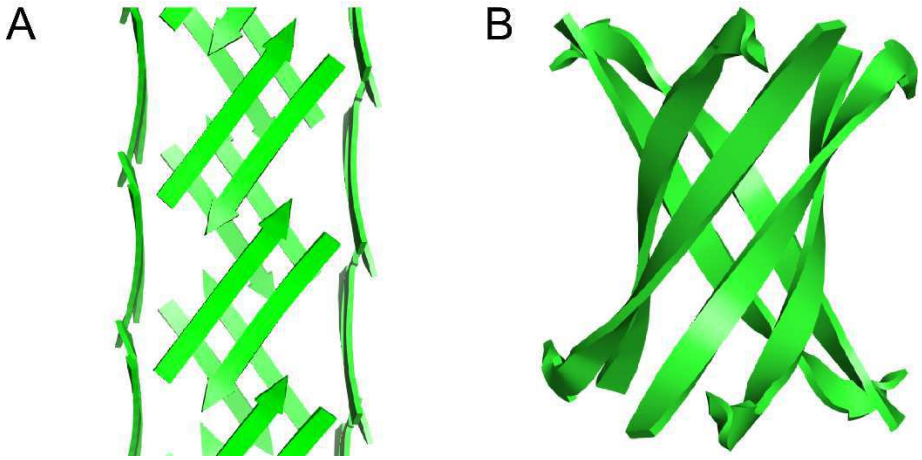

Figure 4.12. (A) Square channel formed by peptide **1**. (B) β-Barrel formed by a peptide fragment from αB crystallin (PDB:3SGO).

The interfaces between the square channels formed by peptide **1** resemble the layered β-sheet structures that compose amyloid fibrils. In amyloid fibrils, β-sheets adjacent to each other to form laminated layers. The interfaces formed by the square channels in the "tilted window" pattern are not as tightly laminated as many amyloid interfaces, such as the "steric zippers" discovered by Eisenberg and coworkers (Figure 4.13).[1]

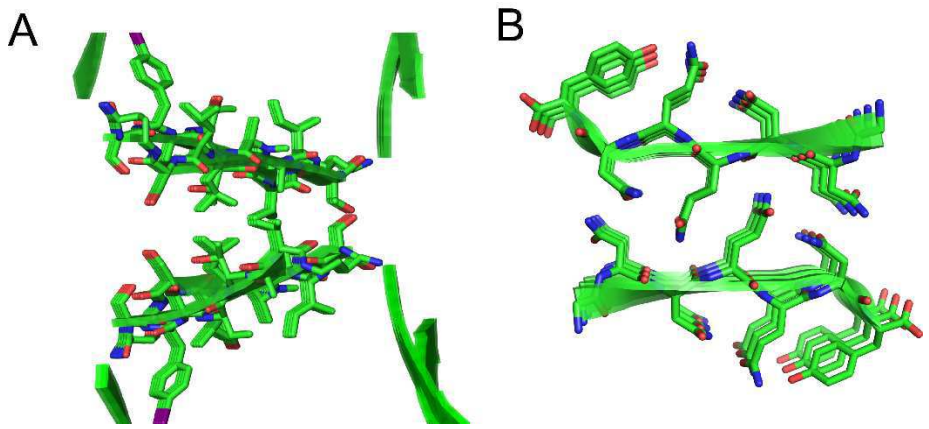

Figure 4.13. (A) Interface between square channels in the "tilted windows" assembly. (B) Layered β-sheet structures formed by a peptide from the yeast prion protein Sup35 (PDB:1YJP).

Although we do not yet understand all of the rules governing the supramolecular assembly of β-sheets, it is clear that the hydrogen-bonding edges impart Lego-like assembly. What makes the square channels formed by macrocyclic β-sheet peptide **1** especially interesting is that I did not design the peptide to assemble in this fashion, but rather this mode of assembly emerged from the structure and sequence of the peptide.

Conclusion

I have designed a macrocyclic peptide derived from TTR. Rather than recapitulating the native TTR tetramer assembly, the peptide formed a square channel assembly that comprises an extended network of hydrogen-bonded β-sheets. This unanticipated result is intriguing because the assembly represents an emergent property of the peptide. I anticipate that this new assembly of β-sheets will serve as a piece of puzzle toward understanding the rules of β-sheet supramolecular assembly. The eventual understanding would yield advances in therapeutics in amyloid diseases and in peptide-based materials by designing structures, functions, and applications.

References and Notes

1. Nelson, R.; Sawaya, M. R.; Balbirnie, M.; Madsen, A. O.; Riekel, C.; Grothe, R.; Eisenberg, D., Structure of the cross-β spine of amyloid-like fibrils. *Nature* **2005**, *435*, 773-778.

2. Sawaya, M. R.; Sambashivan, S.; Nelson, R.; Ivanova, M. I.; Sievers, S. A.; Apostol, M. I.; Thompson, M. J.; Balbirnie, M.; Wiltzius, J. J.; McFarlane, H. T.; Madsen, A. O.; Riekel, C.; Eisenberg, D., Atomic structures of amyloid cross-β spines reveal varied steric zippers. *Nature* **2007**, *44*, 453-457.

3. Petkova, A. T.; Ishii, Y.; Balbach, J. J.; Antzutkin, O. N.; Leapman, R. D.; Delaglio, F.; Tycko, R., A structural model for Alzheimer's β-amyloid fibrils based on experimental constraints from solid state NMR. *Proc. Natl. Acad. Sci. U.S.A.* **2002**, *9*, 16742-165747.

4. Luhrs, T.; Ritter, C.; Adrian, M.; Riek-Loher, D.; Bohrmann, B.; Dobeli, H.; Schubert, D.; Riek, R., 3D structure of Alzheimer's amyloid-β(1-42) fibrils. *Proc. Natl. Acad. Sci. U.S.A.* **2005**, *102*, 17342-17347.

5. Yu, L.; Edalji, R.; Harlan, J. E.; Holzman, T. F.; Lopez, A. P.; Labkovsky, B.; Hillen, H.; Barghorn, S.; Ebert, U.; Richardson, P. L.; Miesbauer, L.; Solomon, L.; Bartley, D.; Walter, K.; Johnson, R. W.; Hajduk, P. J.; Olejniczak, E. T., Structural characterization of a soluble amyloid β-peptide oligomer. *Biochemistry* **2009**, *48*, 1870-1877.

6. Laganowsky, A.; Liu, C.; Sawaya, M. R.; Whitelegge, J. P.; Park, J.; Zhao, M.; Pensalfini, A.; Soriaga, A. B.; Landau, M.; Teng, P. K.; Cascio, D.; Glabe, C.; Eisenberg, D., Atomic view of a toxic amyloid small oligomer. *Science* **2012**, *335*, 1228-1231.

7. Apostol, M. I.; Perry, K.; Surewicz, W. K., Crystal structure of a human prion protein fragment reveals a motif for oligomer formation. *J. Am. Chem. Soc.* **2013**, *135*, 10202-10105.

8. Khakshoor, O.; Lin, A. J.; Korman, T. P.; Sawaya, M. R.; Tsai, S. C.; Eisenberg, D.; Nowick, J. S., X-ray crystallographic structure of an artificial β-sheet dimer. *J. Am. Chem. Soc*. **2010**, *132*, 11622-11628.

9. Liu, C.; Sawaya, M. R.; Cheng, P. N.; Zheng, J.; Nowick, J. S.; Eisenberg, D., Characteristics of amyloid-related oligomers revealed by crystal structures of macrocyclic β-sheet mimics. *J. Am. Chem. Soc.* **2011**, *133*, 6736-6744.

10. Liu, C.; Zhao, M.; Jiang, L.; Cheng, P. N.; Park, J.; Sawaya, M. R.; Pensalfini, A.; Gou, D.; Berk, A. J.; Glabe, C. G.; Nowick, J.; Eisenberg, D., Out-of-register β-sheets suggest a pathway to toxic amyloid aggregates. *Proc. Natl. Acad. Sci. U.S.A.* **2012**, *109*, 20913-20918.

11. Cheng, P. N.; Liu, C.; Zhao, M.; Eisenberg, D.; Nowick, J. S., Amyloid β-sheet mimics that antagonize protein aggregation and reduce amyloid toxicity. *Nat. Chem.* **2012**, *4*, 927-933.

12. Kreutzer, A. G.; Hamza, I. L.; Spencer, R. K.; Nowick, J. S., X-ray crystallographic structures of a trimer, dodecamer, and annular pore formed by an Aβ17-36 β-hairpin. *J. Am. Chem. Soc.* **2016**, 138, 4634-4642

13. Salveson, P. J.; Spencer, R. K.; Nowick, J. S., X-ray crystallographic structure of oligomers formed by a toxic β-hairpin derived from alpha-synuclein: trimers and higher-order oligomers. *J. Am. Chem. Soc.* **2016**, *138*, 4458-4467.

14. Spencer, R. K.; Kreutzer, A. G.; Salveson, P. J.; Li, H.; Nowick, J. S., X-ray crystallographic structures of oligomers of peptides derived from β2-microglobulin. *J. Am. Chem. Soc.* **2015**, *137*, 6304-6311.

15. Rapezzi, C.; Quarta, C. C.; Riva, L.; Longhi, S.; Gallelli, I.; Lorenzini, M.; Ciliberti, P.; Biagini, E.; Salvi, F.; Branzi, A., Transthyretin-related amyloidoses and the heart: a clinical overview. *Nat. Rev. Cardiol.* **2010**, *7,* 398-408.

16. Foss, T. R.; Wiseman, R. L.; Kelly, J. W., The pathway by which the tetrameric protein transthyretin dissociates. Biochemistry **2005**, *44*, 15525-15533.

17. Andersson, K.; Olofsson, A.; Nielsen, E. H.; Svehag, S.-E.; Lundgren, E., Only amyloidogenic intermediates of transthyretin induce apoptosis. *Biochem. Biophys. Res. Commun.* **2002**, *294*, 309-314.

18. Bulawa, C. E.; Connelly, S.; Devit, M.; Wang, L.; Weigel, C.; Fleming, J. A.; Packman, J.; Powers, E. T.; Wiseman, R. L.; Foss, T. R.; Wilson, I. A.; Kelly, J. W.; Labaudiniere, R., Tafamidis, a potent and selective transthyretin kinetic stabilizer that inhibits the amyloid cascade. *Proc. Natl. Acad. Sci. U.S.A.* **2012**, *109*, 9629-9634.

19. Spencer, R.; Chen, K. H.; Manuel, G.; Nowick, J. S., Recipe for β-Sheets: Foldamers containing amyloidogenic peptide sequences. *Eur. J. Org. Chem.* **2013**, 3523-3528.

20. Spencer, R. K.; Nowick, J. S., A Newcomer's guide to peptide crystallography. *Isr. J. Chem.* **2015**, *55*, 698-710.

Supporting Information

Table of Contents

Figure 2.S1. Synthesis of peptides **1**

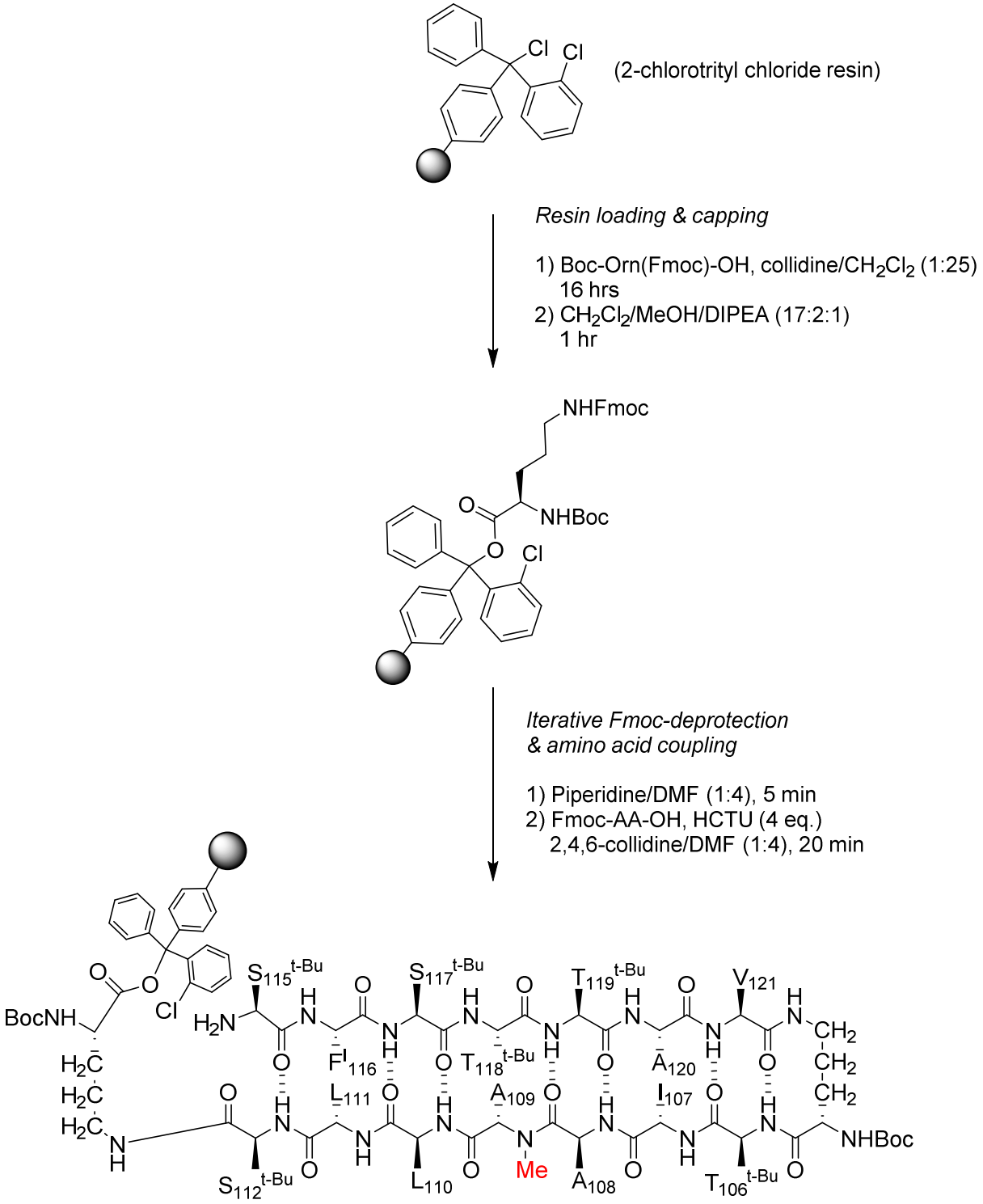

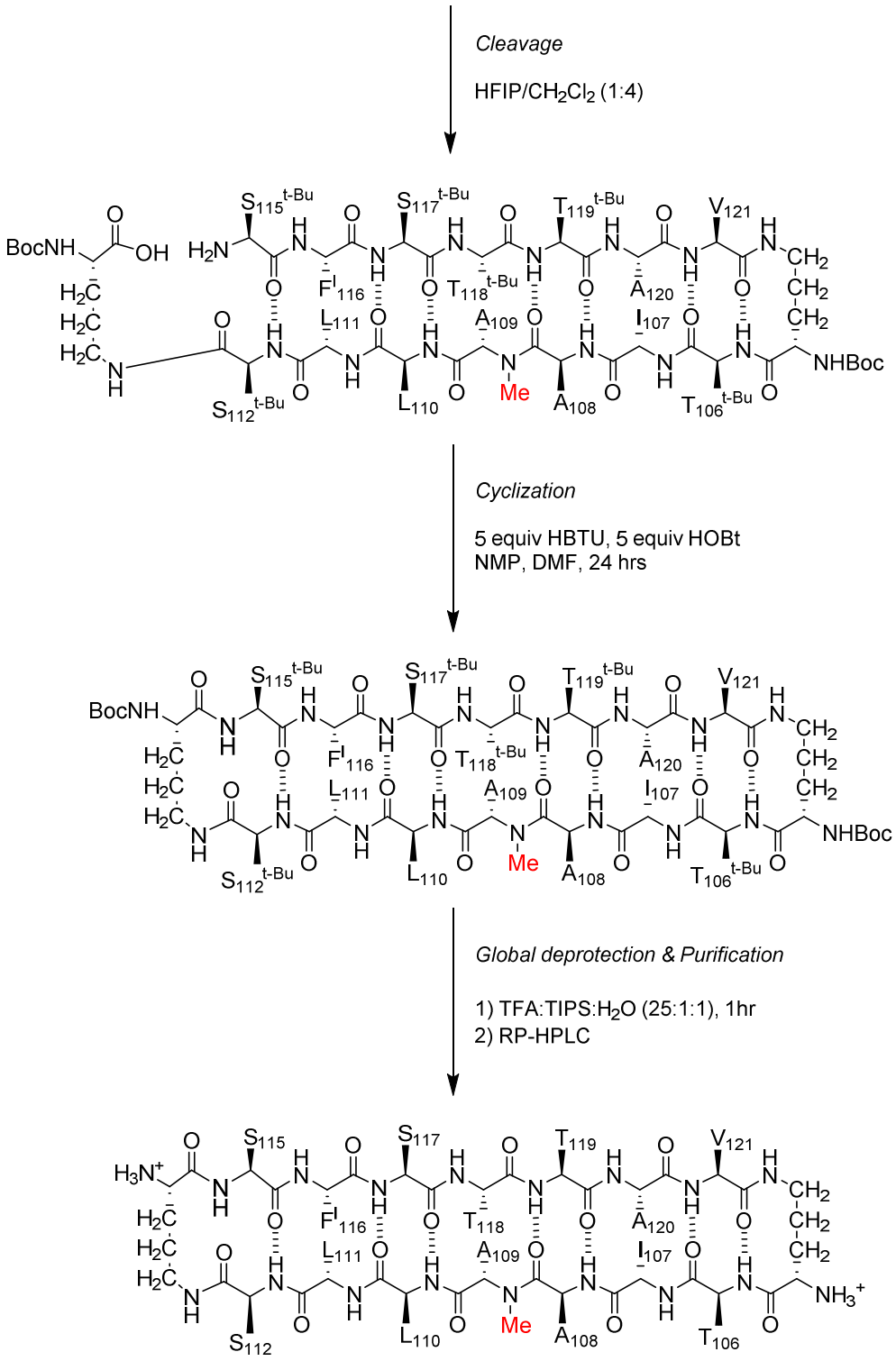

Peptide **1** (TFA salt)

Procedure for the synthesis of peptide 1

Loading resin: 2-Chlorotrityl chloride resin (300 mg, 1.2 g/mol) was added to a Bio-Rad Poly-Prep column. The resin was swollen for 15 minutes in CH_2Cl_2, and the solvent was drained. A 8 mL solution of Boc-Orn(Fmoc)-OH (0.6 equiv, 80 mg, 0.22 mmol) in 4% 2,4,6-collidine in CH_2Cl_2 was added to the resin. The resin was left on a rocker overnight (~16 hours). The solution was drained and a solution of CH_2Cl_2/MeOH/DIPEA (17:2:1) was added to the resin to cap unreacted sites. The suspension was rocked for one hour. The solution was drained and transferred into a reaction vessel for synthesizer or hand-coupling.

Peptide synthesis: The iterative procedure of Fmoc-deprotection and amino acid coupling was done on the PS3 synthesizer or manually as follows: (1) Fmoc-deprotection with 5 mL of 20% piperidine in DMF (5 minutes); (2) washing the resin 3 times with 5 mL DMF; (3) amino acid coupling with 4 equiv of appropriate amino acid (Fmoc-AA-OH) and 4 equiv of HCTU, in 20% 2,4,6-collidine in DMF for 20 minutes. Alanine 108, which follows *N*-methylalanine 109, was coupled twice with 4 equiv of HATU and 4 equiv of HOAt (for one hour per coupling). (4) washing the resin 3 times with 5 mL DMF; (5) final deprotection of Fmoc from the last amino acid coupled; (6) washing 3 times with 5 mL DMF.

Cleavage of the peptide from resin: Resin was transferred to a Bio-Rad Poly-Prep column, washed with 10 mL of CH_2Cl_2, and dried under N_2. A solution of 8 mL of 20% hexafluoroisopropanol (HFIP) in CH_2Cl_2 was added to the resin and agitated for 40 minutes. The filtrate was drained into a 250 mL round bottom flask and the resin was washed with 5 mL CH_2Cl_2. [The resin turns red upon an addition of HFIP solution and turns light yellow/green upon washing with CH_2Cl_2.] An

additional 8 mL of 20% HFIP in CH_2Cl_2 was added and followed by the same procedure. The combined solution was concentrated *in vacuo*, yielding a yellow thin film around the flask.

Cyclization of the peptide: The linear peptide, HOBt (4 equiv), and HBTU (4 equiv) was dissolved in 125 mL DMF and stirred. After 10 minutes of stirring, 0.3 mL of *N*-methylmorpholine was added to the solution and stirred overnight under N_2. The solution was concentrated *in vacuo* to affords the crude cyclic peptide as a yellow oil.

Global deprotection and isolation: The crude cyclized peptide was dissolved in a 20 mL solution of TFA/TIPS/H_2O (25:1:1) and stirred for 1 hour. The solution was concentrated *in vacuo*. The crude peptide was dissolved in 20% ACN in water and filtered through a 0.2 μm syringe filter. The peptide was purified with a C18 column coupled to Beckman preparative HPLC. The fractions were collected over a gradient of 20-60% ACN in water each containing 0.1% TFA. The pure fractions that contained the desired peptide were combined, concentrated *in vacuo*, frozen, and lyophilized to afford the peptide as a white fluffy solid.

Crystallization procedure for peptide 1

Initial screening: Peptide **1** was screened in 864 crystallization conditions using Hampton Research crystallization kits (Crystal Screen, Index, and PEG/ION). This screen was performed using the hanging drop vapor diffusion method in 96-well plates with three 150-nL drops per well. In each hanging drop, a 10 mg/mL solution of peptide **1** in filtered deionized water (18 MΩ) was combined with the crystallization buffer in 1:1, 1:2, and 2:1 ratio. The 96-well plates were set up with a TTP Labtech Mosquito pipetting robot. The 96-well plates were examined daily under a microscope for next seven days to check for crystal growths.

Optimization: Crystallization conditions that grew crystals in the initial screening were optimized further in 4x6 Hampton VDX 24-well plates. The hanging drop vapor diffusion method was used. Each well in optimization plates was set up to contain 1 mL of crystallization buffer based on conditions from the initial screening by varying pH and percent co-solvents. Each hanging drop on siliconized glass cover slides from Hampton Research contained of 10 mg/mL solution of peptide **1** in water and crystallization buffer in 1:1 ratio (2 μL drop), 1:2 ratio (3 μL drop), and 2:1 ratio (3 μL drop). The cover slides were inverted and pressed down onto the 24-well plates with silicon grease to provide a sealed environment in each well.

Data collection and data processing: Data was collected on a Rigaku Micromax-007 HF diffractometer with a Cu rotating anode at 1.54 Å wavelength. The data were integrated, scaled, and merged using iMosflm. Hybrid structure search (HySS) in the Phenix software suite was used to determine the coordinates of the anomalous signal. The electron density maps were generated using the coordinates of the iodine anomalous signal as initial positions in Autosol. Manipulation of the model coordinates was done in Coot. Models were refined with phenix.refine. Table 4.S1 shows the refinement statistics for peptide **1**.

Table 4.S1. **Data collection and refinement statistics for peptide 1**

PDB ID	5HPP
space group	$P4_32_12$
a, *b*, *c* (Å)	42.3, 42.3, 16.3
α, β, λ (°)	90, 90, 90
peptide per asymmetric unit	1
crystallization conditions	0.1 M NaOAc buffer at pH 5.3, 0.2 M $CaCl_2$, and 31% isopropanol
wavelength (Å)	1.54
resolution (Å)	21.15–2.083 (2.157–2.083)
total reflections	2053 (200)
unique reflections	1027 (98)
multiplicity	2.0 (2.0)
completeness (%)	100 (100)
mean I/σ	13.92 (5.49)
Wilson B factor	14.51
R_{merge}	0.04945 (0.1101)
$R_{measure}$	0.06993 (0.1557)
$CC_{1/2}$	0.994 (0.956)
CC^*	0.999 (0.989)
R_{work}	0.1661 (0.1637)
R_{free}	0.1843 (0.2251)
number of non-hydrogen atoms	129
RMS_{bonds}	0.018
RMS_{angles}	1.30
average B-factor	19.33
Number of TLS groups	1

HPLC and ESI-MS of peptide 1

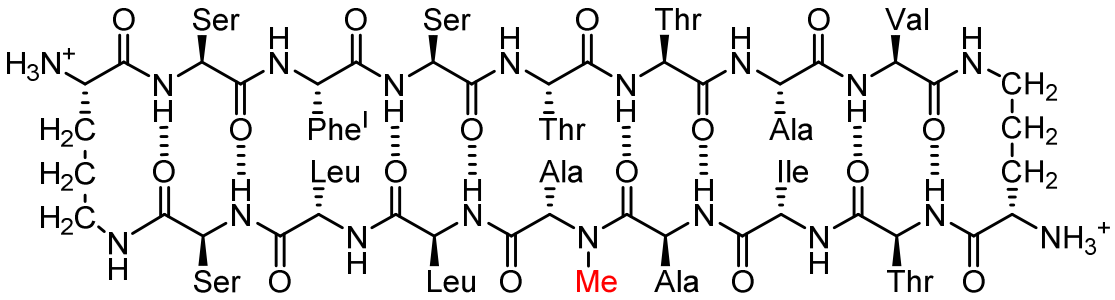

HPLC condition: 5-95 % acetonitrile over 20 minutes

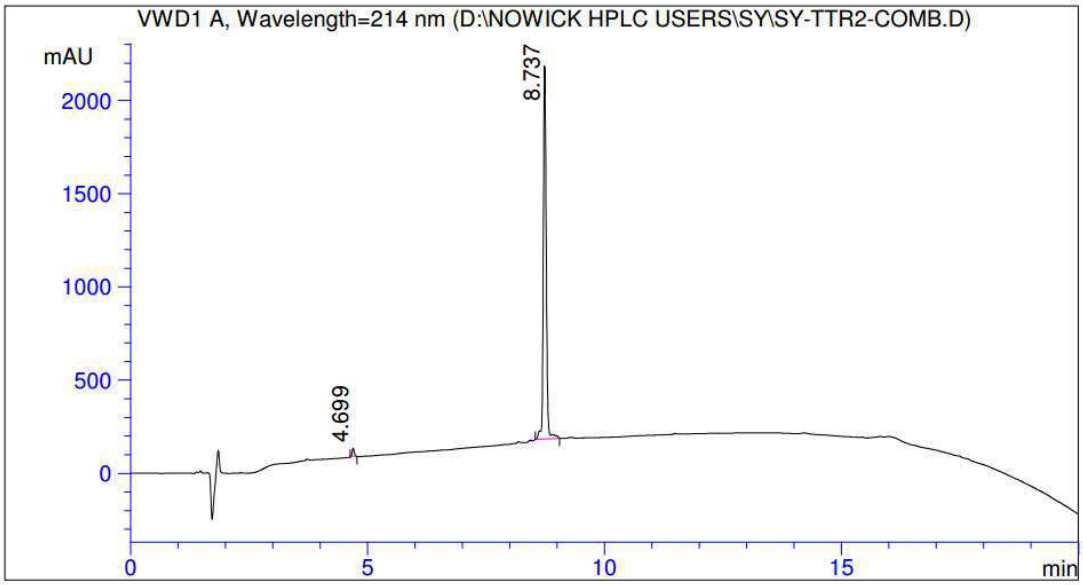

Signal 1:VWD1 A, Wavelength=214 nm

Peak #	RT [min]	Type	Width [min]	Area mAU*s	Height [mAU]	Area %
1	4.699	MM	0.045	122.752	2.166	1.393
2	8.737	MM	0.071	8690.231	97.834	98.607

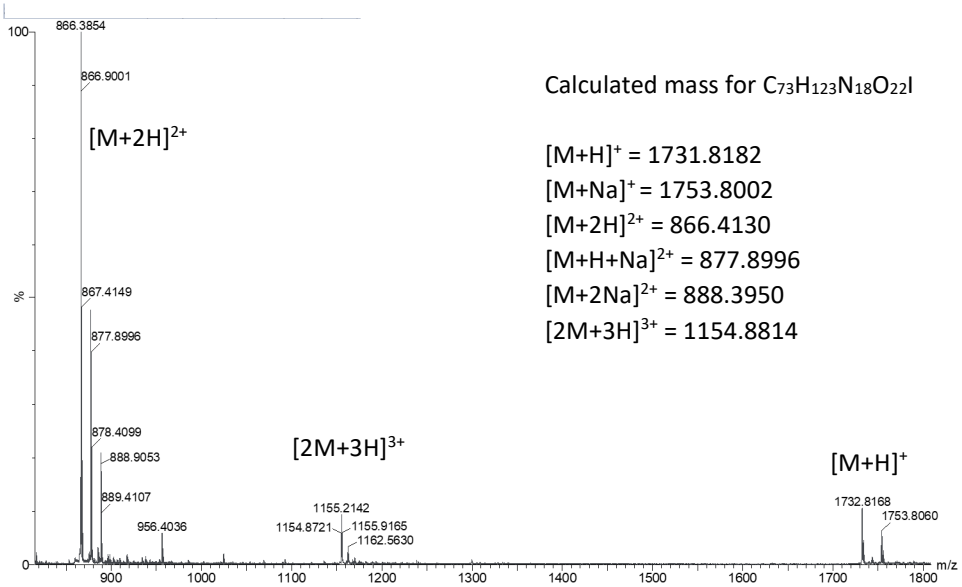

Calculated mass for $C_{73}H_{123}N_{18}O_{22}I$

$[M+H]^+$ = 1731.8182
$[M+Na]^+$ = 1753.8002
$[M+2H]^{2+}$ = 866.4130
$[M+H+Na]^{2+}$ = 877.8996
$[M+2Na]^{2+}$ = 888.3950
$[2M+3H]^{3+}$ = 1154.8814

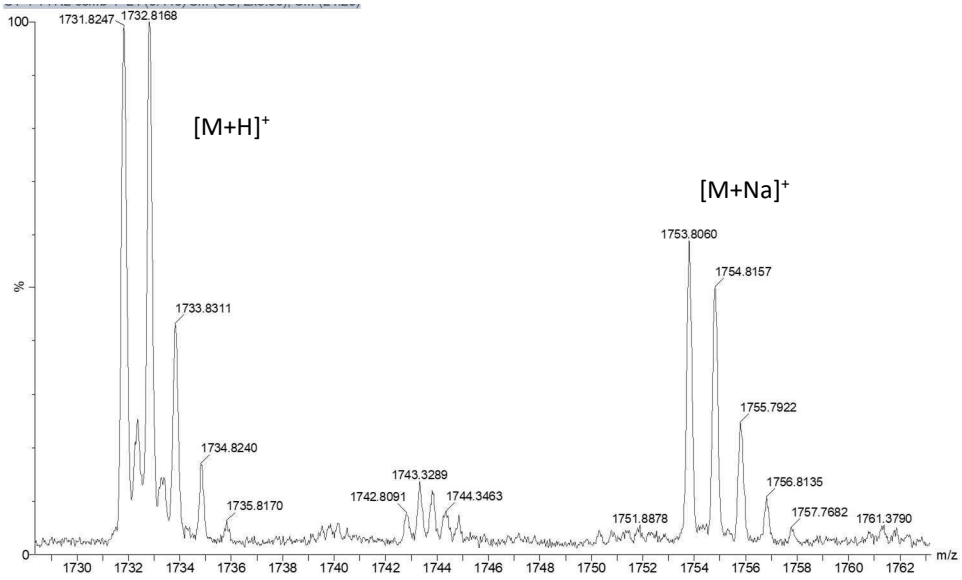

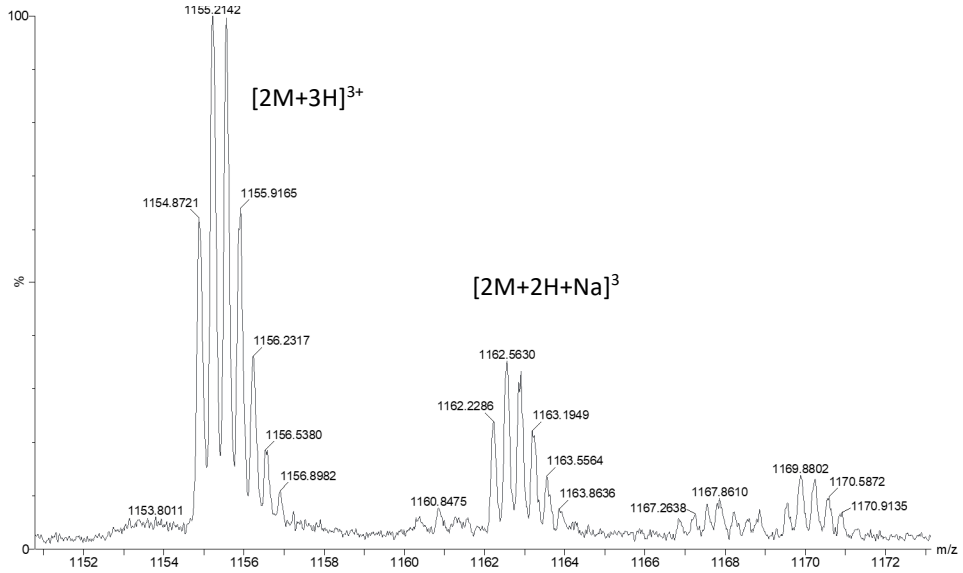

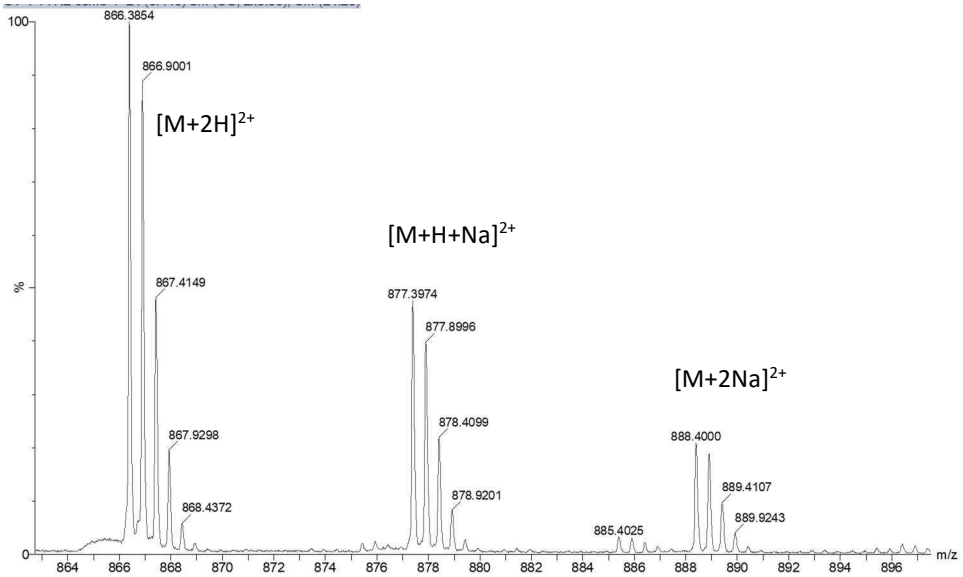

Figure 2.S2. HPLC and ESI-MS of peptide **1**

HPLC and ESI-MS of peptide 2

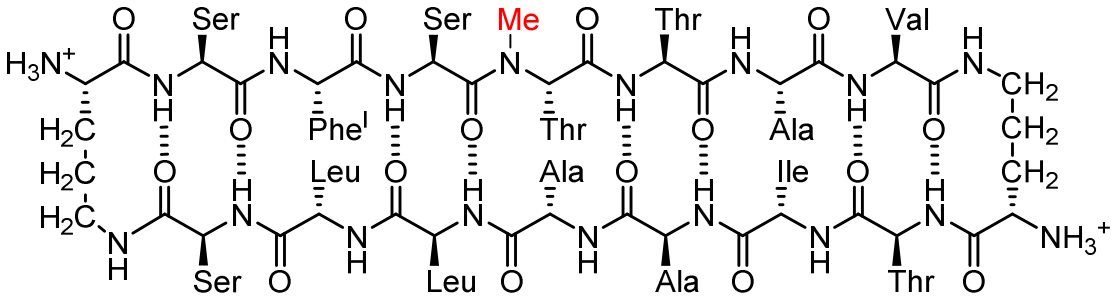

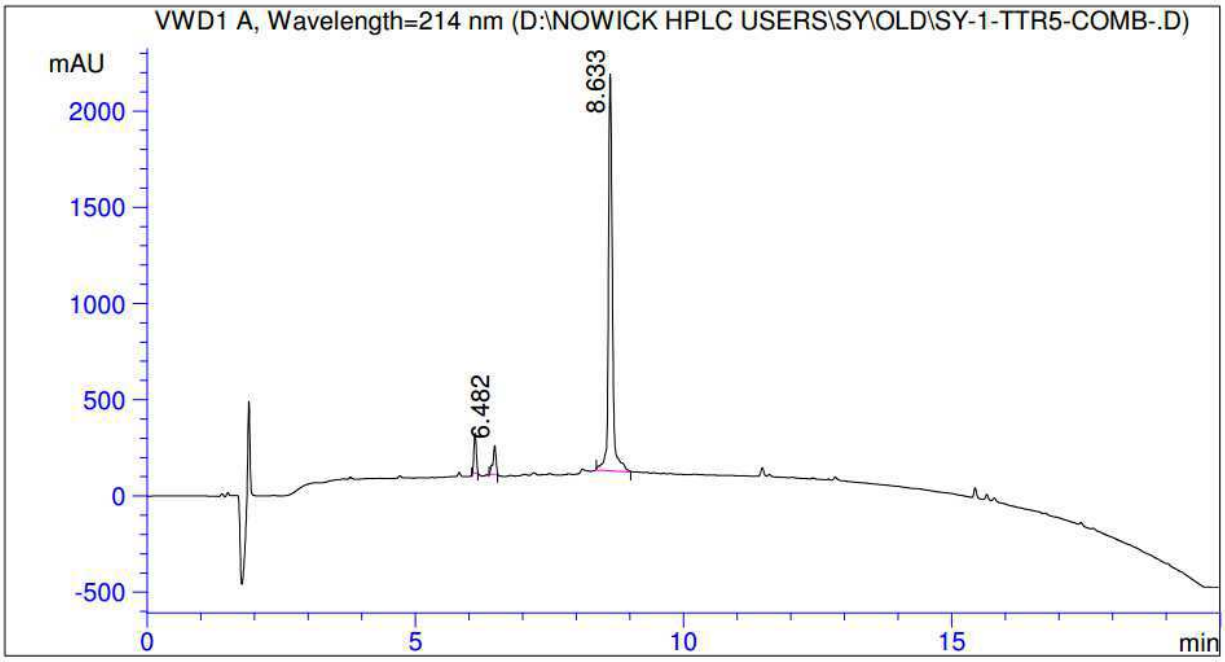

Signal 1:VWD1 A, Wavelength=214 nm

Peak #	RT [min]	Type	Width [min]	Area mAU*s	Height [mAU]	Area %
1	6.115	MM	0.049	618.643	8.593	5.233
2	6.482	MM	0.065	584.652	6.182	4.945
3	8.633	MM	0.085	10618.637	85.225	89.822

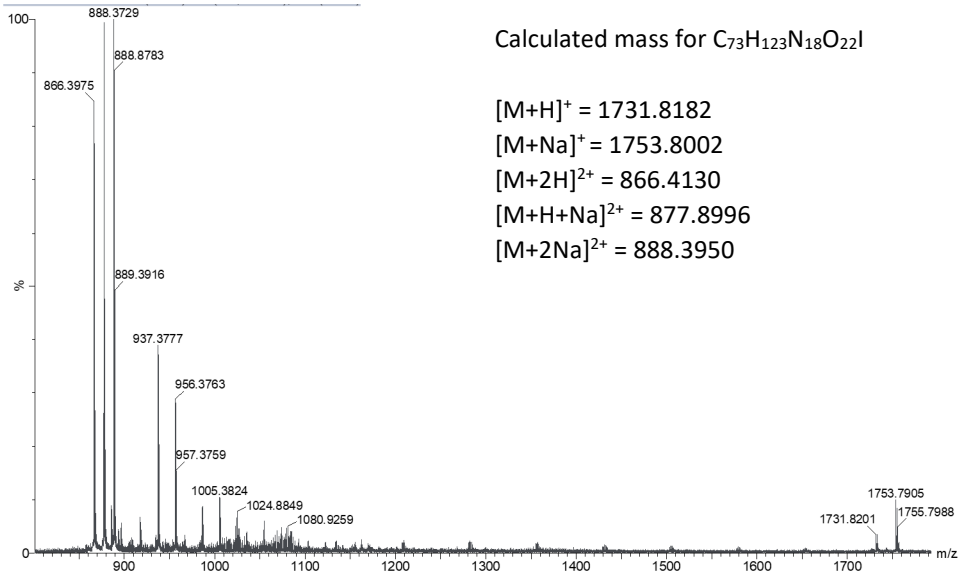

Calculated mass for $C_{73}H_{123}N_{18}O_{22}I$

$[M+H]^+$ = 1731.8182
$[M+Na]^+$ = 1753.8002
$[M+2H]^{2+}$ = 866.4130
$[M+H+Na]^{2+}$ = 877.8996
$[M+2Na]^{2+}$ = 888.3950

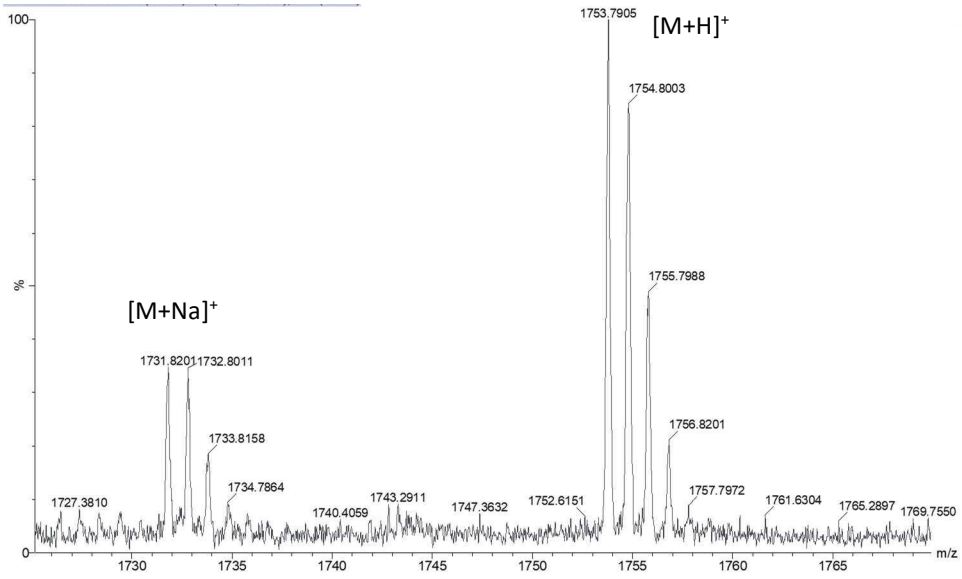

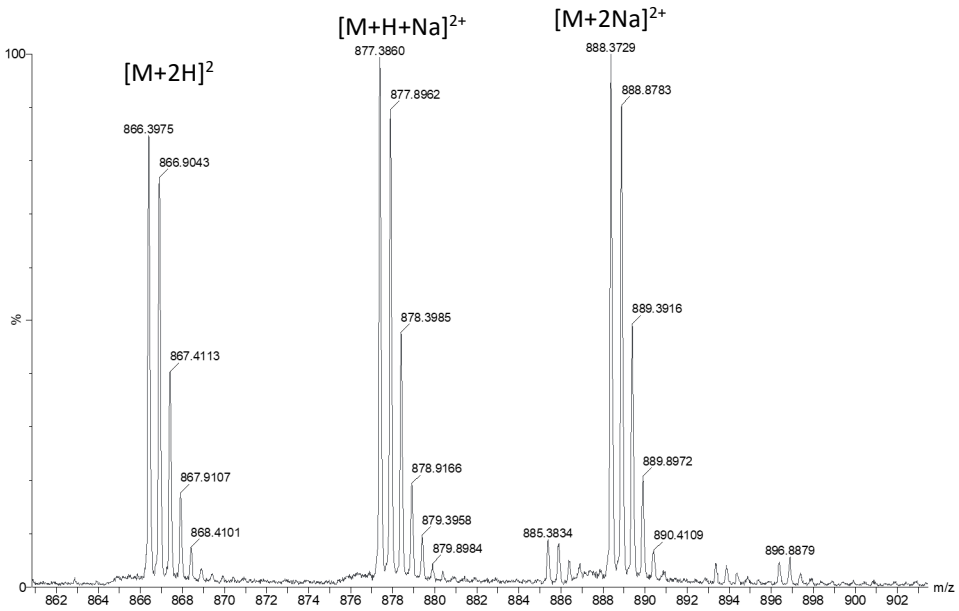

Figure 2.S3. HPLC and ESI-MS of peptide **2**

HPLC and ESI-MS of peptide 3

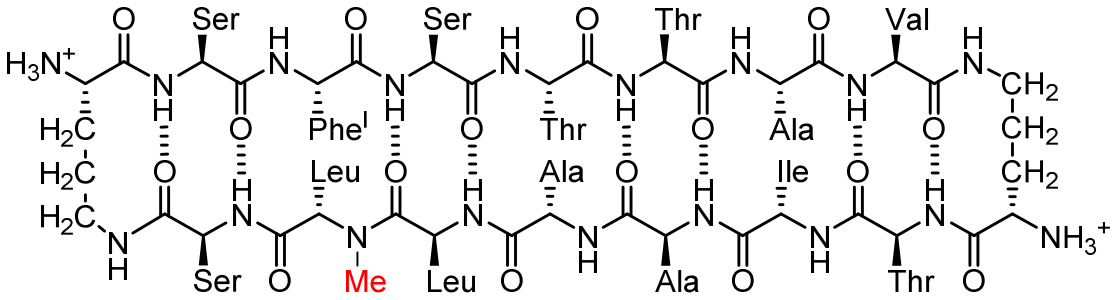

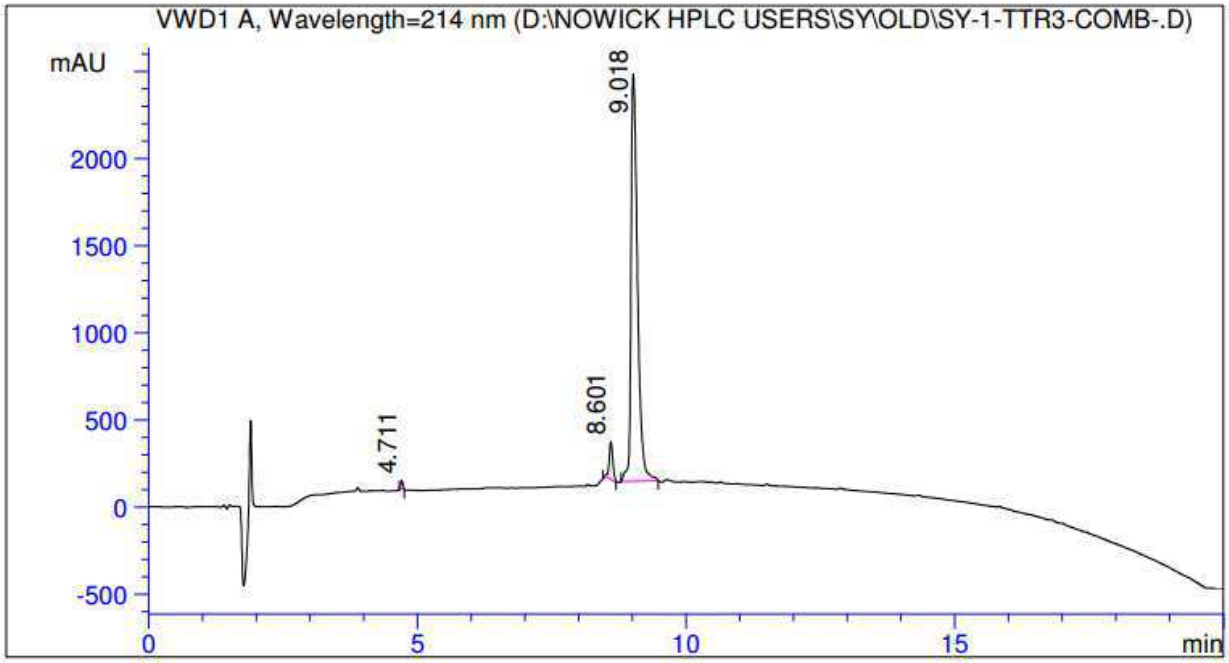

Signal 1:VWD1 A, Wavelength=214 nm

Peak #	RT [min]	Type	Width [min]	Area mAU*s	Height [mAU]	Area %
1	4.711	MM	0.043	116.074	1.720	0.560
2	8.601	MM	0.080	1023.719	8.241	4.939
3	9.018	MM	0.139	19587.502	90.039	94.501

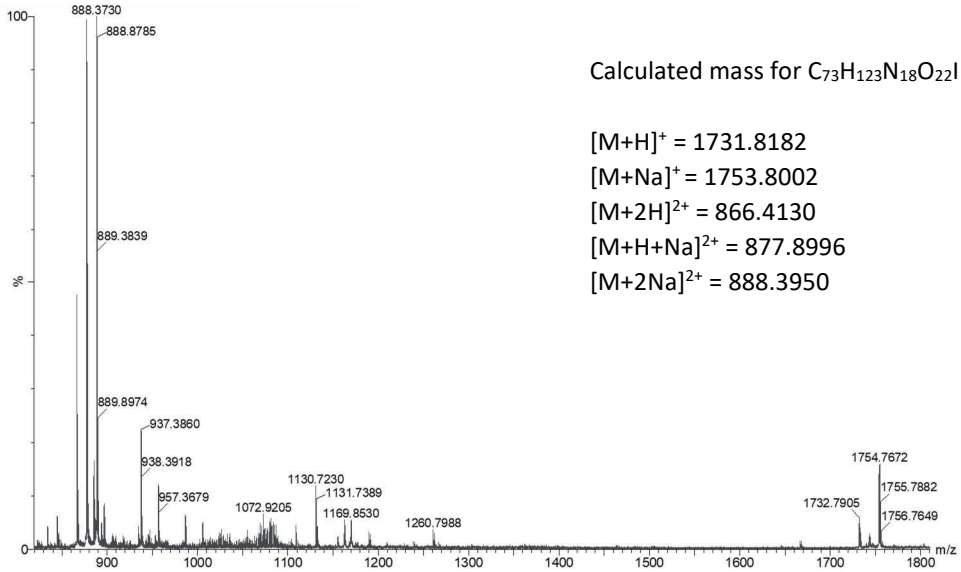

Calculated mass for $C_{73}H_{123}N_{18}O_{22}I$

$[M+H]^+$ = 1731.8182
$[M+Na]^+$ = 1753.8002
$[M+2H]^{2+}$ = 866.4130
$[M+H+Na]^{2+}$ = 877.8996
$[M+2Na]^{2+}$ = 888.3950

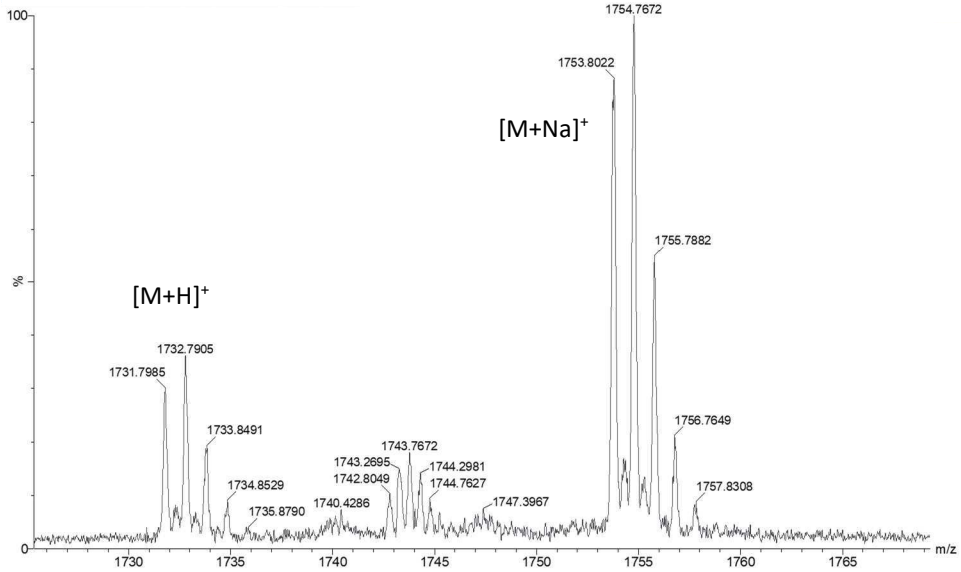

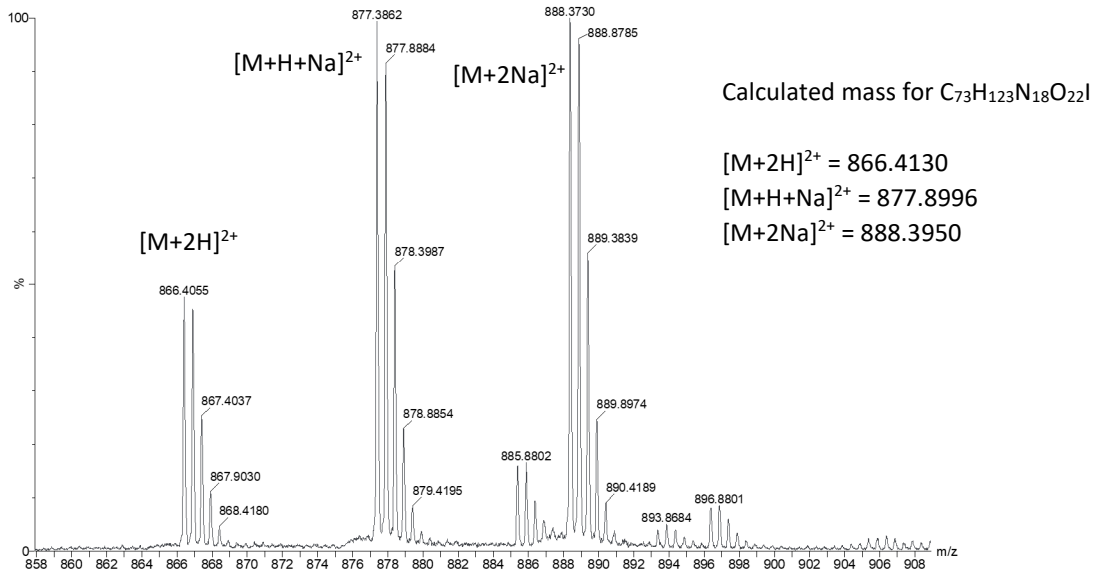

Figure 2.S4. HPLC and ESI-MS of peptide **3**

HPLC and ESI-MS of peptide 4

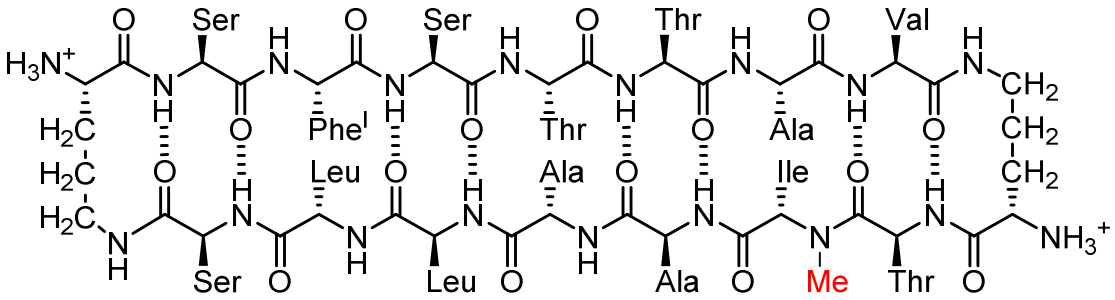

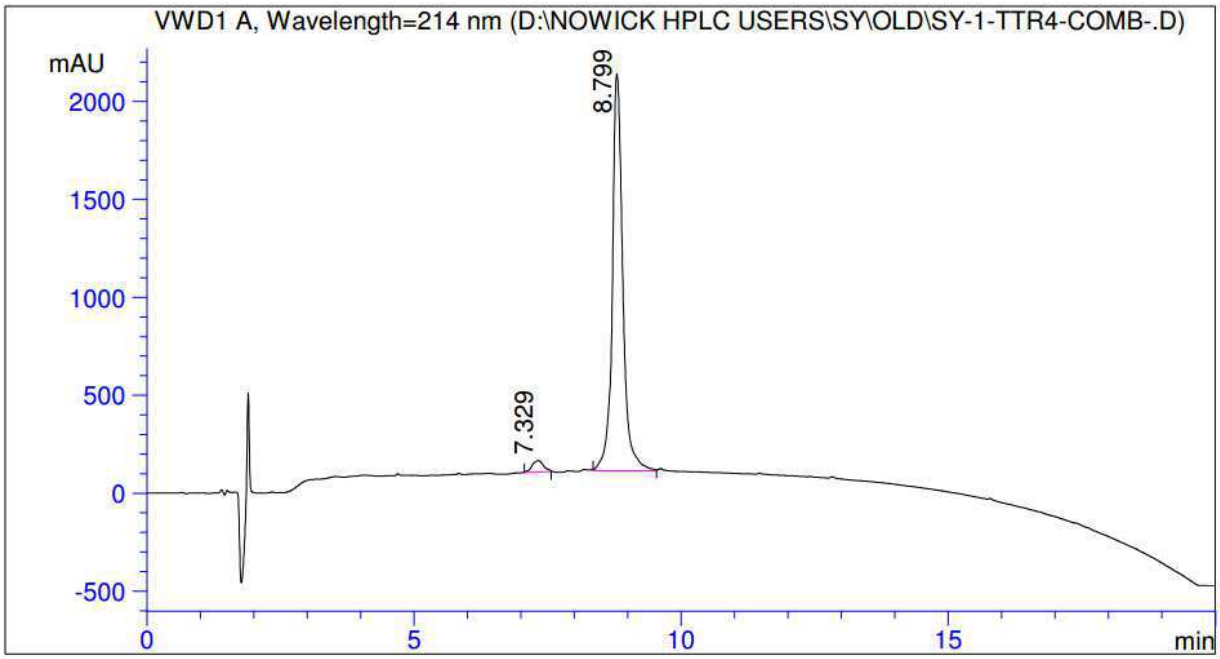

Signal 1:VWD1 A, Wavelength=214 nm

Peak #	RT [min]	Type	Width [min]	Area mAU*s	Height [mAU]	Area %
1	7.329	MM	0.251	879.103	2.803	3.079
2	8.799	MM	0.228	27672.213	97.197	96.921

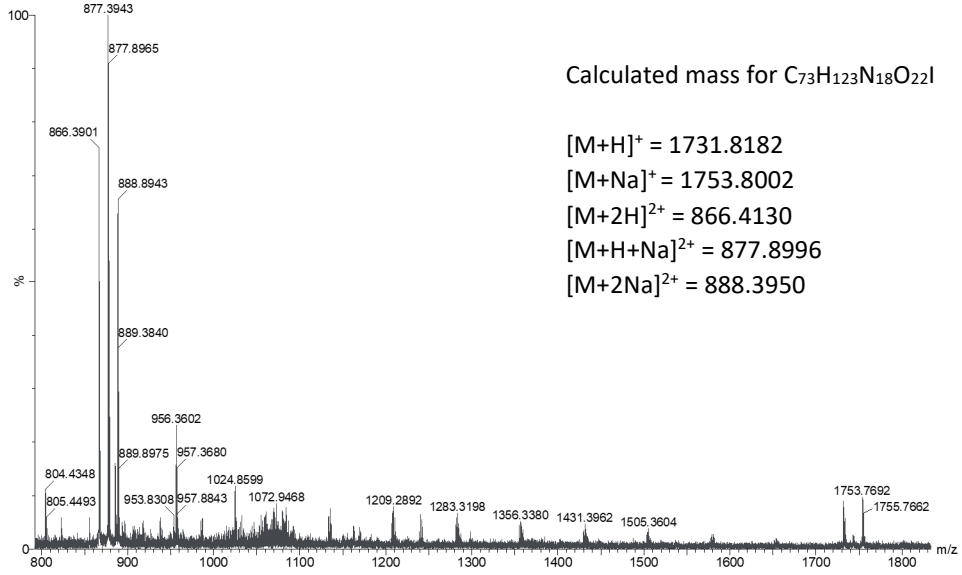

Calculated mass for $C_{73}H_{123}N_{18}O_{22}I$

$[M+H]^+$ = 1731.8182
$[M+Na]^+$ = 1753.8002
$[M+2H]^{2+}$ = 866.4130
$[M+H+Na]^{2+}$ = 877.8996
$[M+2Na]^{2+}$ = 888.3950

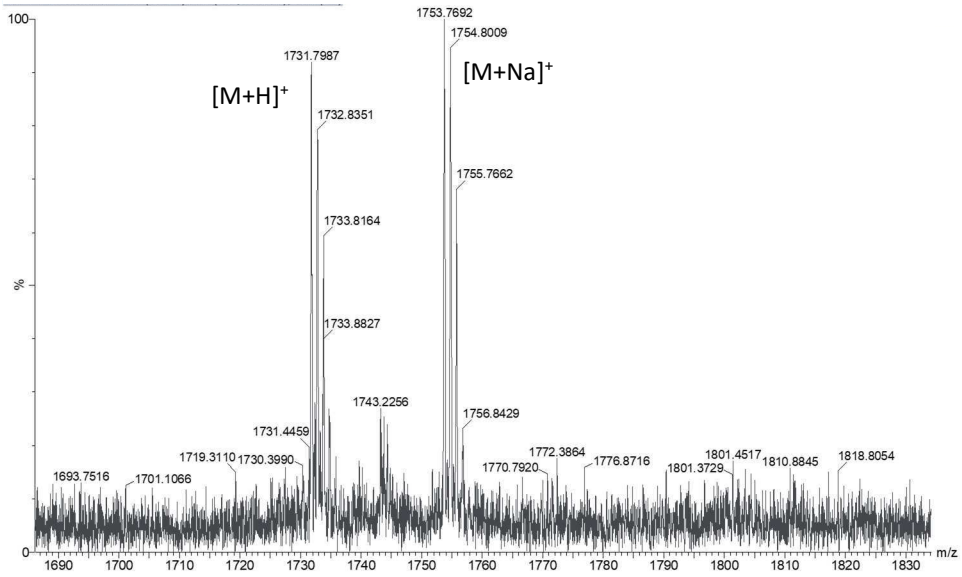

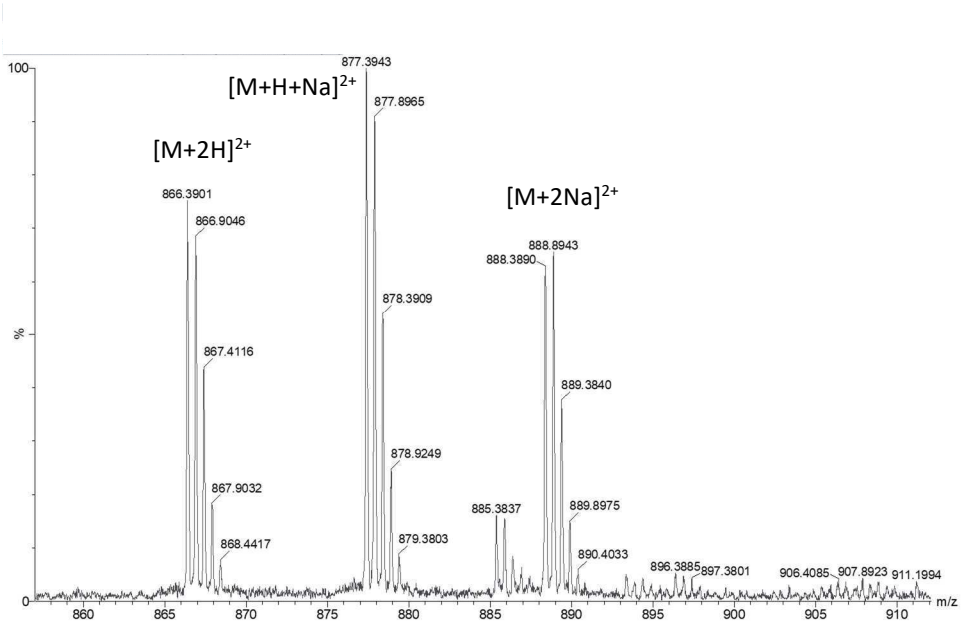

Figure 2.S5. HPLC and ESI-MS of pept**ide 4**

Epilogue:

My Collaborations

in the Nowick Laboratory

Introduction

I was fortunate to have collaborated with many talented members of the Nowick lab as well as other laboratories during my graduate career. In this chapter, I wanted to highlight collaborative projects that I got to give my hands to. These collaborations have been one of the best parts of my research career for a few reasons: (1) I got to learn to work and communicate with researchers with different background; (2) I got to learn many new techniques that I would not have learned otherwise; (3) The researchers who I got to help with their projects also happily helped me with my projects.

Through these collaborations, I learned that I very much enjoy working with colleagues and bringing research goals to fruition through communication and teamwork. Having collaborated with scientists with diverse disciplines: chemists, biologists and immunologists, I have learned to communicate and work with scientists that have different expertise. I believe that communication and collaboration between scientists in different fields are essential for achieving important scientific goals. I wish to continue to build collaborations and synergistic relationships with colleagues in the future in an industry setting.

1. Stabilization, Assembly, and Toxicity of Trimers Derived from Aβ.[1]

In my first year in the Nowick laboratory, I was assigned to assist Dr. Adam Kreutzer with his project which he was trying to covalently stabilize three monomers containing two cysteines each to form covalently stabilized trimers. The design of stabilized trimer originates from our laboratory's previous finding where macrocyclic peptide templating Aβ β-hairpin formed trimeric trimer assembly in its X-ray crystallographic structure.[2] Two amino acids in each vertices of the trimers were mutated to two cysteines and which were then oxidized into covalently linked trimers (Figure 5.1). These triangular trimers represented unprecedented stable oligomeric model that could help researchers understand the oligomerization of Aβ. Biophysical and biological studies of the stabilized trimers showed similar assembly that was observed in the crystallographic structure and similar toxicity mechanism toward a neuronally derived human cell line, SH-SY5Y.

I was tasked to synthesize the covalently stabilized trimers, screen for crystallization, and optimize crystallization conditions. I synthesized large amounts of the monomer unit of the trimer using solid-phase peptide synthesis and optimized the oxidation condition to form stabilized trimers. Next, I set up crystallization screens and optimized crystallization conditions, varying concentrations of buffer, additives, and the peptide. I was able to grow high-quality diffracting crystals to be mounted on X-ray diffractometer. Adam and I collected many X-ray diffraction datasets to solve the crystal structure of the trimer. The X-ray crystallographic structure showed that the stabilized trimers assemble to form hexamers, dodecamers, and annular pore-like structures (Figure 5.2).

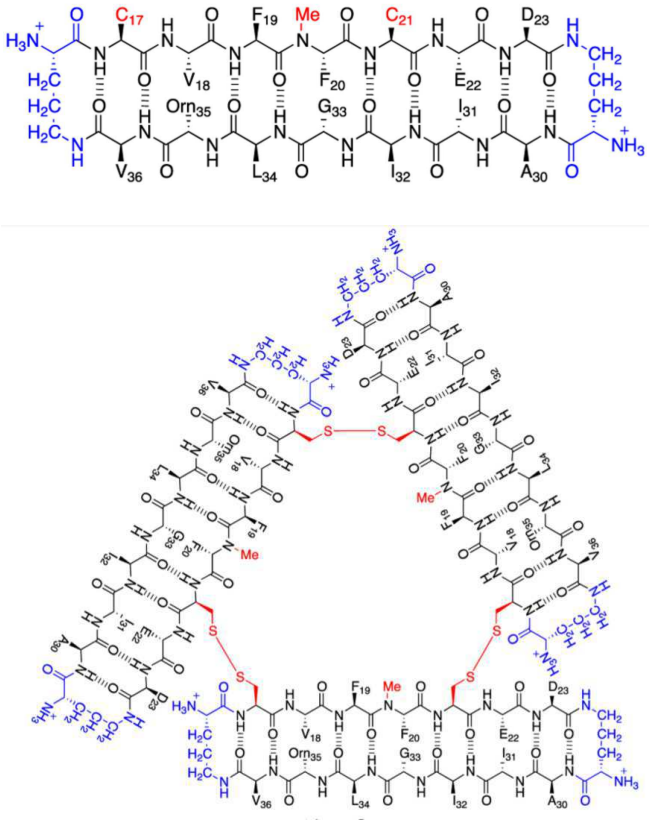

Figure 5.1. (A) The chemical structure of the macrocyclic peptide containing two cysteine mutations (B) The chemical structure of the covalently stabilized trimer after oxidation of the monomer unit.

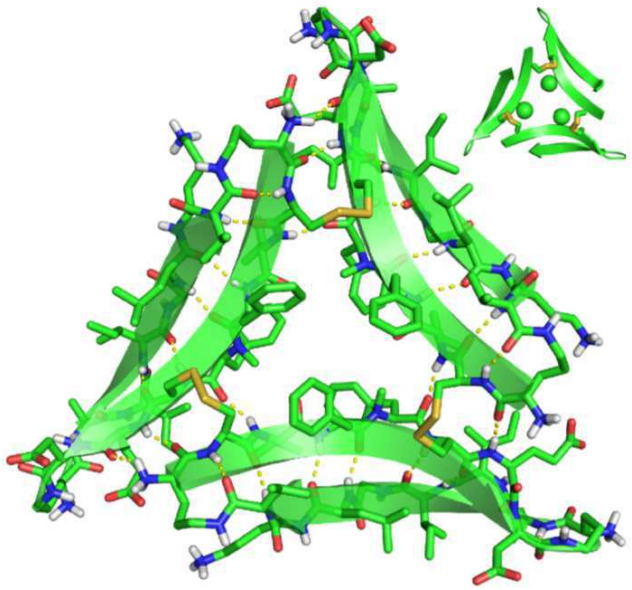

Figure 5.2. The X-ray crystal structure of covalently stabilized trimer.

In another project, I again assisted Adam with project involving development and characterization of another cross-linked trimer with a shifted β-hairpin alignment. I contributed in this project by developing synthesis of the trimer and helping obtain an X-ray crystallographic structure of the trimer. The findings of this project provided additional insights into how trimeric oligomers of full-length Aβ may look like and behave like.

In the project which investigates the assembly and cellular interactions of a trimer derived from Aβ, I provided the fluorescently labeled Aβ to Gretchen Guaglianone. The goal of Gretchen's project was to develop new fluorescently labeled cross-linked trimers to understand and illuminate the solution-phase assembly and cellular interaction of cross-linked trimers. One of the experiments to monitor the cellular interaction of the fluorescently labeled trimer was to incubate those labeled trimers with SH-SY5Y neuronally derived cells with fluorescent microscopy. To investigate the interaction between cross-linked trimers and full-length Aβ, she also incubated the fluorescein labeled Aβ(C1-42) and looked at their colocalization with appropriate wavelength excitation (Figure 5.3). Under fluorescent microscopy, she was able to observe some colocalization between cy3 labeled cross-linked trimers and fluorescein labeled Aβ(C1-42).

Being parts of these projects was incredibly rewarding and fun. Through these projects, I learned a lot of skills and techniques needed for my independent projects, while making positive impacts on these projects which were published in high-impact journals. I learned how to synthesize and purify to produce large quantities of highly pure peptides, as well as X-ray crystallography techniques. These techniques were essential for my own projects. Adam and I have built a strong team while working on these projects and the teamwork brought fruitful results throughout my graduate career.

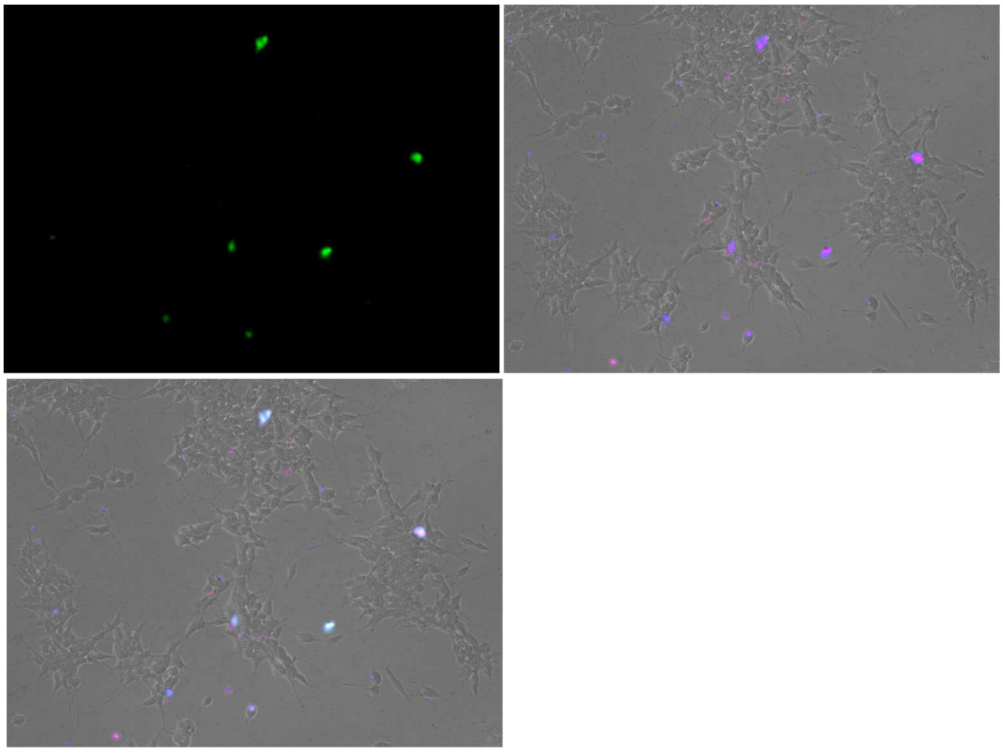

Figure 5.3. Fluorescent microscopy images of SH-SY5Y cells when treated with fluorescein-labeled Aβ, cy3- and cy5-labeled cross-linked trimer. Excited at fluorescein excitation (top, left), at cy3 excitation (top, right), and at cy5 excitation (bottom, left).

2. A Hexamer of a Peptide Derived from Aβ16-36.[3]

In this project, I assisted Dr. Adam Kreutzer with synthesis and X-ray crystallography of a macrocyclic peptide derived from $A\beta_{16-36}$. Unlike the previously studied macrocyclic peptides, the macrocyclic peptide derived from $A\beta_{16-36}$ assembled in solution to form hexamers, trimers, and dimers. The X-ray crystallography, SDS-PAGE, and size exclusion chromatography studies showed that the peptide assembled to form a hexamer in the crystal state and that the hexamer is composed of dimers and trimers. Cytotoxicity assays showed that the oligomers formed by the peptide are toxic toward neuronally derived SH-SY5Y cells.

To further investigate and explore the importance of charge and hydrophobicity in oligomerization, we prepared "chimeric" peptide which contained L17K, E22A, and Orn35M mutations. This mutant peptide assembled differently than the parent peptide by SDS-PAGE and X-ray crystallography. In X-ray crystallographic structure, the columns are composed of antiparallel β-sheet dimers formed by hydrophobic interactions. Each dimer consists of an antiparallel β-sheet formed by two β-hairpins. The dimer is shifted out of registration by two residues toward the C-termini (Figure 5.4). This collaboration resulted a publication in *Biochemistry*.

Through this project, I was able to further polish my laboratory skills in syntheses of peptides and X-ray crystallography. I learned from how Adam executed this project by collaborating with many junior laboratory members. In this project, he worked with three junior laboratory members and an undergraduate student researcher, and distributed tasks efficiently to each collaborator.

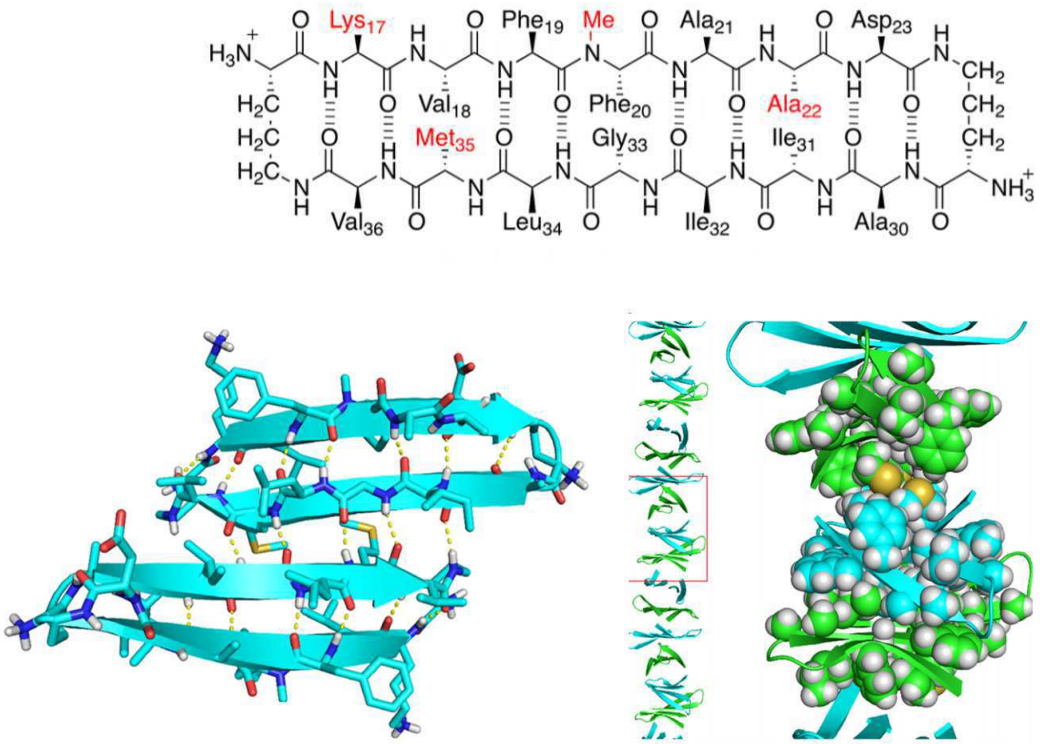

Figure 5.4. The synthesized "chimera" macrocyclic peptide and the X-ray crystallographic structure and assembly of the peptide.

3. Repurposing triphenylmethane dyes to bind to trimers derived from Aβ.[4]

In this project, I collaborated with Dr. Patrick Salveson in his project where he used triphenylmethane dyes as a binder for the cross-linked trimers (Figure 5.5). Patrick developed several variants of crystal violet dyes and investigated how the cross-linked trimers bind to those dyes. The dyes change their colors from purple to blue and become fluorescent when they are bound to trimers. The three-fold symmetric shape of the trimers and triphenylmethane dyes imparts interesting supramolecular interaction between them. I synthesized cross-linked trimer and provided to Patrick in this project. I also demonstrated the utility of the dyes with my model systems.

While I was collaborating on this project, I learned a few lessons from Patrick: I witnessed persistency and innovation in how Patrick works in scientific projects. He executed the project in a careful and thorough manner with many experiments with proper controls. Patrick also showed great leadership during this project by working with many junior laboratory members including undergraduate student researchers. In the end, we were able to publish this work in *Journal of American Chemical Society*.

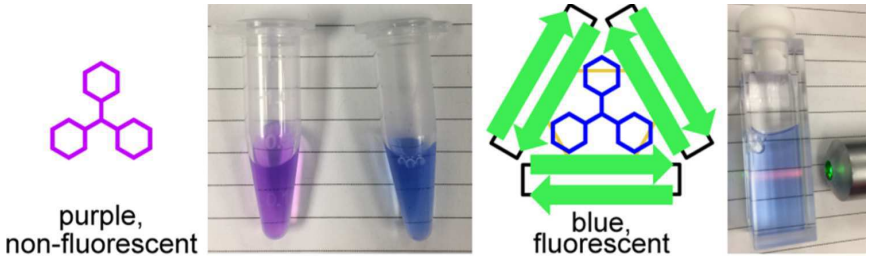

Figure 5.5. Schematics of triphenylmethane dyes with and without binding to cross-linked trimer.

4. Effects of Familial Mutations on the Structural Assembly and Biophysical Properties of a Peptide Derived from Aβ16-36

In this project, I collaborated with Kate McKnelly on project where we questioned what the effects of familial mutations were on assembly of macrocyclic peptide mimicking Aβ β-hairpin (Figure 5.6). Familial mutants of Aβ are associated with early onset Alzheimer's disease and are believed to be more prone to oligomerize into neurotoxic form than unmutated Aβ. I hypothesized that these common familial mutations would affect the assembly of β-hairpin. We synthesized seven mutants within β-hairpin macrocycle and assessed their oligomerization properties by SDS-PAGE. Kate further took on the project by determining structures by X-ray crystallography.

In this project, I developed skills conceiving a new idea, communicating and collaborating with junior laboratory members. Throughout the time we worked on this project, I learned important skills such as project management and working well with junior laboratory workers.

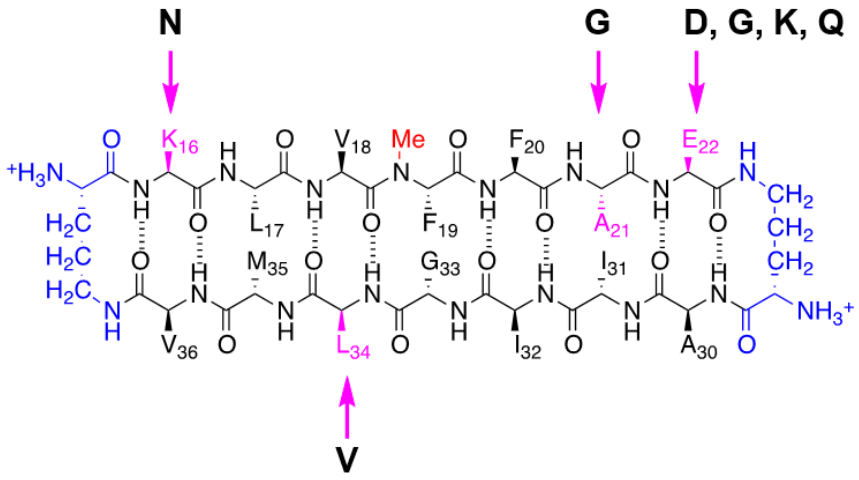

Figure 5.6. Macrocyclic peptide scaffold which familial mutants were synthesized.

5. Antibodies Generated Against a Triangular Trimer Derived from Aβ

In this project, Adam envisioned developing polyclonal antibodies raised from the cross-linked trimer (Figure 5.7). This new antibody selectively recognizes cross-linked trimers and shows unprecedented ring-like staining on brain slices from Alzheimer's disease transgenic mouse brains and human brains. This antibody constitutes a new tool for investigating the role of Aβ oligomers in Alzheimer's disease. I contributed in this project by synthesizing and providing cross-linked trimer for antibody development.

In this project, I was able to help boot up the project as well as to learn new laboratory techniques related to antibody work such as immunoblotting and ELISA. I witnessed how the cross-linked trimer project progressed over the years, and through that I learned a lot from Adam's creativity and persistency. I am excited to what the future holds on this project.

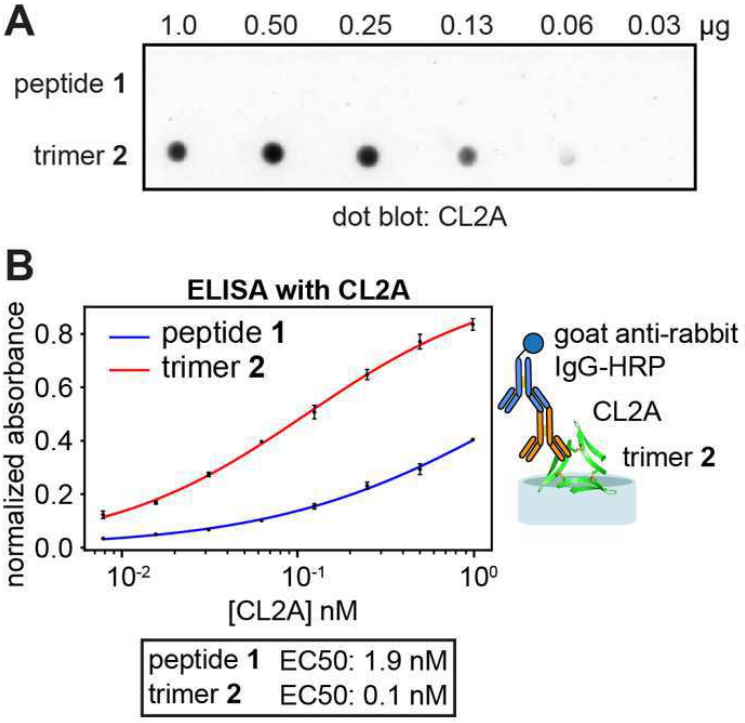

Figure 5.7. Characterization of antibody derived from cross-linked trimer CL2A.

Conclusion

Overall, these collaborations were essential for my growth as a scientist and helped me develop technical and interpersonal skills needed for my future career. Not only did I learn invaluable scientific techniques that made my graduate training easier, but also I learned to work with many different types of people. I witnessed how senior laboratory members executed their projects and learned a lot from their persistency, leadership, and creativity. Together through these collaborations, I was able to publish several co-author publications and another few in the pipeline. I am very proud of us for brining these projects in fruition together.

For the future laboratory members, I highly recommend collaborating with other members constantly along with your own projects. These synergistic efforts go long way. Working with senior members will teach know-how's in laboratory techniques and they will be more likely help you in your projects. Working with junior members will develop your leadership and will make you better mentor. Leadership and mentoring are important in your future career whether it may be in academic or in industry.

Again, I feel so fortunate to have worked with many group members during my time in the Nowick laboratory and appreciate every opportunity for having me work together.

References

1. Kreutzer, A. G.; Yoo, S.; Spencer, R. K.; Nowick, J. S., Stabilization, assembly, and toxicity of trimers derived from Aβ. *J. Am. Chem. Soc.* **2017**, *139*, 966-975.

2. Spencer, R. K.; Li, H.; Nowick, J. S., X-ray crystallographic structures of trimers and higher-order oligomeric assemblies of a peptide derived from Aβ(17-36). *J. Am. Chem. Soc.* **2014**, *136*, 5595-5598.

3. Kreutzer, A. G.; Spencer, R. K.; McKnelly, K. J.; Yoo, S.; Hamza, I. L.; Salveson, P. J.; Nowick, J. S., A hexamer of a peptide derived from Aβ16-36. *Biochemistry* **2017**, *56*, 6061-6071.

4. Salveson, P. J.; Haerianardakani, S.; Thuy-Boun, A.; Yoo, S.; Kreutzer, A. G.; Nowick, J. S., Controlling the oligomerization state of Aβ-derived peptides with light. *J. Am. Chem. Soc.* **2018**, *140*, 5842-5852.